



PONTIFICIA UNIVERSIDAD CATOLICA DE CHILE
ESCUELA DE INGENIERIA

**FINE PARTICULATE MATTER: INDOOR
AND OUTDOOR SOURCE
APPORTIONMENT AT SANTIAGO,
CHILE**

FRANCISCO JAVIER BARRAZA SAAVEDRA

Thesis for the degree of
Doctor of Engineering Sciences

Advisor:
HÉCTOR JORQUERA GONZÁLEZ

Santiago, Chile. September, 2015

© 2015, Francisco Barraza Saavedra



PONTIFICIA UNIVERSIDAD CATOLICA DE CHILE
ESCUELA DE INGENIERIA

MATERIAL PARTICULADO FINO: CONTRIBUCIÓN DE FUENTES INTRADOMICILIARIAS Y AMBIENTALES EN SANTIAGO, CHILE

FRANCISCO JAVIER BARRAZA SAAVEDRA

Tesis para optar al grado de
Doctor en Ciencias de la Ingeniería

Profesor Supervisor:
HÉCTOR JORQUERA GONZÁLEZ

Santiago de Chile, Septiembre, 2015

© 2015, Francisco Barraza Saavedra



PONTIFICIA UNIVERSIDAD CATOLICA DE CHILE
ESCUELA DE INGENIERIA

MATERIAL PARTICULADO FINO: CONTRIBUCIÓN DE FUENTES INTRADOMICILIARIAS Y AMBIENTALES EN SANTIAGO, CHILE

FRANCISCO JAVIER BARRAZA SAAVEDRA

Tesis presentada a la Comisión integrada por los profesores:

HÉCTOR JORQUERA GONZÁLEZ

BÁRBARA LOEB LUSCHOW

LUPITA D. MONTOYA

ERNESTO GRAMSCH LABRA

CLAUDIO GELMI WESTON

CRISTIAN VIAL EDWARS

Para completar las exigencias del grado de
Doctor en Ciencias de la Ingeniería

Santiago de Chile, Septiembre, 2015

ACKNOWLEDGMENTS

To all who gave me their unconditional support and made the development of this thesis possible.

I would like to give special thanks to:

My Family and wife for their patience and infinite love.

My Advisor Professor Héctor Jorquera, whom was of great intellectual and unconditional support, as well as a scientific partner.

Professor Gonzalo Valdivia (Medicine, PUC), for his intellectual support in the design of our monitoring campaign and in the selection of representative households.

To all the volunteers who opened their homes to us so that we could progress in our research.

To all my University, Lab, research and office partners.

Thanks to Ana María Villalobos and Dr. James J. Schauer from the University of Wisconsin-Madison for sharing their knowledge in the publication of: “Chemical speciation and source apportionment of fine particulate matter in Santiago, Chile, 2013”.

And finally, thanks to CONICYT for financing the project (Grant FONDECYT 1121054) and providing economical support through next scholarships: “Apoyo de Tesis Doctoral” and “Beca de Mantención”.

PONTIFICIA UNIVERSIDAD CATOLICA DE CHILE
ESCUELA DE INGENIERIA

PARTICULATE MATTER: INDOOR AND OUTDOOR SOURCE APPORTIONMENT
AT SANTIAGO, CHILE

Thesis submitted to the Office of Research and Graduate Studies in partial fulfillment of
the requirements for the Degree of Doctor in Engineering Sciences by
Francisco Barraza Saavedra

ABSTRACT

Santiago's inhabitants have been exposed to high concentrations of fine particle matter ($PM_{2.5}$) for decades; progress towards a solution to this environmental risk has been slowing down lately. To contribute to a solution to this long-standing problem it is necessary to clearly identify and quantify the agents that contribute to ambient levels of $PM_{2.5}$. The goal of this Thesis is to obtain an enhanced evaluation of Santiago's air quality, through the identification and quantification of the main sources that contribute to $PM_{2.5}$ levels, differentiating Santiago's indoor environment from the outdoor environment. To achieve this goal a source-receptor model was applied to: a) historical database, b) new indoor/outdoor data generated by this thesis and, c) new database collected together with researchers from University of Wisconsin-Madison. From the analyzed data it was found that the main sources that contribute to outdoor $MP_{2.5}$ levels were: motor vehicles, wood burning, sulphates, marine aerosol, copper smelter and soil dust suspension. In indoor environment during spring, six sources were also identified; three of them from outdoor sources: motorized vehicles, street dust and sulphates; and three of them from indoor sources: indoor dust suspension, kitchen + cleaning products and kitchen + tobacco smoke. Also, it was found that the outdoor mean level of $PM_{2.5}$ was slightly lower than indoor mean level.

From the different campaigns we can conclude the existence of significant regional sources that impact on Santiago (marine aerosol and copper smelters); that the main contributions to $PM_{2.5}$ come from emissions from motor vehicles and wood burning, the

latter increasing in the cold months. We also found that indoor $PM_{2.5}$ is different to outdoor $PM_{2.5}$ both in concentration and in composition; this is justified by the existence of emission sources found only indoors that explain ~50% of the total indoor $PM_{2.5}$. We found that only half of indoor households used a fan in their kitchens. Thus, emissions produced by cooking could be further reduced if all households took the cost-effective measure of having a working fan in their kitchens. Likewise, the perspective of this thesis is to help pin down future social-governmental interventions that would allow Santiago to improve its air quality.

Keywords: Air quality, indoor air quality, fine particulate matter, source apportionment of $PM_{2.5}$, exposure to $PM_{2.5}$, sustainable urban development.

Members of the Doctoral Thesis Committee:

Héctor Jorquera González
Bárbara Loeb Luschow
Ernesto Gramsch Labra
Claudio Gelmi Weston
Lupita D. Montoya
Cristian Vial Edwards

Santiago, September, 2015

PONTIFICIA UNIVERSIDAD CATOLICA DE CHILE
ESCUELA DE INGENIERIA

MATERIAL PARTICULADO FINO: CONTRIBUCIÓN INTRADOMICILIARIAS Y
AMBIENTALES EN SANTIAGO

Tesis enviada a la Dirección de Investigación y Postgrado en cumplimiento parcial de los
requisitos para el grado de Doctor en Ciencias de la Ingeniería.

Francisco Barraza Saavedra

RESUMEN

Los habitantes de Santiago han estado expuestos a altas concentraciones de material particulado fino ($PM_{2.5}$) por décadas. La mejoría de los niveles ambientales del $MP_{2.5}$ en Santiago ha ido frenándose en los últimos años. Para poder solucionar esta problemática, es necesario identificar y cuantificar claramente los agentes que contribuyen al aumento de niveles de $PM_{2.5}$. El objetivo de esta Tesis es obtener una evaluación mejorada de la calidad del aire existente para Santiago, mediante la identificación y cuantificación de las principales fuentes que contribuyen al $PM_{2.5}$ en Santiago, diferenciando entre el ambiente intradomiciliario y el exterior. Para cumplir con este objetivo se aplicó un modelo fuente-receptor mediante la utilización del programa computacional PMFv3.0 el cual fue aplicado sobre: a) bases de datos históricos, b) nuevos datos interior/exterior generados por esta tesis y c) nueva base de datos colectados en conjunto con investigadores de la University of Wisconsin-Madison. De los datos analizados se encontró que las principales fuentes que contribuyen al $MP_{2.5}$ exterior en Santiago fueron seis: vehículos motorizados, quema de leña, sulfatos, aerosol marino, fundiciones de cobre y polvo en suspensión. Durante primavera en interior también se identificaron 6 fuentes; tres de ellas de origen exterior: vehículos motorizados, polvo de calle y sulfatos, y tres de origen interior: polvo interior suspendido, cocina + productos de limpieza y cocina + humo de tabaco. Además se encontró el nivel promedio de $PM_{2.5}$ del exterior fue levemente menor al de interior.

De las distintas campañas se puede concluir la existencia de fuentes significativas e intermitentes de contribución regional que impactan sobre Santiago (aerosol marino y

fundiciones de cobre) y que las principales contribuciones al $PM_{2.5}$ provienen de las emisiones generadas por los vehículos motorizados y la quema de leña, incrementando estas últimas sus emisiones durante los meses fríos. El $PM_{2.5}$ intradomiciliario es diferente al encontrado en el exterior, tanto en concentración, como en composición, fenómeno explicado a procesos de generación y resuspensión interna de $PM_{2.5}$ (~50% del total). Dado que aproximadamente la mitad de las viviendas no tenían un ventilador funcionando en la cocina, el aporte proveniente de la cocción de alimentos podría ser reducido si se tomara esa medida, la cual es razonable desde el punto de vista de costo-efectividad. De esta tesis se tiene como perspectiva ayudar a precisar futuras intervenciones socio-gubernamentales que permitan una ciudad con una buena calidad del aire.

Palabras Claves: Calidad del aire, calidad del aire intradomiciliario, material particulado fino, contribución de fuentes al $PM_{2.5}$, exposición al $MP_{2.5}$, desarrollo urbano sustentable

Miembros de la Comisión de Tesis Doctoral

Héctor Jorquera González

Bárbara Loeb Luschow

Ernesto Gramsch Labra

Claudio Gelmi Weston

Lupita D. Montoya

Cristian Vial Edwards

Santiago, Septiembre, 2015

GENERAL INDEX

| | |
|--|-----------|
| List of Papers | 1 |
| 1. Introduction and Thesis Goals | 2 |
| 1.1. General background | 2 |
| 1.2. Hypothesis of the thesis..... | 5 |
| 1.3. Objectives of the thesis | 6 |
| 1.4. Outline of the thesis..... | 7 |
| 2. Source apportionment of PM₁₀ and PM_{2.5} in a desert region in northern Chile..... | 10 |
| 2.1. Highlights | 10 |
| 2.2. Graphical abstract..... | 10 |
| 2.3. Abstract | 11 |
| 2.4. Introduction | 12 |
| 2.5. Methodology | 17 |
| 2.5.1. Sampling and analytical techniques..... | 17 |
| 2.5.2. Receptor modeling analysis for particulate matter | 17 |
| 2.6. Results and discussion..... | 20 |
| 2.6.1. Mass concentration and chemical composition | 20 |
| 2.6.2. Source apportionment for the PM ₁₀ fraction | 23 |
| 2.6.3. Source apportionment for the fine fraction (PM _{2.5})..... | 28 |
| 2.7. Discussion | 33 |
| 2.8. Conclusions | 41 |
| 2.9. Acknowledgments..... | 41 |
| 3. Source apportionment of ambient PM_{2.5} in Santiago, Chile: 1999 and 2004 results | 42 |
| 3.1. Highlights | 42 |
| 3.2. Graphical abstract..... | 42 |
| 3.3. Abstract | 43 |
| 3.4. Introduction | 44 |
| 3.5. Methodology | 48 |
| 3.5.1. Ambient monitoring campaigns..... | 48 |
| 3.5.2. Receptor modeling methodology..... | 49 |

| | |
|---|------------|
| 3.6. Results | 51 |
| 3.6.1. Mass concentration and chemical composition | 51 |
| 3.6.2. Receptor modeling results for the 2004 PM _{2.5} data..... | 52 |
| 3.6.3. Receptor modeling results for the 1999 PM _{2.5} data | 66 |
| 3.7. Discussion of results..... | 75 |
| 3.8. Conclusions | 81 |
| 3.9. Acknowledgments | 82 |
| 4. Indoor PM_{2.5} in Santiago, Chile, spring 2012: Source apportionment and outdoor contributions | 83 |
| 4.1. Highlights | 83 |
| 4.2. Graphical abstract..... | 83 |
| 4.3. Abstract | 84 |
| 4.4. Introduction | 85 |
| 4.4.1. Single zone indoor air quality models | 85 |
| 4.4.2. Multi-zone indoor air quality models | 86 |
| 4.4.3. Case study: Santiago, Chile | 87 |
| 4.4.4. Indoor and outdoor monitoring campaigns..... | 90 |
| 4.4.5. Filter analysis | 92 |
| 4.4.6. Receptor modeling methodology..... | 93 |
| 4.5. Results | 94 |
| 4.5.1. Mass concentration and chemical composition | 94 |
| 4.5.2. Indoor-outdoor relationships..... | 101 |
| 4.5.3. Receptor modeling results for indoor PM _{2.5} | 107 |
| 4.6. Discussion of results..... | 111 |
| 4.7. Conclusions | 113 |
| 4.8. Acknowledgments | 114 |
| 5. Chemical speciation and source apportionment of fine particulate matter in Santiago, Chile, 2013..... | 115 |
| 5.1. Highlights | 115 |
| 5.2. Abstract | 115 |
| 5.3. Introduction | 117 |
| 5.4. Methodology | 122 |
| 5.4.1. Sampling site description..... | 122 |

| | |
|---|------------|
| 5.4.2. Sampling method and selection of samples | 126 |
| 5.4.3. Chemical analysis | 127 |
| 5.4.4. Source apportionment | 129 |
| 5.5. Results and discussion..... | 130 |
| 5.5.1. Particulate matter and composition..... | 130 |
| 5.5.2. CMB results | 141 |
| 5.6. Summary and conclusions..... | 149 |
| 5.7. Acknowledgments | 151 |
| 6. Summary and Conclusion | 152 |
| 6.1. General Conclusions | 152 |
| 6.2. Future prospects | 155 |
| 7. Bibliografía | 157 |
| Annexes | 174 |
| Annex A: Ethical Issues | 175 |

TABLES INDEX

| | |
|---|-----|
| Table 1 Summary of chemical composition of ambient PM ₁₀ , in µg/m ³ . | 21 |
| Table 2 Summary of chemical composition of ambient PM _{2.5} , in µg/m ³ . | 22 |
| Table 3 Source profiles for the five factor solution for PM ₁₀ fraction in µg/m ³ (F _{peak} =0). | 25 |
| Table 4 Source profiles for the six factor solution for PM _{2.5} in µg/m ³ (F _{peak} =-0.05). | 29 |
| Table 5 Summary of source apportionment results. | 32 |
| Table 6 Summary of PM _{2.5} mass and elemental concentrations ^a , 2004 campaign. | 51 |
| Table 7 Summary of PM _{2.5} mass and elemental concentrations ^a , 1999 campaign. | 52 |
| Table 8 Regression diagnostics for a 6 factor solution, 2004 data. | 53 |
| Table 9 Source profiles [ng/m ³] for a 6 factor solution, 2004 data (F _{peak} = -0.15). | 54 |
| Table 10 Comparison of dominant source contributions and wind trajectory analysis for selected days, 2004 campaign. | 62 |
| Table 11 Source apportionment results for 2004 campaign. | 66 |
| Table 12 Regression diagnostics for a 6 factor solution, 1999 data. | 67 |
| Table 13 Source profiles [ng/m ³] for a 6 factor solution, 1999 data (F _{peak} = -0.2). | 67 |
| Table 14 Comparison of dominant source contributions and wind trajectory analysis for selected days, 1999 data. | 71 |
| Table 15 Source apportionment results for 1999 campaign. | 74 |
| Table 16 Summary of 48 h indoor PM _{2.5} elemental concentrations, 2012 campaign [ng/m ³] (N = 47 households) | 95 |
| Table 17 Summary of outdoor 24 h PM _{2.5} elemental concentrations, 2012 campaign [ng/m ³] (N = 41 samples). | 96 |
| Table 18 Results of the comparison tests for group medians, 2012 campaign. | 97 |
| Table 19 Robust fit of Equation 8 for indoor species. | 102 |
| Table 20 Robust fit results of Equation 8 for individual households. | 105 |
| Table 21 Diagnostics for the 6-factor solution for indoor PM _{2.5} . | 107 |
| Table 22 Source profiles [ng/m ³] for a 6 factor solution, indoor PM _{2.5} data. | 107 |

| | |
|---|-----|
| Table 23. Contribution of species to total factor mass (%) for the six factor solution, indoor PM _{2.5} | 109 |
| Table 24 Source apportionment results for indoor PM _{2.5} , 6-factor solution | 110 |
| Table 25 Monthly meteorological data measured at the Meteorological Service station closest to the receptor site. | 118 |
| Table 26 Summary of previous source apportionment results carried out at Santiago. | 121 |
| Table 27 Monthly average gravimetric PM _{2.5} mass and bulk composition (±standard deviation) for fine particulate matter in Santiago, Chile..... | 133 |
| Table 28 Source contributions to ambient PM _{2.5} organic carbon (OC) estimated by CMB. Statistically significant source contributions are shown in bold. | 143 |
| Table 29 Monthly source contribution to PM _{2.5} from March to October. | 147 |

FIGURES INDEX

| | |
|---|----|
| Figure 1 Graphical abstract: Source apportionment of ambient PM _{2.5} in Santiago, Chile: 1999 and 2004 results..... | 10 |
| Figure 2 Location of the ambient monitoring site and the main sources surrounding it.... | 13 |
| Figure 3 Annual box plots of surface meteorological variables measured at Cerro Moreno Airport (23°26'S, 70°26'W), 20 km NNW of Antofagasta, for the years 2000–2010. | 14 |
| Figure 4 Box plots of daily PM ₁₀ concentrations measured using Hi-volume samplers. Top panel: by year; lower panel: by month. Period: January 2004 through December 2009. | 15 |
| Figure 5 Summary of wind measurements during the ambient monitoring campaign. Left panel: diurnal boxplot of wind speed. Eight panel: compass plot of wind speed and direction..... | 16 |
| Figure 6 Source profile concentrations [$\mu\text{g}/\text{m}^3$] for the five factor solution for ambient PM ₁₀ (F _{peak} =0). | 21 |
| Figure 7 Source profile concentrations [$\mu\text{g}/\text{m}^3$] for the six factor solution for ambient PM _{2.5} (F _{peak} =−0.05), factors 1–3..... | 23 |
| Figure 8 Source profile concentrations [$\mu\text{g}/\text{m}^3$] for the six factor solution for ambient PM _{2.5} (F _{peak} =−0.05), factors 4–6..... | 30 |
| Figure 9 Time series plots of source contributions to PM ₁₀ and PM _{2.5} concentrations, in [$\mu\text{g}/\text{m}^3$]. | 33 |
| Figure 10 Backward trajectories arriving at the monitor site on January 15 th , 2008. | 34 |
| Figure 11 Backward trajectories arriving at the monitor site on January 17 th , 2008. | 35 |
| Figure 12 Forward wind trajectories departing from the cement plant on December 29 th , 2007..... | 36 |
| Figure 13 Forward wind trajectories departing from the brine plant on December 19 th , 2007..... | 37 |
| Figure 14 Forward wind trajectories departing from the copper smelter on January 3 rd , 2008..... | 38 |

| | |
|--|----|
| Figure 15 Compass plots of local wind data for December 19th, 2007 and January 17th, 2008..... | 39 |
| Figure 16 Graphical abstract: Source apportionment of ambient PM _{2.5} in Santiago, Chile: 1999 and 2004 results..... | 42 |
| Figure 17 A map depicting the metropolitan region of Chile, major urban areas, and Santiago's ambient monitoring network..... | 45 |
| Figure 18 Annual box plots of daily ambient PM _{2.5} concentrations at Santiago's stations L, M, N and O, in [µg/m ³], for the period 2000–2011. | 46 |
| Figure 19 Monthly box plots of daily ambient PM _{2.5} concentrations at Santiago's stations L, M, N and O, in [µg/m ³], for the period 2000–2011. | 47 |
| Figure 20 Box plots of estimated, ambient PM _{2.5} source contributions by day of the week, 2004 campaign. | 56 |
| Figure 21 Scatterplots of estimated, ambient PM _{2.5} source contributions versus mean daily temperatures, 2004 campaign..... | 57 |
| Figure 22 On May 2004 There was no Presence of wildfires close to Santiago..... | 58 |
| Figure 23 On June 2004 There was no Presence of wildfires close to Santiago..... | 58 |
| Figure 24 Presence of wildfires close to Santiago on February 2004 | 59 |
| Figure 25 Presence of wildfires close to Santiago on December 2004 | 59 |
| Figure 26 Forward trajectories starting a Caletones smelter on March 11 th 2004. | 63 |
| Figure 27 Forward trajectories starting a Chagres and Ventanas smelters on May 28 th 2004..... | 63 |
| Figure 28 Backward trajectories arriving at monitor site on July 26 th 2004..... | 64 |
| Figure 29 Forward trajectories starting at the copper smelters and backward trajectories from the monitor site on March 11 th 2004. | 64 |
| Figure 30 Backward trajectories arriving at monitor site on June 30 th 2004. | 65 |
| Figure 31 Timeline plot of estimated, ambient PM _{2.5} source contributions, 2004 campaign. | 66 |
| Figure 32 Box plots of estimated, ambient PM _{2.5} source contributions by day of the week, 1999 campaign. | 69 |

| | |
|--|-----|
| Figure 33 Scatterplots of estimated, ambient PM _{2.5} source contributions versus mean daily temperatures, 1999 campaign..... | 70 |
| Figure 34 Forward trajectories starting at Caletones smelter on July 7 th 1999. | 72 |
| Figure 35 Forward trajectories starting at Ventanas and Chagres smelters on July 10 th 1999. | 72 |
| Figure 36 Forward trajectories starting at Chagres smelters on August 3 th 1999. | 73 |
| Figure 37 Backward trajectories arriving at monitor site on August 11 th 1999. | 73 |
| Figure 38 Timeline plot of estimated, ambient PM _{2.5} source contributions, 1999 campaign. | 74 |
| Figure 39 Comparison of campaign average and annual average source contributions for the 2004 PM _{2.5} campaign. | 75 |
| Figure 40 Comparison of July–November source contributions [$\mu\text{g}/\text{m}^3$] for the 1999 and 2004 PM _{2.5} campaigns. | 76 |
| Figure 41 Graphical abstract: Indoor PM _{2.5} in Santiago, Chile, spring 2012: Source apportionment and outdoor contributions | 83 |
| Figure 42 Trends in ambient PM _{2.5} measured at Santiago, Chile, 2000-2012 (TEOM uncorrected data). | 88 |
| Figure 43 Aerial photograph of the outdoor sampling site and surrounding structures..... | 91 |
| Figure 44 A map depicting Downtown Santiago, the location of the outdoor monitor | 92 |
| Figure 45 Box plots of PM _{2.5} concentrations for the 24 h outdoor, 48 h indoor and socioeconomic status data categories. | 94 |
| Figure 46 Boxplots of indoor and outdoor concentrations of OC, EC, Na and Mg ($\mu\text{g}/\text{m}^3$) | 98 |
| Figure 47 Same as previous figure but for Al, Si, S and Cl ($\mu\text{g}/\text{m}^3$)..... | 99 |
| Figure 48 Same as previous figure but for K, Ca, Ti and Mn ($\mu\text{g}/\text{m}^3$). | 99 |
| Figure 49 Same as previous figure but for Fe, Cu, Zn and As ($\mu\text{g}/\text{m}^3$). | 100 |
| Figure 50 Same as previous figure but for Se, Br, Sr and Pb ($\mu\text{g}/\text{m}^3$). | 100 |
| Figure 51 Robust linear fit of Equation 8 for total PM _{2.5} and most of its component species | 103 |

| | |
|--|-----|
| Figure 52 Examples of robust linear fit of Equation 8 for all measured species at selected households..... | 104 |
| Figure 53 Plots of the estimated F_{INF} parameter versus..... | 106 |
| Figure 54 Boxplots of source contributions G_1 , G_5 , and G_6 ($\mu\text{g}/\text{m}^3$) versus households without (0) or with (1) smoker occupants. | 110 |
| Figure 55 Histograms of hours per day with windows and doors open for all households included in the springtime campaign. | 112 |
| Figure 56 Map of Santiago showing the geographical center (labeled star), the location of the receptor site, two of the closest air quality monitoring network stations (L, N), and the closest station from the Meteorological Service. | 123 |
| Figure 57 Views of Santiago from the receptor site..... | 123 |
| Figure 58 Plots of rose winds for monitoring stations L and N for March - October 2013. | 124 |
| Figure 59 Plots of monthly averages of pollutants measured at stations N and L, year 2013..... | 125 |
| Figure 60 Monthly comparison of a) $\text{PM}_{2.5}$ mass b) sulfate c) nitrate and d) WSOC of 1) all samples collected and 2) selected samples, including standard error, from March to October. | 127 |
| Figure 61 Concentration of a) $\text{PM}_{2.5}$ mass, b) sulfate, c) nitrate, d) WSOC, e) OC, and f) EC in Santiago from March to October. | 131 |
| Figure 62 Monthly gravimetric $\text{PM}_{2.5}$ mass (\pm standard error) and bulk composition in Santiago from March to October..... | 132 |
| Figure 63 Monthly gravimetric $\text{PM}_{2.5}$ mass (\pm standard error) and bulk composition from May to September, including dust. | 134 |
| Figure 64 Monthly ambient concentrations of a) EC, WIOC, and WSOC and b) WSIN and WSON in Santiago from March to October..... | 136 |
| Figure 65 Monthly concentration of a) levoglucosan, b) PAHs, and c) hopanes in ambient $\text{PM}_{2.5}$ in Santiago from March to October. | 138 |
| Figure 66 Monthly carbon preference indices (CPI)..... | 140 |

| | |
|---|-----|
| Figure 67 Linear regression between mobile source contributions of the base case and the alternative case. | 141 |
| Figure 68 Monthly source contribution to PM _{2.5} OC estimated using CMB model on a) absolute and b) percent scales in Santiago from March to October. | 144 |
| Figure 69 Monthly source contribution to ambient PM _{2.5} mass in Santiago from March to October. | 146 |
| Figure 70 Santiago 2004/1999 campaigns. Summary of outdoor sources apportionment. | 152 |
| Figure 71 Santiago 2012 campaign. Indoor Source Apportionment..... | 153 |
| Figure 72 Santiago 2013 campaign. Outdoor Source Apportionment | 154 |

LIST OF PAPERS

This thesis is based on the following papers, presented in the text in the following chapters:

2. Héctor Jorquera, Francisco Barraza
Source apportionment of PM_{10} and $PM_{2.5}$ in a desert region in northern Chile. *Science of the Total Environment*, 444, 327–335, 2013
3. Héctor Jorquera, Francisco Barraza
Source apportionment of ambient $PM_{2.5}$ in Santiago, Chile: 1999 and 2004 results. *Science of the Total Environment*, 435-436, 418–429, 2012
4. Francisco Barraza, Héctor Jorquera, Gonzalo Valdivia, Lupita D. Montoya
Indoor $PM_{2.5}$ in Santiago, Chile, spring 2012: Source apportionment and outdoor contributions. *Atmospheric Environment*, 94, 692-700, 2014
5. Ana M. Villalobos, Francisco Barraza, Héctor Jorquera, James J. Schauer
Chemical Speciation and Source Apportionment of Fine Particulate Matter in Santiago, Chile, 2013. *Science of the Total Environment*, 512-513, 133–142, 2015

1. INTRODUCTION AND THESIS GOALS

This chapter describes the thesis background, its main goal and specific objectives. It begins with an introduction to the topic of fine particulate matter air pollution in Santiago, followed by the statements of the main goal and specific objectives proposed in this thesis. The next chapters present the publications resulting from this thesis's work.

1.1. General background

Solid particles suspended in the air, denoted as Particulate Matter (PM), are classified according to the aerodynamic diameter of the particles that constitute them. PM_{10} and $PM_{2.5}$ are the most studied and regulated fractions because they can be inhaled and get into deep regions of the respiratory tract. The fine particle matter ($PM_{2.5}$) is the fraction studied in this thesis, corresponding to solid particles suspended in the air with aerodynamic diameter equal or smaller than 2.5 micrometers (μm), originated mainly by anthropogenic emissions. Short term epidemiologic studies have found a consistent statistical association between the mass concentration of these particles in the air and daily morbidity and mortality, even in low environmental concentrations (US EPA 2004; WHO: World Health Organization 2005; D W Dockery et al. 1993; Pope 2007; Lepeule et al. 2012). In the case of premature long-term mortality, cohort studies have conclusively shown that the magnitude of the effect is several times the value of the estimated effect of short-term study (D W Dockery et al. 1993; Lepeule et al. 2012; Cesaroni et al. 2013; Arden Pope et al. 2011).

Short term epidemiologic studies have been performed in Santiago, correlating the increased levels of $PM_{2.5}$ in the environment with health effects. Leiva *et al.* (Leiva et al. 2013) found that for every daily increment of $10 \mu g/m^3$ of $PM_{2.5}$ in the air, the risk of hospitalization from cerebrovascular disease increases 29% (Odds Ratio: 1,29; 95% IC: 0,55-2,03). For a daily increment of $10 \mu g/m^3$ of $PM_{2.5}$, Valdés *et al.* (Valdes et al. 2012) determined a 33% increment of premature mortality because of cardiovascular problems. These authors also highlight that the composition of Particle Matter is relevant, noting that

high contents of chrome, copper and sulfur have a greater association with premature mortality caused by chronic obstructive pulmonary disease (COPD), while zinc and sodium are associated to cerebrovascular disease. Both studies don't conclude definitively about the statistical association since the confidence intervals include the 1.0 value. Nevertheless, their results are plausible for their adequate procedure and the consistency of their findings. Pino *et al.* (Pino et al. 2004) observed in a prospective study that from April 1995 to October 1996, the $PM_{2.5}$ was positively correlated with a lower respiratory tract illnesses in children less than one year old, establishing that a daily increment of $10 \mu g/m^3$ of $PM_{2.5}$ increases in 5% the risk of wheezing bronchitis (95% IC: 0% - 9%). This study used epidemiologic models with temporary delays and confirmed that at the ninth day after acute exposure to $PM_{2.5}$ an increase of a maximum 9% is reached. González *et al.* (González R. et al. 2013) established, through a study of temporal series during the period 2000-2007, that the periods of high PM contamination are correlated with peak values of incidence of diabetes mellitus type 1.

All of the above studies evidence the impact of ambient $PM_{2.5}$ in the health of people, and they have used ambient monitoring of $PM_{2.5}$ to estimate population exposure to $PM_{2.5}$. However, it has been found that people spend most of their time indoors (Caceres et al. 2001). Hence studies that measure indoor air pollution, especially in households, provide a better estimation of total human exposure to $PM_{2.5}$ and its effects on people's health. However, given the high costs and difficulties to perform indoor studies, government agencies often use outdoor measurements to estimate total human exposure to air pollution. To improve this situation, it is useful to characterize the relationship between indoor and outdoor air pollution and how that changes according to the household's characteristics. In this way it would be possible to have better estimates of total human exposure to $PM_{2.5}$ considering the different environments in which people stay during their normal activities.

In recent years the study of indoor $PM_{2.5}$ has increased due to its impact on people's health (Ashmore and Dimitroulopoulou 2009; Junninen et al. 2009; Lai et al. 2010; Ohura et al. 2009), particularly due to solid fuel use in developing countries. On this

regard, WHO has estimated that indoor air pollution is responsible of 36 % of all low respiratory infections, of 22% of the cases of COPD and of 2 million premature deaths (WHO 2002; WHO 2015). Another important feature of indoor $PM_{2.5}$ is the difference it has regarding outdoor $PM_{2.5}$, both in concentration and in composition. The outdoor $PM_{2.5}$ has been identified as one of the main sources that contribute to increase indoor $PM_{2.5}$ particles, because they easily infiltrate through cracks or through ventilation, causing air exchange between the outdoor and indoor air. (Qing Yu Meng et al. 2009). Other sources that have been identified as contributors to increase indoor $PM_{2.5}$ levels are: household cleaners (cleaning process), dust suspension caused by people moving indoor, cooking, the presence of pets and insects, smoking, using candles and incense and indoor space heating. Some studies exclude households with smokers, for a better characterization of indoor pollution (Abt et al. 2000; Bernstein et al. 2008; Saraga et al. 2010; Begum et al. 2009), but this bias the results if the percentage of people who smoke indoor is high.

In Chile there are few recent publications that give information on indoor air quality and its relation to health effects. In general, high concentrations of $PM_{2.5}$, NO_2 , SO_2 and ultra-fine particles (less than $0.1 \mu m$ in size) were found during winter (Ruiz et al. 2010; Rojas-Bracho et al. 2002; Adonis and Gil 2001; Flores et al. 2010). The origin of this behavior is mainly caused by heating combustion and outdoor contributions (Ruiz et al. 2010). Rojas-Bracho *et al.* showed that in central and northeast sectors of Santiago, concentrations of indoor $PM_{2.5}$, PM_{10} and NO_2 are higher than those found in cities across the USA and Canada; this is explained because of high internal and external anthropogenic contributions and the meteorological and geographical conditions related to Santiago's location. (Rojas-Bracho et al. 2002; Muñoz et al. 2010). Adonis and Gil have measured CO , SO_2 , PM_{10} , and polycyclic aromatic hydrocarbons (PAHs) in La Pintana, one of the poorest sectors within Santiago. This study found that low socioeconomic status is more vulnerable to the impacts attributed to poor air quality and has high concentration levels of indoor pollutants (Adonis and Gil 2001). Flores *et al.* found an association between the emissions from the use of coal and firewood with chronic respiratory symptoms, and also found that in adults, those most at risk of COPD are male over 60 years old (Flores et al. 2010); this study identified possible sources of PM through surveys without a quantitative

indoor measurement of pollutant levels. These facts suggest that in order to better understand the impact of air quality on respiratory problems of Santiago's population, it is necessary to quantify the concentration and chemical composition of indoor $PM_{2.5}$, and perform a deeper and more accurate analysis for identifying the main sources that contribute to increase the levels of $PM_{2.5}$ including the own habits of residents which impact upon these concentrations.

1.2. Hypothesis of the thesis

The hypotheses that were the basis of this thesis were:

The analysis of the chemical composition of $PM_{2.5}$ by using receptor models, could allow us to identify and quantify the contributions of different types of sources, differentiating between i) natural and anthropogenic sources; ii) indoor and outdoor sources, and iii) primary and secondary particles.

Outdoor sources could have a significant contribution to indoor $PM_{2.5}$ levels.

Accurate identification and quantification of sources contributing to $PM_{2.5}$ would allow us to obtain: i) a hierarchy of impacts of each source, ii) origin classification (indoor and / or outdoor), and finally iii) contribute to improve social behavior and policies that help to reduce $PM_{2.5}$ levels.

1.3. Objectives of the thesis

The main goal of this thesis is to perform a quantitative air quality evaluation to identify the major sources that contribute to both outdoor and indoor $\text{PM}_{2.5}$ concentrations.

The specific goals are the following ones:

- Achieving a chemical characterization of $\text{PM}_{2.5}$ that provides enough information to identify the main sources contributing to its levels.
- Applying a receptor model for Santiago for identifying the main sources contributing to $\text{PM}_{2.5}$, differentiating between sources of primary and secondary origin.
- Identifying and quantifying the main sources contributing to indoor $\text{PM}_{2.5}$ in Santiago. Such analysis has not been performed before this Thesis.
- Sorting out sources contributing to indoor and outdoor $\text{PM}_{2.5}$, and quantifying the contribution (and infiltration) from outdoor to indoor.

1.4. Outline of the thesis

This thesis has been developed taking as its central theme the identification and quantification of the main sources that explain $PM_{2.5}$ levels in Santiago. The structure of the Thesis responds to the questions that arose during the research process. These questions and their answers are described below.

a) How to identify and quantify the main sources that contribute to $PM_{2.5}$?

The answer to this question is to apply a receptor model, in this case PMF (Positive Matrix Factorization) widely used in developed countries (Reff, Eberly, and Bhawe 2007; Belis et al. 2013), which had already been used by the research group for the city of Tocopilla (Hector Jorquera 2009). In this thesis PMF (3.0 version) model was successfully applied to measured data in the industrial area of La Negra, II Region, where sources of $PM_{2.5}$ were few and already known. From this task, the first article presented in this thesis was generated: "Source apportionment of PM_{10} and $PM_{2.5}$ in a desert region in northern Chile" (See Chapter 2). This training work validated a protocol and chemical profiles from industrial sources and natural contributions to ambient PM_{10} and $PM_{2.5}$ in an industrial area located in the hyper-arid Atacama Desert.

b) Is the methodology applicable to Santiago?

Unlike the work mentioned in a), modeling ambient $PM_{2.5}$ at Santiago has been a greater challenge because it has more contributing sources, and has a marked seasonality not present in the north of Chile. However, it was possible to obtain a feasible model for historical data collected during 2004 and 1999; the same model was applied (PMF 3.0) to data measured in the same sector of the city (Las Condes, eastern side of Santiago) but analyzed at different laboratories; the similarity of the results in both years showed that PMF3.0 is able to identify the main contributing sources to $PM_{2.5}$. In this case six main sources whose contributions for 1999/2004 were estimated as follows: motor vehicles: $28 \pm 2.5\%$ / $31.2 \pm 3.4\%$, biomass burning: $24.8 \pm 2.3\%$ / $28.9 \pm 3.3\%$, sulfates: $18.8 \pm 1.7\%$ /

6.2±2.5%, marine aerosol: 13±2.1% / 9.9±1.5%, copper smelters: 11.5±1.4% / 9.7±3.3% and suspended soil dust: 3.9±1.5% / 4.0±2.4%. This work resulted in the publication of the article: "Source apportionment of ambient PM_{2.5} in Santiago, Chile: 1999 and 2004 results" (See Chapter 3). From this work it is highlighted that although the level of PM_{2.5} has declined over the years, the main sources of contribution remain the same for 2004 and 1999, in almost the same percentages. In addition it provides quantitative evidence of the impact of regional contributions such as marine aerosol and copper smelters near Santiago.

c) From the exposure point of view, is indoor PM_{2.5} equal in concentration and/or composition to the PM_{2.5} found outdoors?

Studies performed in EEUU and Europe cities have determined that indoor PM_{2.5} differs from outdoor PM_{2.5}, yet there is not much information of this for Santiago. That is why a campaign of indoor/outdoor monitoring has been performed in order to find and collect information that enables to answer this question. This effort culminated in the third published article, titled "Indoor PM_{2.5} in Santiago, Chile, spring 2012: Source apportionment and outdoor Contributions ". In this paper it is evidenced in a conclusive way that indoor PM_{2.5} differs regarding concentration, composition and sources of contribution. It should be noted that a work like this (application of a receptor model) is the first one conducted in Santiago; it was found that indoor generated contributions are responsible for about 50% of total indoor PM_{2.5}.

d) Is it possible to obtain a better characterization, especially for the cold season?

A limitation of the model obtained for Santiago described in b) is that it was based solely on elemental analysis of ambient PM_{2.5}. Thus it did not use molecular tracers; neither resolved the sources that emit OC (which can reach up to 70% of the PM_{2.5}). We remark that every combustion process produces organic carbon emissions (vehicle motors and food cooking) and some increase during the colder months (wood burning). In order to answer this question a monitoring campaign was conducted from March to October 2013

at the San Joaquin campus of Pontificia Universidad Católica de Chile (PUC), collecting ambient $PM_{2.5}$ samples that were subsequently analyzed and studied using the model of contribution of sources CMB - Chemical Mass Balance - (U.S. Environmental Protection Agency 2015) by the research group of Dr. James J. Schauer from the University of Wisconsin-Madison. From this collaborative work the following work was published: "Chemical speciation and source apportionment of fine particulate matter in Santiago , Chile, 2013" (See Chapter 5). This article highlights the following aspects: i) a complete molecular speciation of $PM_{2.5}$, including alkanes and alkenes of high molecular weight, PAHs and fatty acids, ii) for the first time, the identification and quantification of sources contributing to organic carbon is obtained for Santiago, including secondary organic aerosols, iii) the contributions of motor vehicles are provided for gasoline and diesel powered vehicles, and iv) similar results are obtained and complemented to those obtained for Santiago 2004-1999, using a completely different basis of chemical species and a different receptor model.

In summary, in this Thesis a quantitative and comprehensive description of the major sources of ambient $PM_{2.5}$ at Santiago has been accomplished, spanning from 1999 through 2013. In addition, an indoor $PM_{2.5}$ campaign has shown that 70% of outdoor $PM_{2.5}$ penetrates the households at Santiago in the warm season and that 50% of indoor $PM_{2.5}$ comes from indoor sources.

2. SOURCE APPORTIONMENT OF PM₁₀ AND PM_{2.5} IN A DESERT REGION IN NORTHERN CHILE

2.1. Highlights

- Ambient PM₁₀ and PM_{2.5} were measured in an industrial zone within an arid region in the North of Chile.
- Dry climate allows accumulation of heavy metals deposited on the ground.
- Soil dust becomes enriched with tracers of anthropogenic activities.
- Average suspended soil dust reaches 9 µg/m³ for PM_{2.5} and 50 µg/m³ for PM₁₀.
- Peak daily soil dust reaches 31.5 µg/m³ for PM_{2.5} and 104 µg/m³ for PM₁₀.

2.2. Graphical abstract

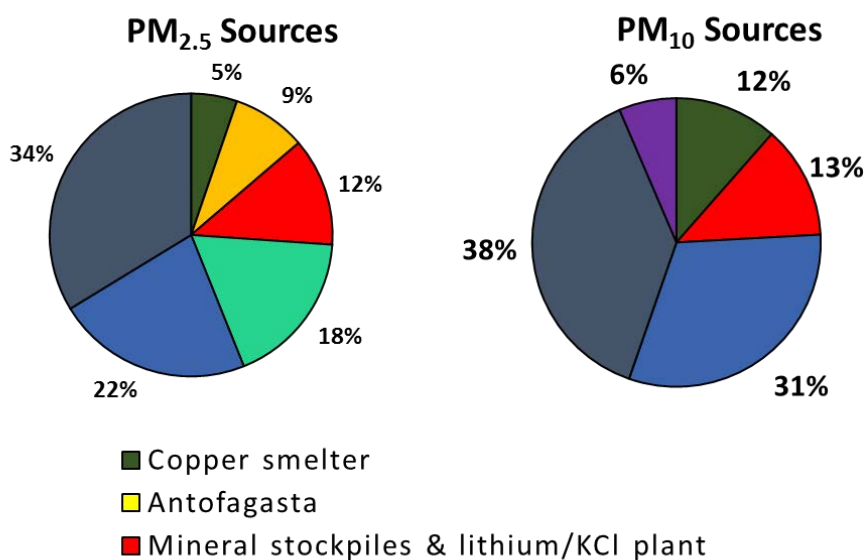


Figure 1 Graphical abstract: Source apportionment of ambient PM_{2.5} in Santiago, Chile: 1999 and 2004 results

2.3. Abstract

Estimating contributions of anthropogenic sources to ambient particulate matter (PM) in desert regions is a challenging issue because wind erosion contributions are ubiquitous, significant and difficult to quantify by using source-oriented, dispersion models. A receptor modeling analysis has been applied to ambient PM₁₀ and PM_{2.5} measured in an industrial zone ~20 km SE of Antofagasta (23.63°S, 70.39°W), a midsize coastal city in northern Chile; the monitoring site is within a desert region that extends from northern Chile to southern Perú. Integrated 24-hour ambient samples of PM₁₀ and PM_{2.5} were taken with Harvard Impactors; samples were analyzed by X Ray Fluorescence, ionic chromatography (NO₃⁻ and SO₄⁻), atomic absorption (Na⁺, K⁺) and thermal optical transmission for elemental and organic carbon determination. Receptor modeling was carried out using Positive Matrix Factorization (US EPA Version 3.0); sources were identified by looking at specific tracers, tracer ratios, local winds and wind trajectories computed from NOAA's HYSPLIT model.

For the PM_{2.5} fraction, six contributions were found — cement plant, $33.7 \pm 1.3\%$; soil dust, $22.4 \pm 1.6\%$; sulfates, $17.8 \pm 1.7\%$; mineral stockpiles and brine plant, $12.4 \pm 1.2\%$; Antofagasta, $8.5 \pm 1.3\%$ and copper smelter, $5.3 \pm 0.8\%$. For the PM₁₀ fraction five sources were identified — cement plant, $38.2 \pm 1.5\%$; soil dust, $31.2 \pm 2.3\%$; mineral stockpiles and brine plant, $12.7 \pm 1.7\%$; copper smelter, $11.5 \pm 1.6\%$ and marine aerosol, $6.5 \pm 2.4\%$. Therefore local sources contribute to ambient PM concentrations more than distant sources (Antofagasta, marine aerosol) do. Soil dust is enriched with deposition of marine aerosol and calcium, sulfates and heavy metals from surrounding industrial activities. The mean contribution of suspended soil dust to PM₁₀ is $50 \mu\text{g}/\text{m}^3$ and the peak daily value is $104 \mu\text{g}/\text{m}^3$. For the PM_{2.5} fraction, suspended soil dust contributes with an average of $9.3 \mu\text{g}/\text{m}^3$ and a peak daily value of $31.5 \mu\text{g}/\text{m}^3$.

2.4. Introduction

Chile's economy is based mainly on mineral, agricultural, forest and marine exports, with primary copper and refined copper production accounting for 34% and 17% - respectively - of worldwide production in 2010 (COCHILCO 2012) northernmost part of Chile, from $\sim 30^{\circ}\text{S}$ up to the border with Perú is where most mining activities are concentrated. Source apportionment and chemical characterization of ambient particles have been reported at three coastal cities in that region. Kavouras et al. (Kavouras et al. 2001) found that at Iquique ($20^{\circ}12'\text{S}$, $70^{\circ}10'\text{W}$) marine aerosol contributes 40% of PM_{10} mass, but only 4.5% of $\text{PM}_{2.5}$ fraction; soil dust was a significant contribution there with 14% of PM_{10} mass but it was not found in the fine fraction. Fiebig-Wittmaack et al. (Fiebig-Wittmaack et al. 2006) found that at La Serena ($29^{\circ}54'\text{S}$, $71^{\circ}15'\text{W}$) sea salt contributes 40 to 50% of the coarse particles, depending on season of the year, and that concentration decreases as the measurement site moves inland, being 10 times lower at 60 km off the coast. Jorquera (Hector Jorquera 2009) found at Tocopilla ($22^{\circ}05'\text{S}$, $70^{\circ}12'\text{W}$) that 50% of $\text{PM}_{2.5}$ is from sulfates originated from coal-fired thermal power plant emissions, and that marine aerosol and soil dust accounted for 35% and 15% of PM_{10} , respectively, in agreement with the results of Kavouras et al. (Kavouras et al. 2001) obtained at Iquique.

The subject of the present analysis is an industrial area that has not been studied before. This industrial zone - with a cement manufacturing facility, a copper smelter, an area of minerals stockpiles and a $\text{Li}_2\text{CO}_3/\text{KCl}$ brine extraction plant among other sources - is located SE from Antofagasta (23.63°S , 70.39°W , population: 360,000 inhabitants in 2009) on the west side of a coastal range — see Figure 2. The landscape is a desert that includes northern Chile and most of southwestern Perú — from 5°S to 30°S ; in both countries mining activities have been on the rise in the last two decades, leading the economic growth in those countries.

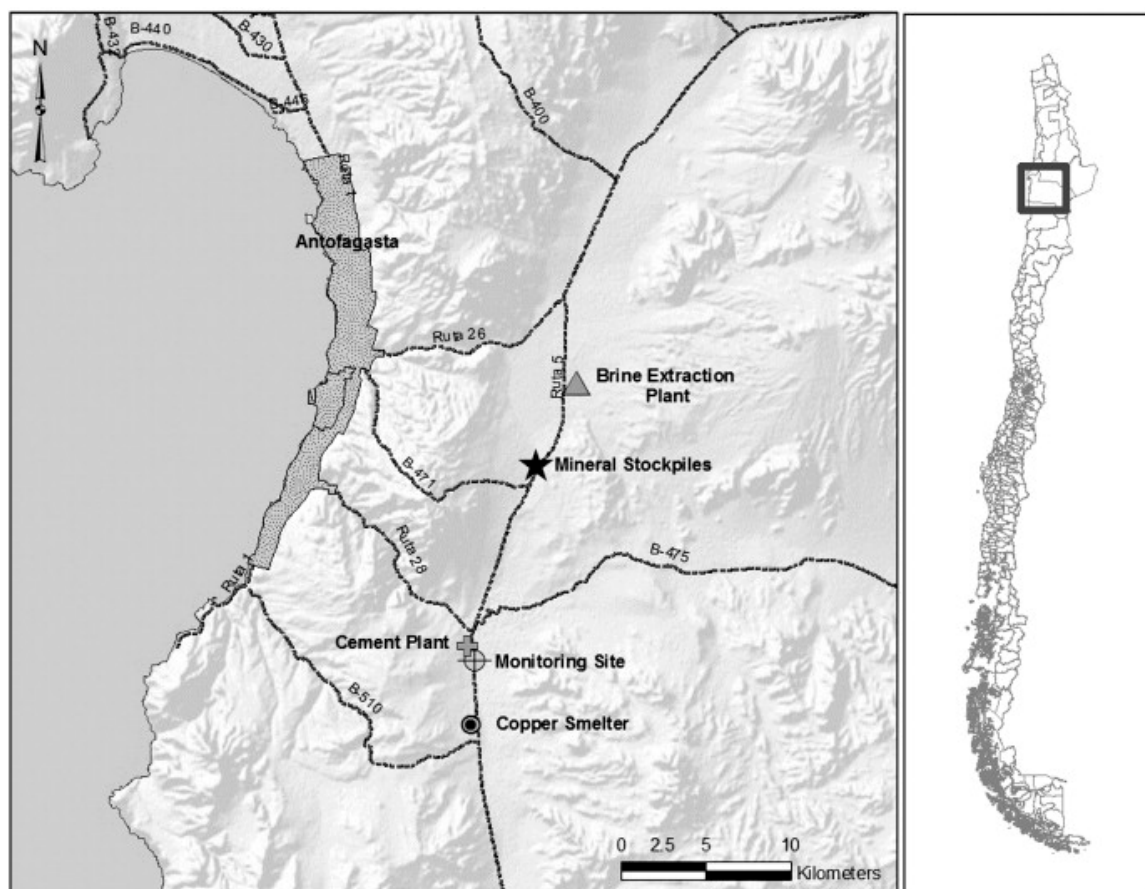


Figure 2 Location of the ambient monitoring site and the main sources surrounding it.

In this study region local meteorological variables have low seasonality — see Figure 3 — for a long term record at Antofagasta's airport. There is a permanent stratus cloud deck which is distinctive of the South American west coast (Xu, Xie, and Wang 2005; Mansbach and Norris 2007; Sun et al. 2010).

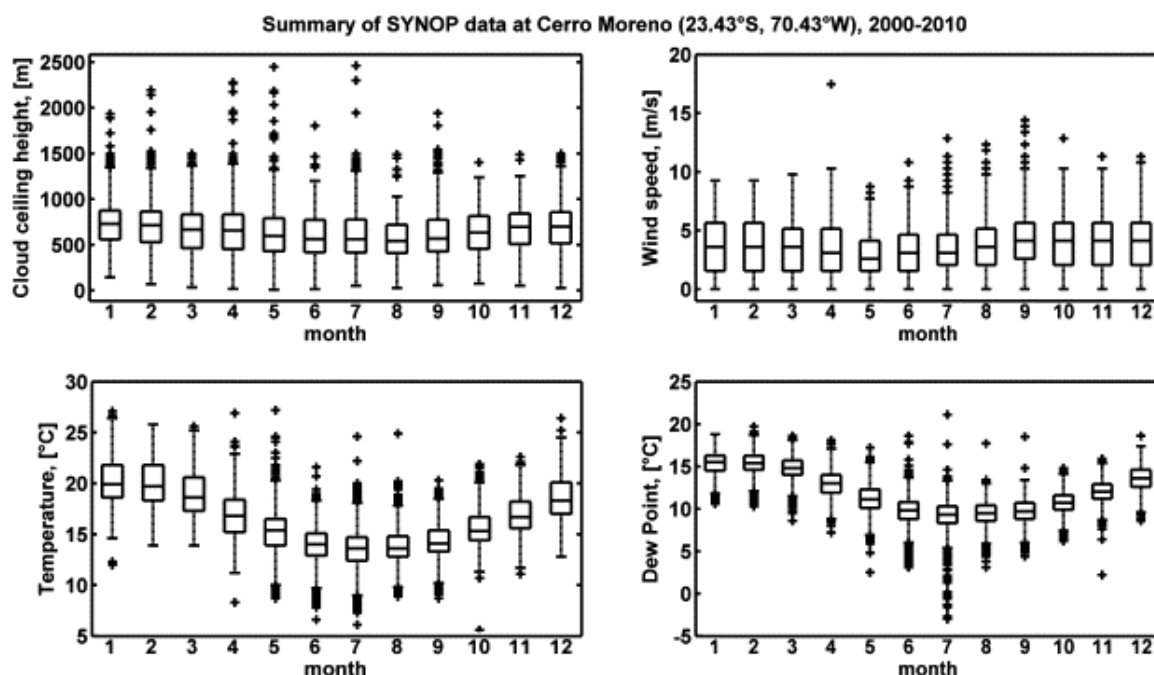


Figure 3 Annual box plots of surface meteorological variables measured at Cerro Moreno Airport (23°26'S, 70°26'W), 20 km NNW of Antofagasta, for the years 2000–2010.

A small seasonality is present in ambient daily PM_{10} concentrations measured at the industrial site every third day with high volume samplers (SINCA 2012) — see Figure 4. Annual PM_{10} concentrations exceed the ambient standard of $50 \mu\text{g}/\text{m}^3$ and in all years, $\sim 25\%$ of measured days exceed the ambient standard of $150 \mu\text{g}/\text{m}^3$. The small seasonality in ambient PM_{10} implies that a short term campaign can capture major features of PM_{10} and $\text{PM}_{2.5}$ in that region.

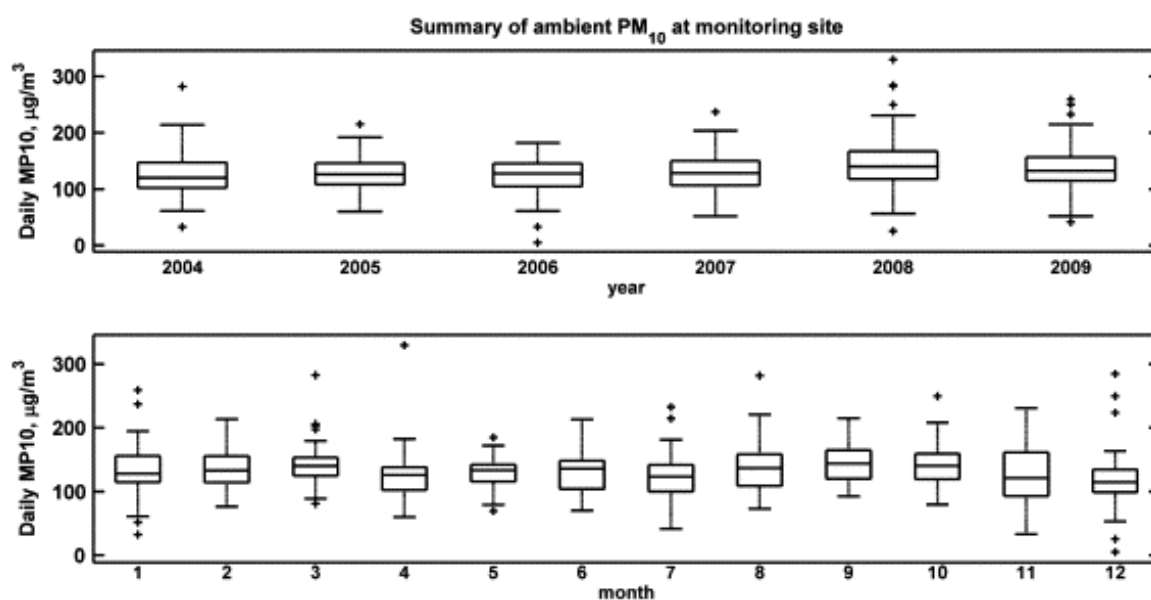


Figure 4 Box plots of daily PM₁₀ concentrations measured using Hi-volume samplers. Top panel: by year; lower panel: by month. Period: January 2004 through December 2009.

At the industrial site, top hourly wind speed values exceed 5 m/s every day so wind gusts may be even larger thus contributing to wind erosion — see Figure 5 for data collected during the measurement campaign. Wind erosion is ubiquitous in desert landscapes and this PM emission is difficult to estimate. Remote sensing of dust plumes is hampered by the permanent cloudiness on this coastal region. Furthermore, even under clear sky conditions, small plumes of diffuse sources are not detected by remote sensing yet they may have a substantial contribution to total dust concentrations for they cover larger areas than stronger dust sources do (Okin et al. 2011). Therefore, source-oriented dispersion models — or inverse modeling using satellite retrievals — may not estimate the total amount of naturally suspended dust in arid regions like the one analyzed herein.

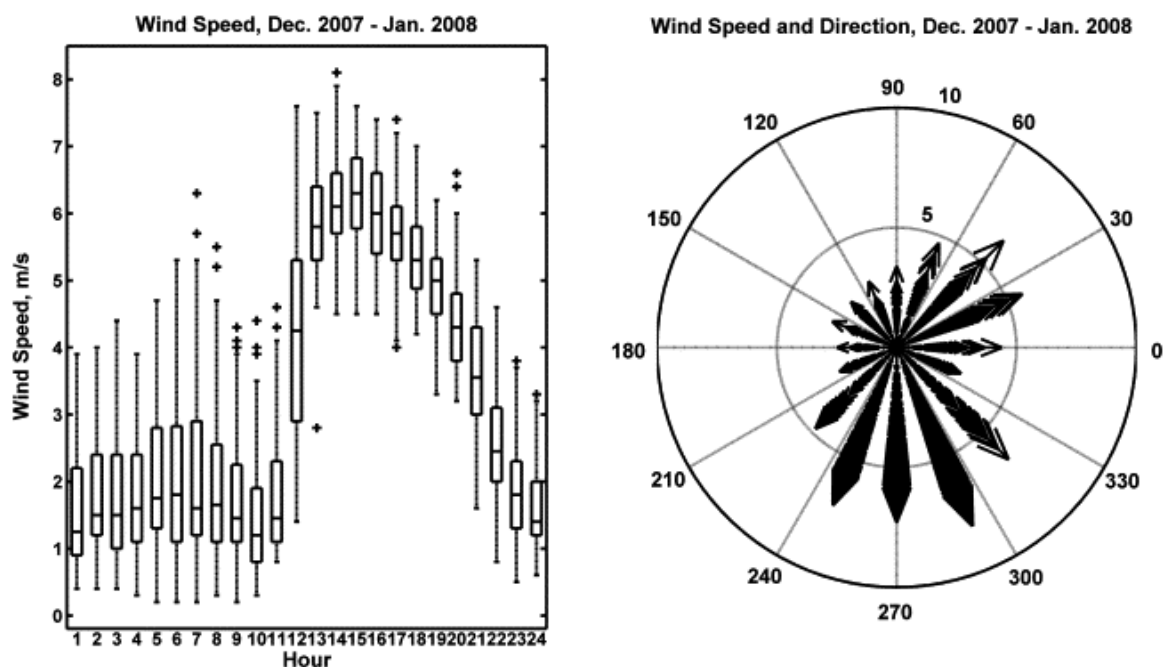


Figure 5 Summary of wind measurements during the ambient monitoring campaign. Left panel: diurnal boxplot of wind speed. Right panel: compass plot of wind speed and direction.

In this work we report results of a short term ambient monitoring campaign of PM_{10} and $PM_{2.5}$, followed by chemical analysis for trace elements and some ions and thermal determination of organic (OC) and elemental carbon (EC). The resulting database was analyzed using EPA's PMF3 receptor model (EPA— US Environmental Protection Agency) to identify and quantify major sources contributing to ambient PM concentrations. The following sections of this paper present a description of the ambient monitoring campaign, the receptor modeling approach, the results of the analysis, a discussion and a closing section with conclusions.

2.5. Methodology

2.5.1. Sampling and analytical techniques

The campaign was carried out between December 17th, 2007 and January 20th 2008 – see Figure 2 for the location of the monitoring site. Since on Sunday December 23rd a sampling was lost, a make-up sample was taken on January 27th, also a Sunday. A total of 35 daily samples of PM₁₀ and PM_{2.5} were taken using low volume Harvard Impactors (Air Diagnostics and Engineering, Inc. Naples, Maine, USA) operating at a constant air flow of 10 L/min; Teflon filters (2 and 3 µm pore size, Gelman Scientific, Ann Arbor, MI, USA) were used to collect both PM size fractions; the Teflon filters were analyzed for elemental composition using X ray fluorescence, for NO₃⁻ and SO₄⁻ in PM_{2.5} using ionic chromatography and for Na⁺ and K⁺ in PM₁₀ using atomic absorption. In addition, quartz fiber filters (#2500 QAT-UP, Gelman Scientific, Ann Arbor, MI, USA) were used for co-located samples of PM_{2.5} that were analyzed with a DRI Model 2001 Thermal Optical Analyzer (Atmoslytic Inc., Calabasas, CA, USA) to measure elemental (EC) and organic (OC) carbon; field blank filters were also included in the sampling protocol. All chemical analysis were performed at the Desert Research Institute, Reno, NV, USA. For more details see Jorquera (Hector Jorquera 2009).

2.5.2. Receptor modeling analysis for particulate matter

Receptor models attempt to identify and quantify sources that contribute to ambient PM concentrations at a given monitoring (receptor) site. Required data are the concentrations of n chemical species measured in m PM samples. Models explain the observed species concentrations as a sum of p source contributions (P. Hopke 2005).

$$X_{ij} = \sum_{k=1}^p g_{ik} f_{kj} + e_{ij}$$

Equation 1

In the above equation X_{ij} is the j -th species mass measured in the i -th PM sample, g_{ik} is the PM mass concentration from the k -th source contributing to the i -th PM sample, f_{kj} is the j -th species mass fraction from the k -th source, e_{ij} is a model residual and p is the total number of resolved sources. It is assumed that source profiles $\{f_{kj}\}$ are constant during the sampling period. Usually five to six sources are identified using this methodology and receptor models require a substantial amount of data points to achieve a robust source apportionment — see Pant and Harrison (Pant and Harrison 2012) for a recent review.

We use in this work the software Positive Matrix Factorization (PMF, version 3.0), available from U.S. EPA (U.S. Environmental Protection Agency 2012b); this software minimizes the weighted sum of squares.

$$Q = \sum_{i=1}^n \sum_{j=1}^m \left[\left(X_{ij} - \sum_{k=1}^p g_{ik} f_{kj} \right) / \sigma_{ij} \right]^2$$

Equation 2

Where σ_{ij} is the estimated uncertainty in the j -th species i -th PM sample. For a properly assigned set of uncertainties the optimal Q should approach the theoretical degrees of freedom for factor analysis: $n \cdot m - p \cdot (m+n)$. Minimization of Equation 2 is carried out using a Huber residual weighting so that results are robust to data outliers (Paatero 1997; Paatero 1999; Reff, Eberly, and Bhave 2007).

The procedure of Polissar et al. (Polissar, Hopke, Malm, et al. 1998) was used to assign input data uncertainties in PMF3.0 — see also Reff et al. (Reff, Eberly, and Bhave 2007). Data uncertainties (σ_{ij} in Equation 2) were computed as Equation 3

$$\sigma_{ij} = \begin{cases} s_{ij} + \frac{DL}{3}, & \text{if } X_{ij} > DL \\ \frac{5DL}{6}, & \text{if } X_{ij} \leq DL \end{cases}$$

Equation 3

Where s_{ij} is the laboratory analytical uncertainty for X_{ij} and DL is the detection limit value - estimated as three times the standard deviation of filter blank values. X_{ij} values below the detection limit (if any) were replaced by half of the DL value. We do not have missing values in the data sets analyzed.

Paatero et al. (Paatero, P Hopke et al. 2005) have shown how to graphically explore the range of potential solutions of Equation 2 varying a parameter named F_{peak} : positive values force most elements to lie on few source profiles, while negative values mean that most source profiles are mixed thus they do not stand for “pure sources”. They suggest varying F_{peak} until correlation among paired source contributions $\{g_{ik}, g_{il}\}$ is minimized; this condition is graphically confirmed when several $\{g_{ik}, g_{il}\}$ points lay on either axis — the so called ‘edge points’ — and this means that k-th or l-th source is not contributing to PM mass on those data points; we follow that approach here.

2.6. Results and discussion

2.6.1. Mass concentration and chemical composition

For this campaign mean daily (24 h) concentrations of PM_{10} and $\text{PM}_{2.5}$ were 161 and 42 $\mu\text{g}/\text{m}^3$, respectively. The highest daily values were 331 $\mu\text{g}/\text{m}^3$ for PM_{10} and 108 $\mu\text{g}/\text{m}^3$ for $\text{PM}_{2.5}$; both happened the same day, December 29th 2007; the lowest measured values were 80 $\mu\text{g}/\text{m}^3$ for PM_{10} and 21 $\mu\text{g}/\text{m}^3$ for $\text{PM}_{2.5}$. Table 1 shows results for PM_{10} elemental concentrations measured with XRF — Na^+ and K^+ were measured by atomic absorption. The listed elements are the ones that had at most two values below the detection limit (DL) reported by the laboratory. The rightmost column in Table 1 has the DL value reported by the laboratory followed by the number of values below the DL, if any, between brackets. The species with the highest concentration is calcium, coming from the cement facility nearby — see Figure 6 — and from suspended soil dust. Other species with high concentrations are silicon, sodium, iron, potassium and aluminum. Silicon and aluminum may come from cement manufacturing or suspended soil dust emissions. Potassium can be released from suspended soil dust and from specific processes such as the $\text{Li}_2\text{CO}_3/\text{KCl}$ brine extraction plant located NNW of the monitoring site. Finally, sodium is assumed to come from marine aerosol reaching the monitoring site — see discussion below on wind trajectory analysis.

Table 1 Summary of chemical composition of ambient PM_{10} , in $\mu\text{g}/\text{m}^3$.

| Species | Stand. dev. | Minimum | Mean | Median | Maximum | DL (# <) |
|-----------------|-------------|---------|-------|--------|---------|-----------|
| Na ⁺ | 1.153 | 1.703 | 4.359 | 4.181 | 6.579 | 0.066 |
| Al | 0.363 | 0.995 | 1.602 | 1.637 | 2.231 | 0.014 |
| Si | 0.808 | 2.100 | 3.662 | 3.761 | 4.916 | 0.027 |
| P | 0.074 | 0.045 | 0.180 | 0.176 | 0.404 | 0.002 |
| S | 2.078 | 1.516 | 5.377 | 5.263 | 11.674 | 0.036 |
| Cl | 0.590 | 0.642 | 1.885 | 1.759 | 3.090 | 0.007 |
| K | 0.535 | 1.054 | 1.946 | 1.875 | 3.360 | 0.005 |
| K ⁺ | 0.782 | 1.056 | 2.385 | 2.296 | 4.724 | 0.022 |
| Ca | 9.305 | 15.78 | 28.97 | 27.59 | 57.13 | 0.060 |
| Ti | 0.035 | 0.075 | 0.138 | 0.137 | 0.226 | 0.001 |
| V | 0.004 | 0.005 | 0.014 | 0.014 | 0.025 | 0.0001 |
| Cr | 0.001 | 0.000 | 0.004 | 0.004 | 0.007 | 0.001(1) |
| Mn | 0.015 | 0.026 | 0.049 | 0.047 | 0.087 | 0.001 |
| Fe | 0.556 | 1.012 | 2.097 | 2.108 | 3.282 | 0.006 |
| Ni | 0.002 | 0.000 | 0.003 | 0.003 | 0.007 | 0.0003(2) |
| Cu | 0.586 | 0.033 | 0.582 | 0.320 | 2.409 | 0.002 |
| Zn | 0.047 | 0.037 | 0.093 | 0.083 | 0.236 | 0.001 |
| As | 0.119 | 0.000 | 0.076 | 0.048 | 0.722 | 0.0002(1) |
| Br | 0.005 | 0.006 | 0.014 | 0.013 | 0.026 | 0.001 |
| Rb | 0.004 | 0.005 | 0.011 | 0.010 | 0.025 | 0.001 |
| Sr | 0.013 | 0.017 | 0.038 | 0.037 | 0.068 | 0.001 |
| Zr | 0.003 | 0.001 | 0.007 | 0.007 | 0.014 | 0.002(2) |
| Pb | 0.010 | 0.005 | 0.021 | 0.020 | 0.051 | 0.002 |

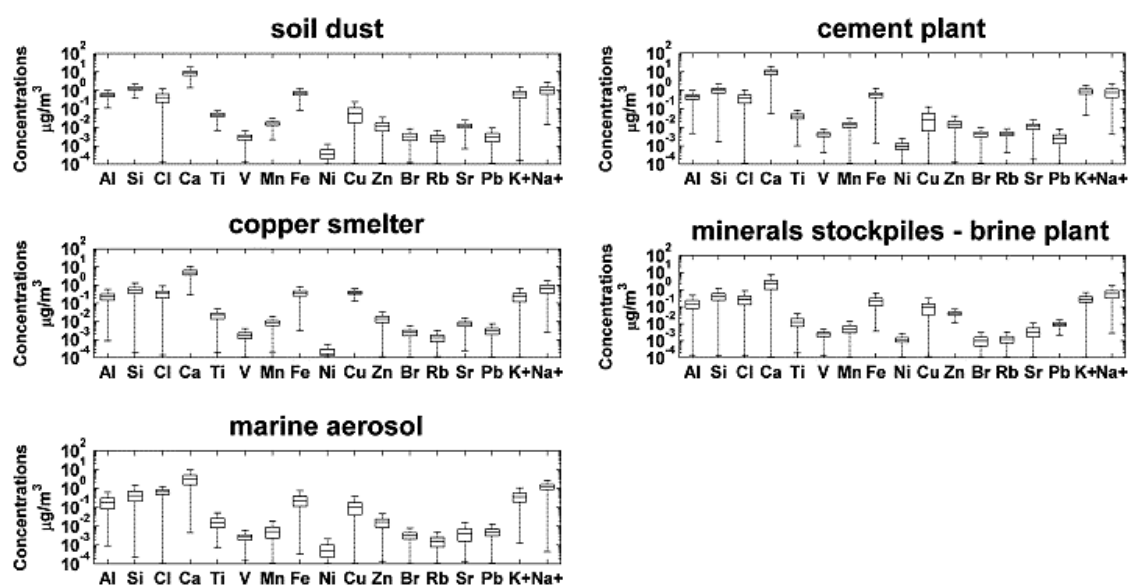
**Figure 6** Source profile concentrations $[\mu\text{g}/\text{m}^3]$ for the five factor solution for ambient PM_{10} (Fpeak=0).

Table 2 shows a summary of species concentrations measured in the PM_{2.5} fraction, using the same format as in Table 1. Species with higher concentrations are sulfates, calcium, organic and elemental carbon. Sulfates may come from primary emissions from cement kiln and copper smelter but may also be generated by the SO_x emissions from those sources through fast oxidation under favorable environmental conditions (see Figure 7); calcium may come from the cement facility and suspended soil, and organic carbon and elemental carbon are tracers of combustion sources. Hence those four dominant species are all anthropogenic and the likely sources emitting them are the same ones already described for the PM₁₀.

Table 2 Summary of chemical composition of ambient PM_{2.5}, in µg/m³.

| Species | Stand. dev. | Minimum | Median | Mean | Maximum | DL (# <) |
|-------------------------------|-------------|---------|--------|--------|---------|-----------|
| Al | 0.117 | 0.087 | 0.216 | 0.224 | 0.722 | 0.006 |
| Si | 0.273 | 0.211 | 0.556 | 0.583 | 1.665 | 0.009 |
| P | 0.043 | 0.062 | 0.120 | 0.128 | 0.209 | 0.002 |
| S | 1.124 | 1.763 | 3.031 | 3.389 | 5.497 | 0.014 |
| Cl | 0.111 | 0.071 | 0.208 | 0.220 | 0.554 | 0.002 |
| K | 0.312 | 0.194 | 0.560 | 0.613 | 1.534 | 0.002 |
| Ca | 2.659 | 1.407 | 3.395 | 3.907 | 16.292 | 0.009 |
| Ti | 0.012 | 0.009 | 0.020 | 0.022 | 0.068 | 0.001 |
| V | 0.003 | 0.003 | 0.006 | 0.007 | 0.013 | 0.0001 |
| Mn | 0.004 | 0.002 | 0.009 | 0.010 | 0.025 | 0.0014 |
| Fe | 0.173 | 0.151 | 0.332 | 0.354 | 1.036 | 0.0025 |
| Ni | 0.001 | 0.000 | 0.002 | 0.002 | 0.007 | 0.0003(2) |
| Cu | 0.043 | 0.017 | 0.058 | 0.068 | 0.212 | 0.0007 |
| Zn | 0.041 | 0.019 | 0.046 | 0.060 | 0.200 | 0.0007 |
| As | 0.080 | 0.003 | 0.029 | 0.050 | 0.476 | 0.0002 |
| Br | 0.001 | 0.002 | 0.004 | 0.004 | 0.007 | 0.0010 |
| Rb | 0.002 | 0.0005 | 0.003 | 0.004 | 0.010 | 0.0007(1) |
| Sr | 0.004 | 0.002 | 0.006 | 0.007 | 0.019 | 0.0013 |
| Pb | 0.009 | 0.004 | 0.012 | 0.014 | 0.049 | 0.0018 |
| NO ₃ ⁻ | 0.130 | 0.145 | 0.331 | 0.350 | 0.683 | 0.020 |
| SO ₄ ⁻² | 4.129 | 6.026 | 10.645 | 11.871 | 21.776 | 0.194 |
| OC | 0.766 | 1.552 | 2.494 | 2.645 | 5.314 | 0.228 |
| EC | 0.440 | 0.304 | 1.007 | 1.084 | 2.145 | 0.152 |
| TC | 1.005 | 1.856 | 3.676 | 3.728 | 5.777 | 0.253 |

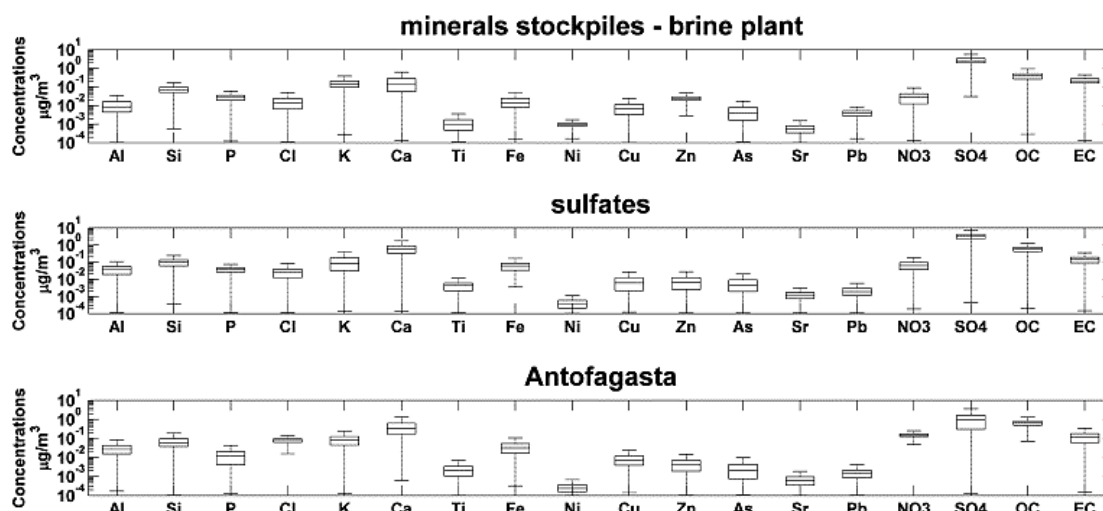


Figure 7 Source profile concentrations [$\mu\text{g}/\text{m}^3$] for the six factor solution for ambient $\text{PM}_{2.5}$ ($F_{\text{peak}} = -0.05$), factors 1–3.

2.6.2. Source apportionment for the PM_{10} fraction

Following the recommendations given in PMF3.0 User Guide (U.S. Environmental Protection Agency 2012b) and in the technical literature (Reff, Eberly, and Bhave 2007), we have run the receptor model for $p = 3, 4$, and 5 factors including an additional, proportional model error originated from deviations from receptor model assumptions: source profile variability, potential sample contamination, etc. This additional model error was varied between 5 and 25% until the theoretical, a priori Q value $-n \cdot m - p \cdot (m+n)$ was close to the *numerical* Q value out of the minimization of Equation 2; this was achieved for an extra model uncertainty of 10%. Then we have applied Multiple Linear Regression (MLR) to the PM_{10} mass concentrations using the p source contributions as independent variables and checked whether MLR coefficients were positive and statistically significant ($p \leq 0.05$).

We have found that a five factor solution explains well measured PM_{10} concentrations. Elements fitted by PMF3.0 are: Al, Si, Cl, Ca, Ti, V, Mn, Fe, Ni, Cu, Zn, Br, Rb, Sr, Pb, Na^+ and K^+ ; all elements have regression coefficients (R^2) greater than 0.80, except two: V (0.73) and Ni (0.78). Kolmogorov–Smirnov test results support a Gaussian error distribution in model residues of all fitted species; all standardized residuals

were lower than 3.0 except two: V (3.02) and Ni (-3.31). It was not possible to extract more sources out of this data set, as diagnosed by negative regression coefficients in the MLR of PM_{10} mass when six sources were chosen in PMF3.0.

Sensitivity analysis of this five-factor solution were performed by applying the *Fpeak* parameter as described in the Methodology section (section 2.4). However we have found that the base simulation ($Fpeak = 0$) produced more plausible results.

Table 3 shows source profiles, in $\mu\text{g}/\text{m}^3$, and ratio of modeled to observed species concentrations for fitted species. All ratios are above 0.97 except Ni (0.83) showing a good model representation of elemental concentrations in ambient PM_{10} samples; Figure 6 shows the variability in source profiles, computed using 1000 bootstrap runs. These results are discussed next.

Table 3 Source profiles for the five factor solution for PM_{10} fraction in $\mu\text{g}/\text{m}^3$ ($F_{\text{peak}}=0$).

| Species | Soil dust | Cement plant | Copper smelter | Mineral stockpiles | Marine aerosol | Modeled conc. | Observed conc. | Ratio M/O |
|-----------------|-----------|--------------|----------------|--------------------|----------------|---------------|----------------|-----------|
| Al | 0.6771 | 0.5355 | 0.1676 | 0.1926 | 0.0285 | 1.6012 | 1.6020 | 0.999 |
| Si | 1.5782 | 1.1685 | 0.3654 | 0.5130 | 0.0200 | 3.6450 | 3.6620 | 0.995 |
| Cl | 0.4530 | 0.4708 | 0.0031 | 0.2402 | 0.7000 | 1.8671 | 1.8850 | 0.990 |
| Ca | 10.3130 | 11.0410 | 4.1303 | 2.3434 | 0.7141 | 28.5418 | 28.9700 | 0.985 |
| Ti | 0.0551 | 0.0477 | 0.0153 | 0.0160 | 0.0031 | 0.1374 | 0.1380 | 0.995 |
| V | 0.0032 | 0.0049 | 0.0008 | 0.0026 | 0.0022 | 0.0135 | 0.0140 | 0.967 |
| Mn | 0.0190 | 0.0158 | 0.0069 | 0.0064 | 0.0004 | 0.0484 | 0.0490 | 0.988 |
| Fe | 0.8399 | 0.6652 | 0.2938 | 0.2612 | 0.0250 | 2.0850 | 2.0970 | 0.994 |
| Ni | 0.0000 | 0.0011 | 0.0000 | 0.0013 | 0.0001 | 0.0025 | 0.0030 | 0.831 |
| Cu | 0.0703 | 0.0021 | 0.3372 | 0.0387 | 0.1330 | 0.5813 | 0.5820 | 0.999 |
| Zn | 0.0099 | 0.0182 | 0.0120 | 0.0471 | 0.0048 | 0.0920 | 0.0930 | 0.989 |
| Br | 0.0035 | 0.0054 | 0.0011 | 0.0003 | 0.0034 | 0.0138 | 0.0140 | 0.989 |
| Rb | 0.0022 | 0.0055 | 0.0010 | 0.0012 | 0.0008 | 0.0107 | 0.0110 | 0.974 |
| Sr | 0.0149 | 0.0123 | 0.0060 | 0.0039 | 0.0000 | 0.0371 | 0.0380 | 0.978 |
| Pb | 0.0028 | 0.0023 | 0.0010 | 0.0107 | 0.0040 | 0.0207 | 0.0210 | 0.986 |
| K ⁺ | 0.5516 | 1.1236 | 0.1503 | 0.2933 | 0.1995 | 2.3183 | 2.3850 | 0.972 |
| Na ⁺ | 1.3220 | 1.0732 | 0.0801 | 0.5597 | 1.2928 | 4.3278 | 4.3590 | 0.993 |

The first source has more than 40% of the Al, Si, Ti, Mn, Fe and Sr measured; its K/Fe ratio is 0.66 so it corresponds to soil dust whose ratio is 0.6 ± 0.2 (Malm et al. 1994). The source profile shows a very stable composition of crustal elements; there is also chloride and sodium in this profile likely coming from marine aerosol deposition. The second source is identified as the cement manufacturing facility. It has the highest Ca concentration and bootstrap results for this profile shows narrow distributions for Ca, Al, Si, and Fe, all major components of cement; hence this stable source profile corresponds to the cement manufacturing facility which includes cement kiln and fugitive emissions from cement storing, handling and shipping.

The third source has 58% of Cu, with a distinctively narrow concentration range so we identify it as the PM_{10} emission from the copper smelter, located ~3.7 km south of the monitoring site. The presence of crustal elements in this profile is an evidence of mixing of suspended soil dust emissions with the smelter plume in route to the monitoring site as shown by inspection of wind trajectories — see section below (section 2.6). Crustal element compositions also have a narrow concentration distribution but their average values are 2.5—4.3 times lower than in the soil dust profile.

The fourth source is identified with fugitive PM_{10} emissions from sulfide mineral stockpiles and from the brine plant. This source has ~51% of Zn, 53% of Ni and 52% of Pb, all tracers of sulfide ores (Fernández-Caliani et al. 2009) and that have stable concentrations in the source profile; the profile contains 13% of soluble potassium — a tracer of brine plant emissions — and also crustal elements but with lower concentrations than in the soil dust profile. The fifth source has 37.5% of Cl, 25% of Br and 30% of Na measured — all with narrow composition ranges distinctive of a stable source profile — so this is the marine aerosol. Crustal elements in this source profile have a broader composition distribution than in other source profiles and their average concentrations are 14 to 79 times lower than in the soil dust profile, showing a good source discrimination obtained by PMF3.0. Wind trajectory analysis confirms that this source is the marine aerosol and it may arrive to the monitoring site from different directions — see Discussion section below.

Table 5 shows results of the MLR of ambient concentrations of PM_{10} against source contributions; since the intercept is not statistically significant ($p = 0.062$), a MLR with a zero intercept was computed. The relative contributions to ambient PM_{10} and their standard deviations are: cement plant, $38.2 \pm 1.5\%$; soil dust, $31.2 \pm 2.3\%$; mineral stockpiles and brine plant, $12.7 \pm 1.7\%$; copper smelter, $11.5 \pm 1.6\%$ and marine aerosol, $6.5 \pm 2.4\%$. For this five factor solution a linear regression of modeled versus observed PM_{10} (not shown) explains 90% of the observed variance in ambient PM_{10} .

In the above analysis for PM_{10} sulfur was not considered because of its low R^2 value in model results when included as input to PMF3. As an ex post check we computed a MLR of sulfur concentrations using as independent variables the five $\{g_{ik}\}$ source contributions resolved with PMF3. The resulting sulfur apportionment equation is:

$$S = 0.56 + 0.94G_1 + 1.78G_2 - 0.01G_3 + 1.36G_4 + 0.73G_5.$$

Equation 4

This result shows that sulfur is apportioned to all sources but the copper smelter and in similar amounts $\sim 1 \mu\text{g}/\text{m}^3$, so its contribution to most source profiles is relevant; the above results in Equation 4 confirm the source identification already obtained for PM_{10} . Nonetheless, we do get a low R^2 in the above equation (0.39, adjusted value) so we chose not to include sulfur in the final model.

We now comment on our choice of soluble potassium — measured by ionic chromatography - in place of total potassium - as measured by XRF — in the receptor model analysis for PM_{10} . A reduced major axis regression applied to those paired data showed consistence among them ($R^2 = 0.88$) and both measurements produced nearly the same fitting R^2 values in PMF3: 0.97 for K^+ and 0.94 for K. A MLR of potassium concentrations against the five $\{g_{ik}\}$ source contributions produced results similar to the ones shown in Table 3 for K^+ . Hence model receptor results are equivalent for either choice of input measurements.

2.6.3. Source apportionment for the fine fraction (PM_{2.5})

PMF3.0 was run for $p = 4, 5$ and 6 factors, and we have found that a six factor solution describes well PM_{2.5} ambient concentrations; an extra modeling uncertainty of 11% produces a numerical Q value close to the theoretical one. The fitted species are: Al, Si, P, Cl, K, Ca, Ti, Fe, Ni, Cu, Zn, As, Sr, Pb, NO₃⁻, SO₄⁻², organic (OC) and elemental carbon (EC). Most fitted species had correlation coefficients higher than 0.84; the exceptions are OC (0.48) and EC (0.49) that were kept in the final solution for they are tracers that help identify sources. Kolmogorov–Smirnov test results support a Gaussian error distribution in model residues for all fitted species; only two standardized residues were higher than 3.0: K (3.39) and Zn (3.37).

For this data set sulfur and sulfate were highly correlated; a reduced major axis regression of these paired data has $R^2 = 0.96$. In Table 4 sulfates have a fitting $R^2 = 0.99$, slightly better than in the case of sulfur ($R^2 = 0.97$) obtained by MLR of sulfur concentrations against the six source contributions $\{g_{ik}\}$. Given this equivalence, we have chosen sulfates as input to PMF3 in the source apportionment of PM_{2.5}.

Table 4 Source profiles for the six factor solution for $PM_{2.5}$ in $\mu g/m^3$ ($F_{peak} = -0.05$).

| Species | Mineral stockpiles & brine plant | Sulfates | Antofagasta | Copper smelter | Soil dust | Cement plant | Modeled conc. | Observed conc. | Ratio M/O |
|------------|--|----------|-------------|-------------------|--------------|-----------------|------------------|-------------------|--------------|
| Al | 0.002 | 0.036 | 0.025 | 0.013 | 0.051 | 0.096 | 0.222 | 0.224 | 0.989 |
| Si | 0.053 | 0.079 | 0.061 | 0.037 | 0.118 | 0.212 | 0.559 | 0.583 | 0.959 |
| P | 0.029 | 0.039 | 0.014 | 0.009 | 0.003 | 0.034 | 0.127 | 0.128 | 0.992 |
| Cl | 0.009 | 0.010 | 0.077 | 0.008 | 0.060 | 0.052 | 0.217 | 0.22 | 0.986 |
| K | 0.128 | – | 0.077 | 0.053 | 0.084 | 0.252 | 0.594 | 0.613 | 0.970 |
| Ca | – | 0.440 | 0.270 | 0.177 | 1.193 | 1.715 | 3.795 | 3.907 | 0.971 |
| Ti | 0.000 | 0.004 | 0.002 | 0.001 | 0.005 | 0.009 | 0.021 | 0.022 | 0.970 |
| Fe | 0.007 | 0.058 | 0.032 | 0.022 | 0.095 | 0.138 | 0.351 | 0.354 | 0.991 |
| Ni | 0.001 | 0.000 | 0.000 | 0.000 | 0.000 | 0.000 | 0.002 | 0.002 | 0.943 |
| Cu | 0.006 | 0.004 | 0.009 | 0.016 | 0.032 | – | 0.067 | 0.068 | 0.992 |
| Zn | 0.024 | 0.002 | 0.005 | 0.010 | 0.008 | 0.007 | 0.057 | 0.06 | 0.946 |
| As | 0.002 | 0.003 | 0.003 | 0.036 | 0.006 | 0.000 | 0.050 | 0.05 | 0.993 |
| Sr | 0.000 | 0.001 | 0.000 | 0.000 | 0.002 | 0.002 | 0.007 | 0.007 | 0.979 |
| Pb | 0.004 | 0.002 | 0.002 | 0.003 | 0.003 | – | 0.014 | 0.014 | 0.988 |
| NO_3^- | 0.025 | 0.069 | 0.153 | 0.018 | 0.004 | 0.081 | 0.348 | 0.35 | 0.995 |
| $SO_4^{=}$ | 2.803 | 3.406 | 1.397 | 0.838 | 0.386 | 2.920 | 11.748 | 11.871 | 0.990 |
| OC | 0.461 | 0.606 | 0.712 | 0.074 | 0.248 | 0.414 | 2.515 | 2.645 | 0.951 |
| EC | 0.214 | 0.098 | 0.128 | 0.126 | 0.263 | 0.106 | 0.935 | 1.084 | 0.863 |

Sensitivity analysis of this six factor solution was performed by applying the *Fpeak* parameter. For this fine fraction we have found that the better source identification was achieved by using $F_{peak} = -0.05$, so this one is presented in this work Table 4 shows source profiles and ratio of modeled to observed concentration for fitted species. All ratios are between 0.94 and 1.0 — except for EC (0.86) — showing a good model representation of measured species concentrations in ambient $PM_{2.5}$ samples

Figure 7 and Figure 8 show the variability in source profiles, computed using 1000 bootstrap runs in PMF3.0. These results are discussed next.

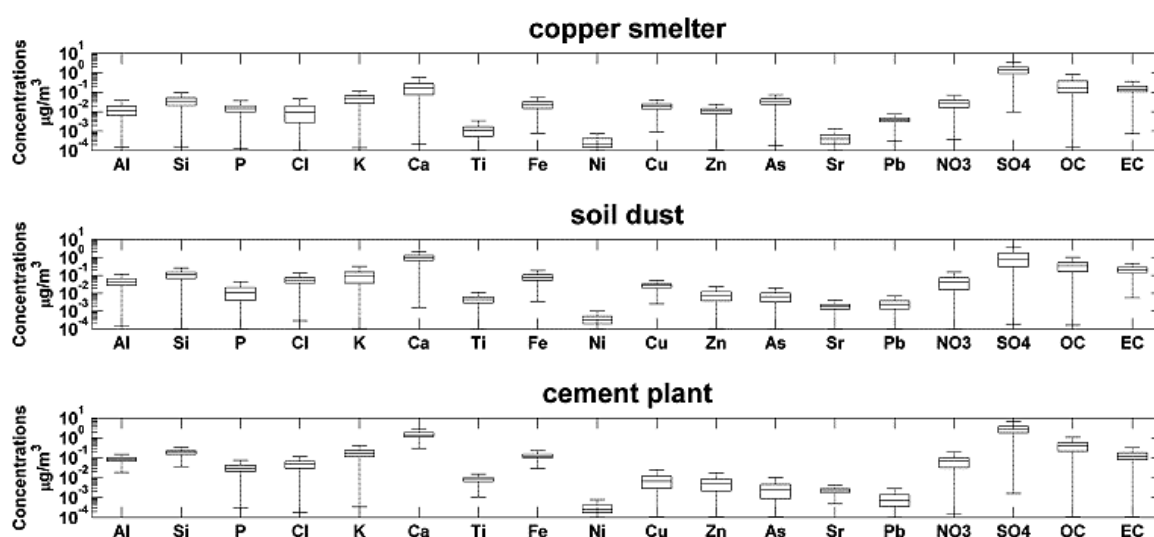


Figure 8 Source profile concentrations [$\mu\text{g}/\text{m}^3$] for the six factor solution for ambient $PM_{2.5}$ ($F_{peak} = -0.05$), factors 4–6.

The first source has more than 50% of Ni, 40% of Zn and 28% of Pb, all with narrow concentration range in the source profile so it corresponds to fugitive $PM_{2.5}$ from mineral stockpiles 12 km NNE of the monitoring site; this source also has 24% of sulfates, 23% of EC, 21% of potassium and 18% of OC showing enrichment with particle deposition from cement kiln, copper smelter and brine plant emissions as well. The second source has 29% of sulfates, 30% of P, 24% of OC and 10.5% of EC, all with narrow concentration ranges so it is a sulfate plume originated from copper smelter emissions. The ratio $S/P \sim 30$ in this profile is similar to values obtained for copper smelter contributions to ambient $PM_{2.5}$ at Santiago (Rojas et al. 1990; Héctor Jorquera and Barraza 2012).

The third source has the highest concentrations of chlorine, nitrate and OC which show a stable source profile hence it comes from combustion sources and it is a plume aged enough to have nitrates within; thus we identify it as the plume of Antofagasta moving inland; the anthropogenic origin is also supported by a ratio $K/Fe = 2.4$. This source includes emissions from vehicular traffic and shipping activities at Antofagasta; the presence of chlorine in this source profile is due to mixing of marine aerosol as air masses move from the coast towards the monitoring site. Nonetheless, secondary and carbonaceous aerosols dominate in this profile so we identify this source as the contribution to $PM_{2.5}$ from Antofagasta. Furthermore, this source is different from the marine aerosol source profile identified in the PM_{10} fraction that is dominated by sea salt (see Table 3).

The fourth source has more than 70% of As, and it has 24% of Cu and Pb and 18% of Zn, all tracers of primary copper smelter emissions (Hedberg, Gidhagen, and Johansson 2005) that have small composition variability in the source profile. The fifth source has crustal species such as Al, Si, K, Ca, Ti, Fe and Sr with small composition variability in the source profile; the ratio $K/Fe = 0.88$ supports that this source is the suspended soil dust; there is a clear enrichment of this source profile with Cl, K and Cu deposited on the ground and accumulated in this desert region. The sixth source has more than 45% of Ca; species such as Al, Si, Ca Fe, sulfates and OC have small composition variability in the source profile. Furthermore the ratios $Ca/Fe = 12.5$ and $Ca/SO_4^{-2} = 0.59$ are characteristic of cement kiln emissions (Watson et al. 2008) thus this is the cement plant source.

A MLR analysis was carried out with ambient $PM_{2.5}$ concentrations and source contributions from the six sources identified. Once again, the intercept was not significant ($p = 0.85$), so a MLR with zero intercept produced the source contributions shown in Table 5. The relative contributions to ambient $PM_{2.5}$ concentrations and their standard errors are: cement plant: $33.7 \pm 1.3\%$, soil dust: $22.4 \pm 1.6\%$, sulfates: $17.8 \pm 1.7\%$, mineral stockpiles and brine plant: $12.4 \pm 1.2\%$, Antofagasta: $8.5 \pm 1.3\%$ and copper smelter: $5.3 \pm 0.8\%$. For this six factor solution a linear regression of modeled versus observed $PM_{2.5}$ (not shown) explains 95% of the variance observed in ambient $PM_{2.5}$.

Table 5 *Summary of source apportionment results.*

| Source | MLR coefficient ($\mu\text{g}/\text{m}^3$) | Standard error ($\mu\text{g}/\text{m}^3$) |
|--|--|---|
| <i>PM₁₀</i> | | |
| Soil dust | 50.3 | 3.8 |
| Cement plant | 61.6 | 2.4 |
| Copper smelter | 18.5 | 2.5 |
| Mineral stockpiles & lithium/KCl plant | 20.4 | 2.7 |
| Marine aerosol | 10.4 | 3.9 |
| <i>PM_{2.5}</i> | | |
| Mineral stockpiles & lithium/KCl plant | 5.15 | 0.49 |
| Sulfates | 7.43 | 0.71 |
| Antofagasta | 3.53 | 0.56 |
| Copper smelter | 2.19 | 0.32 |
| Soil dust | 9.32 | 0.69 |
| Cement plant | 14.05 | 0.52 |

2.7. Discussion

Figure 9 shows time series plots of $PM_{2.5}$ and PM_{10} source contributions for the period of the measurement campaign. In some days the receptor model predicts negative contributions from one or two sources, but total model estimation is quite close to measured concentrations. On December 29th ambient PM_{10} reached a peak of $331 \mu\text{g}/\text{m}^3$ and the receptor model estimated a value of $280 \mu\text{g}/\text{m}^3$; for the $PM_{2.5}$ fraction the peak measured value was $108 \mu\text{g}/\text{m}^3$ and the model predicted $107 \mu\text{g}/\text{m}^3$.

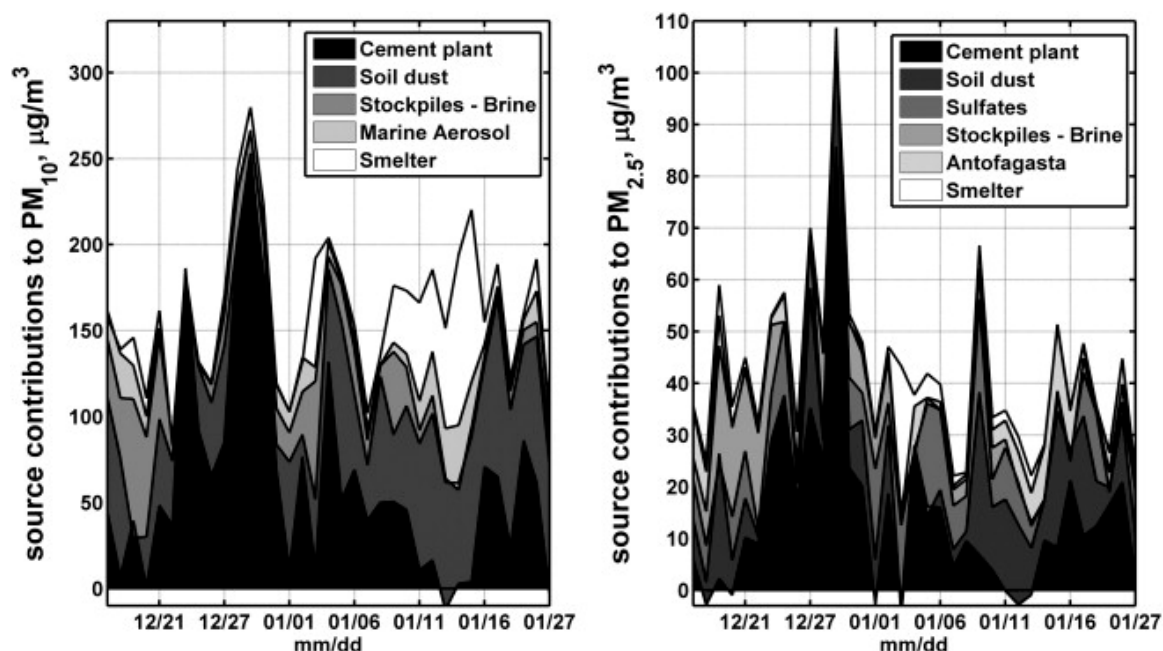


Figure 9 Time series plots of source contributions to PM_{10} and $PM_{2.5}$ concentrations, in $[\mu\text{g}/\text{m}^3]$.

In order to confirm source identification we have conducted an analysis of wind trajectories, using the Hybrid Single-Particle Lagrangian Integrated Trajectory (HYSPLIT) from the USA's National Oceanic and Atmospheric Administration, NOAA (Rolph 2012). We have constructed 24 h monitor-backward and source-forward trajectories to check receptor model results; the NCEP meteorological database has been chosen with an explicit modeling of the vertical wind velocity and initial trajectories have been set at 100 m above ground level. Using this methodology we have found that:

a) The highest soil dust contributions to PM_{10} and $PM_{2.5}$ happen when wind direction is S-SSW-SW and soil dust is mixed with marine aerosol and copper smelter emissions — see Figure 10 for January 15th.

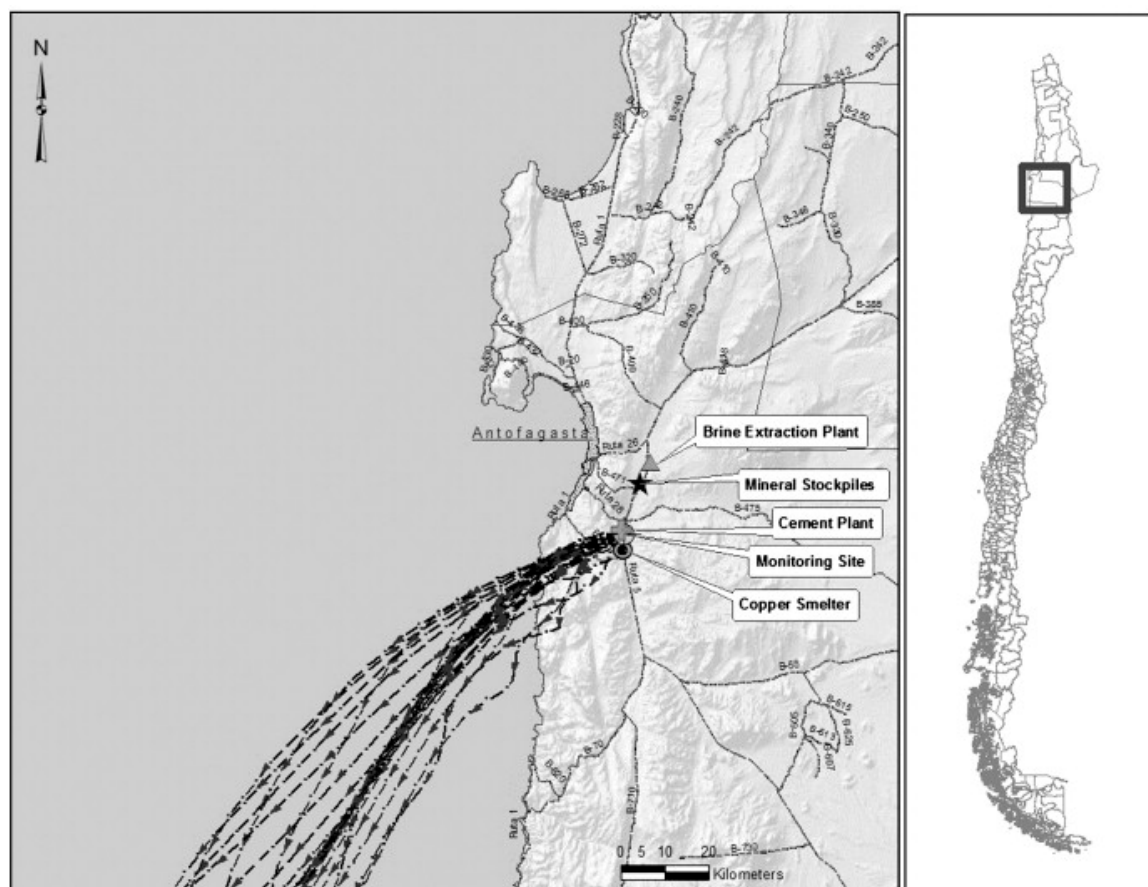


Figure 10 Backward trajectories arriving at the monitor site on January 15th, 2008.

b) When W–WNW winds enter Antofagasta's basin they move towards the monitoring site bringing in contributions from Antofagasta, soil dust and cement plant emissions — see Figure 11 for January 17th.

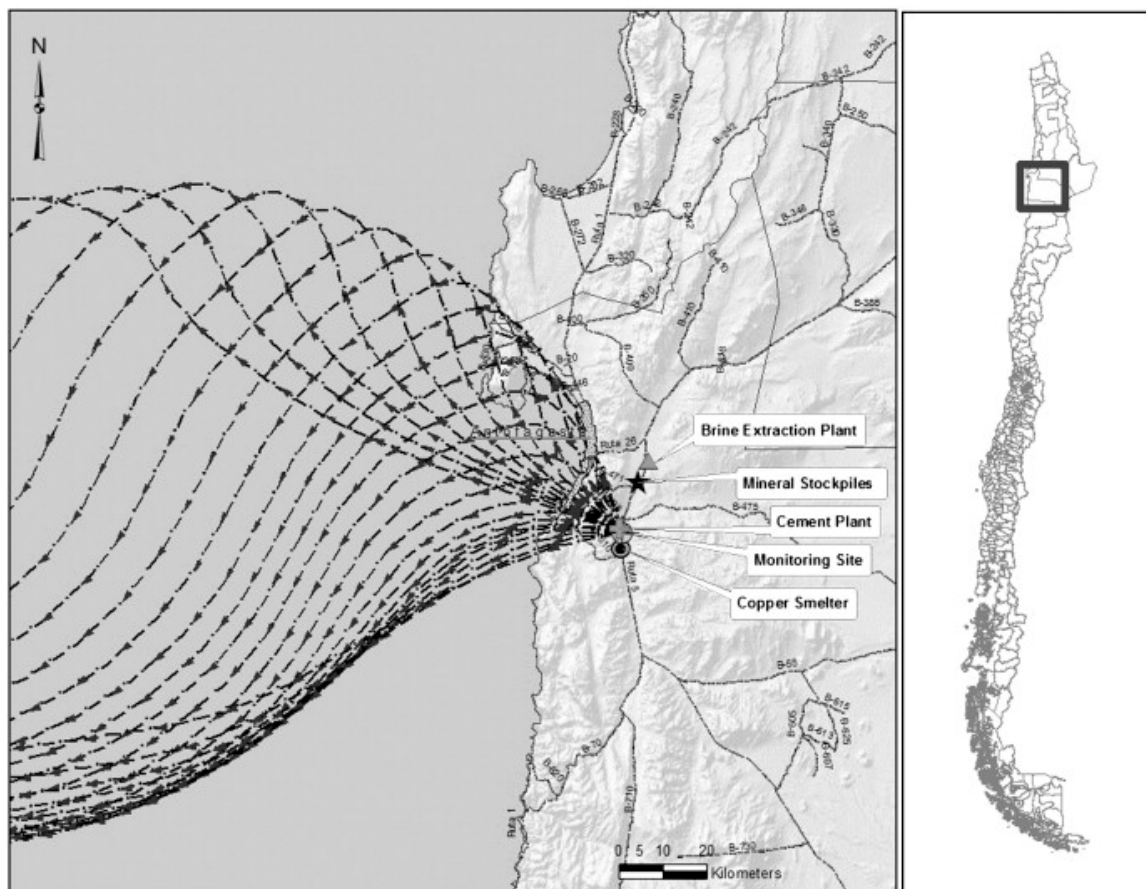


Figure 11 Backward trajectories arriving at the monitor site on January 17th, 2008.

c) When wind trajectories directly go from a source towards the monitor, the impacts of such source on measured values are the highest and this is consistent with the outcomes of the receptor modeling analysis for the very same day. For instance, this happens for the cement plant emissions in December 29th (Figure 12) when the highest values of PM_{10} and $PM_{2.5}$ were recorded, for the mineral stockpiles and brine plant emissions on December 19th — see Figure 13 — and for the copper smelter on January 3rd (Figure 14) when the highest values of As were recorded in both PM size fractions.

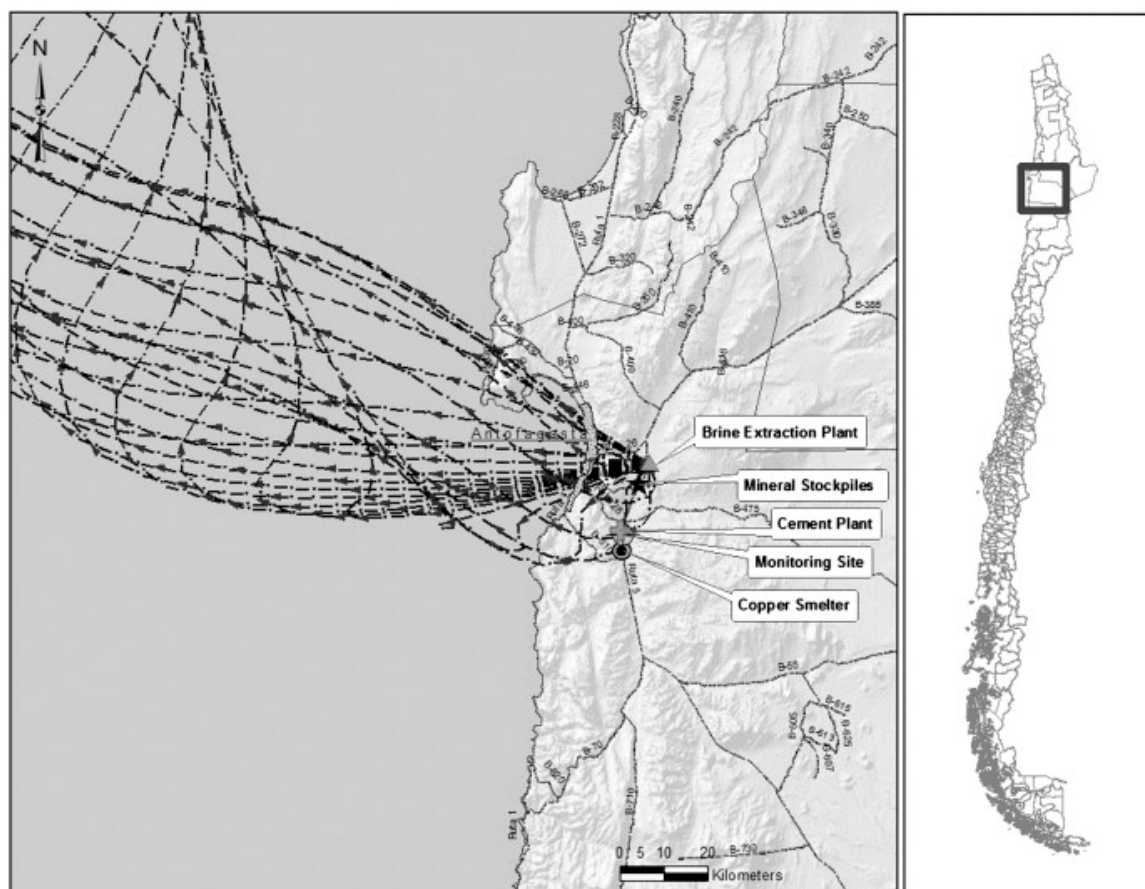


Figure 12 Forward wind trajectories departing from the cement plant on December 29th, 2007.

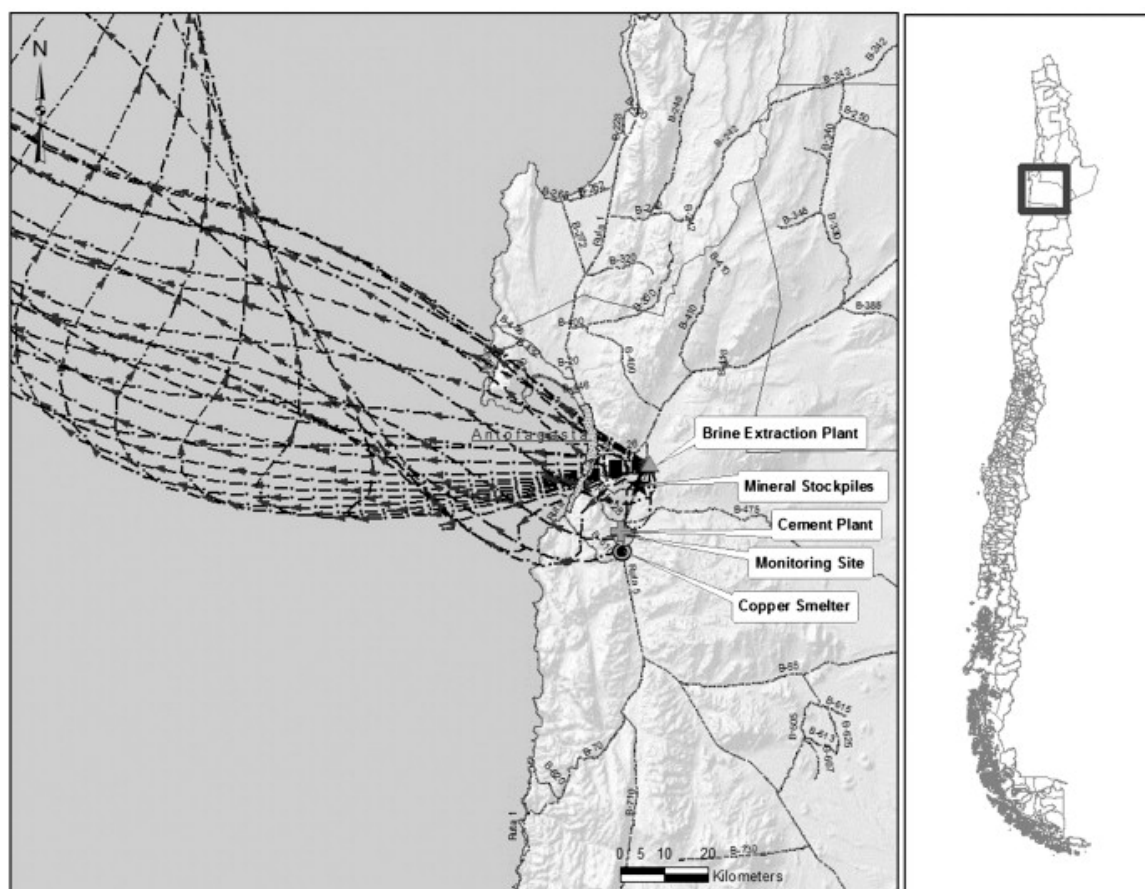


Figure 13 Forward wind trajectories departing from the brine plant on December 19th, 2007.

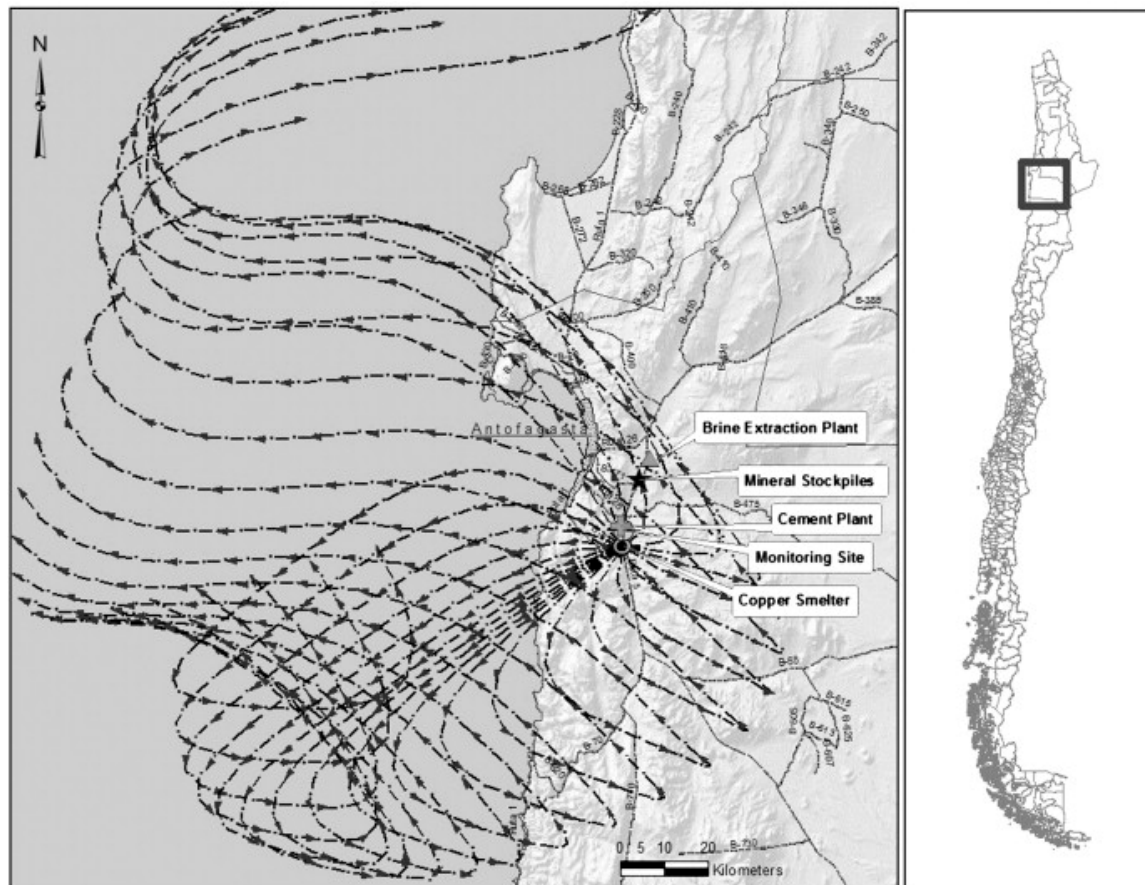


Figure 14 Forward wind trajectories departing from the copper smelter on January 3rd, 2008.

We acknowledge that wind trajectory analysis may not be accurate when terrain features like the coastal range are present. Hence we have checked the above analysis using the local wind measured at the monitoring site for the campaign period. We show in Figure 15 compass plots for December 19th and January 17th; it can be seen that in December 19th there were five hours when wind direction was between 30 and 60°, that is, from the location of the minerals stockpiles and the brine plant towards the monitoring site; likewise in January 17th there were nine hours with wind direction between 270 and 300° thus bringing contributions from Antofagasta and cement plant emissions to the monitoring site. Therefore, local wind data in Figure 15 are in agreement with the wind trajectories shown in Figure 11 and Figure 13.

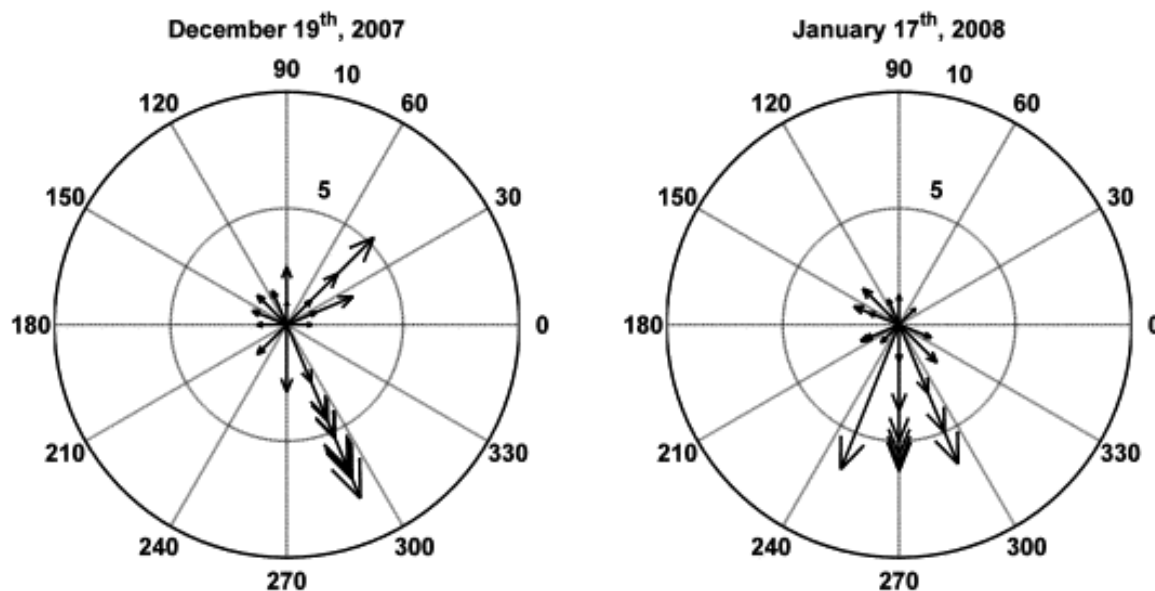


Figure 15 Compass plots of local wind data for December 19th, 2007 and January 17th, 2008.

Inspection of correlation coefficients among $\{g_{ik}\}$ source contributions to $PM_{2.5}$ shows that sulfate contributions are significantly correlated with the copper smelter and Antofagasta contributions ($p < 0.05$); there is a negative — but not statistically significant ($p = 0.14$) — correlation between sulfates and cement plant contributions. In addition, the ratio $S/P \sim 30$ in the sulfates source profile (Table 4) is similar to values obtained for copper smelters contributions to ambient $PM_{2.5}$ at Santiago (Rojas et al. 1990; Héctor Jorquera and Barraza 2012). Hence results suggest that sulfates in the $PM_{2.5}$ fraction come mostly from the copper smelter emissions either as directly emitted sulfates or produced by the oxidation of SO_x emissions from that source.

One source that appears in $PM_{2.5}$ but not in PM_{10} is Antofagasta; this source was characterized by high contents of carbonaceous and secondary aerosols (Table 4), species that were only measured in the $PM_{2.5}$ fraction. On the other hand marine aerosol is resolved in the PM_{10} (Table 3) but not as a single source in the $PM_{2.5}$ analysis; this result is probably due to the small sample size analyzed with PMF3.0.

The anthropogenic source that contributes most at the PM_{10} size fraction is the cement plant, followed by mineral stockpiles–brine plant and the copper smelter source.

For the $PM_{2.5}$ fraction the relative order is cement plant, copper smelter (including sulfates) and mineral stockpiles–brine plant sources; so most pollution come from local sources and not from regional ones. Values of the soil dust contribution are higher than those estimated at other locations in the same region — see Introduction section (2.3 section) — and we ascribe this result to the bare landscape in the study area as compared with urbanized ground landscapes for the cities mentioned in the Introduction section.

The model receptor analysis shows that suspended soil dust is enriched with elements of natural and anthropogenic origin: sodium chloride from marine aerosol, Ca and sulfates from the cement plant, Cu, Zn, As and sulfates from the copper smelter, Zn, Pb, S and Ni from the mineral stockpiles. All these elements deposit and accumulate on the ground due to the lack of precipitation in this desert region and are easily suspended by the local winds therein — see Figure 5; these soil dust accumulation and suspension mechanisms are difficult to be modeled using source-oriented dispersion models. Anthropogenic sources such as copper smelter, cement plant and minerals stockpile emissions get mixed with suspended soil dust at the monitoring site. Wind trajectory analysis and inspection of local winds have confirmed such interpretation — see Figure 11, Figure 13 and Figure 15 and those in the Supplementary material.

2.8. Conclusions

A short term campaign measuring chemical speciation in ambient PM₁₀ and PM_{2.5} size fractions was conducted between December 17th, 2007 and January 27th, 2008 near Antofagasta, a mid-size coastal city in northern Chile. The site is within a desert that includes northern Chile and most of southwestern Perú.

Source apportionment was estimated by applying U.S. EPA's Positive Matrix Factorization receptor modeling software - version 3.0 - to PM₁₀ and PM_{2.5} size fractions. Sources were identified by inspection of source profiles for key tracers, tracer ratios, local winds and wind trajectory analysis. The relative contribution results for the PM_{2.5} fraction are: cement plant: $33.7 \pm 1.3\%$, soil dust: $22.4 \pm 1.6\%$, sulfates: $17.8 \pm 1.7\%$, minerals stockpiles/brine plant: $12.4 \pm 1.2\%$, Antofagasta: $8.5 \pm 1.3\%$ and copper smelter: $5.3 \pm 0.8\%$. For the PM₁₀ fraction the contributions are: cement plant, $38.2 \pm 1.5\%$; soil dust, $31.2 \pm 2.3\%$; sulfide stockpiles/brine plant, $12.7 \pm 1.7\%$; copper smelter, $11.5 \pm 1.6\%$ and marine aerosol, $6.5 \pm 2.4\%$. Hence local sources contribute to ambient PM concentrations more than distant sources (Antofagasta, marine aerosol) do.

Suspended soil dust has a mean contribution of $50 \mu\text{g}/\text{m}^3$ to ambient PM₁₀ and its peak daily value is $104 \mu\text{g}/\text{m}^3$. For the fine fraction, the contributions are $9.3 \mu\text{g}/\text{m}^3$ and $31.5 \mu\text{g}/\text{m}^3$, respectively.

2.9. Acknowledgments

Financial support for this work was provided by the Industria Nacional de Cemento S.A.; the company also provided access to installing ambient samplers. We thank Mrs. Yolanda Silva (<http://www.setec.cl>) ampling and Mr. Steven Kohl for the chemical analysis performed at the Desert Research Institute (www.dri.edu). We acknowledge a CONICYT doctoral fellowship granted to one of us (F. Barraza). The research described in this article has not been subjected to any review by the funding institutions thus no official endorsement should be inferred.

3. SOURCE APPORTIONMENT OF AMBIENT $PM_{2.5}$ IN SANTIAGO, CHILE: 1999 AND 2004 RESULTS

3.1. Highlights

- Regional copper smelters do contribute to ambient $PM_{2.5}$ at Santiago.
- Marine aerosol often arrives at Santiago mixed in with anthropogenic sources.
- A 20-year reduction of $PM_{2.5}$ at Santiago is due to local and regional regulations.
- Regional sources must be further regulated for improving Santiago's air quality.
- Regional sources must be considered in cost–benefit analysis of regulations.

3.2. Graphical abstract

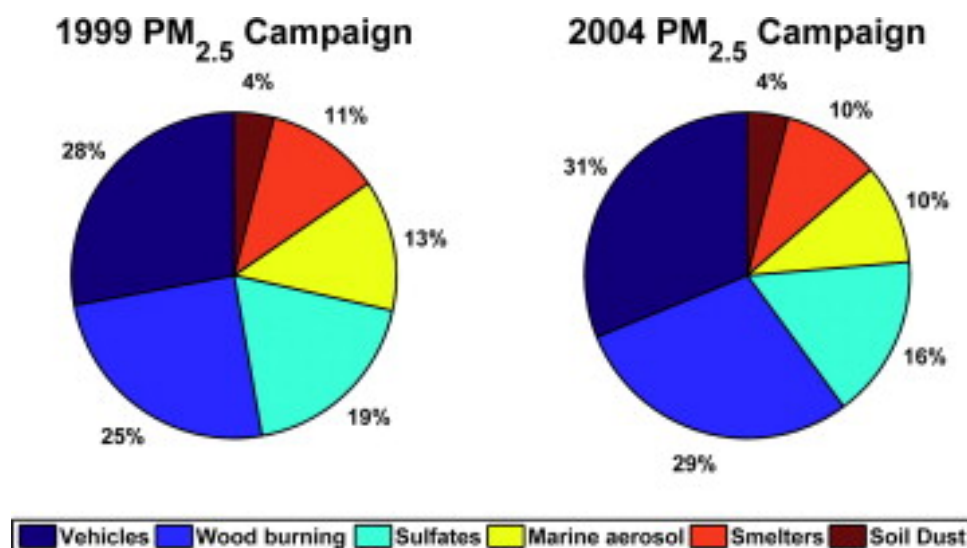


Figure 16 Graphical abstract: Source apportionment of ambient $PM_{2.5}$ in Santiago, Chile: 1999 and 2004 results

3.3. Abstract

A receptor model analysis has been applied to ambient $\text{PM}_{2.5}$ measurements taken at Santiago, Chile (33.5°S , 70.7°W) in 2004 (117 samples) and in 1999 (95 samples) on a receptor site on the eastern side of the city. For both campaigns, six sources have been identified at Santiago and their contributions in 1999/2004 are: motor vehicles: $28 \pm 2.5 / 31.2 \pm 3.4\%$, wood burning: $24.8 \pm 2.3 / 28.9 \pm 3.3\%$, sulfates: $18.8 \pm 1.7 / 16.2 \pm 2.5\%$, marine aerosol: $13 \pm 2.1 / 9.9 \pm 1.5\%$, copper smelters: $11.5 \pm 1.4 / 9.7 \pm 3.3\%$ and soil dust: $3.9 \pm 1.5 / 4.0 \pm 2.4\%$. Hence, relative contributions are statistically the same but the absolute contributions have been reduced because ambient $\text{PM}_{2.5}$ has decreased from 34.2 to 25.1 $\mu\text{g}/\text{m}^3$ between 1999 and 2004 at Santiago. Similarity of results for both data sets — analyzed with different techniques at different laboratory facilities — shows that the analysis performed here is robust.

Source identification was carried out by inspection of key species in source profiles, seasonality of source contributions, comparison with published source profiles and by looking at wind trajectories computed using the Hybrid Single-Particle Lagrangian Integrated Trajectory (HYSPLIT) from USA's National Oceanic and Atmospheric Administration (NOAA); for the wood burning sources the MODIS burned area daily product was used to confirm wildfire events along the year. Using this combined methodology we have shown conclusively that: a) marine air masses do reach Santiago's basin in significant amounts but combined with anthropogenic sources; b) all copper smelters surrounding Santiago — and perhaps coal-fired power plants as well — contribute to ambient $\text{PM}_{2.5}$; c) wood burning is the second largest source, coming from residential wood burning in fall and winter and from regional wildfires in spring and summer.

The results of the present analysis can be used to improve emission inventories, air quality forecasting systems and cost–benefit analysis at local and regional scales.

3.4. Introduction

The greater metropolitan region of Santiago, Chile (33.5°S, 70.7°W) is the 6th largest South American city in population (6 million), and 39% of the country's inhabitants lived there in 2002 (ECLAC: Economic Commission for Latin America 2012; INE: Instituto Nacional de Estadísticas 2012). During fall and winter meteorological conditions lead to pollutant trapping below a thermal inversion, raising all pollutant concentrations. This poor air quality is caused by a combination of atmospheric emissions, the topography of Santiago and specific meteorological conditions (Garreaud, Rutllant, and Fuenzalida 2002; Hector Jorquera et al. 2004; Muñoz et al. 2010; Muñoz and Alcañiz 2012; Rutllant and Garreaud 2004).

The air quality monitoring network in Santiago has been expanded (since 2009) to nine monitoring stations that cover the Greater Metro area of $\sim 40 \times 40$ km of extension — see Figure 17 — and all these stations measure ambient $\text{PM}_{2.5}$ by means of tapered element oscillating mass (TEOM) instruments. In addition, the Ministry of the Environment operates Low-Vol samplers to conduct chemical analysis for integrated, 24-h $\text{PM}_{2.5}$ filter samples. There have been several studies that show how different chemical components of ambient $\text{PM}_{2.5}$ have evolved in the last years (P. Artaxo 1996; P. Artaxo 1998; Paulo Artaxo, Oyola, and Martinez 1999; Koutrakis et al. 2005; Rojas et al. 1990) with decreasing trends in sulfur, lead and other anthropogenic elements.

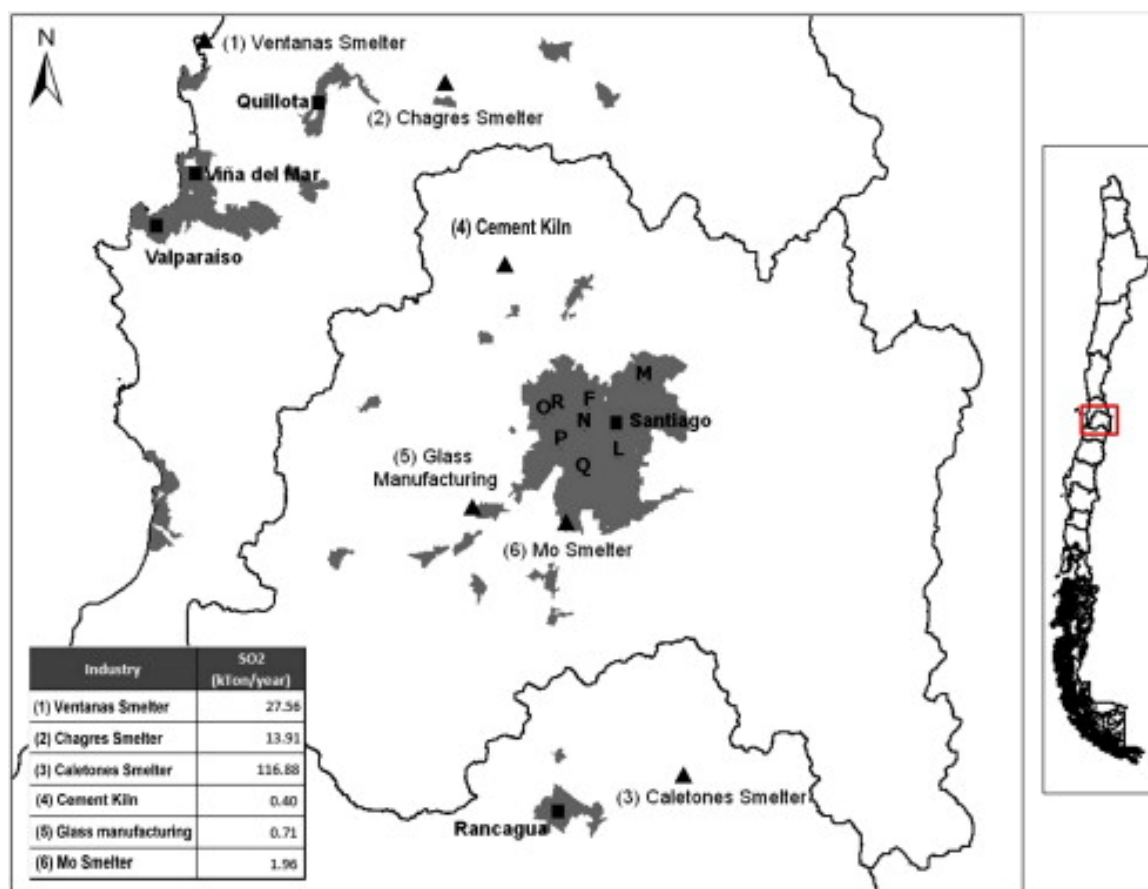


Figure 17 A map depicting the metropolitan region of Chile, major urban areas (gray shade), and Santiago's ambient monitoring network (letters). The location of major SO₂ sources around Santiago are denoted by a triangle, and their emissions are listed in the table.

The longest records of continuous ambient monitoring of PM_{2.5} in Santiago for stations L, M, N and O in Figure 17 and Figure 18, show the evolution of daily (00 to 24 h LST) averages of PM_{2.5} for 2000-2011 in those stations; there is a decreasing trend that is explained by a continuous effort in environmental regulations. Nonetheless, annual averages in 2011 are still above WHO guidelines. Station M is the one with the lowest ambient concentrations and the other three sites show similar values. This difference is explained by the location of monitor M on the Andes foothills, being frequently above of the thermal inversion layer, departing from the monitoring network deployed down on the valley; Gramsch et al. (Gramsch, E; Cereceda-Balic and Oyola, P; Vonbaer 2006) have performed cluster analysis of ambient PM₁₀, PM_{2.5} and ozone recorded at those four stations and have confirmed such a different behavior for ambient pollutant concentrations.

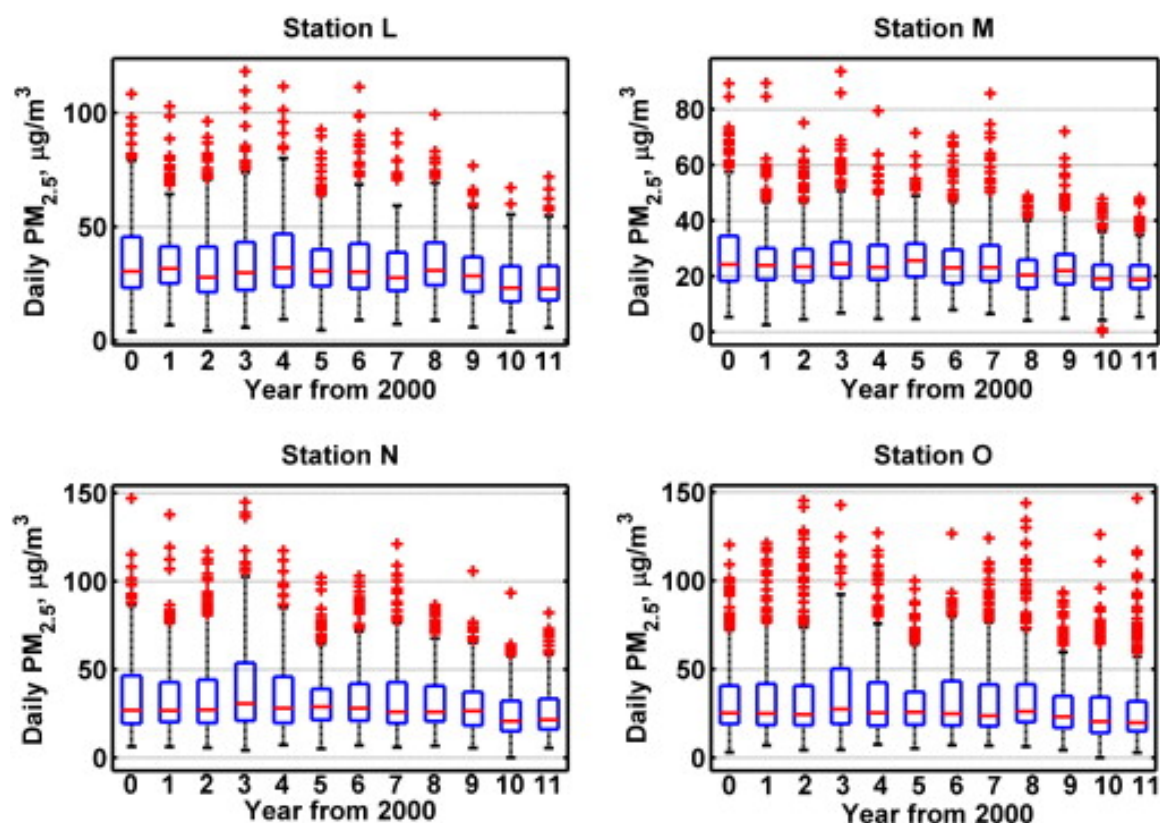


Figure 18 Annual box plots of daily ambient $PM_{2.5}$ concentrations at Santiago's stations L, M, N and O, in [$\mu\text{g}/\text{m}^3$], for the period 2000–2011.

Figure 19 shows a monthly boxplot of $PM_{2.5}$ daily averages at those four monitoring sites; it can be seen that the seasonality of ambient $PM_{2.5}$ is high at all sites; between May and July 50% of daily values exceeded $50 \mu\text{g}/\text{m}^3$ at the downtown and west sides of the city whereas at station M the respective percentage is 25%. In fall and winter the subsidence regime of the Pacific high is enhanced by coastal lows promoting strong drainage flow from the Andes leading to pollution trapping in Santiago's basin (Gallardo et al. 2002; Garreaud, Rutllant, and Fuenzalida 2002; Olivares et al. 2002; Rutllant and Garreaud 2004) so near midnight pollution peaks at site O but reaches low values at site M thus explaining the difference in daily $PM_{2.5}$ concentrations across the city - see Jorquera and Castro (Hector Jorquera and Castro 2010) for an inverse modeling of a fall season episode.

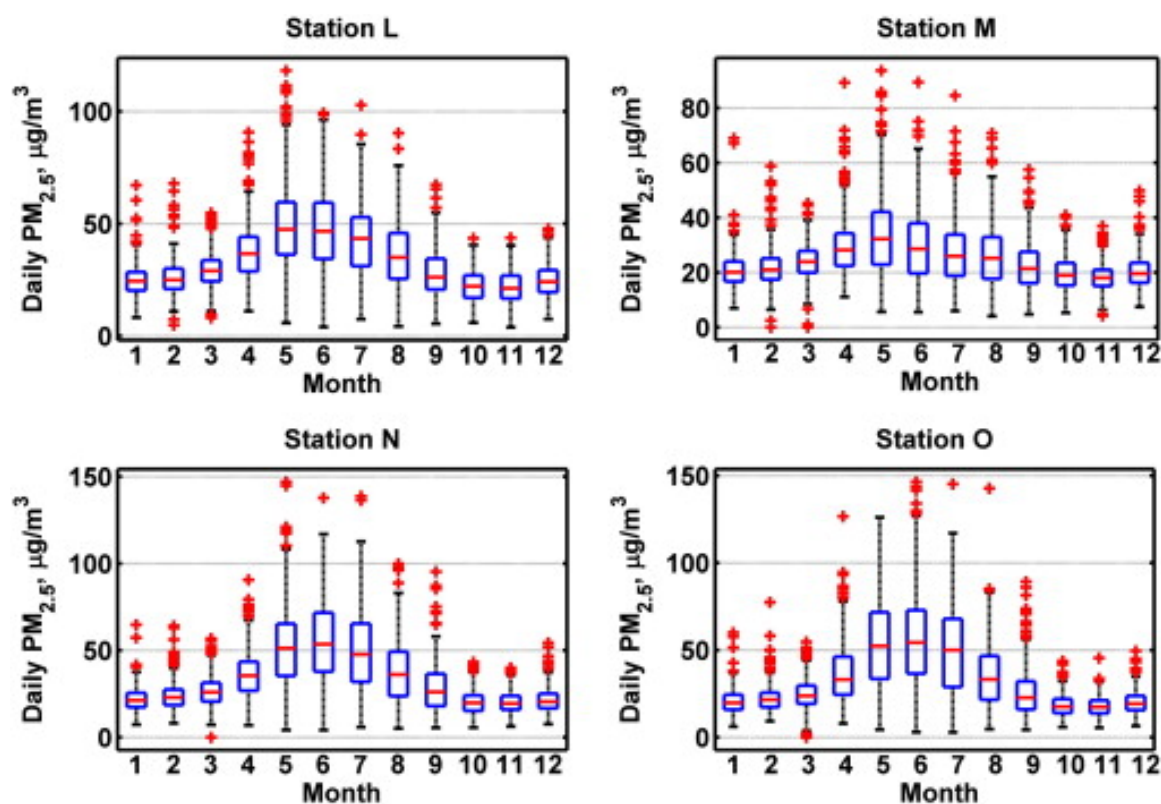


Figure 19 Monthly box plots of daily ambient $PM_{2.5}$ concentrations at Santiago's stations L, M, N and O, in $[\mu g/m^3]$, for the period 2000–2011.

In the diurnal period a valley-to-mountain circulation develops transporting air masses from the city towards site M which can be considered a receptor of Santiago's pollution plume most of the year (Rappenglück et al. 2000; Schmitz 2005). The exceptions are the aforementioned subsidence episodes when a low thermal inversion blocks the valley-to-mountain circulation and segregates station M from the rest of the city's air quality network (Rutllant and Garreaud 2004).

The goal of this work is to conduct a source apportionment of ambient $PM_{2.5}$ concentrations at Santiago to identify major sources. The following sections of this paper present a description of the ambient monitoring campaign, the receptor modeling approach, the results of the analysis, a discussion and the final conclusions.

3.5. Methodology

3.5.1. Ambient monitoring campaigns

3.5.1.1. Santiago 2004 data

Ambient $PM_{2.5}$ samples were collected with Low-Vol dichotomous samplers operating at 15 L/min by the Autoridad Sanitaria de la Región Metropolitana (www.asrm.cl). Data were taken at Las Condes, located in the eastern zone of the city (site M in Figure 17). Samples were collected every day during fall and winter (April–September) and every third day during spring and summer (October–March). From that collection we have selected 117 filters so that all 2004 $PM_{2.5}$ pollution episodes were included; this means higher concentrations are overrepresented in this data base. We have chosen this non-uniform sampling to obtain a detailed source apportionment for all $PM_{2.5}$ episodes recorded in 2004; nonetheless 27% of the samples analyzed belong to spring and summer seasons and so source apportionment results are produced for all year 2004; implications of the above sampling protocol are commented in the Discussion of results section below.

The elemental analysis was conducted by X-ray fluorescence at the Desert Research Institute, Reno, NV, USA. In addition local authorities monitor elemental (EC) and organic (OC) carbon concentrations at the same site M with a Rupprecht and Patashnick Series 5400 monitor. The monitor samples the ambient air for one hour, and then performs a thermal analysis to determine the concentration of EC and OC contained in the $PM_{2.5}$ fraction.

3.5.1.2. Santiago 1999 data

This sampling campaign was conducted between July and November 1999 by researchers of Sao Paulo University, with a total of 95 daily samples taken with Stacked

Filter Unit, SFU samplers (Philip K. Hopke et al. 1997) operating at 17 L/min and using a 0.4- μm pore size Nuclepore filter to collect the fine mode particles with aerodynamic diameter below 2.0 μm ($\text{PM}_{2.0}$). Sampled volume was obtained with volume integrators calibrated with Hastings Precision Mass Flowmeters, to within 1% accuracy. Black carbon concentration was measured using an optical absorption technique, with a diffusion system photometer. The filters were analyzed with proton induced X-ray emissions (PIXE) to measure 20 trace elements (Mg, Al, Si, P, S, Cl, K, Ca, Ti, V, Cr, Mn, Fe, Ni, Cu, Zn, As, Br, Sr, and Pb). Irradiation was performed at the LAMFI — Laboratório de Análise de Materiais por Feixes Iônicos from the Institute of Physics, University of São Paulo. More details of the methodology can be found in Artaxo, 1996, Artaxo, 1998 and Artaxo et al. 1999. (P. Artaxo 1996; P. Artaxo 1998; Paulo Artaxo, Oyola, and Martinez 1999)

3.5.2. Receptor modeling methodology

Receptor models are mathematical procedures for identifying and quantifying the sources of ambient air pollution and their effects at a receptor site, on the basis of concentration measurements therein, without neither emission inventories nor meteorological data (Willis 2000). In mathematical terms, the general receptor modeling problem can be stated in terms of the contributions from p independent sources to n chemical species measured in a set of m samples as follows (P K Hopke et al. 2006):

$$X_{ij} = \sum_{k=1}^p g_{ik} f_{kj} + e_{ij}$$

Equation 5

where X_{ij} is the j -th species mass measured in the i -th sample, g_{ik} is the PM mass concentration from the k -th source contributing to the i -th sample, f_{kj} is the j -th species mass fraction from the k -th source, e_{ij} is a model residual associated with the j -th species concentration measured in the i -th sample, and p is the total number of independent sources. The above equation stands for a mass balance for each measured species.

In the positive matrix factorization (PMF) approach, non-negative constraints upon f_{kj} and g_{ik} are integrated into the computational process (Paatero 1997; Paatero 1999). PMF has been extensively applied to source apportionment of PM_{10} and $PM_{2.5}$ at many places worldwide — see Paatero et al. (Paatero, P Hopke et al. 2005) and Reff et al. (Reff, Eberly, and Bhave 2007) for a detailed bibliography. We use in this work PMF version 3.0, available from U.S. EPA (U.S. Environmental Protection Agency 2012a); the task of this computer software is to minimize the weighted sum of squares

$$Q = \sum_{i=1}^n \sum_{j=1}^m \left[\left(X_{ij} - \sum_{k=1}^p g_{ik} f_{kj} \right) / \sigma_{ij} \right]^2$$

Equation 6

Where σ_{ij} is the estimated model uncertainty in the j -th species in i -th sample. This model uncertainty must include the laboratory analytical uncertainty (see below), but it also has a component that takes into account deviations from model assumptions: variability in source profiles, number of sources, data contamination, etc. which is expressed as an additional relative uncertainty in PMF3.0 (Reff, Eberly, and Bhave 2007).

Paatero et al. (Paatero, P Hopke et al. 2005) have shown how to explore the range of potential solutions of Equation 6 varying a parameter named F_{peak} : positive values force most elements to lie on few source profiles, while negative values mean that most source profiles are mixed thus they do not stand for “pure sources”; they suggest varying F_{peak} until no correlation among paired source contributions is evident, usually when some points lay on either axis — the so called ‘edge points’.

The value of the analytical uncertainty — reported by the laboratory for each data set — plus one third of the limit of detection was assigned as uncertainty to each measured value. Values below the detection limit were replaced by half of the detection limit values, and their overall uncertainties were set at 5/6 of the detection limit values, following the approach of Polissar et al. (Polissar, Hopke, Paatero, et al. 1998).

3.6. Results

3.6.1. Mass concentration and chemical composition

The mass and elemental concentration data for the 2004 campaign are shown in Table 6; recall that the sampling was non-uniform and more samples were taken in fall and winter seasons when concentrations are higher — see Figure 19. A summary of results for the 1999 campaign is shown in Table 7. Almost all species in $PM_{2.5}$ have decreased between 1999 and 2004; this same trend has been found for downtown site N (Koutrakis et al. 2005; Sax et al. 2007); the exception is potassium, a tracer of wood burning that has increased between 1999 and 2004 at site M.

Table 6 Summary of $PM_{2.5}$ mass and elemental concentrations^a, 2004 campaign.

| Component | Mean | Std. dev. | Minimum | Maximum | No. of samples ^b |
|------------|------|-----------|---------|---------|-----------------------------|
| $PM_{2.5}$ | 32.3 | 16.7 | 6.0 | 83.0 | 117 |
| EC | 1.5 | 0.9 | 0.2 | 5.9 | 65 |
| OC | 7.3 | 2.8 | 2.9 | 15.3 | 65 |
| Al | 104 | 65 | 32 | 609 | 117 |
| Si | 194 | 89 | 53 | 497 | 117 |
| P | 38.6 | 19.9 | 3.5 | 134.5 | 117 |
| S | 950 | 548 | 133 | 3631 | 117 |
| Cl | 31.2 | 43.6 | 1.2 | 258.5 | 117 |
| K | 244 | 108 | 74 | 625 | 117 |
| Ca | 92 | 37 | 29 | 239 | 117 |
| Ti | 9.7 | 3.7 | 2.3 | 22.2 | 117 |
| V | 0.5 | 0.3 | 0.3 | 1.5 | 63 |
| Cr | 1.7 | 1.2 | 0.1 | 5.4 | 116 |
| Mn | 11.9 | 7.0 | 1.4 | 41.1 | 117 |
| Fe | 244 | 90 | 84 | 578 | 117 |
| Ni | 0.4 | 0.3 | 0.1 | 1.6 | 112 |
| Cu | 19.3 | 9.0 | 3.7 | 52.6 | 117 |
| Zn | 46 | 26 | 6.5 | 127 | 117 |
| As | 10.3 | 6.6 | 0.6 | 29.9 | 110 |
| Se | 1.1 | 0.9 | 0.1 | 3.6 | 77 |
| Br | 10.8 | 7.6 | 0.7 | 33.9 | 117 |
| Mo | 2.8 | 1.9 | 0.2 | 11.2 | 113 |
| Ba | 7.9 | 4.0 | 1.3 | 21.7 | 116 |
| Pb | 18.9 | 10.4 | 0.3 | 46.5 | 117 |

^a All concentrations are in $[ng/m^3]$ except $PM_{2.5}$, EC and OC which are in $[μg/m^3]$.

^b Below detection limit values are not accounted for in the statistics.

Table 7 Summary of $PM_{2.5}$ mass and elemental concentrations^a, 1999 campaign.

| Component | Mean | Std. dev. | Minimum | Maximum | No. of samples ^b |
|------------|------|-----------|---------|---------|-----------------------------|
| $PM_{2.5}$ | 36.9 | 20.7 | 4.09 | 114 | 95 |
| BC | 5.87 | 2.97 | 0.56 | 15 | 95 |
| Mg | 86.9 | 68.2 | 14.2 | 385 | 30 |
| Al | 251 | 187 | 32.9 | 1687 | 95 |
| Si | 624 | 478 | 46.3 | 4305 | 95 |
| P | 15.3 | 6.38 | 6.87 | 36.8 | 59 |
| S | 1654 | 1031 | 180 | 4270 | 95 |
| Cl | 43.8 | 27.5 | 7.44 | 124 | 95 |
| K | 187 | 79.8 | 35.5 | 481 | 95 |
| Ca | 234 | 189 | 18.9 | 1757 | 95 |
| Sc | 10.6 | 6.12 | 1.63 | 31.2 | 48 |
| Ti | 32 | 18.5 | 4.18 | 160 | 95 |
| V | 4.26 | 1.97 | 1.43 | 15.8 | 95 |
| Cr | 4.84 | 3.74 | 2.01 | 23 | 41 |
| Mn | 13.4 | 6.77 | 1.12 | 37.6 | 95 |
| Fe | 396 | 216 | 40.4 | 1850 | 95 |
| Ni | 1.58 | 0.66 | 0.57 | 3.06 | 23 |
| Cu | 29.6 | 14.7 | 2.29 | 74 | 95 |
| Zn | 41.6 | 22 | 4.08 | 98.4 | 95 |
| As | 28.6 | 30.4 | 0.84 | 119 | 95 |
| Br | 16.6 | 9.49 | 2.06 | 45.1 | 95 |
| Sr | 2.53 | 1.51 | 0.66 | 12.1 | 95 |
| Zr | 1.87 | 0.88 | 0.58 | 4.35 | 34 |
| Mo | 4.99 | 3.3 | 1.06 | 20.8 | 50 |
| Pb | 82.9 | 52.3 | 7.3 | 281 | 95 |

^a All concentrations are in $[ng/m^3]$ except and $PM_{2.5}$ and BC which are in $[μg/m^3]$.

^b Below detection limit values are not accounted for in the statistics.

3.6.2. Receptor modeling results for the 2004 $PM_{2.5}$ data

We have run the receptor model for different number of factors and examined source profiles looking for specific tracers/tracer ratios and to the seasonality of source contributions to identify potential sources; then we have applied multiple linear regression (MLR) to the daily concentrations of $PM_{2.5}$ using source contributions as independent variables and checked whether the regression coefficients were positive and statistically significant ($p \leq 0.05$). We have found that a six factor solution explains well the measured $PM_{2.5}$ concentrations. The statistical results for the 15 species fitted are shown in Table 8.

Most fitted elements have regression coefficients (R^2) greater than 0.8, except Ba and Cr that were kept for they are tracers of mobile sources (Fujiwara et al. 2011).

Table 8 Regression diagnostics for a 6 factor solution, 2004 data.

| Species | Intercept | Slope | Std. error | R^2 |
|---------|-----------|-------|------------|-------|
| Si | 14.12 | 0.92 | 16.96 | 0.959 |
| P | - 0.86 | 1.02 | 2.15 | 0.989 |
| S | 0.66 | 1.00 | 19.86 | 0.999 |
| Cl | 0.23 | 0.99 | 0.86 | 1.000 |
| K | 4.69 | 0.98 | 11.43 | 0.989 |
| Ca | 10.43 | 0.87 | 10.62 | 0.903 |
| Ti | 0.91 | 0.90 | 0.87 | 0.936 |
| Cr | 0.53 | 0.68 | 0.43 | 0.775 |
| Mn | 3.36 | 0.69 | 2.36 | 0.808 |
| Fe | 5.38 | 0.97 | 19.69 | 0.952 |
| Zn | 4.76 | 0.87 | 5.87 | 0.938 |
| As | 0.04 | 0.99 | 0.15 | 1.000 |
| Br | 2.00 | 0.76 | 2.64 | 0.830 |
| Ba | 2.14 | 0.67 | 2.15 | 0.613 |
| Pb | 2.20 | 0.85 | 3.87 | 0.840 |

Sensitivity analysis of this six factor solution were performed by varying the *Fpeak* parameter — cf. Receptor modeling methodology (section 3.5.2). Following (Paatero, P Hopke et al. 2005), we look for solutions that produce ‘edges’ in G-space scatter plots. We have found that a solution with *Fpeak* = -0.15 is the most plausible one. Positive values of *Fpeak* lead to G-space correlation coefficients higher than the base case results, hence they were not considered as credible solutions. In other words PMF model results support some amount of mixing of source profiles that we comment below in the Discussion of results section (section 3.7). The source profiles, in ng/m^3 , for the rotated solution with *Fpeak* = -0.15 are shown in Table 9.

Table 9 Source profiles [ng/m^3] for a 6 factor solution, 2004 data ($F_{\text{peak}} = -0.15$).

| Species | Motor vehicles | Marine aerosol | Copper smelters | Soil dust | Secondary sulfates | Wood burning |
|---------|----------------|----------------|-----------------|-----------|--------------------|--------------|
| Si | 0.0 | 0.0 | 1.2 | 146.3 | 15.0 | 29.4 |
| P | 2.1 | 0.0 | 7.4 | 0.9 | 27.5 | 0.6 |
| S | 0.0 | 41.6 | 181.3 | 0.0 | 726.8 | 0.0 |
| Cl | 1.3 | 28.7 | 0.0 | 1.3 | 0.0 | 0.0 |
| K | 0.0 | 14.5 | 0.0 | 60.6 | 14.7 | 153.0 |
| Ca | 17.9 | 0.0 | 1.7 | 58.4 | 5.4 | 7.3 |
| Ti | 1.5 | 0.1 | 0.0 | 6.0 | 0.7 | 1.2 |
| Cr | 1.3 | 0.0 | 0.0 | 0.3 | 0.0 | 0.0 |
| Mn | 7.6 | 0.0 | 0.0 | 3.9 | 0.1 | 0.0 |
| Fe | 106.8 | 2.6 | 7.8 | 103.2 | 8.1 | 13.2 |
| Zn | 34.5 | 0.0 | 0.0 | 6.0 | 4.3 | 0.0 |
| As | 0.1 | 0.0 | 9.6 | 0.0 | 0.0 | 0.0 |
| Br | 5.2 | 0.9 | 0.3 | 0.0 | 0.0 | 3.8 |
| Ba | 4.6 | 0.1 | 0.3 | 2.1 | 0.0 | 0.3 |
| Pb | 11.5 | 0.6 | 2.1 | 1.4 | 1.3 | 1.3 |

The first source has more than 60% of measured Pb, Ba and Mn and 75% of Cr and Zn, all tracers of traffic emissions (Fujiwara et al. 2011). From this source profile we have a ratio $\text{Zn}/\text{Fe} = 0.32$; similar ratios have been found in $\text{PM}_{2.5}$ source profiles at the Chilean cities of Temuco (0.34), Rancagua (0.31) and Iquique (0.31) by (Kavouras et al. 2001); comparable results have been found in PM_{10} receptor modeling analysis at Quillota (0.31) by (Hedberg, Gidhagen, and Johansson 2005). Thus, we have identified the first source as motor vehicles. The second source has more than 95% of the Cl so we identify it as marine aerosol reaching Santiago's basin; this has been confirmed by using wind trajectory analysis (see Section 3.6.2.1 below). The third source has almost all As measured; for this source the ratio $\text{S}/\text{As} = 18.9$ is close to the value 16.5 obtained for a copper smelter profile in Rancagua by Kavouras et al. (Kavouras et al. 2001) and 14.6 for one copper smelter profile in Quillota (Hedberg, Gidhagen, and Johansson 2005); therefore we identify this source as the copper smelters surrounding Santiago (see Figure 17). The fourth source has most of Si, Ca and Ti and has a ratio $\text{K}/\text{Fe} = 0.59$ that indicates soil dust emission (Malm et al. 1994); this is confirmed by the ratio $\text{Si}/\text{Ca} = 2.5$ that compares well with the source apportionment results of Kavouras et al. (Kavouras et al. 2001) for Rancagua ($\text{Si}/\text{Ca} = 2.3$). The fifth source has most of sulfur so it is a secondary sulfate source with a profile

dominated by sulfur in mass, like the ones identified in other cities near Santiago by Kavouras et al. (Kavouras et al. 2001); the ratio S/P = 26.4 is quite similar to the value 29.7 found by Rojas et al. (Rojas et al. 1990) at Santiago for samples taken in the summer of 1987. Finally the sixth source has more than 60% of potassium suggesting residential wood burning and wildfire emissions. This kind of source profile varies according to the vegetative species being burned (Chow et al. 2004), so comparisons are difficult to establish with other source apportionment studies. Nonetheless, we have found order-of-magnitude similarities for some elemental ratios. For instance the ratio K/Fe = 11.6 compares well with the value 14.1 found by Rojas et al. (Rojas et al. 1990) at Santiago; likewise the ratio K/Br = 40 is similar to the value 58 found by Kavouras et al. (Kavouras et al. 2001) at Rancagua for samples taken in 1998.

We have also checked the identified sources by making a stepwise regression of elemental (EC) and organic carbon (OC), using the six source contributions as independent variables — we did not use EC nor OC as inputs of the PMF model for the number of valid data (65) was low compared with the total samples analyzed (117). The outcome of the stepwise regressions is given in the following equation

$$EC = 0.96 + 0.684G_1$$

$$OC = 4.04 + 2.44G_1 + 0.48G_2 + 0.99G_6$$

Equation 7

Hence, EC is apportioned only to motor vehicles and OC is apportioned to motor vehicles, wood burning and marine aerosol. This result implies that marine air masses pick up emissions from rural areas upwind of Santiago where wood burning is customarily used for cooking and space heating and where wildfires are frequent, especially in spring and summer.

We have also inspected the weekly seasonality of source contributions — see Figure 20 — motor vehicles and soil dust clearly decrease in weekends showing their

traffic origin. Wood burning has an opposite trend: it rises slightly over weekends; since the monitor site is within a residential neighborhood, people spend more time indoors over the weekend and so increase their use of wood stoves for space heating in fall and winter seasons. Finally, the regional sources — smelters, sulfates and marine aerosol — do not have any clear weekly pattern for they depend upon synoptic scale dynamics.

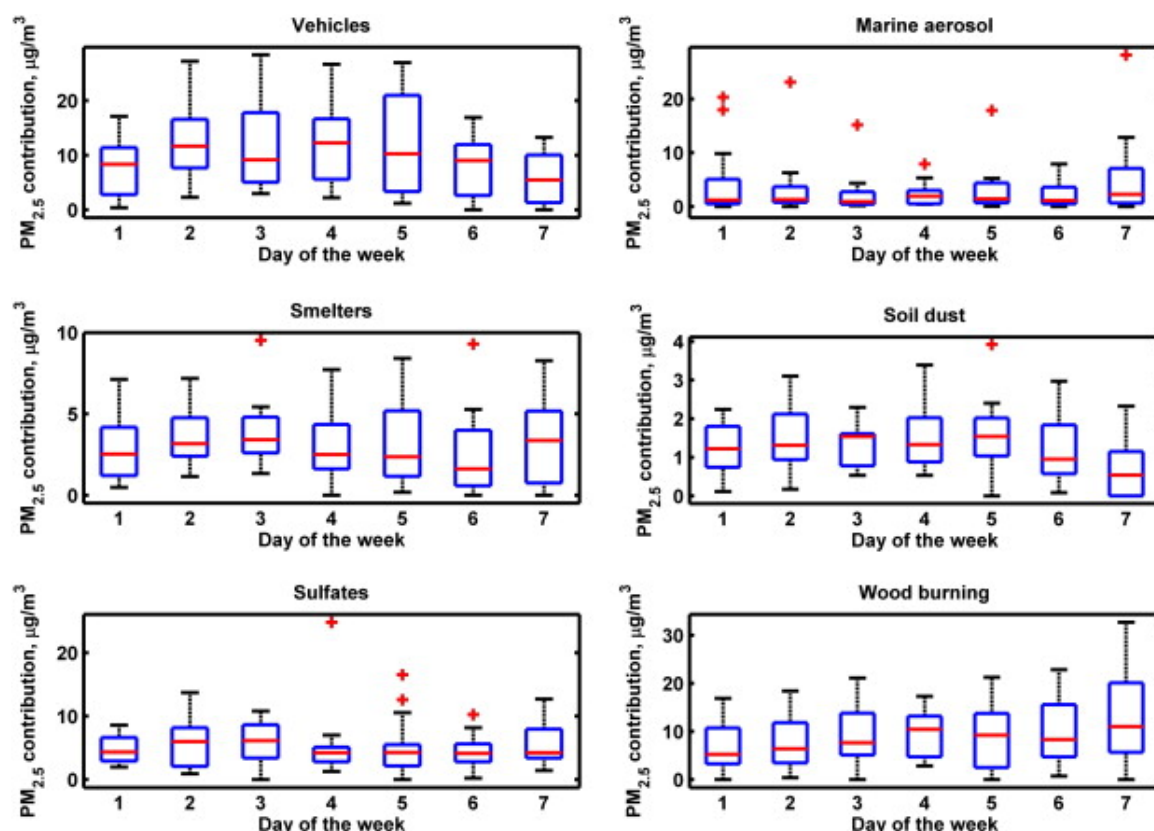


Figure 20 Box plots of estimated, ambient $PM_{2.5}$ source contributions by day of the week, 2004 campaign.

The wood burning contribution increases in winter when ambient temperatures are lowest — see Figure 21; by inspecting the MODIS burned area product (<http://firefly.geog.umd.edu/firemap/>) we have checked that there were no wildfires in the region in fall and winter 2004 — see Figure 22 and Figure 23 — hence such emission must come from residential wood burning within the city; conversely in spring and summer the high contributions of the wood burning source can be explained by regional scale wildfires — see Figure 24 and Figure 25.

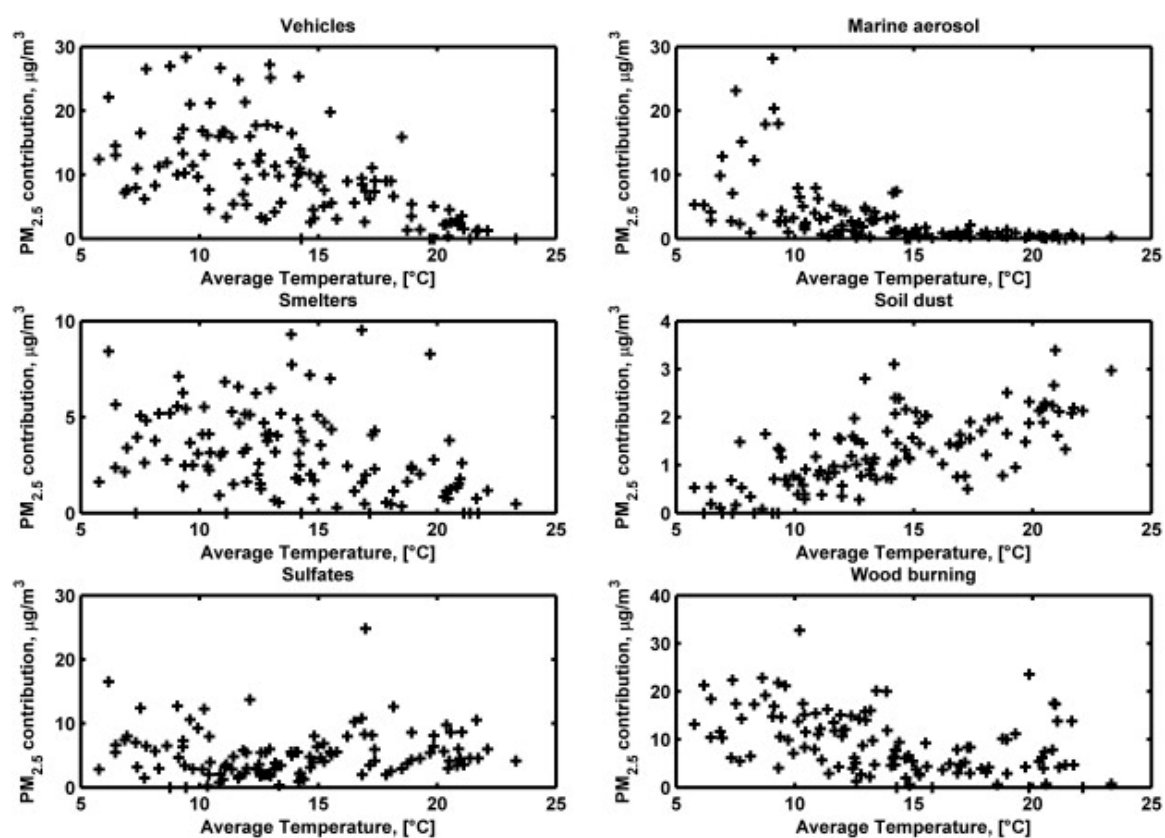


Figure 21 Scatterplots of estimated, ambient $PM_{2.5}$ source contributions versus mean daily temperatures, 2004 campaign.

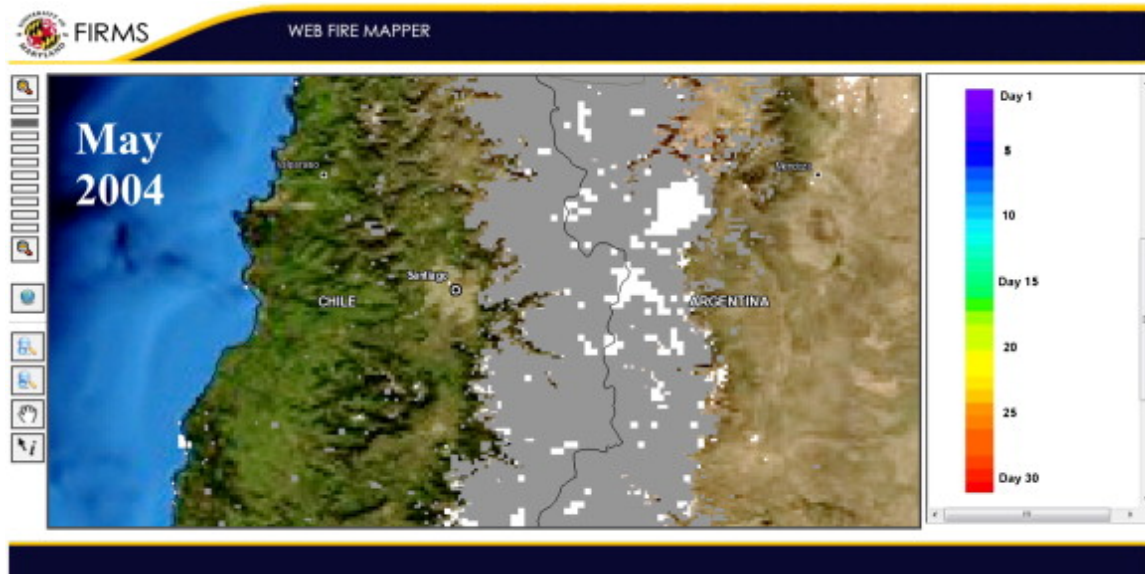


Figure 22 *On May 2004 there was no presence of wildfires close to Santiago.*

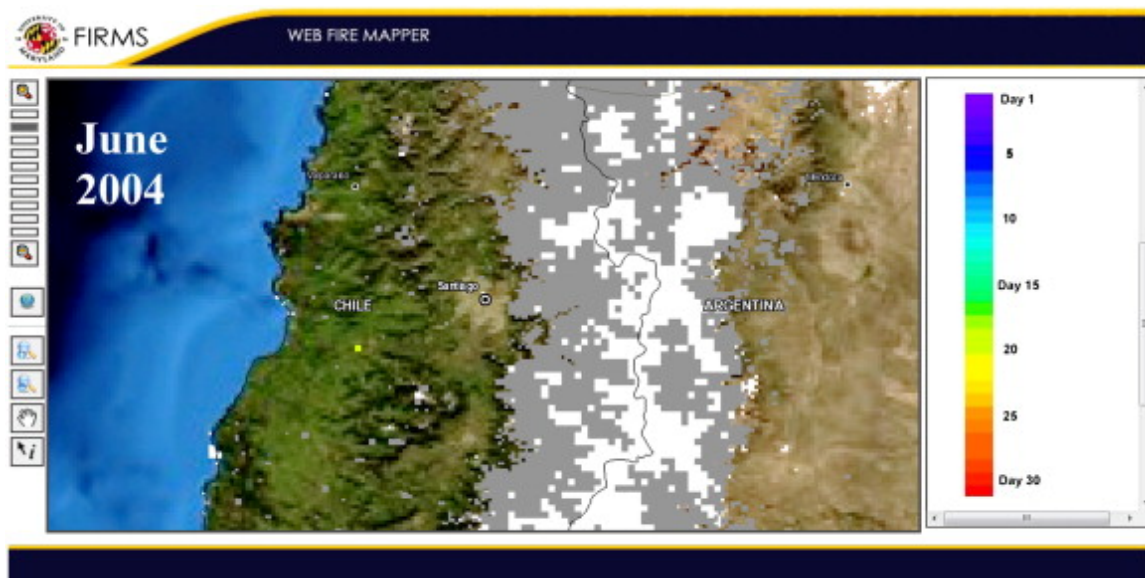


Figure 23 *On June 2004 there was no presence of wildfires close to Santiago*



Figure 24 Presence of wildfires close to Santiago on February 2004



Figure 25 Presence of wildfires close to Santiago on December 2004

Regional sources do not have a correlation with ambient temperatures — see Figure 21 — the negative correlation of temperature with motor vehicles is explained because lower surface air temperatures are correlated with ground level atmospheric stability (Rutllant and Garreaud 2004). The positive correlation of dust soil with ambient temperatures is explained by regional winds that increase in spring and summer — when the subsidence regime of the Pacific high brings in clear skies, warmer air and SW winds, transporting soil dust onto the city and also because in fall and winter higher relative humidity and rainfall reduce fugitive soil dust emissions.

3.6.2.1. Use of wind trajectory analysis to confirm source identification

In previous studies of source apportionment conducted at Santiago (P. Artaxo 1996; P. Artaxo 1998; Paulo Artaxo, Oyola, and Martinez 1999), up to five factors have been found in ambient $PM_{2.5}$, and in an earlier study by Rojas et al. (Rojas et al. 1990) at Downtown Santiago six factors had been found in ambient $PM_{2.5}$; however our present work is the first one in finding smelter contributions as single sources at Santiago. We have verified these findings using wind trajectory analysis, using the Hybrid Single-Particle Lagrangian Integrated Trajectory (HYSPLIT) model (Rolph 2012) from USA's National Oceanic and Atmospheric Administration (NOAA) to construct back trajectories arriving at Santiago and forward trajectories departing from the smelters shown in Figure 17. We have selected several days with the highest contributions for each of the six factors found and plotted forward and backward trajectories, running HYSPLIT using as input the NCEP reanalysis dataset and the default option of modeling vertical velocities. We have chosen wind trajectories departing at 100 m above ground level (AGL) to construct the plots; trajectories computed at 300 and 500 m AGL have produced essentially the same plots.

The sample date, the dominant source contributions according to the receptor model and their estimated magnitudes in $[\mu g/m^3]$, and the responsible sources according to HYSPLIT or MODIS are shown in Table 10. It can be seen that all three copper smelters are responsible for the high contributions of the ‘smelter’ and ‘sulfates’ sources; depending

on prevailing meteorology some days one or more smelter plumes arrive at site M — see Figure 26 , Figure 27 and Figure 28 . For the soil dust we have only found one day with a peak value, that correspond to a springtime SW circulation that brought marine air masses traveling through rural regions SW of Santiago and carrying a soil dust signature — see Figure 29. For the marine aerosol we have found several days with high chlorine values at Santiago; most of them correspond to marine air masses that enter to Santiago's basin from the W or WNW bringing air masses from the greater Valparaiso metro area and from the Ventanas and Chagres industrial zones as well — see Figure 30 — this explains why sulfur appears in the marine aerosol source profile; presence of potassium indicates that the marine aerosol plume is mixed with wood burning from rural areas, coming from typical residential (cooking, space heating) and agricultural (frost preventing) activities upwind of Santiago. For the sulfates contribution, almost all of them are correlated with the smelter source indicating their common origin. The receptor model is able to discriminate between primary smelter emissions and secondary sulfates produced en route to Santiago, although the latter could have also been produced from SO₂ emissions from coal fired power plants near the Ventanas and Chagres smelters and from SO₂ sources closer to Santiago as well — see Figure 17.

Table 10 Comparison of dominant source contributions and wind trajectory analysis for selected days, 2004 campaign.

| Date | Dominant source contribution | Contribution, $\mu\text{g}/\text{m}^3$ | Likely source(s) | Additional information |
|------------|------------------------------|--|------------------------------|------------------------|
| 1/4/04 | Wood burning | 4.7 | Regional wildfire | MODIS |
| 2/6/04 | Wood burning | 13.8 | Regional wildfire | MODIS |
| 3/5/04 | Sulfates | 12.6 | Chagres, Ventanas | HYSPLIT |
| 3/11/04 | Sulfates | 24.8 | Caletones | HYSPLIT |
| 3/13/04 | Sulfates | 10.3 | Ventanas | HYSPLIT |
| 3/29/04 | Sulfates | 8.3 | Chagres | HYSPLIT |
| 4/6/04 | Sulfates/smelters | 8.0/2.4 | Ventanas + Chagres | HYSPLIT |
| 4/10–11/04 | Wood burning | 11.2–10.2 | Local wood burning | MODIS |
| 5/1–2/04 | Wood burning | 20.0–20.1 | Local wood burning | MODIS |
| 5/16/04 | Wood b./Sulfates | 32.7/12.3 | Local wood b. + Chagres | MODIS, HYSPLIT |
| 5/28/04 | Smelters/Sulfates | 8.4/16.5 | Ventanas + Chagres | HYSPLIT |
| 6/6/04 | Wood burning | 22.3 | Local wood burning | MODIS, HYSPLIT |
| 6/30/04 | Marine aerosol | 15.2 | Ventanas + Chagres | HYSPLIT |
| 7/9/04 | Marine aerosol | 17.9 | Ventanas | HYSPLIT |
| 7/26/04 | Marine aerosol/sulfates | 18.0/7.3 | NW flow from ocean + Chagres | HYSPLIT |
| 8/11/04 | Smelters/Sulfates | 3.1/9.3 | Ventanas + Chagres | HYSPLIT |
| 9/15/04 | Smelters/Sulfates | 9.5/10.8 | Caletones | HYSPLIT |
| 10/22/04 | Soil dust | 3.9 | SW flow from ocean | HYSPLIT |
| 10/24/04 | Marine aerosol | 7.4 | SW flow from ocean | HYSPLIT |
| 11/23/04 | Sulfates | 8.4 | Ventanas + Chagres | HYSPLIT |
| 11/29/04 | Sulfates | 6.0 | Caletones | HYSPLIT |
| 12/29/04 | Wood burning | 13.8 | Regional wildfires | HYSPLIT, MODIS |

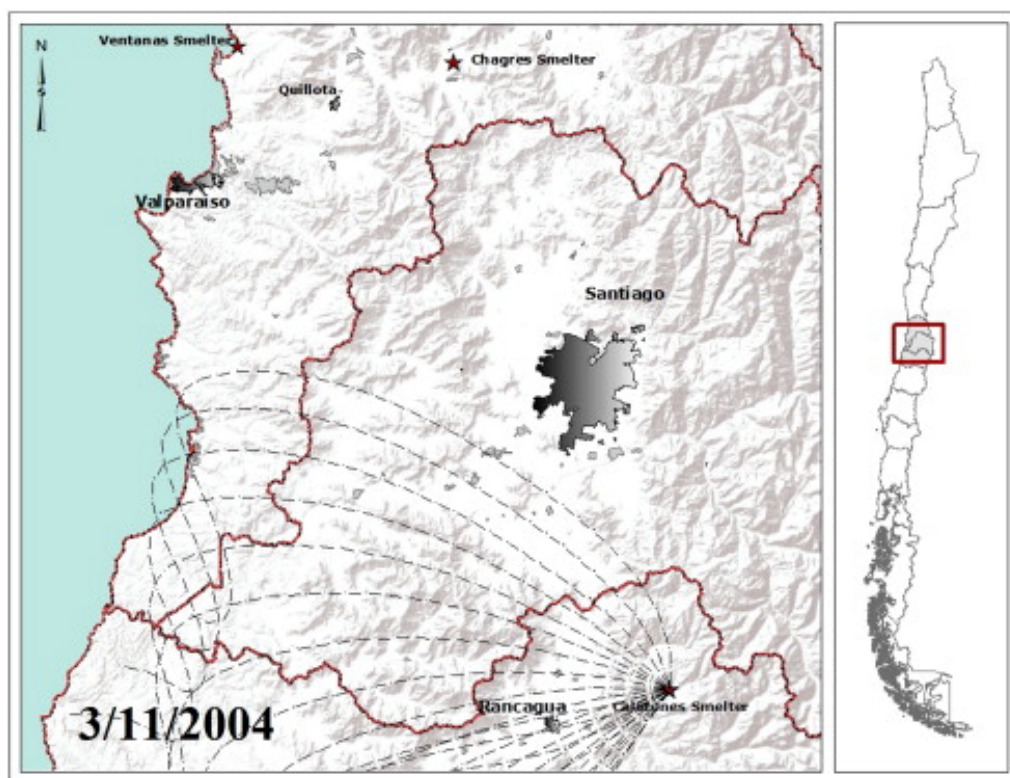


Figure 26 Forward trajectories starting a Caletones smelter on March 11th 2004.

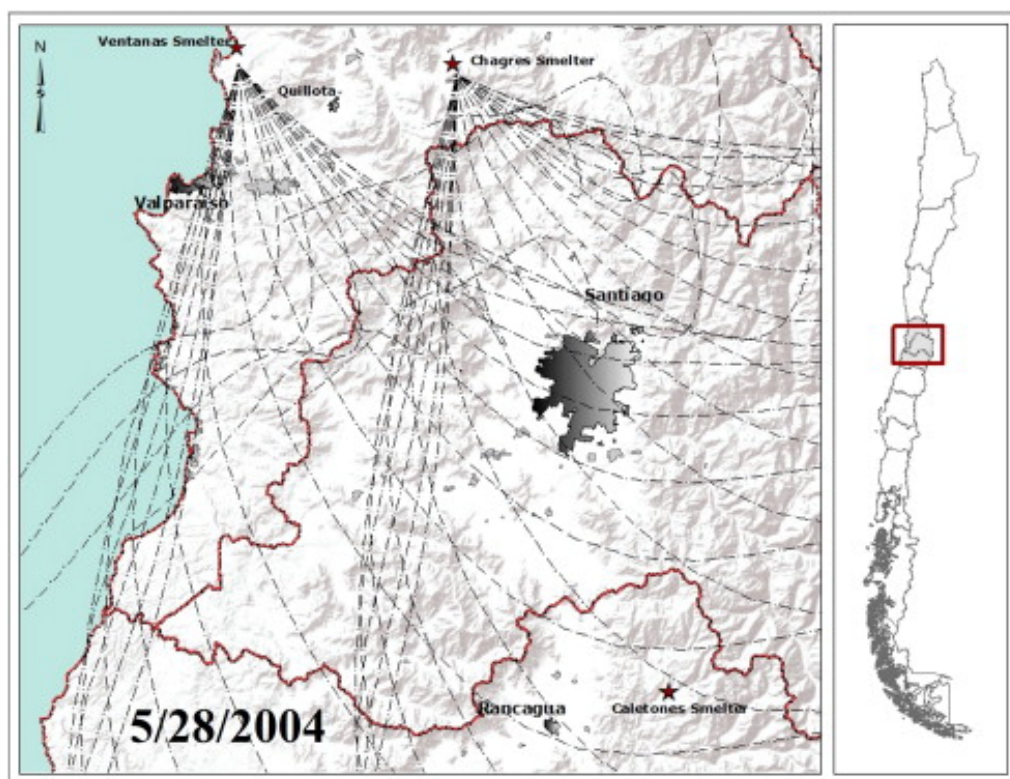


Figure 27 Forward trajectories starting a Chagres and Ventanas smelters on May 28th 2004.

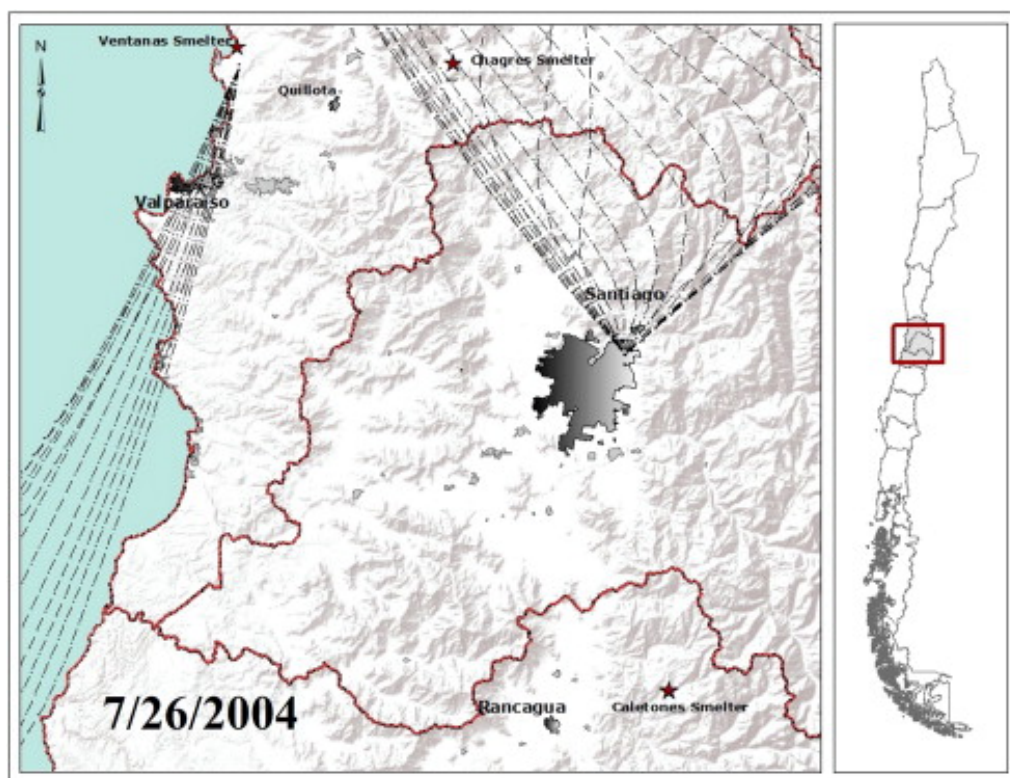


Figure 28 Backward trajectories arriving at monitor site on July 26th 2004.

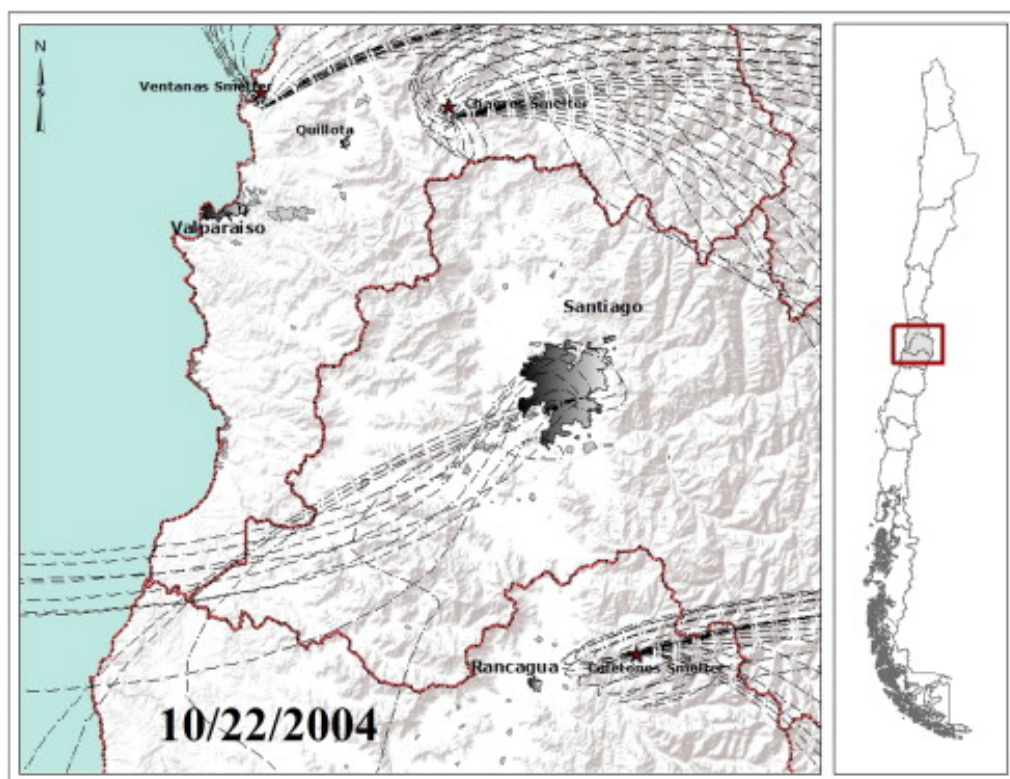


Figure 29 Forward trajectories starting at the copper smelters and backward trajectories from the monitor site on March 11th 2004.

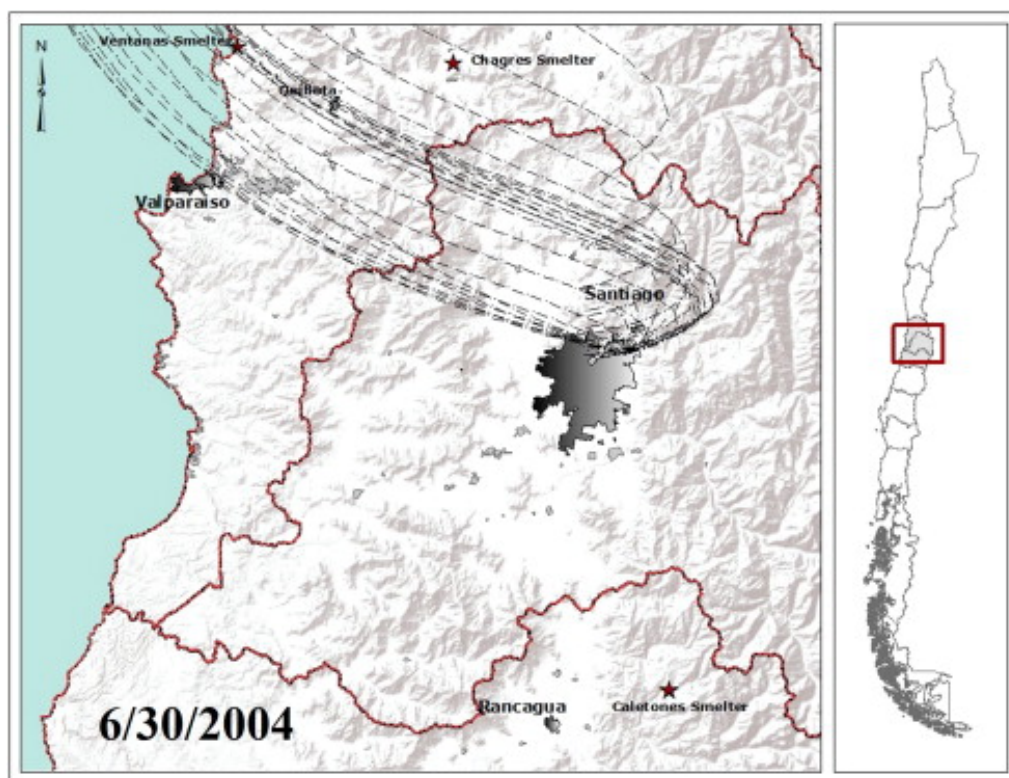


Figure 30 Backward trajectories arriving at monitor site on June 30th 2004.

Figure 31 shows a timeline plot of all six source contributions along the year; the seasonality of motor vehicles, wood burning and soil dust sources is clearly seen and regional contributions happen all year long. Table 11 summarizes the contributions to ambient $PM_{2.5}$ for the six sources identified; the values have been obtained using multiple linear regressions where we have dropped the constant term for not being significant; the six factor model explains 86% of the observed variance as measured by a linear regression of modeled versus observed $PM_{2.5}$.

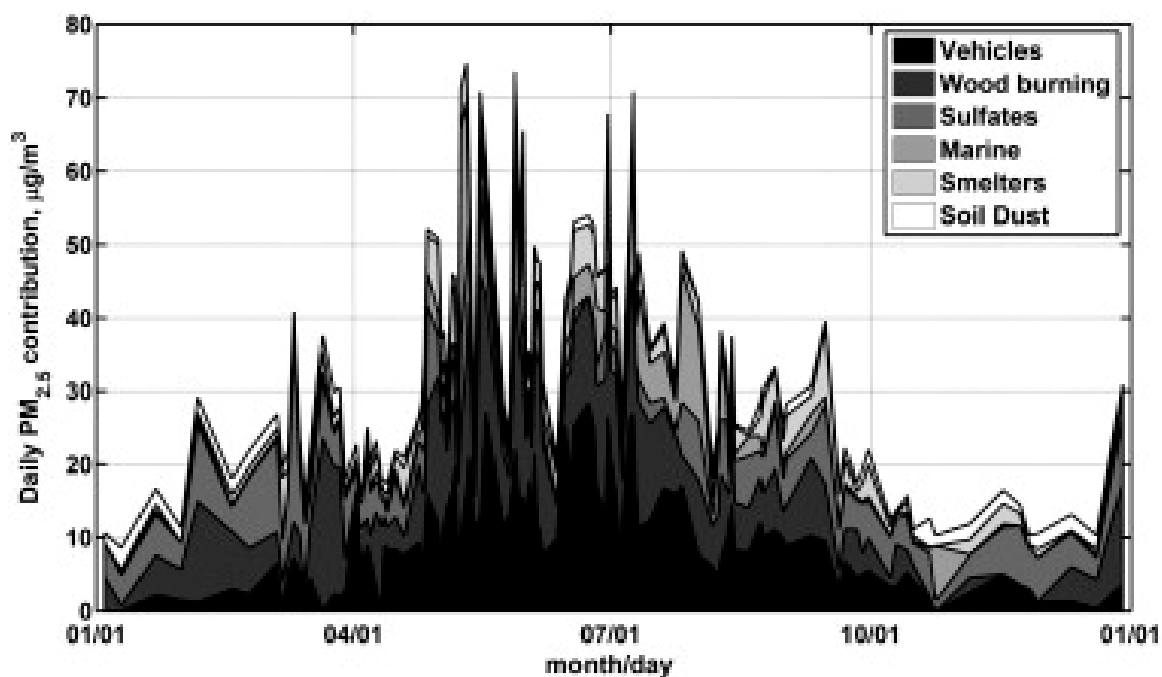


Figure 31 Timeline plot of estimated, ambient $PM_{2.5}$ source contributions, 2004 campaign.

Table 11 Source apportionment results for 2004 campaign.

| Source | Coefficient [$\mu\text{g}/\text{m}^3$] | Std. dev. [$\mu\text{g}/\text{m}^3$] |
|----------------|--|--|
| Vehicles | 9.99 | 1.07 |
| Wood burning | 9.27 | 1.04 |
| Sulfates | 5.20 | 0.80 |
| Marine aerosol | 3.18 | 0.47 |
| Smelters | 3.12 | 1.06 |
| zDust | 1.29 | 0.76 |

3.6.3. Receptor modeling results for the 1999 $PM_{2.5}$ data

Applying the same methodology as in Section 3.6.2, we have found again that a six-factor solution explains well the measured $PM_{2.5}$ concentrations. The statistical results for the 15 species fitted are shown in Table 12. Most fitted elements have regression coefficients (R^2) greater than 0.9, except Cu ($R^2 = 0.80$).

Table 12 Regression diagnostics for a 6 factor solution, 1999 data.

| Species | Intercept | Slope | Std. error | R ² |
|---------|-----------|-------|------------|----------------|
| BC | 222.2 | 0.941 | 682.3 | 0.944 |
| Al | 9.3 | 0.953 | 18.3 | 0.990 |
| Si | 40.1 | 0.920 | 41.6 | 0.991 |
| S | 60.8 | 0.952 | 145.1 | 0.979 |
| Cl | 4.8 | 0.855 | 4.9 | 0.958 |
| K | - 3.0 | 0.994 | 27.3 | 0.895 |
| Ca | 41.3 | 0.787 | 30.0 | 0.961 |
| Ti | - 1.4 | 1.038 | 3.4 | 0.969 |
| Mn | 0.0 | 0.983 | 1.8 | 0.934 |
| Fe | - 5.8 | 1.010 | 22.4 | 0.990 |
| Cu | 4.3 | 0.790 | 5.8 | 0.802 |
| Zn | 1.1 | 0.960 | 5.2 | 0.944 |
| As | 0.5 | 0.973 | 4.6 | 0.977 |
| Br | 0.6 | 0.938 | 2.1 | 0.946 |
| Pb | 9.4 | 0.835 | 12.6 | 0.924 |

Sensitivity analysis of this six-factor solution were performed by applying the *Fpeak* parameter — cf. Section Methodology (section 3.5). The source profiles, in ng/m³, for the rotated solution with *Fpeak* = -0.2 that was the most plausible solution are shown in Table 13.

Table 13 Source profiles [ng/m³] for a 6 factor solution, 1999 data (*Fpeak* = -0.2).

| Species | Wood burning | Copper smelters | Secondary sulfates | Soil dust | Marine aerosol | Motor vehicles |
|---------|--------------|-----------------|--------------------|-----------|----------------|----------------|
| BC | 2022 | 118 | 583 | 292 | 589 | 2149 |
| Al | 2.5 | 16.7 | 7.6 | 165.1 | 28.1 | 29.8 |
| Si | 0.2 | 40.3 | 12.0 | 405.2 | 61.8 | 96.3 |
| S | 21.3 | 466 | 712 | 5.2 | 179 | 254 |
| Cl | 8.0 | 2.6 | 5.8 | 3.7 | 22.3 | 0.0 |
| K | 53.7 | 7.1 | 27.2 | 30.9 | 52.2 | 12.3 |
| Ca | 0.0 | 10.7 | 0.0 | 135.8 | 31.1 | 48.9 |
| Ti | 1.2 | 2.1 | 1.7 | 17.7 | 3.1 | 6.2 |
| Mn | 1.1 | 0.0 | 0.3 | 4.1 | 0.4 | 7.2 |
| Fe | 26.2 | 21.2 | 12.5 | 191.7 | 35.9 | 108 |
| Cu | 1.0 | 4.3 | 2.8 | 3.9 | 6.8 | 9.0 |
| Zn | 3.5 | 2.4 | 2.2 | 2.5 | 11.0 | 19.5 |
| As | 0.1 | 22.7 | 2.2 | 1.0 | 1.1 | 1.3 |
| Br | 8.2 | 0.4 | 1.6 | 0.0 | 3.0 | 3.1 |
| Pb | 35.2 | 2.0 | 0.7 | 0.2 | 6.7 | 33.9 |

The first source has the highest K concentration and the second largest in BC; the ratio K/Al for this profile is 21.5, close to the value of 18.3 reported by Rojas et al. (Rojas et al. 1990) for a wood burning profile at Santiago, so we identify it as the wood burning source. The second source has more than 90% of the As; the ratio S/As = 20.5 is similar to the value 16.5 found for a smelter profile at Rancagua by Kavouras et al. (Kavouras et al. 2001), so we identify it as copper smelter plumes reaching Santiago's basin. The third source has the highest S concentration measured so we identify it as the secondary sulfates source. The fourth source has most of crustal elements (Al, Ca, Ti, and Fe); the ratio Al/Si = 0.40 is closer to the values found by Kavouras et al. (Kavouras et al. 2001) for soil dust profiles at Valparaiso (0.39) and Viña del mar (0.42); the ratio Si/Fe = 2.1 is close to the results obtained in that same work at Rancagua (2.6) and Viña del Mar (2.0) hence this fourth source is a soil dust emission. The fifth source has most of chlorine so it is a marine aerosol plume mixed with wood burning (K) and sulfates. Finally the sixth source has most of BC, Mn, Fe, Cu, Zn and Pb suggesting motor vehicle emissions; the ratio Mn/Fe = 0.067 in this profile is close to the ratio measured in the motor vehicle profile for the 2004 data (0.070, see Table 9, and to the value of 0.068 obtained by Kavouras et al. (Kavouras et al. 2001) in Rancagua in 1998. These similarities confirm that this source is the motor vehicle emission.

An inspection of weekly seasonality of source contributions — see Figure 32 — shows the same patterns observed for the 2004 results, so the sources are the same ones identified in the 2004 campaign data. Correlation of source contributions and ambient temperatures also has a similar behavior as in the 2004 campaign; in Figure 33 the clear correlations are for soil dust, motor vehicles and wood burning whereas all regional sources show no clear trend with ambient temperatures.

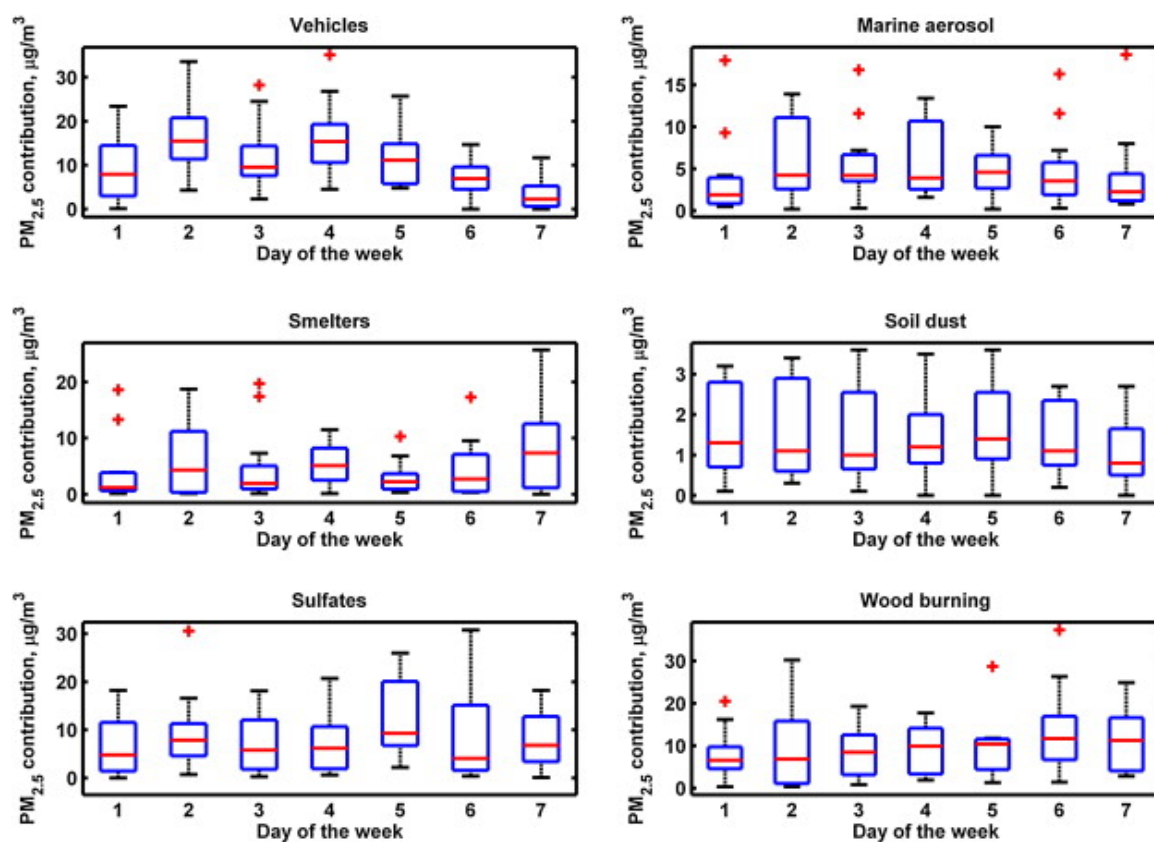


Figure 32 Box plots of estimated, ambient PM_{2.5} source contributions by day of the week, 1999 campaign.

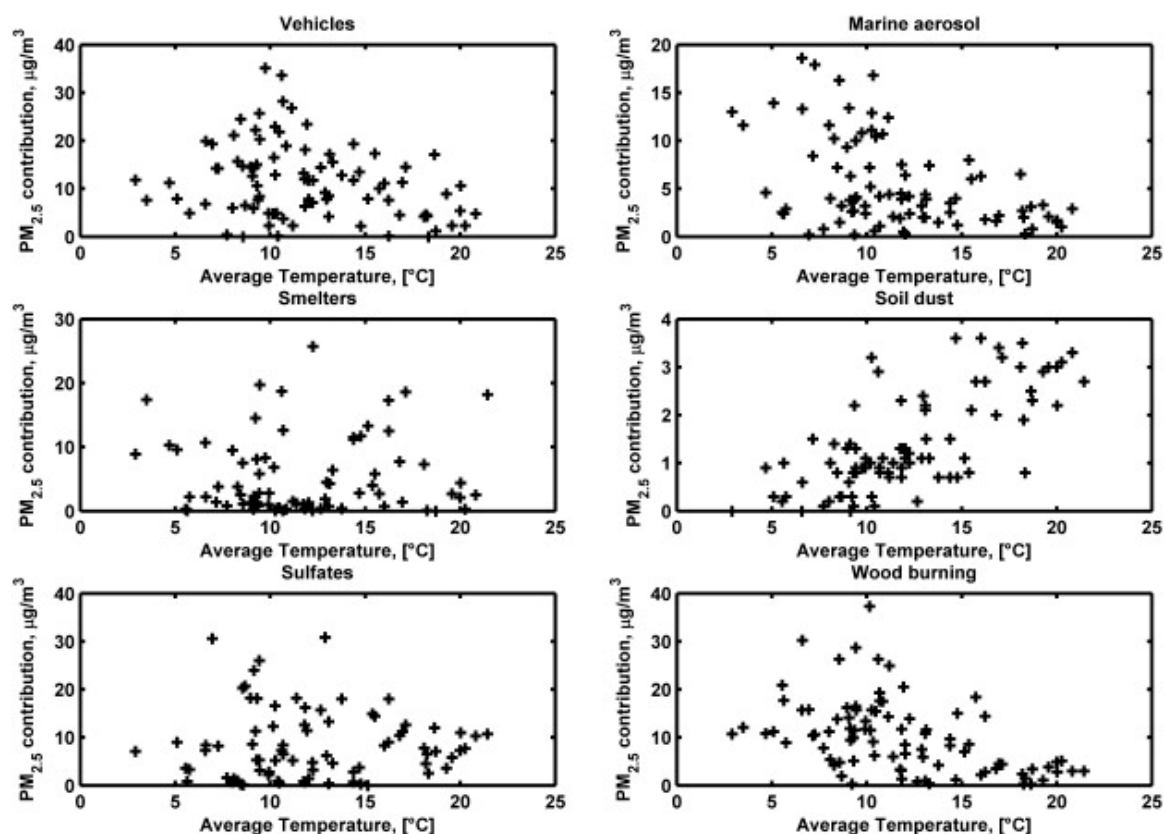


Figure 33 Scatterplots of estimated, ambient $PM_{2.5}$ source contributions versus mean daily temperatures, 1999 campaign.

Using HYSPLIT wind trajectories for the days with distinctively high contributions from the six sources we obtain analogous results as before — see Table 14 for a summary of findings and Figure 34, Figure 35, Figure 36 and Figure 37. Table 15 presents the regression results and the six source contributions for the 1999 campaign data and Figure 38 presents a timeline plot of the source contributions for the campaign period. The seasonality of local sources (vehicles, wood burning and soil dust) has the same pattern as in the 1999 results; for regional sources no significant seasonality is apparent, like in the 2004 results. The six factor model explains 90% of the observed variance as measured by a linear regression of modeled versus observed $PM_{2.5}$.

Table 14 Comparison of dominant source contributions and wind trajectory analysis for selected days, 1999 data.

| Date | Dominant source contribution | Source contribution, [$\mu\text{g}/\text{m}^3$] | Likely source(s) | Additional information |
|----------|------------------------------|---|--|------------------------|
| 7/6/99 | Smelters/Sulfates | 18.7/7.3 | Caletones, Chagres | HYSPLIT |
| 7/7/99 | Smelters/Sulfates | 19.7/3.1 | Caletones | HYSPLIT |
| 7/9/99 | Sulfates | 26.0 | Chagres | HYSPLIT |
| 7/10/99 | Sulfates/Smelters | 20.3/7.5 | Chagres, Ventanas | HYSPLIT |
| 7/16/99 | Smelters | 10.3 | Chagres | HYSPLIT |
| 7/19/99 | Marine/Sulfates | 17.9/8.2 | Coast WNW of Santiago + Ventanas + Chagres | HYSPLIT |
| 7/28/99 | Sulfates | 18.1 | Chagres, Ventanas | HYSPLIT |
| 8/3/99 | Sulfates | 30.6 | Chagres | HYSPLIT |
| 8/8/99 | Smelters | 25.7 | Chagres, Ventanas | HYSPLIT |
| 8/11/99 | Marine/dust | 16.8/13.5 | Coast SW of Santiago | HYSPLIT |
| 8/16/99 | Sulfates | 18.2 | Chagres, Ventanas | HYSPLIT |
| 8/19/99 | Sulfates/Marine | 8.6/13.4 | Ventanas | HYSPLIT |
| 8/22/99 | Smelters/Sulfates | 12.6/6.5 | Ventanas | HYSPLIT |
| 8/27/99 | Sulfates | 24.0 | Chagres, Ventanas | HYSPLIT |
| 9/18/99 | Smelters/Sulfates | 17.3/9.0 | Caletones | HYSPLIT |
| 9/26/99 | Sulfates | 18.2 | Chagres | HYSPLIT |
| 9/30/99 | Sulfates | 20.7 | Chagres, Ventanas | HYSPLIT |
| 10/5/99 | Marine/Sulfates | 12.9/5.2 | Chagres | HYSPLIT |
| 10/7/99 | Smelters/Sulfates | 5.8/14.4 | Caletones | HYSPLIT |
| 10/17/99 | Smelters/Sulfates | 12.5/18.0 | Chagres, Ventanas | HYSPLIT |
| 10/23/99 | Sulfates | 18.0 | Chagres | HYSPLIT |
| 10/27/99 | Sulfates | 13.3 | Chagres, Ventanas | HYSPLIT |
| 11/4/99 | Smelters/Sulfates | 7.7/10.4 | Caletones | HYSPLIT |
| 11/28/99 | Smelters/Sulfates | 18.2/10.7 | Caletones | HYSPLIT |

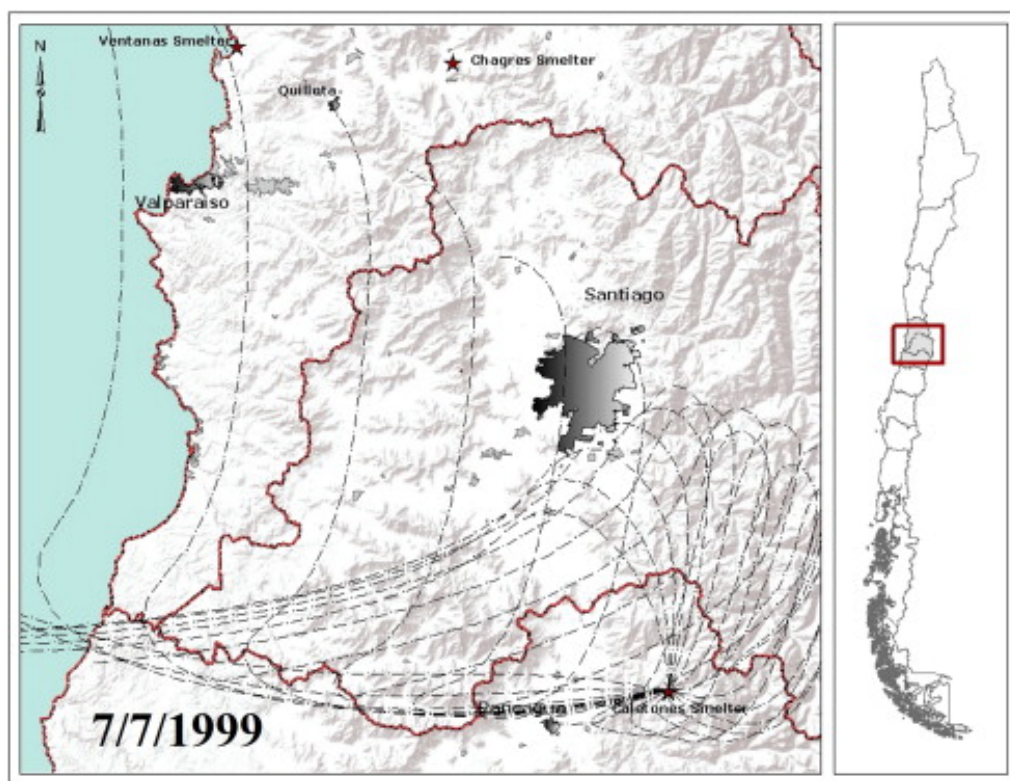


Figure 34 Forward trajectories starting at Caletones smelter on July 7th 1999.

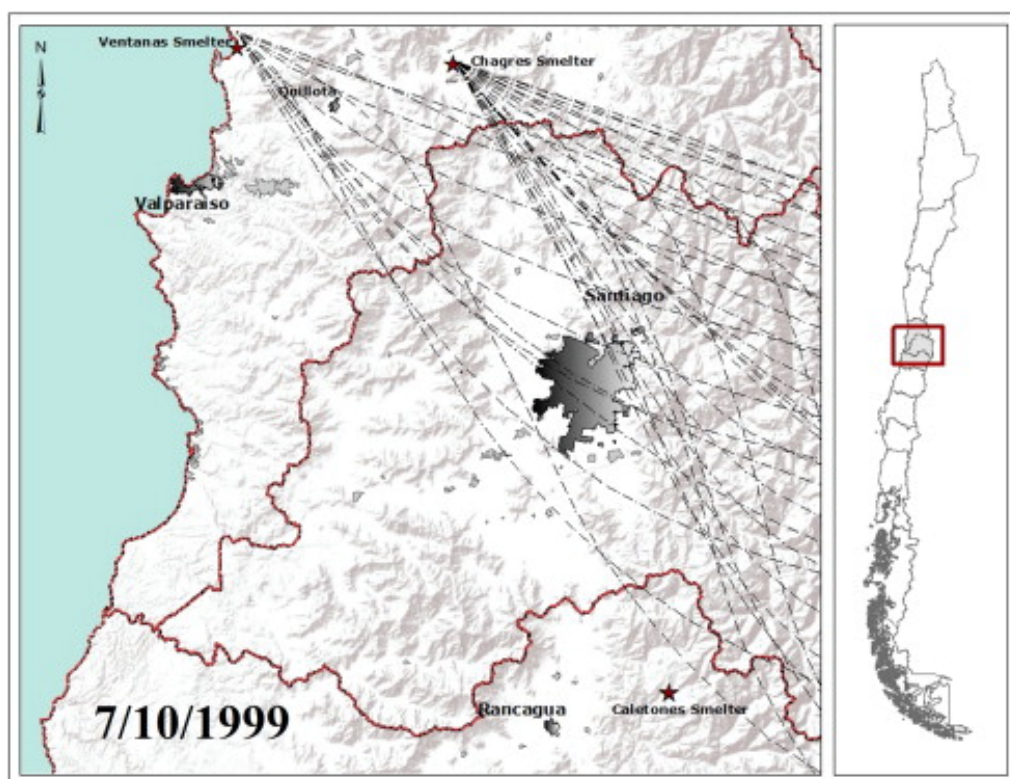


Figure 35 Forward trajectories starting at Ventanas and Chagres smelters on July 10th 1999.

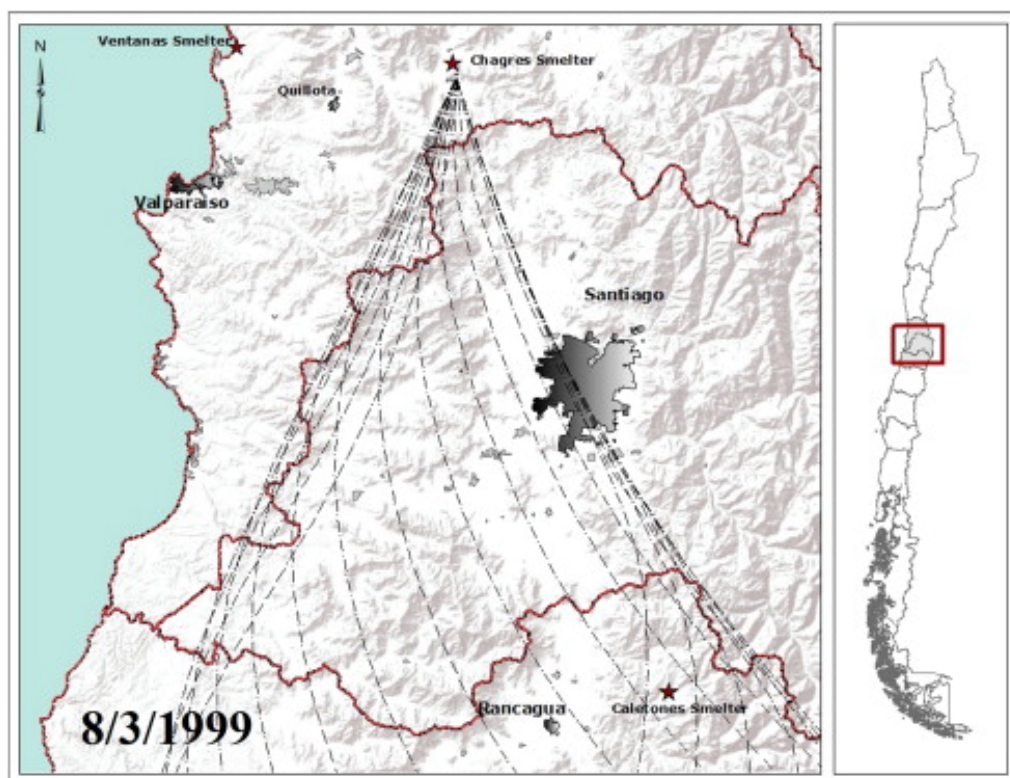


Figure 36 Forward trajectories starting at Chagres smelters on August 3th 1999.

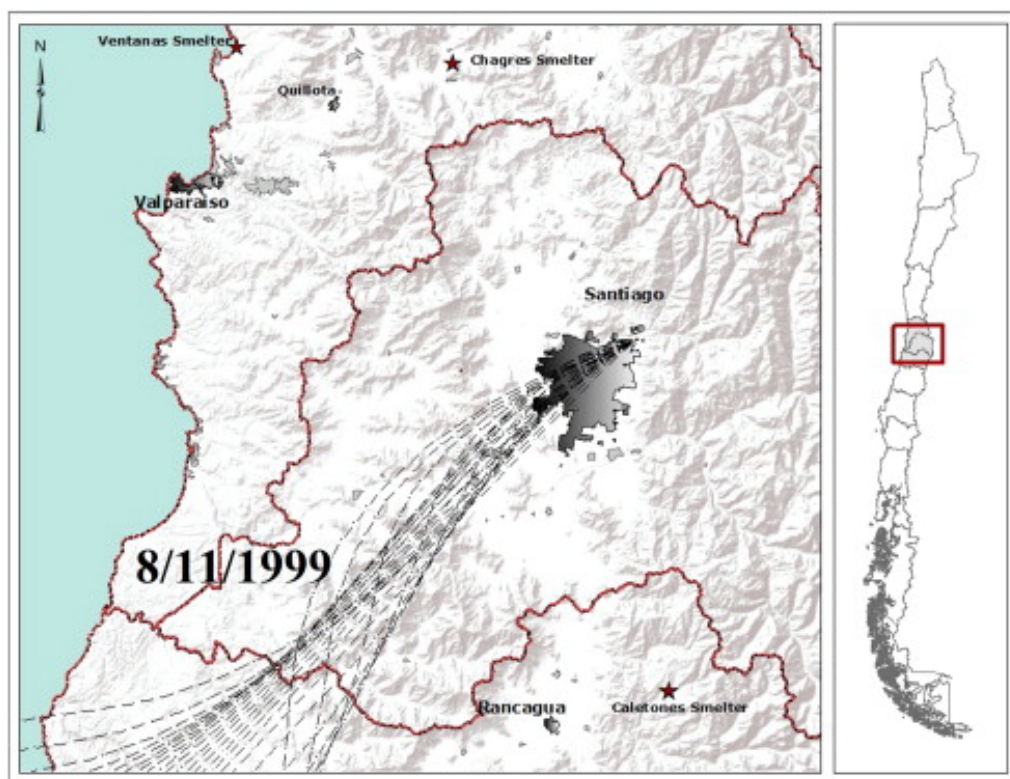
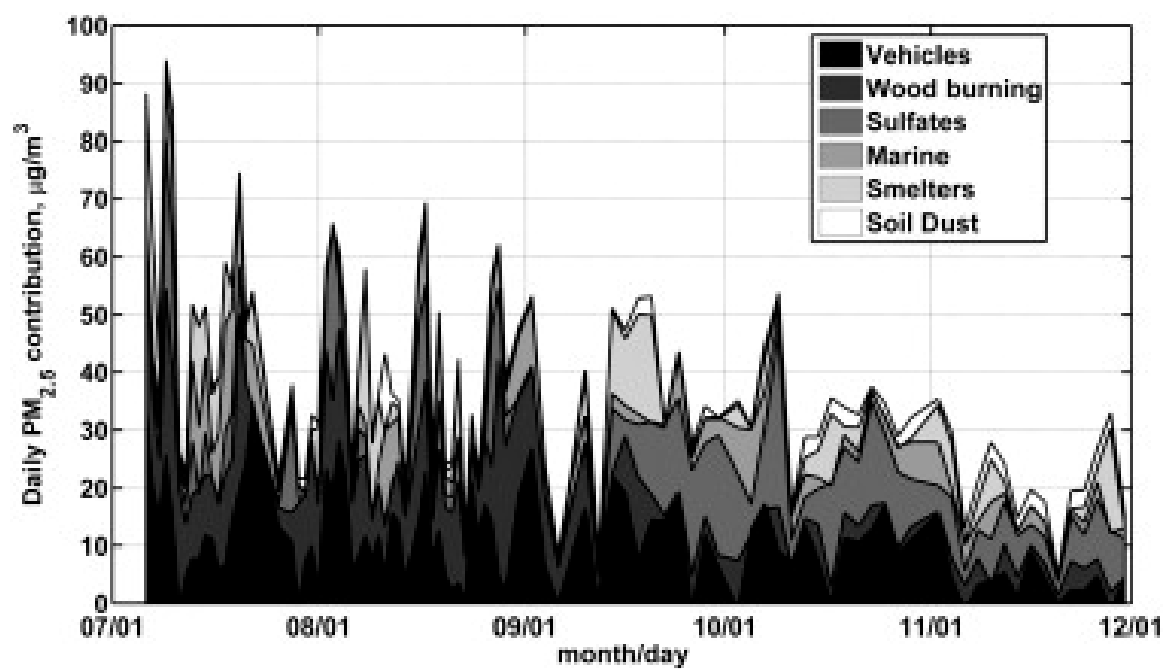


Figure 37 Backward trajectories arriving at monitor site on August 11th 1999.

Table 15 Source apportionment results for 1999 campaign.

| Source | Coefficient [$\mu\text{g}/\text{m}^3$] | Std. dev. [$\mu\text{g}/\text{m}^3$] |
|----------------|--|--|
| Vehicles | 10.58 | 0.95 |
| Wood burning | 9.39 | 0.85 |
| Sulfates | 7.11 | 0.65 |
| Marine aerosol | 4.93 | 0.79 |
| Smelters | 4.35 | 0.52 |
| Dust | 1.50 | 0.57 |

**Figure 38** Timeline plot of estimated, ambient $\text{PM}_{2.5}$ source contributions, 1999 campaign.

3.7. Discussion of results

Robustness of the PMF3.0 solution was tested by adding or discarding species considered in the receptor model. For the 2004 campaign data the two species with the lowest R^2 values (Ba and Cr) were discarded one at a time and altogether yet the resulting contributions were not statistically different from those shown in Table 11. For the 1999 data set the same analysis was done discarding BC concentrations and the resulting source contributions did not change significantly with respect to those in Table 15.

We comment here on the choice of sampling more days in fall and winter 2004 (85 samples) than in spring and summer 2004 (32 samples). Since the long term average of $PM_{2.5}$ is a key metric to assess public health impacts, we have computed monthly averages of the source apportionment results for 2004; with these averages we have estimated source contributions to $PM_{2.5}$ on an annual basis and compared them with the campaign average results in Figure 39; the major changes occur for motor vehicles that reduce their contribution to 27.5% and sulfates and dust that increase their contributions to 20.4% and 5.6%, respectively, with respect to the campaign average values. All changes shown in Figure 39 are within the estimated uncertainties shown in Table 11 hence the non-uniform sampling has a small effect on the relative source contributions estimated for 2004.

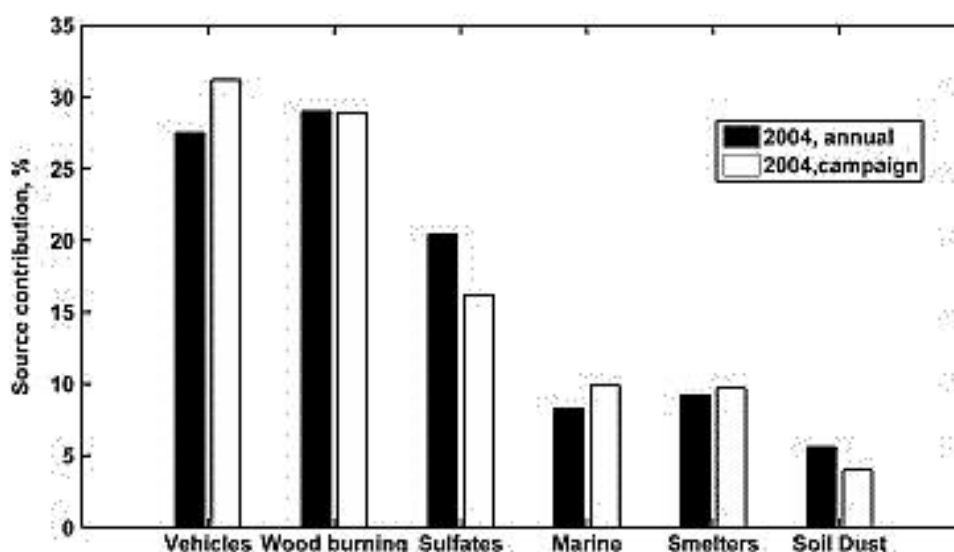


Figure 39 Comparison of campaign average and annual average source contributions for the 2004 $PM_{2.5}$ campaign.

We have also estimated average source contributions for July through November 2004 to make a detailed comparison with the receptor model results for the 1999 campaign; Figure 40 shows that a clear reduction on $PM_{2.5}$ has been achieved for all sources between 1999 and 2004; this is consistent with the observed reduction in ambient $PM_{2.5}$ at Santiago at that site: 34.2 and 25.1 $\mu g/m^3$ between 1999 and 2004, respectively, for the integrated, 24 h filter samples.

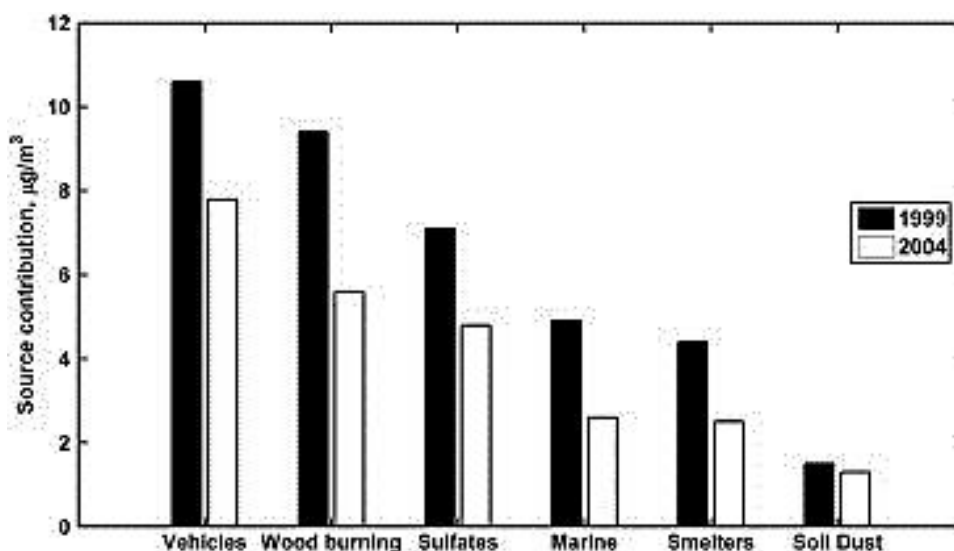


Figure 40 Comparison of July–November source contributions [$\mu g/m^3$] for the 1999 and 2004 $PM_{2.5}$ campaigns.

Contribution of copper smelters to ambient $PM_{2.5}$ has been detected before in the chemical composition of ambient samples taken at Santiago (P. Artaxo 1996; P. Artaxo 1998; Paulo Artaxo, Oyola, and Martinez 1999) but it had not been quantified as a single source contribution before. Dispersion of copper smelter emissions has been modeled at the regional scale by Olivares et al. (Olivares et al. 2002), Gallardo et al. (Gallardo et al. 2002) and by Gidhagen et al. (Gidhagen et al. 2002); the first two works were focused on SO_2 and sulfates and they did not produce an estimate of primary smelter contributions to ambient $PM_{2.5}$. Gidhagen et al.'s work (Gidhagen et al. 2002) was focused on modeling copper smelters As contributions to ambient PM_{10} in central and northern Chile; these authors also carried out a source apportionment and found that As contributions from copper smelters were far more important than As coming from soil dust suspension.

Kavouras et al. (Kavouras et al. 2001) have conducted source apportionment studies at several cities in Chile, and found at Rancagua — 80 km south of Santiago, see Figure 17 — a clear copper smelter profile accounting for 26% of ambient $PM_{2.5}$. Hedberg et al. (Hedberg, Gidhagen, and Johansson 2005) carried out source apportionment of ambient PM_{10} in year 2000 at two small cities: Quillota (see Figure 17) and Linares, 300 km south of Santiago. For Quillota — located at 20 km east of the Pacific Ocean — contributions of the Ventanas and Chagres copper smelters to ambient PM_{10} were between 10 and 16% depending on the season; since soil dust and marine aerosol contributions to PM_{10} were significant we infer that the smelters contributions to ambient $PM_{2.5}$ at Quillota must have been higher than 20% that year. They have also estimated that the Caletones smelter was impacting Quillota and we have found by using wind trajectory analysis that in some meteorological conditions that indeed happens — see Figure 34.

Our results for July 6th-10th in Table 14 can be compared with those of Gallardo et al. (Gallardo et al. 2002) who modeled contributions of the three copper smelters to ambient sulfate concentrations measured at Downtown Santiago (site N in Figure 17). We agree with them that on July 6th–7th the Caletones smelter is responsible for the measured sulfate at site N and that on July 9th–10th the Caletones smelter is not contributing at all to sulfates there. We also agree with those authors that under conditions of downslope easterly wind the Caletones smelter plume can reach Santiago while the other two smelter plumes cannot; our results in Table 10 and Table 14 support that interpretation and Figure 26 and Figure 34 show examples of such meteorological conditions.

In this work we explicitly quantify, for the very first time, smelters contributions to ambient $PM_{2.5}$ at Santiago as two distinct sources: primary emissions and secondary sulfates. Furthermore, we show that all copper smelters surrounding Santiago contribute to ambient $PM_{2.5}$, depending upon meteorology. Sometimes W, NW or WNW winds transport air masses from the Ventanas and Chagres smelters towards Santiago — see Figure 30, — sometimes downslope easterly flow develops and the Caletones smelter plume reaches Santiago — see Figure 34. Our estimate of primary smelter contribution at Santiago in 1999 is $11.4 \pm 1.4\%$, a value significantly lower than the estimated primary

contribution of smelters at Quillota for the $PM_{2.5}$ fraction in 2000 (Hedberg, Gidhagen, and Johansson 2005); thus our results are consistent with the smelters' impact estimated at a receptor closer to those sources. We also conclude that our results for the smelter contributions at Santiago are lower bounds of actual contributions to ambient $PM_{2.5}$ at populated areas (gray areas in Figure 17) *closer* to the copper smelters — recall that in 1998 copper smelters contributed with 26% of $PM_{2.5}$ at Rancagua (Kavouras et al. 2001). Comparison of annual As concentrations at Santiago — Table 6 and Table 7 — and those of cities closer to the copper smelters (MMA: Ambiente Ministerio del Medio 2012) also support this conclusion.

The sulfate contribution to $PM_{2.5}$ at Santiago has been reduced from 50% in the late 80s (Rojas et al. 1990) to ~ 19% in 1999 and ~ 16% in 2004. Regarding our estimates we have to consider that SOx ($SO_2 + SO_3$) emissions coming from the Ventanas and Chagres industrial zones also include emissions from thermal power plants and several industries located therein; furthermore there are also SOx sources near Santiago (see Figure 17). Since the receptor model results cannot discriminate more than one sulfate source, a feasible way to quantify all contributions to secondary sulfates at Santiago is to carry out dispersion modeling of all SOx sources. Thus we acknowledge that our estimates of the ‘smelters’ + ‘sulfates’ contributions are upper bounds of the total copper smelters contributions to ambient $PM_{2.5}$ at Santiago.

We also conclude that *part* of the reduction in ambient $PM_{2.5}$ at Santiago between 2000 and 2011 - see Figure 18 and Figure 40 - is a result of the increasing regulations upon regional copper smelters and *not* from just regulating local sources at Santiago. Emissions of SO_2 from the Caletones and Ventanas smelters have been decreasing between 1990 and 2011 (MMA: Ambiente Ministerio del Medio 2012), although As emissions have been actually increasing between 2008 and 2011 (CODELCO 2012). Emissions from the Chagres smelter have been reduced since 1990 as a consequence of an improvement in the emission abatement process (Anglo American 2012). Since it is likely that all smelters currently contribute to ambient $PM_{2.5}$ in the urban areas shown in Figure 17, we conclude that further regulations are required upon those industrial sources.

Chlorine has been measured in ambient $\text{PM}_{2.5}$ samples at Santiago in previous studies, but its origin had not been clearly identified before; in some cases it has been found mixed with soil dust (Paulo Artaxo, Oyola, and Martinez 1999) or identified by microscopic analysis (Rojas et al. 1990) but not quantified as a single source; in this work we show that marine aerosol does intrude into Santiago's basin with SW, W and WNW circulations. This marine aerosol is mixed with soil dust, wood burning from rural areas and industrial emissions from copper smelters and coal-fired power plants — see Figure 29 and Figure 37 — this also explains why receptor model results show mixed source profiles diagnosed by negative values of the F_{peak} parameter in the PMF results. A dispersion model may help in quantifying the relative contributions of sea salt, soil dust, wood burning, etc. within the ‘marine aerosol’ source identified in this work.

Soil dust has long been recognized as a source in $\text{PM}_{2.5}$ at Santiago, although mixed with industrial and wood burning sources (Rojas et al. 1990; Paulo Artaxo, Oyola, and Martinez 1999), so its contribution to total $\text{PM}_{2.5}$ was an upper bound, estimated at 12% by Rojas et al. (Rojas et al. 1990) and at 15% by Artaxo et al. (Paulo Artaxo, Oyola, and Martinez 1999). In this work we find a clearly distinctive soil dust profile that accounts only for 4% of the $\text{PM}_{2.5}$ mass, with a source profile that has little contribution from traffic emissions like carbonaceous particles, Pb and Br and from other anthropogenic trace elements. We think that our estimate is a sharper one because of the receptor model used in this work: it is known that *positive matrix factorization* is able to resolve more sources than alternate methods do (Willis 2000) because it poses the receptor model problem in a different mathematical setting than other methodologies do (Paatero 1997). This result for the soil dust contribution — and its seasonality — is also relevant for constraining diffuse sources such as street dust suspended by traffic at Santiago (Hector Jorquera and Castro 2010). We also acknowledge that the soil dust estimate for 2004 is not a significant one ($p = 0.11$) but we have decided to keep it because it is usual that smaller sources are difficult to be resolved by receptor models — perhaps more data points are required for a robust estimate — and because its retention in the solution makes results comparable for the 1999 and 2004 ambient campaigns.

Another implication of our results has to do with forecasting $\text{PM}_{2.5}$ at Santiago: current levels of daily ambient $\text{PM}_{2.5}$ observed at Santiago — see Figure 19 — imply that an early warning system needs to be implemented like the current operational PM_{10} forecast for Santiago (MMA: Ministerio del Medio Ambiente 2012). The results found in the present work suggest that under specific meteorological conditions regional sources may contribute to ambient $\text{PM}_{2.5}$ in a non-negligible amount and that those specific conditions may happen all year long — see daily $\text{PM}_{2.5}$ values above $35 \mu\text{g}/\text{m}^3$ in Figure 19 in spring and summer at all monitoring stations — this has to be considered in developing $\text{PM}_{2.5}$ forecasting systems. For instance, a forecasting approach based on *local* correlation of CO and $\text{PM}_{2.5}$ (Saide et al. 2011) may suffer from biases brought by unaccounted regional sources. As another example the current ambient PM_{10} operational forecast at Santiago (MMA: Ministerio del Medio Ambiente 2012) is based upon a multiple linear regression using as predictors synoptic scale meteorology — which is appropriate for including regional wind patterns - but without considering emission data from copper smelters — a shortcoming likely to induce some forecast bias. Finally, in order to properly model regional source contributions reaching Santiago a high spatial resolution is needed to consider the complex terrain surrounding all three copper smelters and their pathways towards Santiago, perhaps using an adaptive grid scheme to reduce numerical diffusion (Garcia-Menendez et al. 2010).

3.8. Conclusions

We have applied a receptor model analysis to integrated 24 h ambient $\text{PM}_{2.5}$ concentrations taken in 2004 (117 samples) and in 1999 (95 samples) at the same site in Santiago. For both campaigns, the same six sources were found and their relative contributions in 1999/2004 are: motor vehicles: $28 \pm 2.5/31.2 \pm 3.4\%$, wood burning: $24.8 \pm 2.3/28.9 \pm 3.3\%$, sulfates: $18.8 \pm 1.7/16.2 \pm 2.5\%$, marine aerosol: $13 \pm 2.1/9.9 \pm 1.5\%$, copper smelters: $11.5 \pm 1.4/9.7 \pm 3.3\%$ and soil dust: $3.9 \pm 1.5/4.0 \pm 2.4\%$. Hence relative contributions are statistically the same but the absolute contributions have been reduced because ambient $\text{PM}_{2.5}$ has been reduced between 1999 and 2004 at Santiago. This is a robust result because those two campaigns were conducted at different times and analyzed with different techniques at different laboratory facilities.

This is the very first time that so many sources of $\text{PM}_{2.5}$ have been clearly identified in Santiago, especially copper smelters (primary emissions and secondary sulfates) and marine aerosol. We have confirmed source identification by adding information from wind trajectories computed using NOAA's HYSPLIT modeling tool and the MODIS burned area product to check seasonality and location of wood burning sources. Using this combined methodology we have shown that: a) marine air masses do reach Santiago's basin in significant amounts, often combined with anthropogenic sources; b) all copper smelters surrounding Santiago contribute to ambient $\text{PM}_{2.5}$; c) wood burning is the second largest source, coming from residential wood burning in fall and winter and from regional wildfires in spring and summer.

Since ambient $\text{PM}_{2.5}$ at Santiago has been reduced from 1999 to 2011 — Figure 18 — this suggests that both local and regional sources must have decreased their emissions and we have shown that this is the case for the 1999–2004 period — see Figure 40; nonetheless there are still spring and summertime daily concentrations that exceed $35 \mu\text{g}/\text{m}^3$ across the city, which suggests that regional sources still influence ambient $\text{PM}_{2.5}$ at Santiago.

The results of the present analysis can be used to improve emission inventories, air quality forecasting systems and cost–benefit analysis at local and regional scales. For the mixed sources found — such as sulfates and marine aerosol — further source apportionment may be accomplished by conducting dispersion modeling of the participating sources.

3.9. Acknowledgments

Financial support for this work was provided by Fondecyt grant 1050662. We thank Mr. Victor Berrios and Mrs. Edith Balcarce (Autoridad Sanitaria de la Región Metropolitana, (www.asrm.cl)) for providing the filters sampled for 2004, to Mr. Roberto Martínez (Environmental Ministry, www.mma.gob.cl) for providing the 1999 campaign database and to Mr. Steven Kohl for the chemical analysis performed at the Desert Research Institute (www.dri.edu); they have provided valuable insights and comments upon technical details of ambient monitoring and chemical analysis. Comments and suggestions from two reviewers have significantly improved the original manuscript. We also thank CONICYT for a doctoral fellowship grant awarded to one of us (F. Barraza). The research described in this article has not been subjected to any review by the funding or collaborating institutions so it does not necessarily reflect their views and no official endorsement should be inferred.

4. INDOOR $PM_{2.5}$ IN SANTIAGO, CHILE, SPRING 2012: SOURCE APPORTIONMENT AND OUTDOOR CONTRIBUTIONS

4.1. Highlights

- First source apportionment of indoor $PM_{2.5}$ conducted at Santiago, Chile.
- Outdoor and indoor sources each contribute half of the measured indoor $PM_{2.5}$.
- Traffic and indoor cooking are the strongest sources of indoor $PM_{2.5}$.
- Indoor concentrations of $PM_{2.5}$ were affected by socioeconomic status.

4.2. Graphical abstract

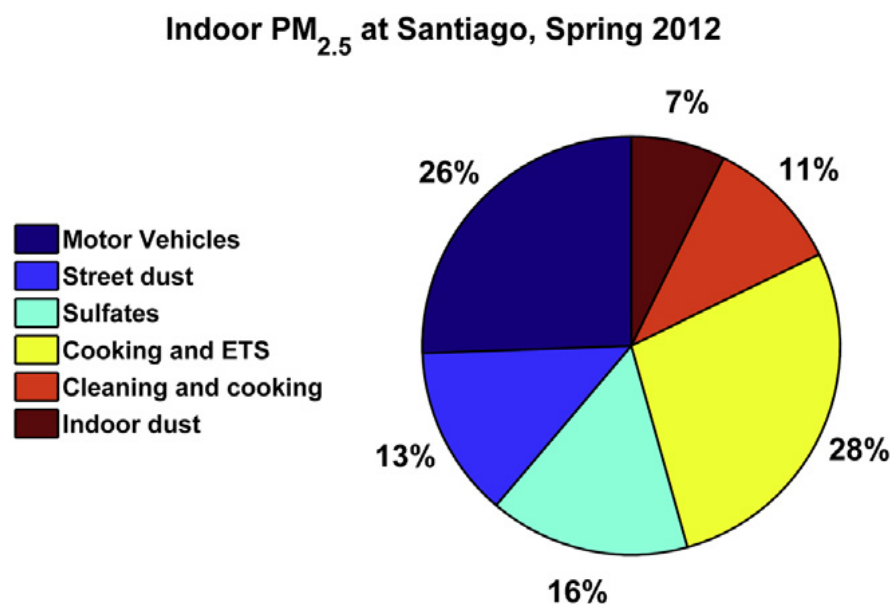


Figure 41 Graphical abstract: Indoor $PM_{2.5}$ in Santiago, Chile, spring 2012: Source apportionment and outdoor contributions

4.3. Abstract

Indoor and outdoor PM_{2.5} sampling campaigns were carried out at Santiago, Chile (6 million inhabitants, 33.5°S, 70.6°W) in spring 2012. A pair of samplers was placed inside each household studied and an additional pair of samplers was placed at a fixed outdoor location for measuring trace elements and elemental (EC) and organic carbon (OC) in Teflon and quartz filters, respectively. A total of 47 households in downtown Santiago were included in this study. Mean outdoor and indoor PM_{2.5} concentrations were 19.2 and 21.6 µg/m³, respectively. Indoor concentrations of PM_{2.5} were affected by socioeconomic status ($p = 0.048$) but no such evidence was found for PM_{2.5} species, except lead ($p = 0.046$). Estimated species infiltration factors were 0.70 (± 0.19), 0.98 (± 0.21), 0.80 (± 0.12) and 0.80 (± 0.03) for PM_{2.5}, OC, EC and sulfur, respectively. Estimated household infiltration factors had a median of 0.75, mean of 0.78, standard deviation of 0.18 and interquartile range (IQR) 0.67 - 0.86.

For the very first time, Positive Matrix Factorization (PMF3) was applied to an indoor PM_{2.5} chemical composition data set measured at Santiago. Source identification was carried out by inspection of key species and by comparison with published source profiles; six sources were identified. Three of them were outdoor contributions: motor vehicles with 5.6 (± 0.7) µg/m³, street dust with 2.9 (± 0.5) µg/m³ and secondary sulfates with 3.4 (± 0.5) µg/m³. The indoor sources were: indoor dust with 1.6 (± 0.3) µg/m³, cleaning and cooking with 2.3 (± 0.3) µg/m³ and cooking and environmental tobacco smoke with 6.1 (± 0.7) µg/m³. There is potential for further reducing PM_{2.5} population exposure in the short term - by improving ventilation of indoor air and controlling indoor sources - and in the long term - with filtration of outdoor air and household improvements to reduce air change rates.

4.4. Introduction

Indoor suspended particulate matter (PM) consists of ambient particles that infiltrate indoors and remain suspended, particles emitted indoors (primary), and sometimes particles formed indoors (secondary) through reactions of gas-phase precursors emitted both indoors and outdoors (Weschler and Shields 1997). Outdoor particles can enter indoor environments by convection (through an open window or by the air conditioning system) or by infiltration through cracks and fissures in the housing envelope. These two combined mechanisms determine the residence time of air — or its reciprocal, the air exchange rate, AER — within a household. Outdoor PM_{2.5} can be a significant contributor to indoor particle concentrations, especially when AERs are high (Abt et al. 2000; Q Y Meng et al. 2005). When indoor sources are present, indoor PM concentrations can be substantially higher than outdoor PM concentrations (Ruiz et al. 2010; Q. Zhang et al. 2010). Indoor anthropogenic PM sources include smoking, cooking, unvented space heaters, cleaning, washing and walking (Chao, Tung, and Burnett 1998; Abt et al. 2000; W. X. Zhao et al. 2006; W. Zhao et al. 2007; Abdullahi, Karimatu L., Delgado-Saborit, Juana Maria Harrison, Roy M. 2013).

Several mechanistic and statistical models have been applied to quantitatively describe factors modifying indoor PM. There are two approaches that have been applied: i) models that assume a well-mixed indoor air volume, like the steady state, single-zone mass balance (Abt et al. 2000; Ott, Wallace, and Mage 2000), and ii) models that regard each household as several compartments (rooms) which may or may not be well-connected depending on when and how internal doors are opened. Both approaches are described in the following paragraphs.

4.4.1. Single zone indoor air quality models

The single zone mass balance model describes households as completely mixed flow reactors, where the indoor PM concentration depends on the outdoor PM concentration in the following way (Abt et al. 2000; Q Y Meng et al. 2005):

$$C_I = \frac{PaC_O}{a+k} + \frac{Q_I}{V(a+k)} \equiv F_{INF}C_O + C_{IG}$$

Equation 8 *single zone mass balance model*

Where C_I and C_O are the measured indoor and outdoor $PM_{2.5}$ ($\mu g/m^3$), respectively, P is the penetration coefficient (dimensionless), a is the household air exchange rate (AER, h^{-1}), Q_I the rate of indoor generation and resuspension of PM ($\mu g/h$), k the rate of removal of PM by reaction or surface deposition (h^{-1}), and V the household volume (m^3). The term $Pa/(a+k)$ is called the infiltration factor (F_{INF}) and it quantifies the fraction of C_O that is found indoors; C_{IG} accounts for indoor-generated concentration. Contributions of outdoor sources to indoor $PM_{2.5}$ concentrations of 23-67% have been estimated in previous studies (Abt et al. 2000; Q Y Meng et al. 2005).

The Random Component Superposition (RCS) statistical model (Ott, Wallace, and Mage 2000) uses the linear regression of indoor on the outdoor PM concentration — equivalent to Equation 8 — to estimate means and distributions of the outdoor and indoor contributions to indoor PM concentrations. Other approaches include multivariate linear regression and receptor models (Abt et al. 2000; Qing Yu Meng et al. 2007; W. X. Zhao et al. 2006; W. Zhao et al. 2007).

4.4.2. Multi-zone indoor air quality models

Several approaches have been proposed to model the dynamics of indoor concentrations due to spatial and temporal variation of indoor sources, internal and external window and door opening activities, occupant's behavior, presence of air conditioning systems, etc. (Klepeis and Nazaroff 2006; Sohn et al. 2007; Du et al. 2012; Fabian, Adamkiewicz, and Levy 2012; McGrath et al. 2014). In this approach each housing unit is regarded as a set of rooms connected by internal doors or windows.

Briefly, multi zone models capture spatial and temporal variations in indoor pollutants that provide more information than the single-zone model. However the resources needed to apply those models are substantially higher: AERs need to be measured for each room and for different combinations of window and door positions, occupants' behavior and emission sources need to be resolved with high temporal and spatial detail and some physical parameters — deposition losses — need to be validated using actual measurements (McGrath et al. 2014).

4.4.3. Case study: Santiago, Chile

The greater metropolitan area of Santiago, Chile (33.5°S, 70.7°W) is the sixth largest South American city in population (6 million inhabitants). Ambient $PM_{2.5}$ has been measured at Santiago since 1989. Despite steady economic growth, ambient $PM_{2.5}$ concentrations have continuously decreased in the last 24 years (Sax et al. 2007; Hector Jorquera et al. 2004; Koutrakis et al. 2005; Moreno et al. 2010). Nonetheless, $PM_{2.5}$ ambient concentrations still exceed the World Health Organization (WHO) daily and annual guidelines of 25 and 10 $\mu\text{g}/\text{m}^3$, respectively (WHO: World Health Organization 2005).

Figure 42 shows the evolution of ambient $PM_{2.5}$ at four monitoring sites — from TEOM data, uncorrected for volatile losses. The decrease in ambient $PM_{2.5}$ across the city in the last years is ascribed to improvements of the public transportation system at Santiago, initiated in 2007.

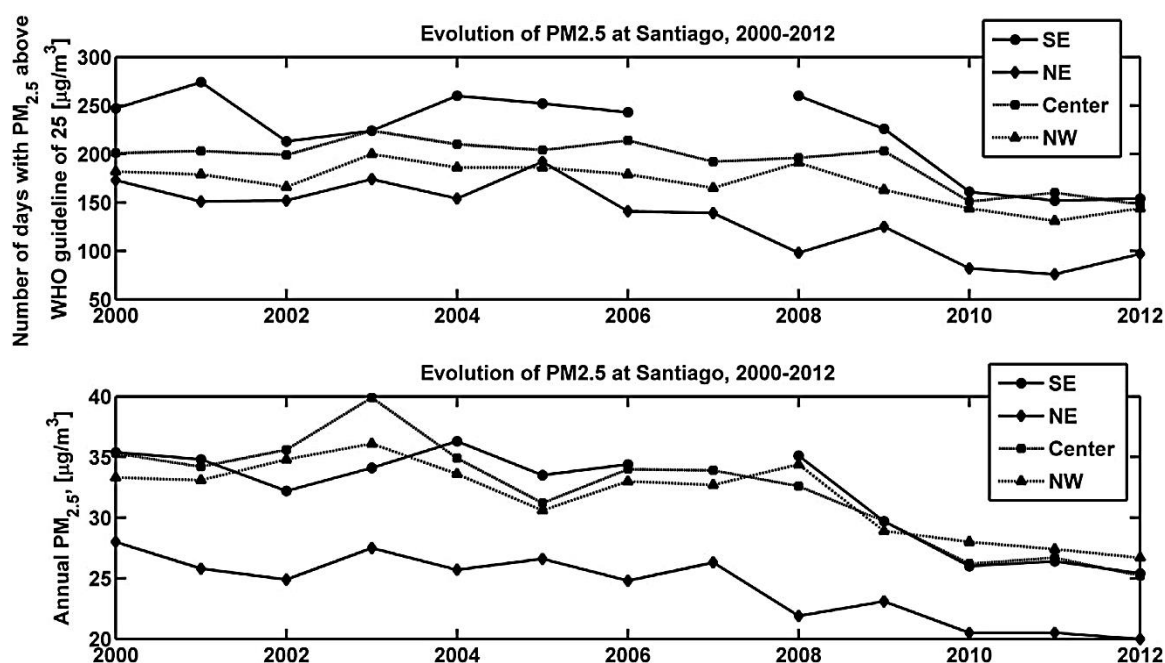


Figure 42 Trends in ambient $PM_{2.5}$ measured at Santiago, Chile, 2000-2012 (TEOM uncorrected data). The location of ambient $PM_{2.5}$ monitors is presented in the next figure.

Several studies have shown how the composition of outdoor $PM_{2.5}$ has evolved in the last years (Paulo Artaxo, Oyola, and Martinez 1999; Sax et al. 2007; Koutrakis et al. 2005; Héctor Jorquera and Barraza 2012) with decreasing trends in sulfur, lead and other anthropogenic elements. Few studies have characterized indoor $PM_{2.5}$ at Santiago; below we summarize them.

Rojas-Bracho et al. (Rojas-Bracho et al. 2002) measured personal, indoor and outdoor $PM_{2.5}$ concentrations for school children in Santiago's central and NE areas. Each participant carried a personal sampler, while Harvard Impactors (Marple et al. 1987), located in their homes, simultaneously collected 24 h samples in the winter of 1999 ($N = 20$). They found a slope (F_{INF}) of 0.61 ($p = 0.0001$) and an intercept (C_{IG}) of $18.9 \mu\text{g}/\text{m}^3$ ($p < 0.0001$) with $R^2 = 0.54$; the median I/O ratio was 0.95 and 10% of ratios were above 1.6.

Ruiz et al. (Ruiz et al. 2010) measured 48 h indoor and outdoor concentrations of $PM_{2.5}$ and its chemical components in winter 2007 at downtown and NE areas in Santiago.

A total of 16 households were measured — 13 apartments and 3 homes — to estimate contributions of unvented space heaters to indoor air pollution. Average outdoor $\text{PM}_{2.5}$ was $55.9 \mu\text{g}/\text{m}^3$, and average indoor $\text{PM}_{2.5}$ varied according to the type of space heater used. They found slope (F_{INF}) values of 0.64, 0.94, 0.66, 0.63 and 0.66 for $\text{PM}_{2.5}$, EC, OC, S and Al, respectively. The contributions of kerosene and LPG heaters to indoor $\text{PM}_{2.5}$ were 44.2 and $18.6 \mu\text{g}/\text{m}^3$, respectively. Elemental carbon (EC) was only generated by kerosene heaters with an average of $9.3 \mu\text{g}/\text{m}^3$ of $\text{PM}_{2.5}$ in those households. Organic carbon (OC) was generated by kerosene and LPG heaters in concentrations of 6.5 and $4.9 \mu\text{g}/\text{m}^3$, respectively.

Burgos et al. (Burgos, Ruiz, and Koifman 2013) compared indoor and outdoor $\text{PM}_{2.5}$ in the west side of Santiago where families were relocated from slums to public housing apartments. The campaign was conducted in winter 2009 and 71 slum units and 98 public housing apartments were measured. Average 24 h indoor $\text{PM}_{2.5}$ concentrations were 55.7 and $77.8 \mu\text{g}/\text{m}^3$, and ratios of average I/O values were 1.08 and 1.18 for public housing and slums, respectively. They estimated an infiltration factor of 0.5 (± 0.1) and the following contributions to indoor 24 h $\text{PM}_{2.5}$ concentrations (in $\mu\text{g}/\text{m}^3$): allocation to public housing was -10.4 (± 5.1), smoking more than 3 cigarettes was 29 (± 11), using biofuels was 25.6 (± 10.0), and presence of an infant was -9.5 (± 4.6). Negative numbers represent negative contributors to these levels.

All these studies were conducted in the winter season when residential heating is active and households restrict opening windows and doors to minimize heat losses; therefore, air exchange rates are kept to their minimum possible values.

The goal of the present study was to conduct a source apportionment of indoor $\text{PM}_{2.5}$ at Santiago, Chile to identify the major contributing sources. The campaign was conducted in springtime when residential heating is turned off and households are more ventilated.

Methodology

4.4.4. Indoor and outdoor monitoring campaigns

Two Partisol samplers (model 2000i Thermo Scientific, USA, 16.67 L/min) were deployed on a building roof at downtown Santiago, to measure urban background $PM_{2.5}$ levels in 24-h integrated filter samples from November 6th through December 22nd, 2012. For this period of the year, the seasonal variation of outdoor $PM_{2.5}$ in Santiago is negligible — as shown by Koutrakis et al. (Koutrakis et al. 2005) (Table 17) and Sax et al. (Sax et al. 2007) (Table 18). Traffic sources did not change in intensity during that period, showing no traffic emission trends throughout the campaign.

In parallel, two TAS Minivol samplers (Airmetrics, Eugene, OR, USA, 5 L/min) were used to collect 48-h indoor $PM_{2.5}$ integrated filter samples; this sampling period was chosen to ensure we had enough material for all the required analysis planned for this study. Before and after deploying the TAS samplers, their volumetric flow rate was checked using a digital manometer (model 600-003, Airmetrics, Eugene, OR, USA). The TAS samplers were located in the living room of each house at about 1.5 m above the floor; the distance from the kitchen to the samplers varied for each household. The samplers could not be placed in the bedroom because they were noisy.

At each household, one TAS was loaded with a Teflon filter (46.2 mm PTFE, Whatman, NJ, USA) and the other with a quartz filter (47 mm, Tissuquartz 2500QAT-UP, Pall Life Sciences, USA) for trace elemental masses and elemental carbon (EC) and organic carbon (OC) quantification, respectively; a household and activity survey was conducted as well. The protocol for the household survey and the consented information letter were approved by the Ethics Committee of the Pontificia Universidad Católica de Chile Medical School. Continuous sampling of indoor temperature, relative humidity and CO_2 concentrations was performed using portable sensors (HOBO, OnSet Computer Corp., Bourne, MA, USA) and located next to the TAS samplers.

The outdoor monitoring site was chosen on the roof of a six-story building in downtown Santiago as representative of urban background conditions — see Figure 43 . Participant households were selected as a subset of those included in the Platino project (<http://www.platino-alat.org/>), which estimated COPD incidence in Latin American countries. Fifty households were selected from the Platino database and were within a 7.5 km radius of the outdoor monitor location (Figure 44). Since Chile's income distribution is quite uneven (ECLAC: Economic Commission for Latin America 2014) downtown Santiago was selected because it is a zone where socioeconomic statuses may be more evenly represented across households. In this work, status 1, 2 and 3 represent high, middle and low income, respectively; poorer dwellings — like slums or publicly subsidized housing — were not considered in this study. In six different households, one of the TAS samplers had a battery discharged while measuring causing the loss of one exposed filter. Consequently, a total of 47 households with $PM_{2.5}$ mass and elemental concentrations were included and 44 of them had complete measurements (including EC and OC concentrations).

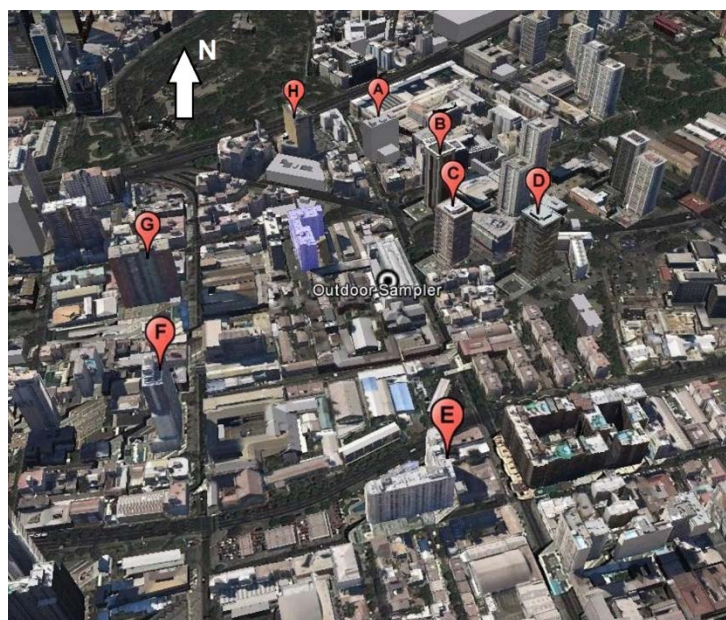


Figure 43 Aerial photograph of the outdoor sampling site and surrounding structures. Distances (m) to elevated buildings are: A: 239; B: 152; C: 86; D: 134; E: 170; F: 190; G: 197; H: 249.

The sampling campaign was conducted in the spring of 2012 so that no residential heating sources of PM_{2.5} were active. Survey results showed that the average times windows and doors were open were 11 and 5.3 h per day, respectively.

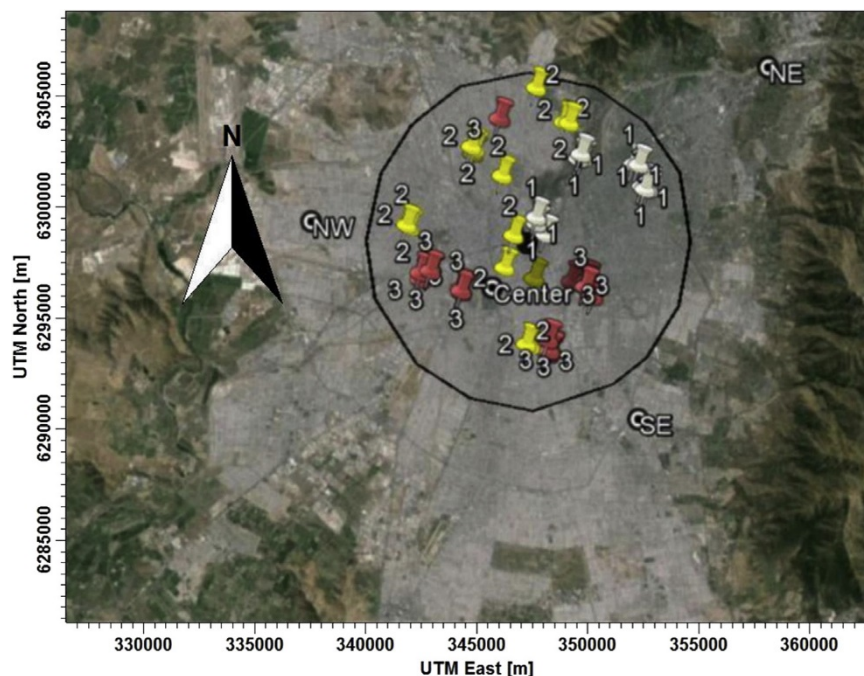


Figure 44 A map depicting Downtown Santiago, the location of the outdoor monitor (black circle, 33°26'36.73"S, 70°38'27.52"W), a circle of 7.5 km radius around it and all households monitored (numbers indicate socioeconomic status).

4.4.5. Filter analysis

Teflon filters were conditioned in a room with controlled temperature ($20 \pm 2^\circ\text{C}$) and relative humidity (35-40%) for 24 h before being weighted with a microbalance (Sartorius, model Cubis-DF LSM011, Goettingen, Germany) with a resolution of 1 μg . Field blank filters — 10% of sampled filters — were also taken to the outdoor site and households along with the exposed filters. All filters were enclosed in Petri dishes (gamma radiation sterilized, VWR, USA), sealed with Teflon tape and placed within screwed aluminum holders, stored in coolers and kept refrigerated at -20°C until analysis.

The elemental analysis was conducted by X-ray fluorescence (XRF) at Chester Labnet Laboratory (Tigard, OR, USA) following method IO-3.3(U.S. Environmental

Protection Agency 1999). For QA/QC purposes, XRF analysis were duplicated for at least 10% of the filters. EC and OC concentrations were measured at University of Colorado Boulder using NIOSH870 method, which is a total optical transmittance (TOT) method. Two blank samples were taken every day and a sucrose standard was added onto them for calibration purposes. These results were compared with previous records to discard any potential drift. Finally, 10% of the filters were punched twice for duplicate analysis. Blank field filters were also analyzed and the detection limit (DL) of each species measured was defined as three times the standard deviation of those blank results. All measured species were blank corrected by subtracting median blank values from the laboratory reported concentrations.

4.4.6. Receptor modeling methodology

In this study, the Positive Matrix Factorization method (PMF), a widely used receptor model for ambient particulate matter samples, was applied. The theoretical basis and practical implementation issues have been described elsewhere (Belis et al. 2013; Reff, Eberly, and Bhave 2007). In this work, PMF version 3.0 (U.S. Environmental Protection Agency 2004) was applied to the 44 households with complete concentration measurements; thus there were no missing values in this analysis.

4.5. Results

4.5.1. Mass concentration and chemical composition

Figure 45 summarizes the 24 h outdoor and 48 h indoor $PM_{2.5}$ mass concentration data for the 2012 campaign and the associated socioeconomic status. The larger variability of indoor $PM_{2.5}$ — $\sigma = 9 \mu g/m^3$ versus $\sigma = 5.7 \mu g/m^3$ for outdoor $PM_{2.5}$ — indicates that indoor concentrations were more heterogeneous in the sampled households than in the outdoor samples. Moreover, maximum $PM_{2.5}$ values clearly exceeded outdoor $PM_{2.5}$ levels.

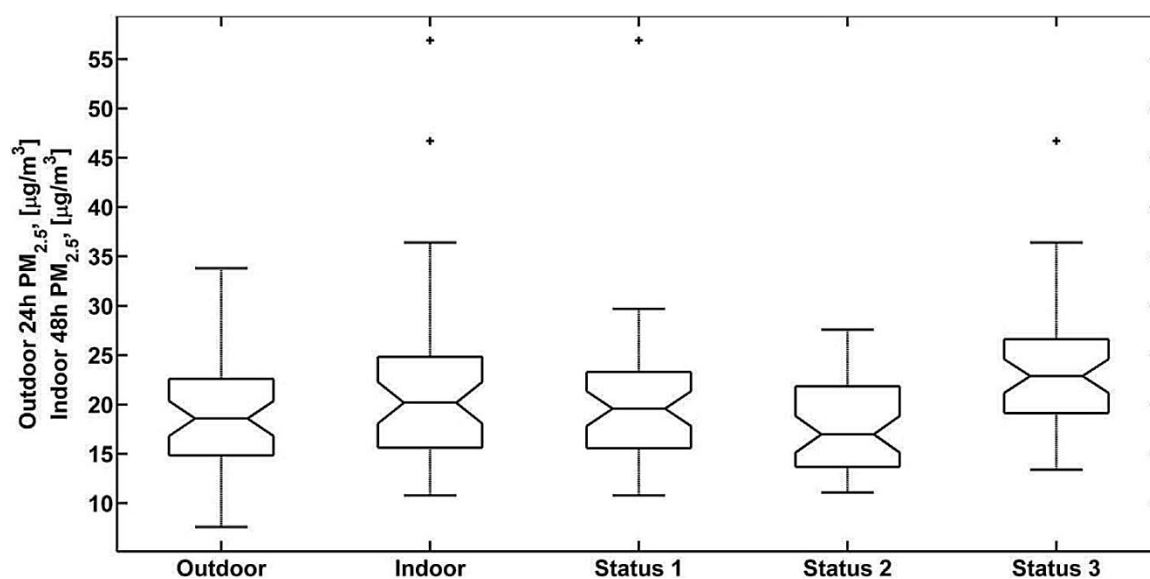


Figure 45 Box plots of $PM_{2.5}$ concentrations for the 24 h outdoor, 48 h indoor and socioeconomic status data categories.

Table 16 and Table 17 summarize the elemental composition data for 48 h indoor and 24 h outdoor samples, respectively. The rightmost column reports the number of samples that fell below the detection limit — henceforth denoted as BDL samples. Only species whose BDL values were less than 45% of the total samples were reported here.

Table 16 Summary of 48 h indoor $PM_{2.5}$ elemental concentrations, 2012 campaign [ng/m^3] (N = 47 households)

| Species | Min. | Perc. 25 | Median | Mean | Perc. 75 | Max. | Stand. Dev. | # BDL ^a |
|-----------------|------|----------|--------|------|----------|--------|-------------|--------------------|
| OC ^b | 2646 | 5210 | 6173 | 7091 | 7284 | 23,762 | 3547 | 0 |
| EC ^b | 288 | 938 | 1196 | 1227 | 1488 | 2017 | 395 | 0 |
| Na | 68 | 160 | 240 | 248 | 336 | 901 | 143 | 9 |
| Mg | 6 | 16 | 35 | 47 | 48 | 682 | 97 | 11 |
| Al | 26 | 67 | 98 | 107 | 124 | 633 | 87 | 2 |
| Si | 86 | 195 | 265 | 339 | 342 | 2244 | 359 | 2 |
| S | 251 | 303 | 440 | 512 | 557 | 1467 | 286 | 2 |
| Cl | 8 | 19 | 41 | 82 | 98 | 543 | 108 | 2 |
| K | 34 | 105 | 136 | 170 | 199 | 639 | 102 | 2 |
| Ca | 59 | 109 | 139 | 252 | 179 | 5413 | 771 | 2 |
| Ti | 4.5 | 7.1 | 9.2 | 11.8 | 10.9 | 85.4 | 13.0 | 2 |
| Mn | 1.3 | 4.9 | 6.1 | 7.8 | 8.4 | 37.5 | 6.1 | 3 |
| Fe | 79 | 113 | 148 | 183 | 176 | 1399 | 190 | 2 |
| Cu | 2.5 | 5.1 | 5.9 | 7.3 | 7.7 | 30.6 | 5.1 | 2 |
| Zn | 10.2 | 14.5 | 18.1 | 28.8 | 32.8 | 134.7 | 26.3 | 2 |
| As | 0.2 | 0.2 | 0.9 | 1.1 | 1.6 | 4.8 | 1.0 | 16 |
| Se | 0.0 | 0.7 | 1.3 | 1.7 | 1.9 | 9.7 | 1.7 | 6 |
| Br | 0.6 | 1.8 | 2.3 | 2.6 | 3.0 | 8.0 | 1.6 | 8 |
| Sr | 0.2 | 0.5 | 0.8 | 0.9 | 1.1 | 7.7 | 1.1 | 12 |
| Pb | 0.7 | 2.8 | 4.6 | 10.5 | 7.5 | 247.5 | 35.5 | 7 |

^a Whenever a given species had BDL samples, these values were replaced by half the detection limit before statistics were computed.

^b There are three missing values in EC and OC concentrations.

Table 17 Summary of outdoor 24 h $PM_{2.5}$ elemental concentrations, 2012 campaign [ng/m^3] ($N = 41$ samples).

| Species | Min. | Perc. 25 | Median | Mean | Perc. 75 | Max. | Stand. Dev. | # BDL ^a |
|---------|------|----------|--------|-------|----------|-------|-------------|--------------------|
| OC | 2400 | 3445 | 4280 | 4280 | 5078 | 6100 | 1046 | |
| EC | 870 | 1180 | 1520 | 1583 | 1918 | 3160 | 510 | |
| Na | 99 | 99 | 226 | 245 | 336 | 592 | 142 | 15 |
| Mg | 14 | 14 | 33 | 37 | 50 | 89 | 24 | 15 |
| Al | 24 | 102 | 128 | 147 | 181 | 497 | 83 | |
| Si | 85 | 260 | 347 | 375 | 454 | 1192 | 195 | |
| S | 209 | 431 | 597 | 706 | 897 | 1595 | 376 | |
| Cl | 7 | 35 | 53 | 97 | 134 | 563 | 108 | |
| K | 58 | 106 | 146 | 160 | 196 | 459 | 77 | |
| Ca | 64 | 148 | 177 | 199 | 221 | 687 | 113 | |
| Ti | 4 | 10 | 13 | 15 | 16 | 63 | 10 | |
| V | 0.40 | 0.40 | 1.10 | 1.08 | 1.50 | 3.00 | 0.63 | 15 |
| Cr | 0.40 | 0.70 | 1.40 | 1.45 | 1.80 | 3.60 | 0.84 | 10 |
| Mn | 3.00 | 7.03 | 10.20 | 11.17 | 13.03 | 43.10 | 7.87 | |
| Fe | 88 | 169 | 219 | 249 | 274 | 859 | 142 | |
| Ni | 0.2 | 0.2 | 0.6 | 0.6 | 0.8 | 1.4 | 0.4 | 17 |
| Cu | 2.7 | 6.5 | 8.1 | 9.2 | 11.0 | 17.9 | 3.5 | |
| Zn | 6.3 | 17.5 | 25.4 | 27.7 | 35.0 | 69.8 | 13.3 | |
| As | 0.1 | 0.6 | 1.4 | 1.5 | 2.0 | 4.2 | 1.1 | 5 |
| Se | 0.2 | 1.2 | 1.8 | 3.7 | 2.4 | 63.0 | 9.6 | 1 |
| Br | 1.3 | 2.3 | 3.1 | 4.2 | 4.2 | 36.6 | 5.4 | |
| Sr | 0.1 | 0.6 | 1.0 | 1.0 | 1.3 | 2.9 | 0.6 | 4 |
| Pb | 1.8 | 3.3 | 4.6 | 5.8 | 6.7 | 26.1 | 4.3 | |

^a Whenever a given species had BDL samples, these values were replaced by half the detection limit before statistics were computed.

Kruskal-Wallis tests were ran to check whether socioeconomic status was associated to changes in indoor $PM_{2.5}$ species and no significant differences among the three socioeconomic group medians were found. This was true for all species except $PM_{2.5}$ ($p = 0.0478$) and lead ($p = 0.0460$), as shown in Table 18. Then Wilcoxon rank sum tests were also ran on pairs of groups and it was found that for $PM_{2.5}$, status 2 and 3 had a significant difference in their medians ($p = 0.0166$). Likewise, for lead status 1 and 2 presented significant median differences ($p = 0.0198$). Finally, for sulfur a significant difference between status 2 and 3 ($p = 0.0351$) was found. Table 3 reports the p values for both tests and all species analyzed. Most indoor $PM_{2.5}$ species show no significant

differences in median values by socioeconomic status; this may be ascribed to similar cooking and cleaning activities across the sampled households.

Table 18 Results of the comparison tests for group medians, 2012 campaign.

| Species | Indoor socio-economic status comparisons | | | | O–I comparisons | |
|-------------------|--|----------------------------------|----------------------------------|----------------------------------|----------------------|----------------|
| | Status 1, 2 and 3 ^a | Status 1 / Status 2 ^b | Status 1 / Status 3 ^b | Status 2 / Status 3 ^b | p-value ^b | Higher median? |
| PM _{2.5} | 0.0478* | 0.2706 | 0.1969 | 0.0166# | 0.2843 | |
| OC | 0.1349 | 0.4175 | 0.2184 | 0.0610 | 0.0000# | I |
| EC | 0.6549 | 0.4668 | 0.8582 | 0.4279 | 0.0003# | O |
| Na | 0.1528 | 0.0805 | 0.3016 | 0.2332 | 0.9766 | |
| Mg | 0.7734 | 0.6764 | 0.8266 | 0.4924 | 0.6325 | |
| Al | 0.9876 | 0.9172 | 0.9367 | 0.8997 | 0.0004# | O |
| Si | 0.6312 | 0.7552 | 0.2928 | 0.7053 | 0.0066# | O |
| S | 0.1057 | 0.1637 | 0.8272 | 0.0351# | 0.0031# | O |
| Cl | 0.8026 | 0.7238 | 0.6479 | 0.5889 | 0.2204 | |
| K | 0.2779 | 0.4669 | 0.4389 | 0.1171 | 0.9001 | |
| Ca | 0.2364 | 0.4927 | 0.0916 | 0.3583 | 0.0021# | O |
| Ti | 0.7354 | 0.9503 | 0.6623 | 0.4175 | 0.0000# | O |
| Mn | 0.9207 | 0.7393 | 0.9525 | 0.7456 | 0.0003# | O |
| Fe | 0.9194 | 0.9172 | 0.5920 | 0.9856 | 0.0000# | O |
| Cu | 0.8335 | 0.7236 | 0.7206 | 0.6139 | 0.0002# | O |
| Zn | 0.2378 | 0.2891 | 0.0954 | 0.5889 | 0.0663 | |
| As | 0.3518 | 0.2237 | 0.7953 | 0.2181 | 0.1432 | |
| Se | 0.6799 | 0.5596 | 0.3926 | 0.8568 | 0.0233# | O |
| Br | 0.4856 | 0.2515 | 0.8270 | 0.3959 | 0.0033# | O |
| Sr | 0.6911 | 0.4636 | 0.8253 | 0.5017 | 0.2576 | |
| Pb | 0.0460* | 0.0198# | 0.0702 | 0.4823 | 0.7569 | |

^a Outcome from the Kruskal–Wallis test for three grouped samples; ‘*’ means the medians present significant differences ($p < 0.05$).

^b Outcome from the Wilcoxon rank sum test for two samples; ‘#’ means paired medians present significant differences ($p < 0.05$).

The most abundant species — in all samples — were organic carbon, elemental carbon, sulfur and crustal elements. Wilcoxon rank sum tests were ran for indoor and outdoor samples for all species; these results are also presented in Table 18. For PM_{2.5}, Na, Mg, Cl, K, Zn, As, Sr and Pb, the null hypothesis that both data have the same median values ($p > 0.05$) could not be rejected. For EC, Al, Si, S, Ca, Ti, Mn, Fe, Cu, Se and Br, outdoor medians were significantly higher than indoor medians ($p < 0.05$); this result suggests that

all these species have no indoor sources. Finally, only indoor OC had median values significantly higher ($p < 0.05$) than the corresponding outdoor values suggesting that there were indoor source contributions to OC. This result is consistent with a large body of evidence that indoor cooking is a substantial contributor to indoor $PM_{2.5}$ and that its source profile is dominated by organic carbon (Abdullahi, Karimatu L., Delgado-Saborit, Juana Maria Harrison, Roy M. 2013). From Figure 46 to Figure 50, show box plots of indoor and outdoor concentrations for all species; outliers are more frequent in indoor samples.

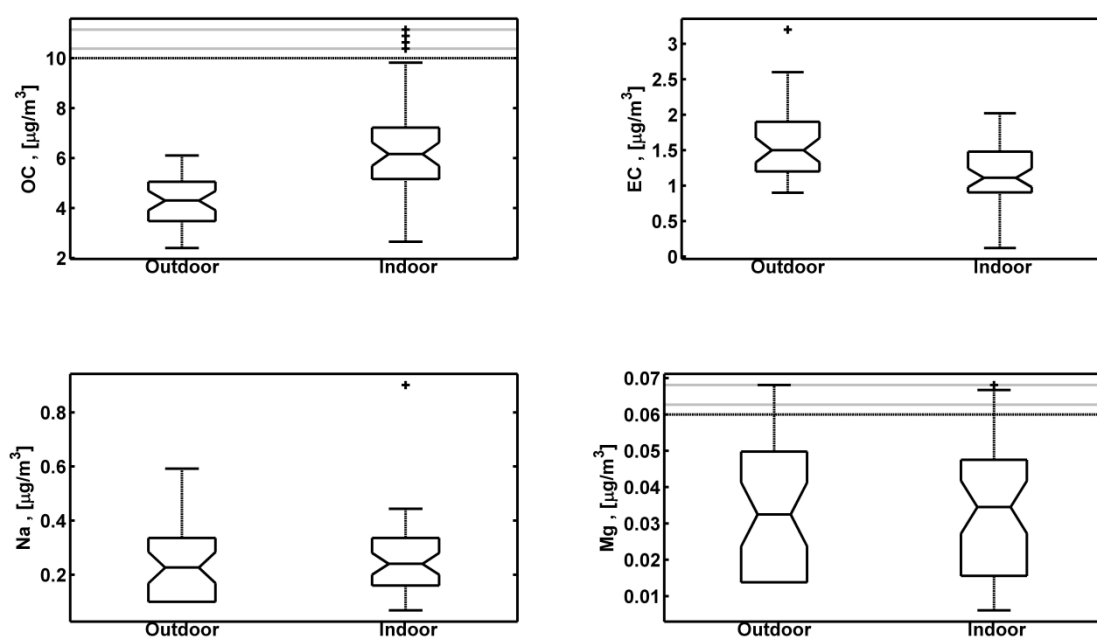


Figure 46 Boxplots of indoor and outdoor concentrations of OC, EC, Na and Mg ($\mu g/m^3$). For easier visualization, outliers are displayed 'compressed'; notches indicate confidence intervals for median values.

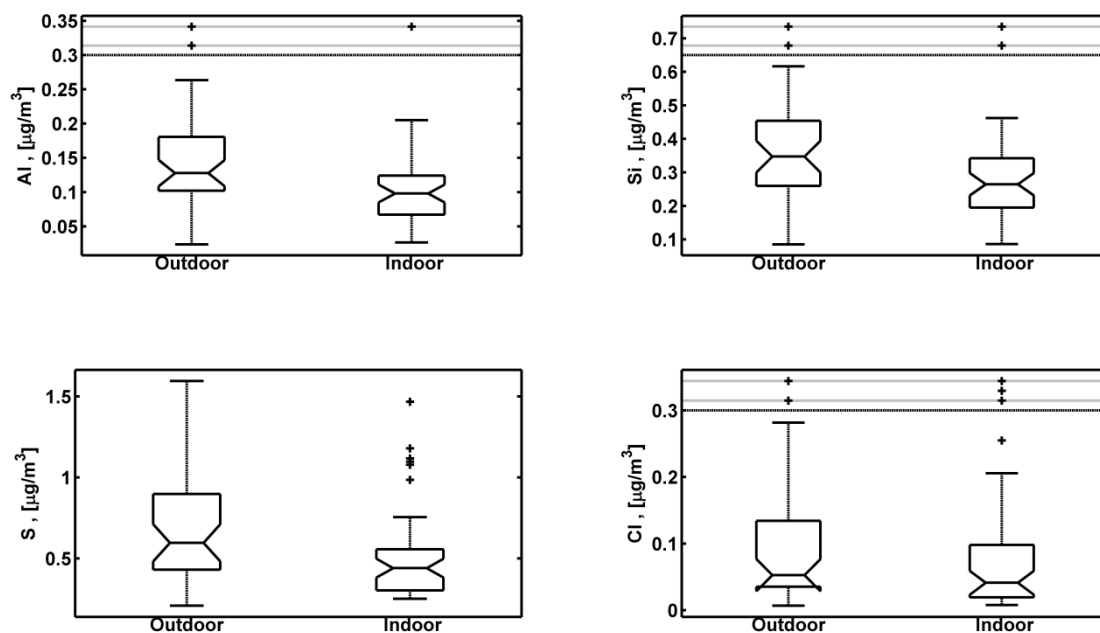


Figure 47 Same as previous figure but for Al, Si, S and Cl ($\mu\text{g}/\text{m}^3$).

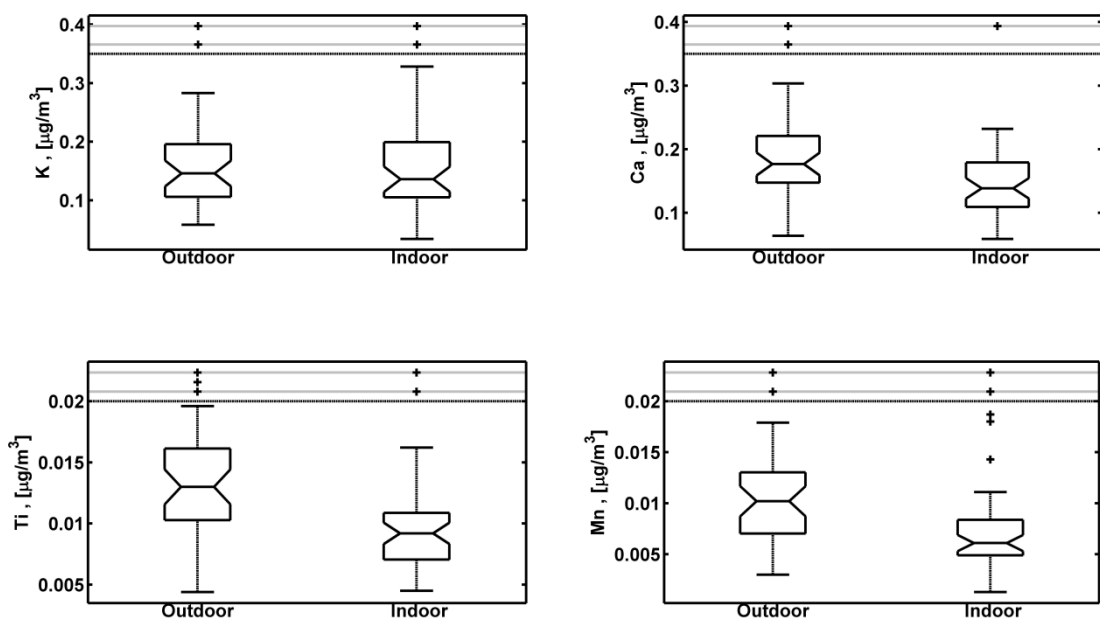


Figure 48 Same as previous figure but for K, Ca, Ti and Mn ($\mu\text{g}/\text{m}^3$).

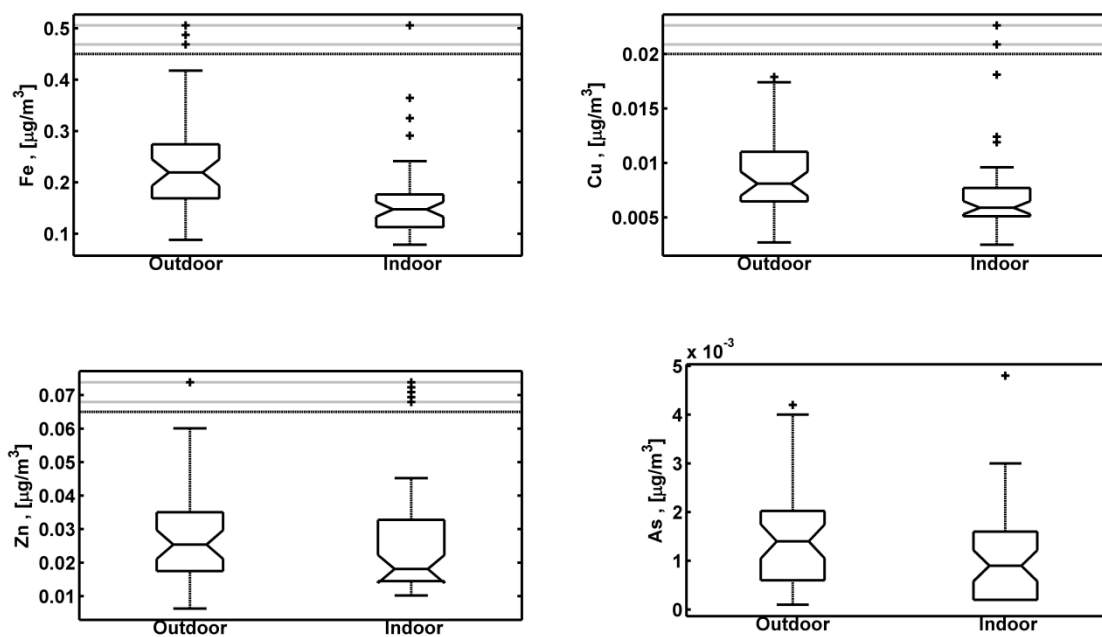


Figure 49 Same as previous figure but for Fe, Cu, Zn and As ($\mu\text{g}/\text{m}^3$).

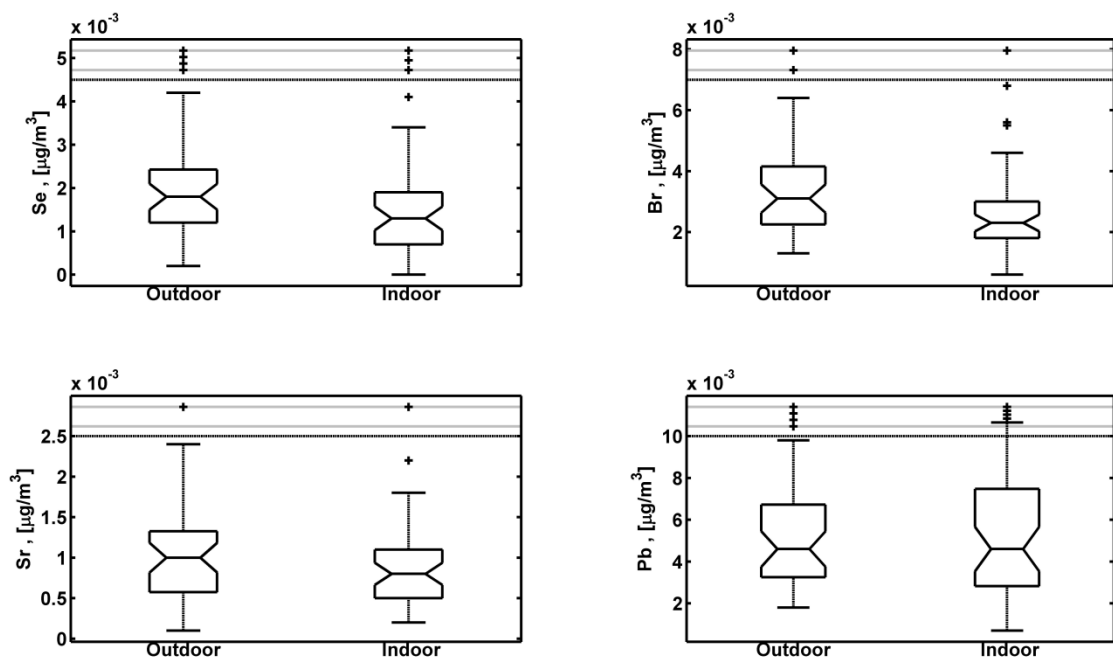


Figure 50 Same as previous figure but for Se, Br, Sr and Pb ($\mu\text{g}/\text{m}^3$).

4.5.2. Indoor-outdoor relationships

Two consecutive outdoor, 24 h data sets were averaged to construct the outdoor counterpart of each 48 h household data set. Then indoor to outdoor concentrations were regressed — using Equation 8 — for $\text{PM}_{2.5}$ and its measured components. A robust regression fit was applied to minimize influence of outliers — likely coming from indoor sources — on fitted parameters. The campaign was carried out in the spring, when warmer temperatures promote frequent door and window opening, effectively increasing α and decreasing the influence of k on F_{INF} . Since P and k still depend upon particle size and household features (Abt et al. 2000; Riley et al. 2002), two different approaches (Qing Yu Meng et al. 2005) to analyze the data were tried:

- a) Fitting Equation 8 for each species and all households to obtain home-average F_{INF} values.
- b) Fitting Equation 8 for each household and all species to obtain F_{INF} estimates for each sampled household.

In approach a) the variability in strength of indoor sources, household geometry, occupants' behavior and location of $\text{PM}_{2.5}$ sampler is smoothed out in the fitted parameters; in approach b) each household captures that variability in the fitted parameters.

Table 19 shows results from applying approach a) to the indoor-outdoor species data and Figure 51 shows robust fits for selected species. A robust linear fitting algorithm — robustfit in MATLAB Release 2009 — was used (Street, Carroll, and Ruppert 1988). The sharpest estimate of F_{INF} was obtained for sulfur ($t\text{-ratio} = 27.5$) because it is a tracer that has no indoor sources (Sarnat et al. 2002). This value (0.80 ± 0.03) is similar to the one reported by Meng et al. (Qing Yu Meng et al. 2007) of 0.78 ± 0.03 for households in three regions of the USA. For $\text{PM}_{2.5}$ the estimated value was 0.70 ± 0.19 , close to the highest values reported in a literature review (Chen and Zhao 2011). For crustal elements (Al, Si, K, Ti), F_{INF} values were lower because $\text{PM}_{2.5}$ crustal particles have larger diameters than sulfate particles; therefore, P decreased and k increased as compared with

sulfur parameters. Some species had significant intercept estimates ($p < 0.05$), which meant their concentrations had indoor-generated contributions. This was the case for Na, Mg, Si, Cl, K, Ti and Fe, among others.

Table 19 Robust fit of Equation 8 for indoor species.

| Species | Intercept | σ | p value | Slope | σ | p value |
|-------------------|-----------|----------|-----------|--------|----------|-----------|
| PM _{2.5} | 6.835 | 3.682 | 0.070 | 0.704* | 0.194 | 0.001 |
| OC | 1.809 | 0.923 | 0.057 | 0.975* | 0.213 | 0.000 |
| EC | -0.088 | 0.198 | 0.658 | 0.799* | 0.119 | 0.000 |
| Na | 0.085* | 0.030 | 0.007 | 0.595* | 0.109 | 0.000 |
| Mg | 0.032* | 0.011 | 0.007 | 0.011 | 0.283 | 0.969 |
| Al | 0.018 | 0.011 | 0.119 | 0.588* | 0.069 | 0.000 |
| Si | 0.101* | 0.042 | 0.020 | 0.484* | 0.103 | 0.000 |
| S | -0.027 | 0.022 | 0.214 | 0.798* | 0.029 | 0.000 |
| Cl | 0.033* | 0.011 | 0.003 | 0.099 | 0.086 | 0.256 |
| K | 0.088* | 0.026 | 0.001 | 0.334* | 0.153 | 0.034 |
| Ca | 0.102 | 0.071 | 0.158 | 0.197 | 0.320 | 0.541 |
| Ti | 0.004* | 0.001 | 0.012 | 0.436* | 0.083 | 0.000 |
| Mn | 0.005* | 0.001 | 0.000 | 0.132 | 0.086 | 0.134 |
| Fe | 0.128* | 0.025 | 0.000 | 0.077 | 0.094 | 0.418 |
| Cu | 0.005* | 0.001 | 0.000 | 0.102 | 0.131 | 0.441 |
| Zn | 0.003 | 0.004 | 0.484 | 0.602* | 0.139 | 0.000 |
| As | 0.000* | 0.000 | 0.017 | 0.355* | 0.108 | 0.002 |
| Se | 0.001* | 0.000 | 0.000 | 0.148* | 0.017 | 0.000 |
| Br | 0.002* | 0.000 | 0.000 | 0.152* | 0.035 | 0.000 |
| Sr | 0.000* | 0.000 | 0.032 | 0.429* | 0.154 | 0.008 |
| Pb | 0.002 | 0.003 | 0.478 | 0.407 | 0.465 | 0.386 |

^a The '*' symbol indicates significant results ($p < 0.05$).

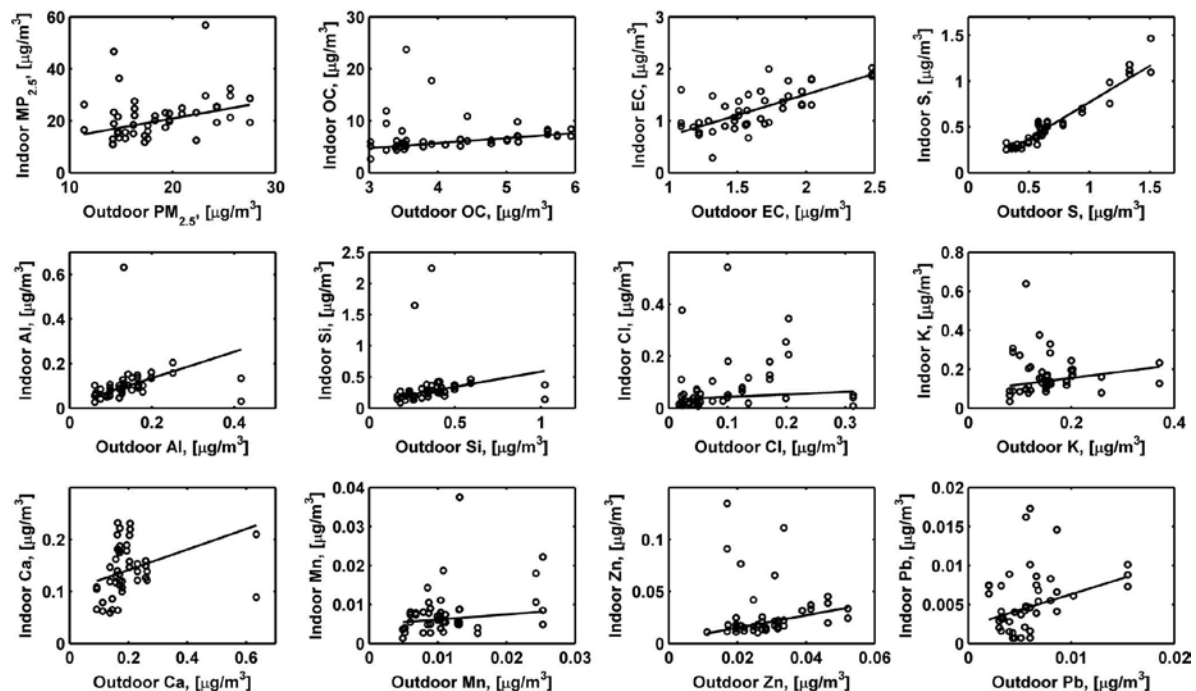


Figure 51 Robust linear fit of Equation 8 for total $PM_{2.5}$ and most of its component species

Figure 52 presents examples of scatter plots and robust fits that arise when Equation 8 was fitted to a single household — approach b). Table 20 presents results for all household fits; the estimated slopes (F_{INF}) are all statistically significant ($p < 0.05$). The median F_{INF} value was 0.75, mean = 0.78, $\sigma = 0.18$ and IQR = (0.67, 0.86). Five of the estimated slopes were higher than 1.0 likely due to the limitations of the single-zone model used Equation 8, which assumes that: i) a single outdoor site was representative of outdoor $PM_{2.5}$ for all households measured, and ii) each household indoor air was well mixed. To address the first issue, the estimated F_{INF} was plotted against the distance of each household to the outdoor monitor — see Figure 53 — and no correlation was found, meaning assumption i) was met. The estimated F_{INF} was also plotted against the household surface — see Figure 53 — all those 5 households were among the larger ones, suggesting assumption ii) was not met for those households. The assumption of well-mixed indoor air requires frequent opening of internal doors and connectedness of multi-zones within a given household. The five high slope estimates suggest that in those households the measured indoor $PM_{2.5}$ at the living room is an underestimation of the actual average household concentration.

Despite these limitations the present estimates are similar to those obtained in another study in which more data were collected — Meng et al. (Qing Yu Meng et al. 2007) — this is likely due to the small number of households at which model assumption ii) was not met in the present study.

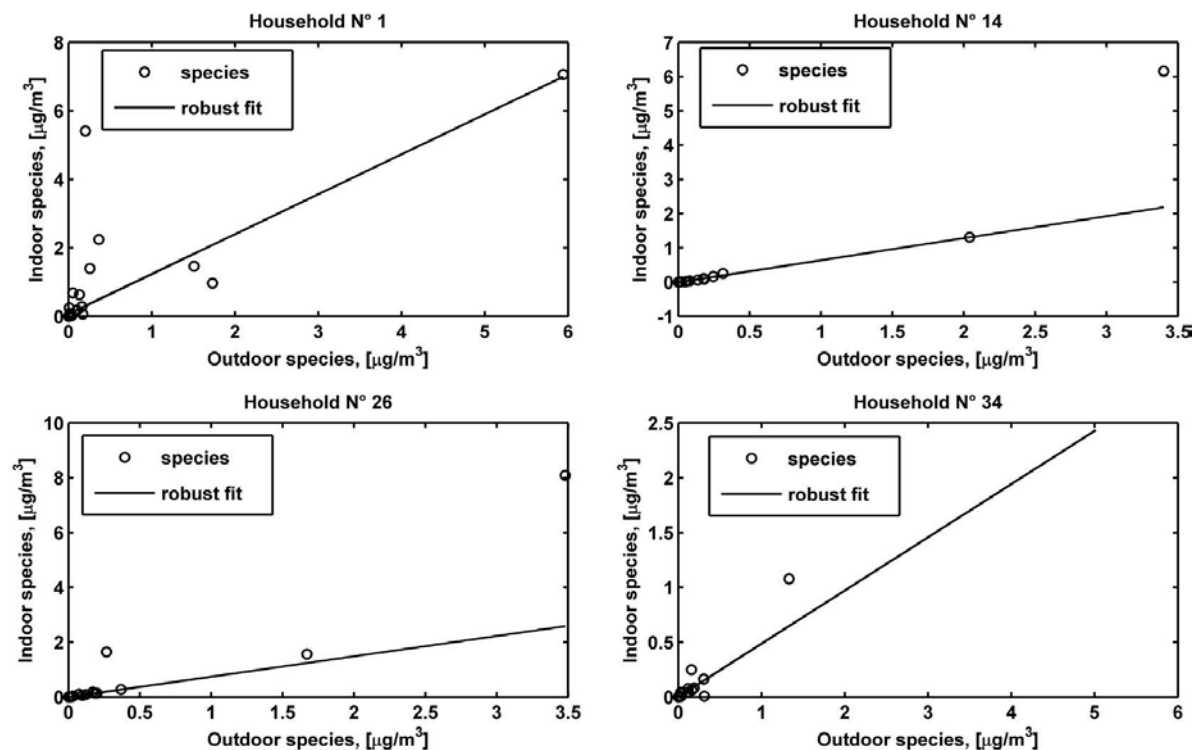


Figure 52 Examples of robust linear fit of Equation 8 for all measured species at selected households (numbers are the same as in Table 20).

Table 20 Robust fit results of Equation 8 for individual households.

| Household | Intercept | σ | p value | slope | σ | p value | R | p value |
|-----------|-----------|----------|---------|-------|----------|---------|-------|---------|
| 1 | 0.069 | 0.14 | 0.621 | 1.17 | 0.10 | 0.000 | 0.757 | 0.0001 |
| 2 | -0.018 | 0.02 | 0.477 | 1.16 | 0.02 | 0.000 | 0.992 | 0.0000 |
| 3 | -0.001 | 0.03 | 0.983 | 0.66 | 0.03 | 0.000 | 0.928 | 0.0000 |
| 4 | -0.008 | 0.04 | 0.857 | 0.96 | 0.04 | 0.000 | 0.981 | 0.0000 |
| 5 | -0.003 | 0.02 | 0.898 | 0.82 | 0.03 | 0.000 | 0.980 | 0.0000 |
| 6 | -0.003 | 0.03 | 0.919 | 0.85 | 0.03 | 0.000 | 0.980 | 0.0000 |
| 7 | -0.001 | 0.03 | 0.977 | 0.73 | 0.03 | 0.000 | 0.979 | 0.0000 |
| 8 | -0.003 | 0.04 | 0.923 | 1.06 | 0.05 | 0.000 | 0.955 | 0.0000 |
| 9 | 0.000 | 0.07 | 0.999 | 0.60 | 0.06 | 0.000 | 0.959 | 0.0000 |
| 10 | -0.001 | 0.03 | 0.973 | 0.55 | 0.03 | 0.000 | 0.978 | 0.0000 |
| 11 | -0.007 | 0.02 | 0.734 | 0.65 | 0.02 | 0.000 | 0.979 | 0.0000 |
| 12 | 0.001 | 0.03 | 0.968 | 0.55 | 0.03 | 0.000 | 0.975 | 0.0000 |
| 13 | 0.000 | 0.03 | 0.994 | 1.05 | 0.03 | 0.000 | 0.975 | 0.0000 |
| 14 | -0.002 | 0.05 | 0.973 | 0.64 | 0.05 | 0.000 | 0.941 | 0.0000 |
| 15 | -0.002 | 0.01 | 0.869 | 0.96 | 0.02 | 0.000 | 0.993 | 0.0000 |
| 16 | 0.007 | 0.03 | 0.800 | 0.69 | 0.02 | 0.000 | 0.983 | 0.0000 |
| 17 | 0.002 | 0.02 | 0.939 | 0.78 | 0.02 | 0.000 | 0.987 | 0.0000 |
| 18 | 0.003 | 0.02 | 0.879 | 0.70 | 0.03 | 0.000 | 0.948 | 0.0000 |
| 19 | 0.020 | 0.03 | 0.564 | 0.74 | 0.04 | 0.000 | 0.970 | 0.0000 |
| 20 | 0.003 | 0.04 | 0.932 | 0.77 | 0.03 | 0.000 | 0.980 | 0.0000 |
| 21 | -0.004 | 0.03 | 0.881 | 0.70 | 0.02 | 0.000 | 0.987 | 0.0000 |
| 22 | 0.001 | 0.04 | 0.973 | 0.75 | 0.03 | 0.000 | 0.978 | 0.0000 |
| 23 | -0.006 | 0.03 | 0.825 | 0.72 | 0.03 | 0.000 | 0.978 | 0.0000 |
| 24 | -0.001 | 0.02 | 0.972 | 0.68 | 0.02 | 0.000 | 0.981 | 0.0000 |
| 25 | 0.004 | 0.04 | 0.915 | 0.65 | 0.04 | 0.000 | 0.963 | 0.0000 |
| 26 | 0.001 | 0.06 | 0.987 | 0.74 | 0.06 | 0.000 | 0.952 | 0.0000 |
| 27 | -0.001 | 0.02 | 0.967 | 0.54 | 0.02 | 0.000 | 0.984 | 0.0000 |
| 28 | -0.001 | 0.02 | 0.971 | 0.65 | 0.02 | 0.000 | 0.991 | 0.0000 |
| 29 | 0.000 | 0.02 | 0.992 | 0.83 | 0.02 | 0.000 | 0.987 | 0.0000 |
| 30 | -0.001 | 0.03 | 0.980 | 0.30 | 0.03 | 0.000 | 0.968 | 0.0000 |
| 31 | 0.002 | 0.07 | 0.984 | 0.90 | 0.09 | 0.000 | 0.962 | 0.0000 |
| 32 | -0.001 | 0.04 | 0.988 | 1.18 | 0.05 | 0.000 | 0.981 | 0.0000 |
| 33 | 0.006 | 0.03 | 0.823 | 0.89 | 0.02 | 0.000 | 0.985 | 0.0000 |
| 34 | 0.002 | 0.02 | 0.923 | 0.49 | 0.02 | 0.000 | 0.954 | 0.0000 |
| 35 | 0.001 | 0.02 | 0.977 | 0.84 | 0.02 | 0.000 | 0.989 | 0.0000 |
| 36 | -0.003 | 0.02 | 0.860 | 0.87 | 0.02 | 0.000 | 0.989 | 0.0000 |
| 37 | -0.003 | 0.03 | 0.932 | 0.85 | 0.03 | 0.000 | 0.976 | 0.0000 |
| 38 | 0.004 | 0.18 | 0.982 | 0.95 | 0.21 | 0.000 | 0.942 | 0.0000 |
| 39 | 0.002 | 0.02 | 0.927 | 0.74 | 0.02 | 0.000 | 0.982 | 0.0000 |
| 40 | -0.005 | 0.04 | 0.898 | 0.78 | 0.03 | 0.000 | 0.971 | 0.0000 |
| 41 | -0.002 | 0.04 | 0.949 | 0.78 | 0.04 | 0.000 | 0.960 | 0.0000 |
| 42 | 0.002 | 0.02 | 0.933 | 0.66 | 0.01 | 0.000 | 0.993 | 0.0000 |
| 43 | -0.001 | 0.01 | 0.966 | 0.95 | 0.01 | 0.000 | 0.996 | 0.0000 |
| 44 | 0.000 | 0.03 | 0.998 | 0.78 | 0.03 | 0.000 | 0.980 | 0.0000 |
| 45 | 0.005 | 0.02 | 0.807 | 0.75 | 0.02 | 0.000 | 0.990 | 0.0000 |
| 46 | 0.001 | 0.13 | 0.994 | 0.73 | 0.13 | 0.000 | 0.950 | 0.0000 |
| 47 | -0.001 | 0.03 | 0.975 | 0.68 | 0.03 | 0.000 | 0.979 | 0.0000 |

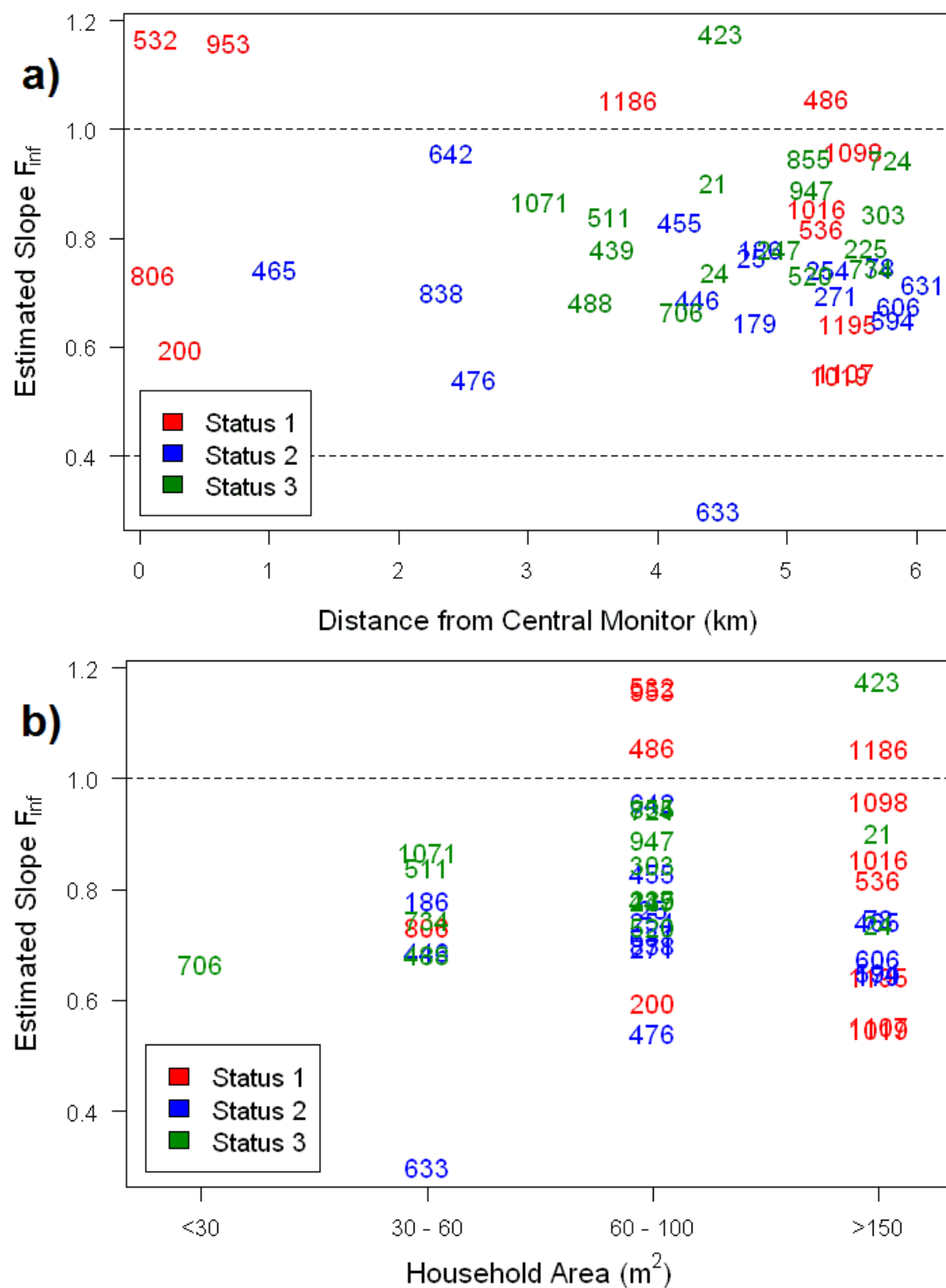


Figure 53 Plots of the estimated F_{INF} parameter versus: a) distance from household to outdoor monitor site (km), and b) household area (m^2). All households are depicted by socioeconomic status.

4.5.3. Receptor modeling results for indoor $PM_{2.5}$

A six-factor solution that explains 85% of the variability of the measured $PM_{2.5}$ indoor concentrations was found. Most fitted elements have regression coefficients (R^2) greater than 0.8, except Si (0.65) — see Table 21. Table 22 presents the resolved source profiles, in ng/m^3 , for the six-factor solution; these are discussed next.

Table 21 Diagnostics for the 6-factor solution for indoor $PM_{2.5}$.

| Species | Intercept | Slope | Std. error | R^2 | KS Test | P Value |
|---------|-----------|-------|------------|-------|---------|---------|
| OC | 1.46 | 0.76 | 0.78 | 0.92 | 0.12 | 0.58 |
| EC | 0.17 | 0.85 | 0.14 | 0.85 | 0.09 | 0.90 |
| Al | -0.02 | 1.21 | 0.02 | 0.95 | 0.06 | 1.00 |
| Si | 0.07 | 0.72 | 0.20 | 0.65 | 0.31 | 0.00 |
| S | -0.01 | 1.01 | 0.01 | 1.00 | 0.10 | 0.76 |
| Cl | 0.00 | 1.03 | 0.00 | 1.00 | 0.14 | 0.32 |
| K | -0.01 | 1.04 | 0.01 | 0.99 | 0.08 | 0.95 |
| Ca | 0.11 | 0.20 | 0.03 | 0.96 | 0.20 | 0.06 |
| Ti | 0.00 | 0.73 | 0.00 | 0.80 | 0.20 | 0.05 |
| Mn | 0.00 | 0.93 | 0.00 | 0.92 | 0.09 | 0.84 |
| Fe | 0.02 | 0.86 | 0.03 | 0.98 | 0.08 | 0.93 |
| Cu | 0.00 | 0.84 | 0.00 | 0.89 | 0.12 | 0.56 |
| Sr | 0.00 | 0.83 | 0.00 | 0.85 | 0.11 | 0.65 |

Table 22 Source profiles [ng/m^3] for a 6 factor solution, indoor $PM_{2.5}$ data.

| Species | F1 | F2 | F3 | F4 | F5 | F6 |
|---------|------|------|------|-----|-----|------|
| OC | 2408 | 961 | 2165 | 365 | 0 | 950 |
| EC | 155 | 155 | 840 | 41 | 6 | 10 |
| Al | 17 | 0 | 25 | 16 | 46 | 8 |
| Si | 44 | 6 | 63 | 52 | 134 | 23 |
| S | 122 | 58 | 71 | 250 | 4 | 0 |
| Cl | 9.4 | 13.3 | 0.0 | 4.7 | 0.0 | 51.6 |
| K | 101 | 31 | 0 | 0 | 14 | 23 |
| Ca | 19 | 5 | 35 | 28 | 65 | 15 |
| Ti | 1.9 | 0.4 | 2.5 | 1.3 | 4.7 | 0.4 |
| Mn | 0.0 | 4.1 | 1.4 | 0.2 | 2.1 | 0.3 |
| Fe | 13 | 26 | 42 | 17 | 72 | 11 |
| Cu | 0.1 | 3.4 | 1.7 | 0.0 | 1.6 | 0.3 |
| Sr | 0.0 | 0.0 | 0.0 | 0.4 | 0.3 | 0.1 |

The first source (factor) is dominated in mass by carbonaceous particles and it has a high OC/EC ratio (15.5) that suggests it is the indoor cooking source; there is a high percentage of K in this source (60%). OC, EC and potassium are also tracers of

environmental tobacco smoke (ETS) (W. Zhao et al. 2007; W. X. Zhao et al. 2006) and in 11 of the 44 households analyzed, people acknowledged smoking habits. Hence, this indoor source was identified as a mixture of cooking and ETS. The second source was dominated in mass by OC and it had the highest percentage of Mn and Cu, which are accepted tracers of traffic sources (Pant and Harrison 2013). Since it also had crustal elements, this source was identified as suspended street dust. The third source identified had 70% of the measured EC, more than 30% of OC, more than 14% of Al, Si, S, Ca and Ti — tracers of suspended street dust and tire wear — and more than 17% of Mn and Cu, tracers of traffic emissions (Pant and Harrison 2013). The OC/EC ratio was 2.58 and more than 92% of the mass in this profile was explained by OC and EC — see

Table 23 — so this source was identified as motor vehicles. The fourth source identified had 49% of sulfur so it was a secondary sulfate source with a profile dominated by sulfur in mass; this source had already been identified for Santiago in 1999 and 2004 by Jorquera and Barraza (Héctor Jorquera and Barraza 2012). The fifth source was dominated in mass by crustal elements, so it represents a suspended indoor soil; it has the largest concentrations of Al, Si, Ca, Ti and Fe. Support for this identification comes from the ratios $\text{Si/Ca} = 2.1$ and $\text{Al/Si} = 0.34$ similar to the values 2.5 and 0.40, found in Santiago in 2004 and 1999 outdoor samples, respectively (Héctor Jorquera and Barraza 2012). The sixth source had more than 65% of the Cl, which suggests cleaning activities and drinking water use; chlorine-based cleaners are often used in Santiago's households. Organic carbon dominates this profile in mass and it is ascribed to activities like boiling water and cooking. Similar indoor source profiles have been obtained by Zhao (W. X. Zhao et al. 2006; W. Zhao et al. 2007) in three US locations. This source was denoted as cleaning and cooking.

Table 23. *Contribution of species to total factor mass (%) for the six factor solution, indoor $PM_{2.5}$.*

| Species | F1 | F2 | F3 | F4 | F5 | F6 |
|---------|------|------|------|------|------|------|
| OC | 83.3 | 76.2 | 66.7 | 47.1 | 0.0 | 87.0 |
| EC | 5.4 | 12.3 | 25.9 | 5.3 | 1.7 | 1.0 |
| Al | 0.6 | 0.0 | 0.8 | 2.0 | 13.1 | 0.7 |
| Si | 1.5 | 0.5 | 2.0 | 6.6 | 38.5 | 2.1 |
| S | 4.2 | 4.6 | 2.2 | 32.2 | 1.1 | 0.0 |
| Cl | 0.3 | 1.1 | 0.0 | 0.6 | 0.0 | 4.7 |
| K | 3.5 | 2.5 | 0.0 | 0.0 | 3.9 | 2.1 |
| Ca | 0.7 | 0.4 | 1.1 | 3.7 | 18.7 | 1.4 |
| Ti | 0.1 | 0.0 | 0.1 | 0.2 | 1.3 | 0.0 |
| Mn | 0.0 | 0.3 | 0.0 | 0.0 | 0.6 | 0.0 |
| Fe | 0.4 | 2.0 | 1.3 | 2.2 | 20.6 | 1.0 |
| Cu | 0.0 | 0.3 | 0.1 | 0.0 | 0.5 | 0.0 |
| Sr | 0.0 | 0.0 | 0.0 | 0.0 | 0.1 | 0.0 |

The above three indoor source profiles (1, 5 and 6) were expected to be each a combination of several sources because they represent average profiles for all 44 households analyzed. For instance, they had similar Al/Si ratios suggesting suspended soil was present in all profiles. Potassium — a tracer of ETS but also of soil dust — is present in those three sources, suggesting more potential mixing of sources. To check the presence of ETS in the indoor source profiles, box plots were constructed of each indoor source contribution versus a categorical variable that was 1 or 0 depending on whether a household had a smoker resident or not.

Figure 54 shows those plots; only source 1 showed a systematic shift to higher values for households with smokers. This supports the identification of source 1 as a mixture of cooking and ETS and that ETS did not appear in sources 5 and 6.

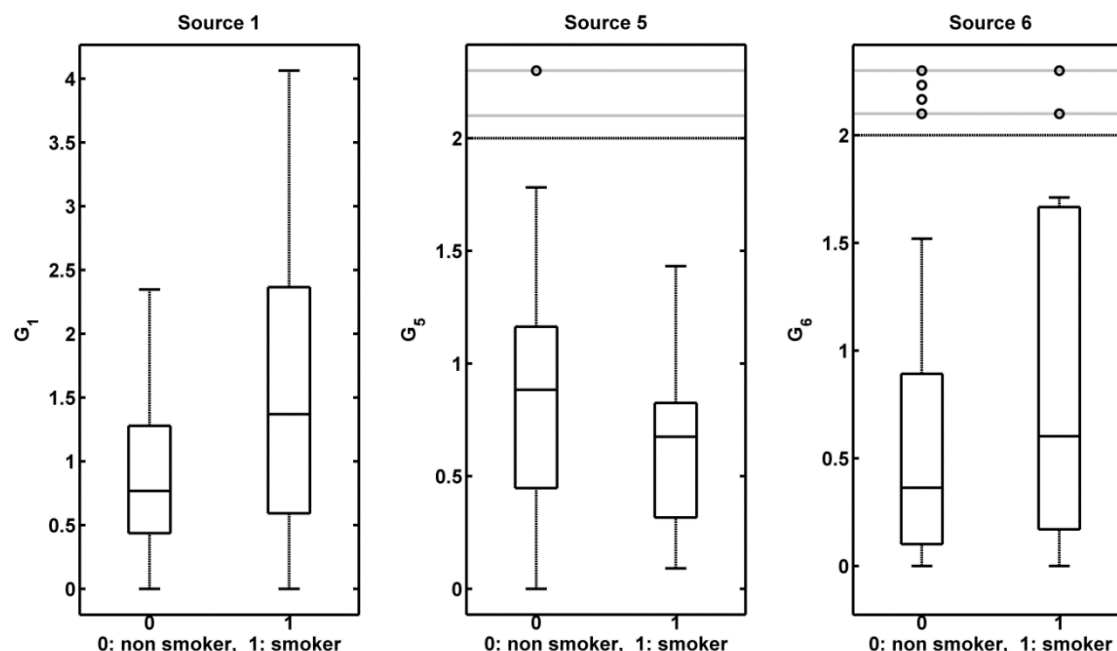


Figure 54 Boxplots of source contributions G_1 , G_5 , and G_6 ($\mu\text{g}/\text{m}^3$) versus households without (0) or with (1) smoker occupants.

A linear regression of indoor $\text{PM}_{2.5}$ concentrations against the source contributions produced the average contributions of the above six sources that are shown in Table 24; the adjusted R^2 value is 0.85 so the six factor solution explains 85% of variance in indoor $\text{PM}_{2.5}$. Traffic (motor vehicles and suspended street dust) was the highest source with 39% of indoor $\text{PM}_{2.5}$, followed by cooking and ETS (28%), sulfates (15%), cleaning and cooking (10%) and indoor dust (8%). Receptor model performance was considered good given the variability in $\text{PM}_{2.5}$ indoor sources that was described with 3 factors for the 44 households. Combined outdoor sources contributed to 54% of indoor $\text{PM}_{2.5}$ concentrations.

Table 24 Source apportionment results for indoor $\text{PM}_{2.5}$, 6-factor solution.^a

| Source | Coefficient [$\mu\text{g}/\text{m}^3$] | Std. dev. [$\mu\text{g}/\text{m}^3$] |
|----------------------|--|--|
| Cooking and ETS | 6.1 | 0.7 |
| Street dust | 2.9 | 0.5 |
| Motor vehicles | 5.6 | 0.7 |
| Sulfates | 3.4 | 0.5 |
| Indoor dust | 1.6 | 0.3 |
| Cleaning and cooking | 2.3 | 0.3 |

^a All estimated coefficients have p values $<10^{-4}$. Linear regression was carried out without considering an intercept term.

4.6. Discussion of results

The infiltration factors — F_{INF} in Equation 8 — obtained here were higher than the ones estimated in previous studies for Santiago in the cold season (see section 4.4.1). This difference is ascribed to the higher values of a in Equation 8 for the spring campaign described here, when windows and doors are more frequently opened which led to higher values of F_{INF} than in previous winter campaigns at Santiago. The estimates reported here — Table 19 — are slightly higher than those reported by Meng et al. (Qing Yu Meng et al. 2007) for USA households: Zn (0.54 ± 0.03) and S (0.76 ± 0.03); hence the present results are consistent with the expected seasonal increase of AERs and consequent rise in F_{INF} in Equation 8, when compared with results from other studies that have used the same single-zone model to analyze data.

The present study had a limitation in that indoor $PM_{2.5}$ was sampled only at the living room in each household. When more detailed analysis of inter-zonal airflow within a household are considered, indoor $PM_{2.5}$ concentrations show spatial gradients, especially when internal doors and windows are kept closed and indoor sources are on. In this extreme case, McGrath et al. (McGrath et al. 2014) showed that a time scale of 4 h is needed in order to propagate (and dilute) peak concentrations from the room with emissions to the other rooms. The sampling period of 48 h used here smoothed out those differences within rooms, especially considering outdoor air infiltration. Du et al. (Du et al. 2012) showed that inter-zonal airflow is relatively less important as compared with outdoor airflow infiltration whenever household AERs are high — their measured AERs had an IQR of 0.32-0.90 h^{-1} . In this present campaign, AERs were not measured at Santiago but an estimate can be made from the average summertime AER measured in California in the RIOPA study (Yamamoto et al. 2010) which was 1.13 h^{-1} ; therefore, the present campaign was conducted in a scenario in which spatial gradients should have been modest for 48 h average indoor $PM_{2.5}$ concentrations. Klepeis and Nazaroff (Klepeis and Nazaroff 2006) have shown through detailed simulations for a household with all outside windows closed that single-zone model values — i.e. Equation 8 — are within 20% of simulated multi-

zone results when air conditioning is intermittently used. A similar increase in household ventilation should have happened in the present study when occupants opened doors and windows — see Figure 55 — hence it is concluded that the single-zone model was adequate to analyze household indoor $\text{PM}_{2.5}$ and its relation with outdoor concentrations in the present study.

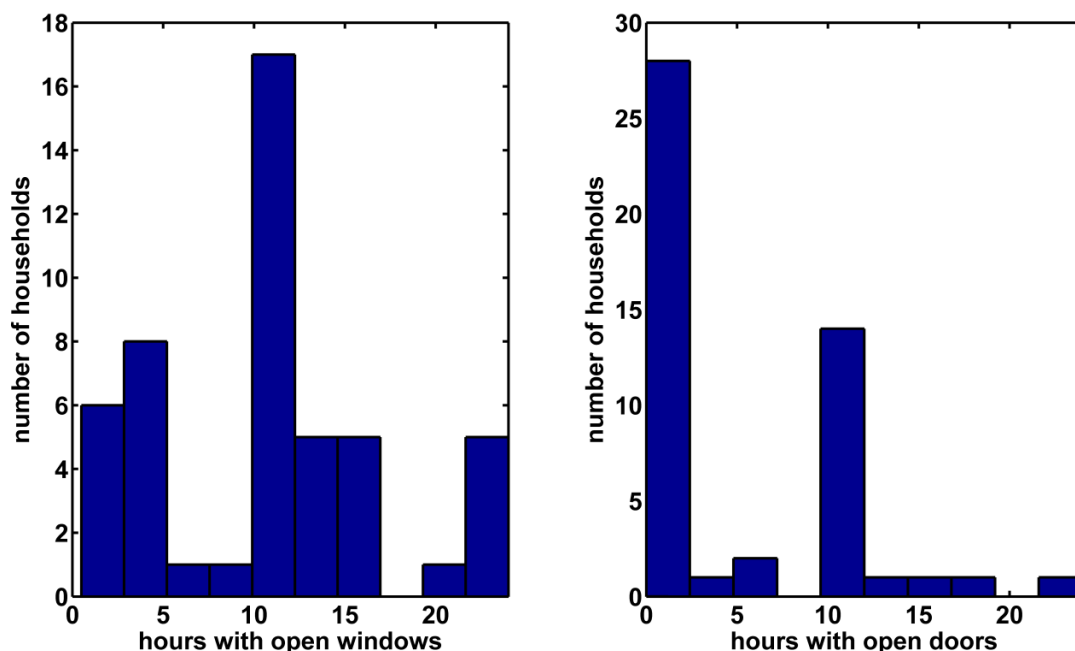


Figure 55 Histograms of hours per day with windows and doors open for all households included in the springtime campaign.

In summary, outdoor and indoor sources each contribute half of the measured indoor $\text{PM}_{2.5}$; there is potential for further reducing $\text{PM}_{2.5}$ population exposure by improving ventilation of indoor air (55% of households in the present study did not have a range hood), filtration of outdoor air, reducing household AER and controlling indoor sources like smoking, cooking or lighting incense. For instance, Singer et al. (Singer et al. 2012) estimated a 55% of removal efficiency for working range hoods in California homes, Fabian et al. (Fabian, Adamkiewicz, and Levy 2012) estimated that a working kitchen fan reduced $\text{PM}_{2.5}$ originated from cooking by $17 \text{ } (\mu\text{g}/\text{m}^3)$ in average in Boston public housing apartments and MacNeill et al. (MacNeill et al. 2012) estimated mean F_{INF} values of 0.26-0.36 for $\text{PM}_{2.5}$ — roughly half of the values found at Santiago — in tightly built homes in Windsor, ON, Canada.

4.7. Conclusions

A springtime indoor $\text{PM}_{2.5}$ campaign was carried out at Santiago, Chile in 2012, including 44 households — three different socioeconomic statuses — in the downtown area. Indoor concentrations of $\text{PM}_{2.5}$ were affected by socioeconomic status ($p = 0.048$) but no such evidence was found for $\text{PM}_{2.5}$ species, except lead ($p = 0.046$); we acknowledge this result is valid only for the warm season.

An urban background site was used to monitor outdoor $\text{PM}_{2.5}$ during the same period as in the indoor campaign. Then the single-zone indoor air quality model — Equation 8 — was applied to estimate infiltration factors that quantify what fraction of outdoor species is found indoors. Estimated values for this study were higher than the ones estimated at Santiago in the cold season — reflecting AER seasonality — yet similar to other studies with more households analyzed (Qing Yu Meng et al. 2007). Individual household infiltration factors had values higher than in developed countries where tighter household envelopes are built; five of the households measured had values higher than 1.0 and this is ascribed to departures of the single-zone model assumptions. This is a limitation of the present study that may be removed by applying multi-zone models in future studies.

For the first time, Positive Matrix Factorization (PMF3) was applied to an indoor $\text{PM}_{2.5}$ chemical composition data set measured at Santiago. Six sources of key species were identified; three were outdoor sources: motor vehicles, street dust and secondary sulfates and three were indoor sources: indoor dust, cleaning and cooking and environmental tobacco smoke; outdoor and indoor sources each contribute to half of the measured indoor $\text{PM}_{2.5}$. There is potential for further reducing $\text{PM}_{2.5}$ population exposure by: a) short-term interventions such as improving ventilation of indoor air and elimination of indoor sources like candle and incense lighting, and b) long-term initiatives such as reducing household AER and the filtration of outdoor air.

4.8. Acknowledgments

HJ and GV were supported by FONDECYT Grant 1121054. FB was supported by a CONICYT doctoral fellowship grant. HJ was also supported by Centro de Desarrollo Urbano Sustentable (CEDEUS, www.cedeus.cl), Grant CONICYT/FONDAP/15110020.

5. CHEMICAL SPECIATION AND SOURCE APPORTIONMENT OF FINE PARTICULATE MATTER IN SANTIAGO, CHILE, 2013

5.1. Highlights

- Strong seasonal trends in $PM_{2.5}$ and source contributions, highest levels in winter
- In winter, the most important sources of $PM_{2.5}$ were wood smoke and nitrate.
- In fall and winter, wood smoke contributed around 60% of OC and 20% of $PM_{2.5}$.
- Secondary inorganic ions accounted for about 30% of $PM_{2.5}$ in fall and winter.
- Secondary organic aerosols contributed significantly to $PM_{2.5}$ in summer and spring.

5.2. Abstract

Santiago is one of the largest cities in South America and has experienced high fine particulate matter ($PM_{2.5}$) concentrations in fall and winter months for decades. To better understand the sources of fall and wintertime pollution in Santiago, $PM_{2.5}$ samples were collected for 24 h every weekday from March to October 2013 for chemical analysis. Samples were analyzed for mass, elemental carbon (EC), organic carbon (OC), water soluble organic carbon (WSOC), water soluble nitrogen (WSTN), secondary inorganic ions, and particle-phase organic tracers for source apportionment. Selected samples were analyzed as monthly composites for organic tracers. $PM_{2.5}$ concentrations were considerably higher in the coldest months (June–July), averaging (mean \pm standard deviation) $62 \pm 15 \mu\text{g}/\text{m}^3$ in these two months. Average fine particle mass concentration during the study period was $40 \pm 20 \mu\text{g}/\text{m}^3$. Organic matter during the peak winter months was the major component of fine particles comprising around 70% of the particle mass. Source contributions to OC were calculated using organic molecular markers and a chemical mass balance (CMB) receptor model. The four combustion sources identified were wood smoke, diesel engine emission, gasoline vehicles, and natural gas. Wood smoke was the predominant source of OC, accounting for $58 \pm 42\%$ of OC in fall and winter.

Wood smoke and nitrate were the major contributors to $\text{PM}_{2.5}$. In fall and winter, wood smoke accounted for $9.8 \pm 7.1 \mu\text{g}/\text{m}^3$ ($21 \pm 15\%$) and nitrate accounted for $9.1 \pm 4.8 \mu\text{g}/\text{m}^3$ ($20 \pm 10\%$) of fine PM. The sum of secondary inorganic ions (sulfate, nitrate, and ammonium) represented about 30% of $\text{PM}_{2.5}$ mass. Secondary organic aerosols contributed only in warm months, accounting for about 30% of fine PM during this time.

5.3. Introduction

Large urban cities in Latin America, like Santiago (Chile), Sao Paulo (Brazil), and Mexico City (Mexico), have been facing serious air pollution problems because of population and industry growth, as well as increasing numbers of motor vehicles (Bell et al. 2006). Numerous studies have shown the negative effects on human health resulting from high levels of particulate matter, such as respiratory problems and premature death from cardiovascular disease (Analitis et al. 2006; Douglas W Dockery and Stone 2007; Pope and Dockery 2006; Pope et al. 2004). Due to the evidence of these adverse effects, the World Health Organization (WHO) recommends a 24-h standard of $25 \mu\text{g}/\text{m}^3$ for $\text{PM}_{2.5}$ (WHO: World Health Organization 2005), which are particles with an aerodynamic diameter of less than $2.5 \mu\text{m}$.

Santiago is the largest city in Chile and has about 6 million inhabitants (approximately 40% of the Chilean population). Santiago is located in subtropical South America ($33^{\circ}27'S$, $70^{\circ}40'W$) between a coastal range to the west (height ~ 1000 m.a.s.l., meters above sea level) and the Andes mountain range to the east (heights above 3000 m.a.s.l.). Transport of pollution in Santiago's basin is controlled by the surrounding topography, persistence of subsidence conditions and associated low mixing heights (Muñoz et al. 2010), and thermally driven winds that peak in the warmer months. Southwesterly winds occur during daytime both in winter (Rutllant and Garreaud 2004) and summer (Schmitz 2005; Viale and Garreaud 2014). In summertime conditions, pollutants from Santiago are transported towards the northeast out of the basin by up-slope winds reaching up to 4000 m (Schmitz 2005). The climate is Mediterranean with dry spring and summer seasons and wet fall and winter seasons as shown in Table 25 for year 2013.

Table 25 *Monthly meteorological data measured at the Meteorological Service station closest to the receptor site.*

| Month | Temperature(°C) | | | Relative humidity (%) | | Cloud Cover (oktas) | | Wind direction / speed (knots) | | Precipitation |
|-----------|-----------------|--------|--------|-----------------------|--------|---------------------|--------|--------------------------------|--------|---------------|
| | Mean | Max 1h | Min 1h | 08 LST | 14 LST | 08 LST | 14 LST | 08 LST | 14 LST | Total (mm) |
| January | 21.5 | 36.2 | 12.6 | 82 | 41 | 1.7 | 1.6 | CALM / 0 | SW / 6 | |
| February | 21.1 | 35.5 | 10.0 | 78 | 35 | 1.6 | 1.9 | CALM / 0 | SW / 5 | |
| March | 17.9 | 32.2 | 8.6 | 82 | 35 | 1.6 | 1.8 | CALM / 0 | SW / 5 | |
| April | 14.6 | 31.8 | 5.0 | 85 | 37 | 3.4 | 2.5 | NE / 2 | SW / 4 | |
| May | 10.8 | 26.6 | 0.8 | 88 | 47 | 3.5 | 3.6 | CALM / 0 | SW / 4 | 116.5 |
| June | 9.5 | 24.4 | -0.6 | 88 | 48 | 2.6 | 2.8 | NE / 3 | SW / 2 | 36.2 |
| July | 8.5 | 24.4 | -3.5 | 91 | 53 | 3.6 | 4.2 | NE / 2 | SW / 3 | 7.3 |
| August | 9.3 | 29.4 | -0.5 | 90 | 51 | 4.2 | 3.5 | E / 3 | SW / 3 | 33.3 |
| September | 11.1 | 27.8 | -1.6 | 81 | 41 | 4.7 | 4.1 | CALM / 0 | SW / 4 | 9 |
| October | 14.8 | 29.9 | 4.8 | 77 | 37 | 3.4 | 3.0 | CALM / 0 | SW / 6 | |
| November | 17.0 | 33.0 | 7.2 | 70 | 34 | 1.8 | 1.6 | SW / 3 | SW / 6 | |
| December | 20.7 | 35.0 | 7.7 | 39 | 37 | 1.0 | 0.9 | CALM / 0 | SW / 7 | |

The city has been facing air pollution problems for more than three decades. The poor air quality is believed to be the result of the growing industrial sector, fast growing population, and increased number of motor vehicles (Ministerio de Transporte 2014), worsened by the aforementioned geophysical constraints for pollutant dispersion in Santiago's basin: in fall and winter seasons subsidence conditions induce thermal inversion layers that increase ambient levels of pollutant concentrations and produce a characteristic seasonality of air quality in the city (Didyk et al. 2000; Héctor Jorquera, Palma, and Tapia 2000; Sax et al. 2007; Tsapakis et al. 2002).

The Chilean government has been implementing regulations in recent decades to control air pollution in Santiago (Héctor Jorquera, Palma, and Tapia 2000; Mena-Carrasco et al. 2014). Efforts have been directed at modernizing the public transport system by replacing old buses with lower-emission buses, using cleaner fuels (including the removal of lead from gasoline in 2001), and reducing the sulfur level in diesel fuel. Policies for emissions reduction from industrial sources were also promulgated, along with street sweeping and cleaning programs to reduce fugitive dust emissions. Contingency measures are implemented every year from April 1 to August 31 (fall and winter) for high pollution events that include activity restrictions on vehicles, industries, residential wood stoves, and exclusive lanes for public buses (Ministerio del Medio Ambiente (MMA) 2014). Restrictions applied during critical days have been effective in reducing levels of particulate matter and NO_x (Troncoso, De Grange, and Cifuentes 2012). These regulations have decreased the average concentrations of PM_{10} and $\text{PM}_{2.5}$ in Santiago; however, levels in winter are still significantly above WHO guidelines (Barraza et al. 2014; Héctor Jorquera and Barraza 2013; Koutrakis et al. 2005; Sax et al. 2007).

In this work we focus on $\text{PM}_{2.5}$ because its health impacts are greater than those of coarse particles, and currently the particulate matter problems for $\text{PM}_{2.5}$ concentrations in Santiago are more complex to manage. This is because secondary $\text{PM}_{2.5}$ has become more relevant as primary emissions have been reduced with the aforementioned policies. Hence new pollution abatement strategies ought to include abatement of gaseous precursors and primary $\text{PM}_{2.5}$ emissions as well.

Policies and regulations implemented in Santiago during recent decades have not only decreased the concentration of particulate matter, they also have changed the relative chemical composition of particles. Table 26 summarizes previous studies in Santiago that have used the chemical composition of $PM_{2.5}$ to determine its sources; the most relevant sources identified between 1987 and 2005 were motor vehicles, wood burning, secondary aerosols, industrial sources and soil dust. In that period, sulfate concentrations were decreasing while organic carbon concentrations were increasing. However, none of those studies used a chemical mass balance (CMB) receptor model with organic molecular tracers. This method has been applied in other cities around the world (Daher et al. 2011; Daher et al. 2012; Heo et al. 2013; E. a. Stone et al. 2007; Elizabeth Stone et al. 2010) but not in Chile.

The goal of this work is to characterize the chemical composition of $PM_{2.5}$ in Santiago through elemental and organic carbon (ECOC), water soluble organic carbon (WSOC), water soluble total nitrogen (WSTN), ionic, elemental, and organic tracer analysis, and to use organic tracers in the CMB model to better identify sources of fine particles and estimate their apportionment. Santiago still needs to reduce the levels of fine particles, so it is expected that the results of this research will better direct control strategies to reduce particulate matter concentrations.

Table 26 *Summary of previous source apportionment results carried out at Santiago.*

| Reference | Dates/location/mean PM _{2.5} (µg/m ³) | Methodology | Results |
|-----------------------------|---|---|---|
| Rojas et al. (1990) | West center, January–February 1987; 34 (µg/m ³) | Dichotomous sampler; XRF analysis of filters. Principal Factor Analysis for source apportionment. | Sulfates: 49%; wood burning and traffic: 26%; residual oil combustion: 13%; soil dust and metal works: 6.4%; soil dust and wood burning: 5.6% |
| Artaxo (1996) | Center, July–August 1996; 54.4 (µg/m ³) | SFU filter samples with PIXE analysis. Absolute Principal Factor Analysis for Source Apportionment. | Sulfates and industry: 64%; motor vehicles: 16%; soil dust: 15.5%; copper smelter: 8.7%; residual oil combustion: 1.9% |
| Artaxo (1998) | Center, July–August 1998; 39.7 (µg/m ³) | SFU filter samples with PIXE analysis. Absolute Principal Factor Analysis for Source Apportionment. | Motor vehicles: 35.8%; soil dust: 31.3%; residual oil combustion and industry: 23.2%; Sulfates and copper smelter: 9.7%; |
| Artaxo (1999) | Center, 27 June–1st December 1999; 28 (µg/m ³) | SFU filter samples with PIXE analysis and BC measurements. Absolute Principal Factor Analysis for Source Apportionment. | Motor Vehicles: 40%, Sulfates + As: 39%, Soil dust: 17%, Metal works: 4% |
| | East, 26 June–30 November 1999; 34 (µg/m ³) | | Motor vehicles + industry: 70%, Sulfates + As: 15%, Soil dust: 7% |
| Gramsch (2005) | Center, July–August 2001; 61.4 (µg/m ³) | Speciation Sampler 2300 for chemical characterization, SFU samples with PIXE elemental analysis. | Nitrate: 19%; sulfate: 8%; ammonia: 12%; EC: 22%; OC: 15%; chlorine: 2% |
| | Center, July–August 2003; 69.4 (µg/m ³) | | Nitrate: 15%; sulfate: 5%; ammonia: 7%; EC: 10%; OC: 33%; chlorine: 2% |
| | Center, July–August 2005; 44.2 (µg/m ³) | | Nitrate: 18%; sulfate: 8%; ammonia: 17%; EC: 11%; OC: 36%; chlorine: 4% |
| Moreno (2010) | Center, April 1998–August 2007 | Dichotomous sampler; XRF analysis of filters. Principal Factor Analysis for source apportionment. | Soil: 24.6%; Motor Vehicles: 12.3%; Residual Oil: 13.6%; Secondary sulfates: 13.6%. |
| Jorquera and Barraza (2012) | East, June–December 1999 (reanalysis of Artaxo's, 1999 data set); 34 (µg/m ³) | PMF3.0 on filter analysis of trace elements + BC; back trajectory analysis to confirm sources. | Motor vehicles: 28%; wood burning: 25%; sulfates: 19%; marine aerosol: 13%; copper smelters: 11%; soil dust: 4% |
| | East, January–December 2004; 25 (µg/m ³) | | Motor vehicles: 31%; wood burning: 29%; sulfates: 16%; marine aerosol: 10%; copper smelters: 10%; soil dust: 4% |

5.4. Methodology

5.4.1. Sampling site description

The chosen monitoring site ($33^{\circ} 29' 51.7''$ S, $70^{\circ} 36' 39.2''$ W) was located on a roof of a 4-story building at the Campus San Joaquín, Pontificia Universidad Católica de Chile, close to Santiago's geographical center; see Figure 56 for a map showing the urban site and nearby air quality and meteorological monitoring stations. The site is located above the tree line, far enough from nearby buildings — see Figure 57 the closest busy street is 470 m away, making it representative of urban conditions as recommended by US EPA's ambient air quality monitoring guidelines (US EPA 1997). Figure 58 shows wind rose plots — for diurnal and nocturnal conditions during the monitoring campaign — for the two closest monitoring stations from Santiago's ambient air quality monitoring network. It can be seen that during diurnal conditions the prevalent winds are S–SW–W while nocturnal winds are E, SE and SW; this corresponds to a mountain-valley circulation that happens all year long. Therefore, the receptor site samples air masses from different parts of the city that pass through the center. The climate of Santiago is Mediterranean, with a dry warm season from October through March and a wet season from April through September; Table 25 shows monthly weather summaries for 2013 at a monitoring site from Chile's Meteorological Service which is close to the urban monitoring site chosen in this study.

As was mentioned in the Introduction section (section 5.3), air pollution has a distinctive seasonality in Santiago; stagnation conditions promoted by subsidence conditions become more frequent in fall and winter when mixing heights reach low levels above Santiago's basin (Muñoz et al. 2010). Figure 59 shows monthly averages of CO, SO₂, O₃, NO, NO₂, PM_{2.5} and PM₁₀ measured at two air quality monitoring stations closest to the central urban site for the year 2013; there is a strong seasonality as all pollutants but ozone increase in fall and winter. These results are characteristic of Santiago

and have been previously reported (Héctor Jorquera, Palma, and Tapia 2000; Héctor Jorquera, Palma, and Tapia 2002; Koutrakis et al. 2005; Sax et al. 2007).

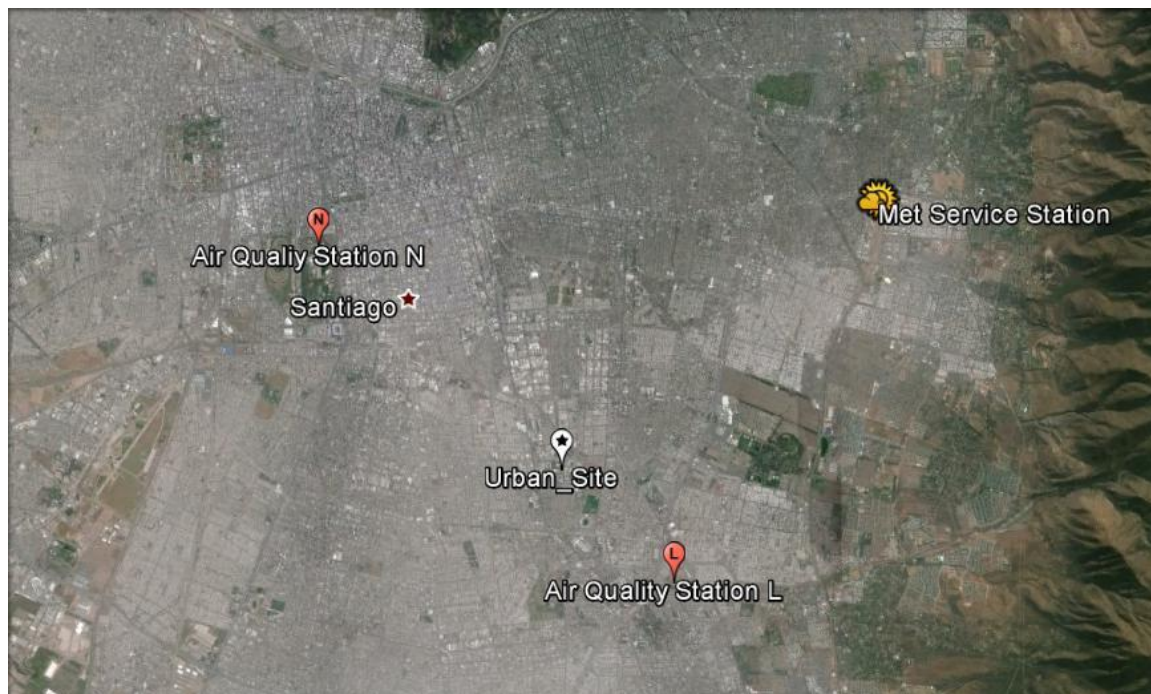


Figure 56 Map of Santiago showing the geographical center (labeled star), the location of the receptor site, two of the closest air quality monitoring network stations (L, N), and the closest station from the Meteorological Service.



West view of Santiago



East view of Santiago

Figure 57 Views of Santiago from the receptor site.

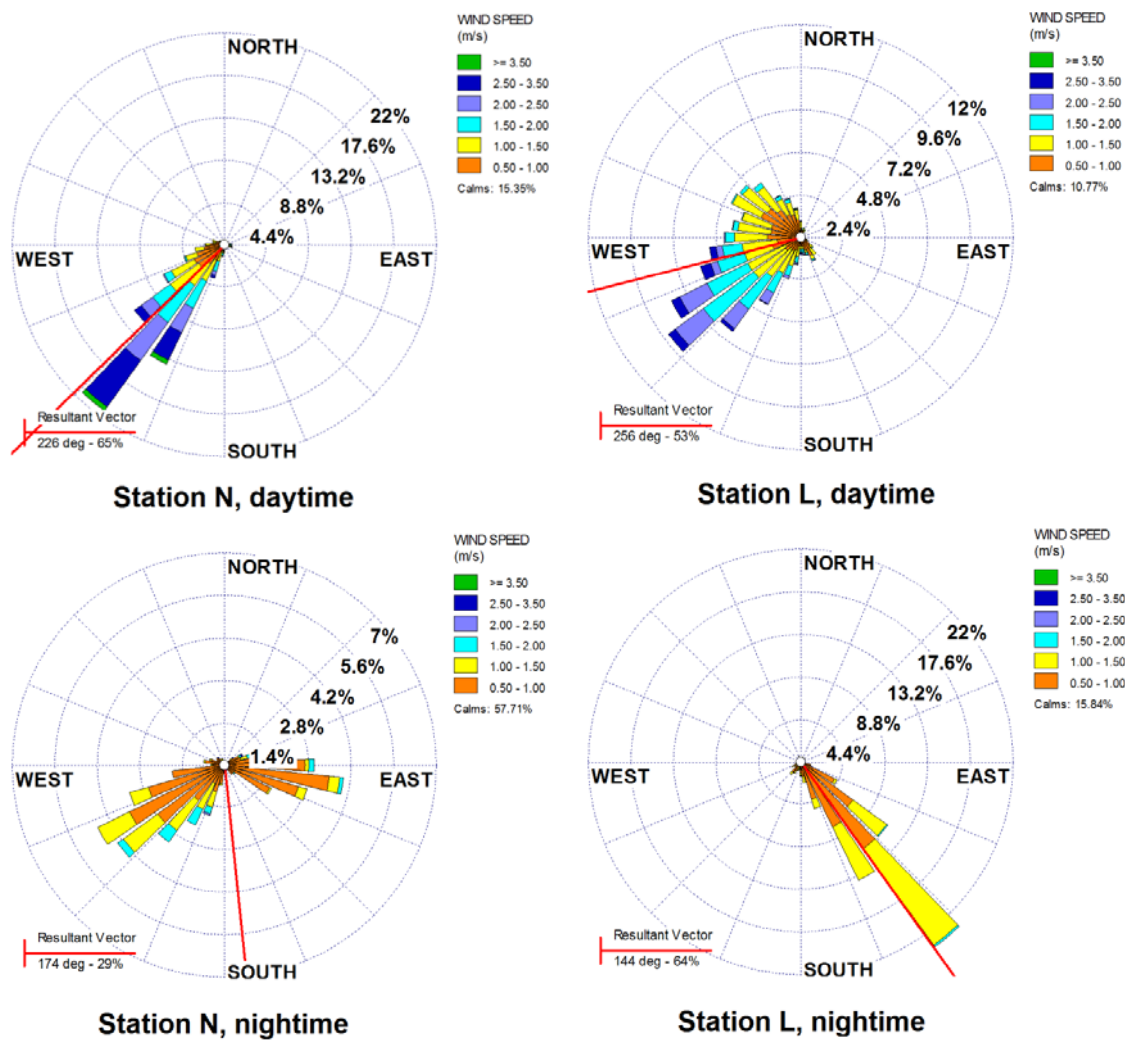


Figure 58 Plots of rose winds for monitoring stations L and N for March - October 2013.

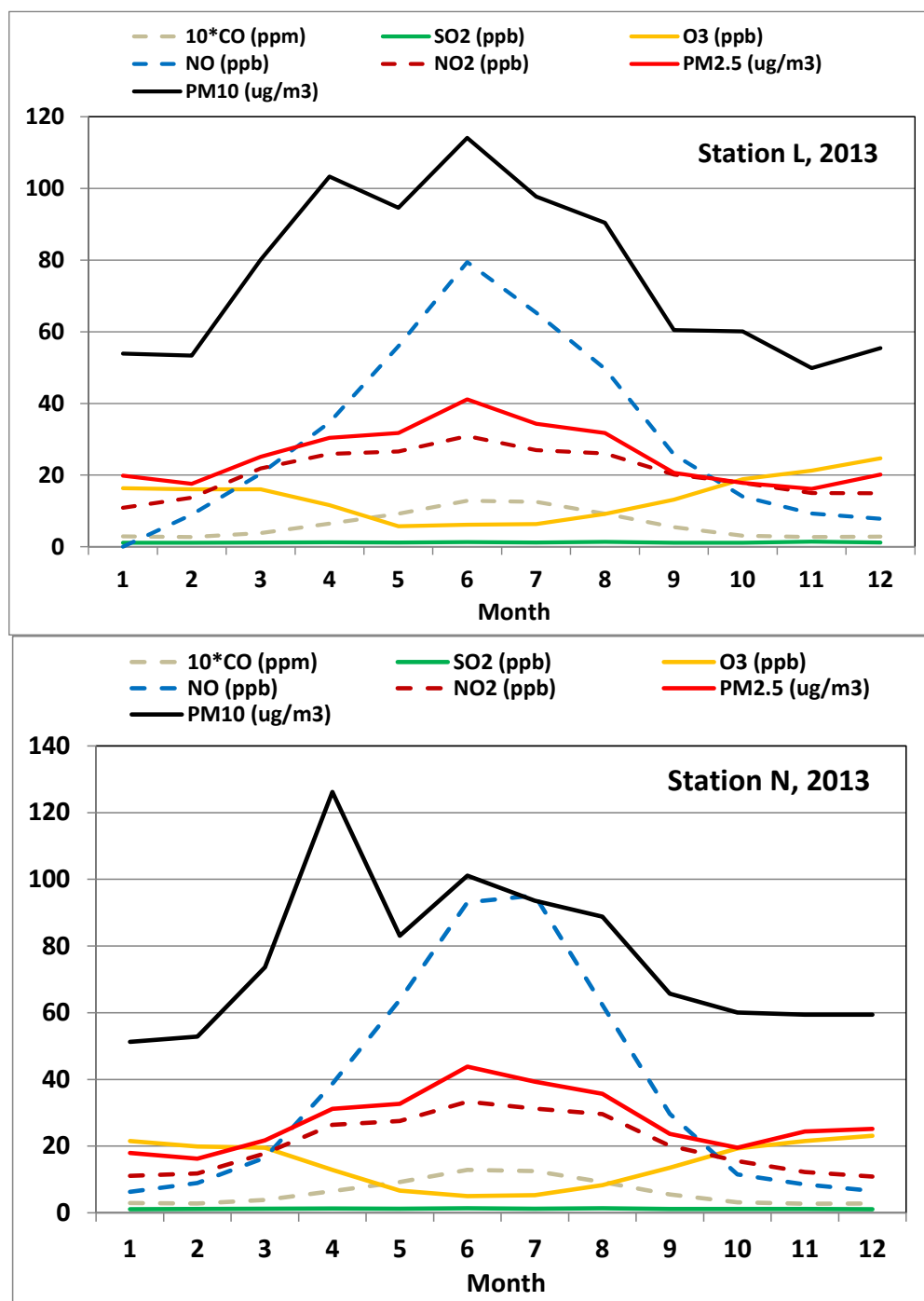


Figure 59 Plots of monthly averages of pollutants measured at stations N and L, year 2013.

5.4.2. Sampling method and selection of samples

Paired Partisol samplers (model 2000i Thermo Scientific, USA, 16.67 L/min) were deployed to measure urban background $PM_{2.5}$ levels in 24-h integrated filters. Samples were collected from March to October 2013 every weekday, except on holidays, beginning at 12:00 local time. One Partisol was loaded with a Teflon filter (46.2 mm PTFE, Whatman, NJ, USA) to determinate $PM_{2.5}$ mass and trace metals, and the other with a quartz filter (47 mm, Tissuquartz 2500QAT-UP, Pall Life Sciences, USA) for purposes of chemical speciation. Field blank filters are 10% of samples. All filters were enclosed in Petri dishes (gamma radiation sterilized, VWR, USA), sealed with Teflon tape and placed within screwed aluminum holders, stored in coolers, and kept refrigerated at $-20^{\circ}C$ until analysis.

In order to reduce the number of samples for ECOC analysis, and to obtain appropriate mass loading for Gas Chromatography/Mass Spectrometry (GC-MS) analysis, five samples per month were selected to be analyzed for ECOC and subsequently for organic tracers. The samples selected for ECOC analysis were chosen to represent every sixth day samples. When a particular sample was missing, the sample taken the day after or before the target day was selected. In each month, the average of $PM_{2.5}$ mass of all the samples was compared with the average mass of the five selected samples to ensure that the selected mass was representative of the mass average. As shown in Figure 60, the selected samples were representative of each month as indicated by the fact that monthly averages were not statistically different. In addition, sulfate, nitrate, and WSOC concentrations of all the samples had similar trends.

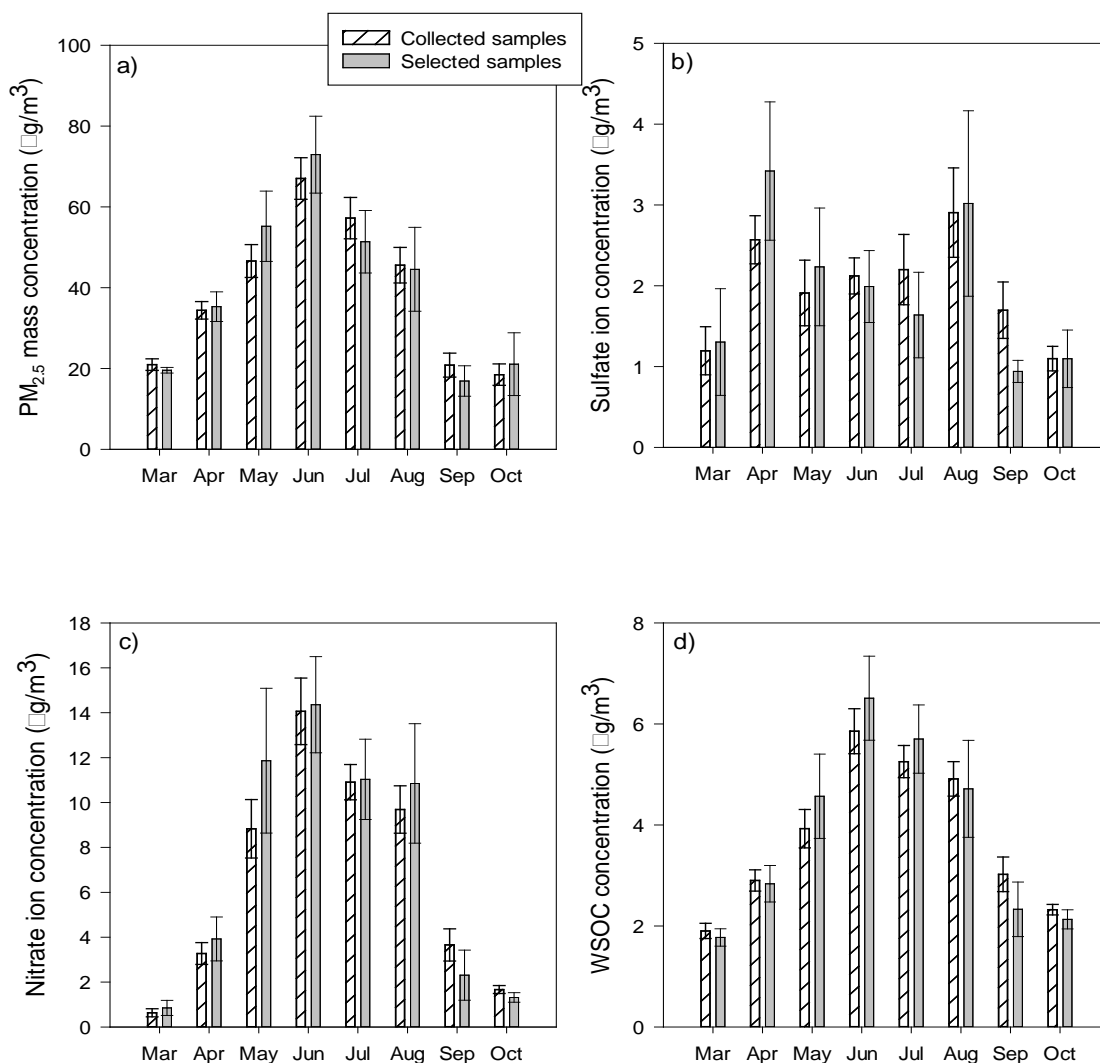


Figure 60 Monthly comparison of a) PM_{2.5} mass b) sulfate c) nitrate and d) WSOC of 1) all samples collected and 2) selected samples, including standard error, from March to October.

5.4.3. Chemical analysis

Teflon filters were conditioned in a room with controlled temperature (20 ± 2 °C) and relative humidity (35–40%) for 24 h before being weighed with a microbalance (Sartorius, model Cubis-DF LSM011, resolution: 1 µg, Goettingen, Germany). The elemental analysis was conducted by X-ray fluorescence at Chester Labnet Laboratory (Tigard, OR, USA) following method IO-3.3 (US EPA 1999). A piece of each quartz filter (1.0 cm²) was analyzed in a Thermal Optical Analyzer (Sunset Laboratories, Forest Grove,

OR, USA) to determine elemental carbon (EC) and organic carbon (OC) through the NIOSH thermal optical transmission method. In the first stage, samples were heated at increasing temperature levels to evolve OC and pyrolysis products in a free oxygen atmosphere. Subsequently, in a second stage, EC was evolved in a He/oxygen atmosphere. EC and OC were quantified using FID. Laser transmittance through the filter was monitored continuously to determinate the split point which separates OC and EC, and to correct for pyrolysis products. Details of the method have been described elsewhere (J. J. Schauer et al. 2003). WSOC and WSTN were measured using a TOC-V SCH Shimadzu total organic carbon analyzer. For the analysis, 1.5 cm² of each quartz filter was water extracted in 15 mL of Milli-Q water for 6 h in a shaker, and filtered using 0.45 µm syringe filters before the analysis (Miyazaki et al. 2011; Yang, Li, and Yu 2003). Water insoluble organic carbon (WIOC) was calculated as the difference between OC and WSOC, and the uncertainty for WIOC was calculated by the propagation of the uncertainties. After TOC/TN analysis, a fraction of the remaining solution was used to determine water soluble inorganic ions. Seven ions (sulfate (SO₄²⁻), nitrate (NO₃⁻), chloride (Cl⁻), sodium (Na⁺), ammonium (NH₄⁺), potassium (K⁺), and calcium (Ca²⁺), were measured using ion chromatography (IC) (Dionex ICS 2100 and Dionex ICS 100) (Wang et al. 2005). Monthly composites containing equal parts of 5 quartz filters per month were prepared to analyze organic compounds by gas chromatography–mass spectrometry (GC-6980, quadrupole MS-5973, Agilent Technology). To ensure that organic compounds would be detected by GC–MS, composites had approximately 500 µg of OC. Before the extraction, composites were spiked with isotopically-labeled standard solutions. Composite samples were extracted using 50/50 dichloromethane and acetone. Samples were sonicated in 20 min increments, alternating between the solvents (four successive extractions), then evaporated in a rotavapor, and finally reduced in volume by blowing down using ultrapure nitrogen. Extracts were analyzed twice by GC–MS. An aliquot was methylated with diazomethane, and in other aliquot, a silylating reagent derivatizes hydroxyl and carboxyl groups (Nolte et al. 2002). Additional details of the method can be found elsewhere Stone et al. (Elizabeth Stone et al. 2010). For quality control of the organic tracer analysis, a sample of SRM 1649a (Urban Dust) from the National Institute of Standards and Technology (NIST) and a standard spike sample were analyzed with each batch of samples. For all of the tracers used

in the CMB model, spike recoveries were in the range of 90–140%. For the inorganic measurements and ECOC, the spike recoveries were in the range of 90–107%. All concentrations were blank corrected, and uncertainties were estimated using standard deviation of field blanks and detection limit of the instruments.

5.4.4. Source apportionment

Primary source contributions to organic carbon were estimated using chemical mass balance receptor model software developed by EPA (EPA CMB v8.2). This software solves a linear system of equations, which includes ambient concentration and source profiles, using the effective variance weighted least-squares method (Watson, Cooper, and Huntzicker 1984). The model was run with eight monthly composite samples that represent a monthly composite for each month from March to October. Due to the resources and particulate matter mass required for the organics analysis, it was not feasible to analyze individual daily samples for organic tracers. Organic compounds selected as tracers were stable during the transport from the source to the receptor, they did not react or volatilize, and all main sources were included in the model in order to obtain good results (James J. Schauer et al. 1996). Twenty one molecular markers were selected, which includes EC, benzo(b)fluoranthene, benzo(k)fluoranthene, benzo(e)pyrene, indeno(1,2,3-cd)pyrene, benzo(ghi)perylene, picene, 17 α (H)-22,29,30-trisnorhopane, 17 α (H)-21 β (H)-30-norhopane, 17 α (H)-21 β (H)-hopane, ABB-20R-C27-cholestane, ABB-20R-C29-sitostane, ABB-20S-C29-sitostane, n-alkanes with carbon numbers from 27 to 33, and levoglucosan. Five source profiles were selected according to previous studies conducted at Santiago — see Table 26 — and to the results of the organic tracer analysis; hence we selected wood smoke (Fine, Cass, and Simoneit 2004), natural gas (Rogge, Hildemann, et al. 1993), diesel emission (Lough et al. 2007), gasoline vehicle (Lough et al. 2007), and smoking vehicle (Lough et al. 2007) as source candidates. CMB results are considered acceptable if $R^2 > 0.9$. If some sources show co-linearity problems, sensitivity analysis will be done to select the appropriate major sources of OC.

5.5. Results and discussion

5.5.1. Particulate matter and composition

PM_{2.5} mass, sulfate, nitrate, and WSOC of all samples collected are shown in Figure 61. PM_{2.5} mass, nitrate, and WSOC concentrations showed similar seasonality: concentrations were much higher from June to August. In contrast, sulfate concentrations did not show seasonality. Figure 60 shows clearly that samples selected for EC/OC and GC–MS analysis were representative of all samples collected. As shown in Figure 61, OC and EC concentrations of the selected samples peaked from June to August. Information on OC and EC concentrations was necessary for particle-phase organic tracer analysis, whose results are the focus of the present study.

Monthly averaged ambient concentrations of PM_{2.5} and reconstructed mass from March to October are shown in Figure 62 and Table 27. Average concentration of fine particles was 40 ± 20 (average \pm standard deviation) $\mu\text{g}/\text{m}^3$; higher concentrations were registered in colder months (June–July), averaging 62 ± 15 $\mu\text{g}/\text{m}^3$. The highest monthly average concentration was in June, 73 $\mu\text{g}/\text{m}^3$, and the single highest concentration measured was 140 $\mu\text{g}/\text{m}^3$ (in July). Although these concentrations are significantly lower than concentrations reported in Chinese and Indian cities (Cao et al. 2012; Deshmukh and Mkoma 2011), 80% of the samples collected during fall–winter (April–September) exceeded 24-h WHO guidelines (25 $\mu\text{g}/\text{m}^3$), and for the same period, 50% of the samples are above 24-h Chilean national standard (50 $\mu\text{g}/\text{m}^3$). Higher concentrations of PM_{2.5} in colder months can be attributed to the topography and the persistence of subsidence conditions that induce thermal inversion layers which increase ambient levels of pollutant concentrations. The lowest concentrations were registered in March and October, summer and spring seasons respectively, averaging about 20 $\mu\text{g}/\text{m}^3$.

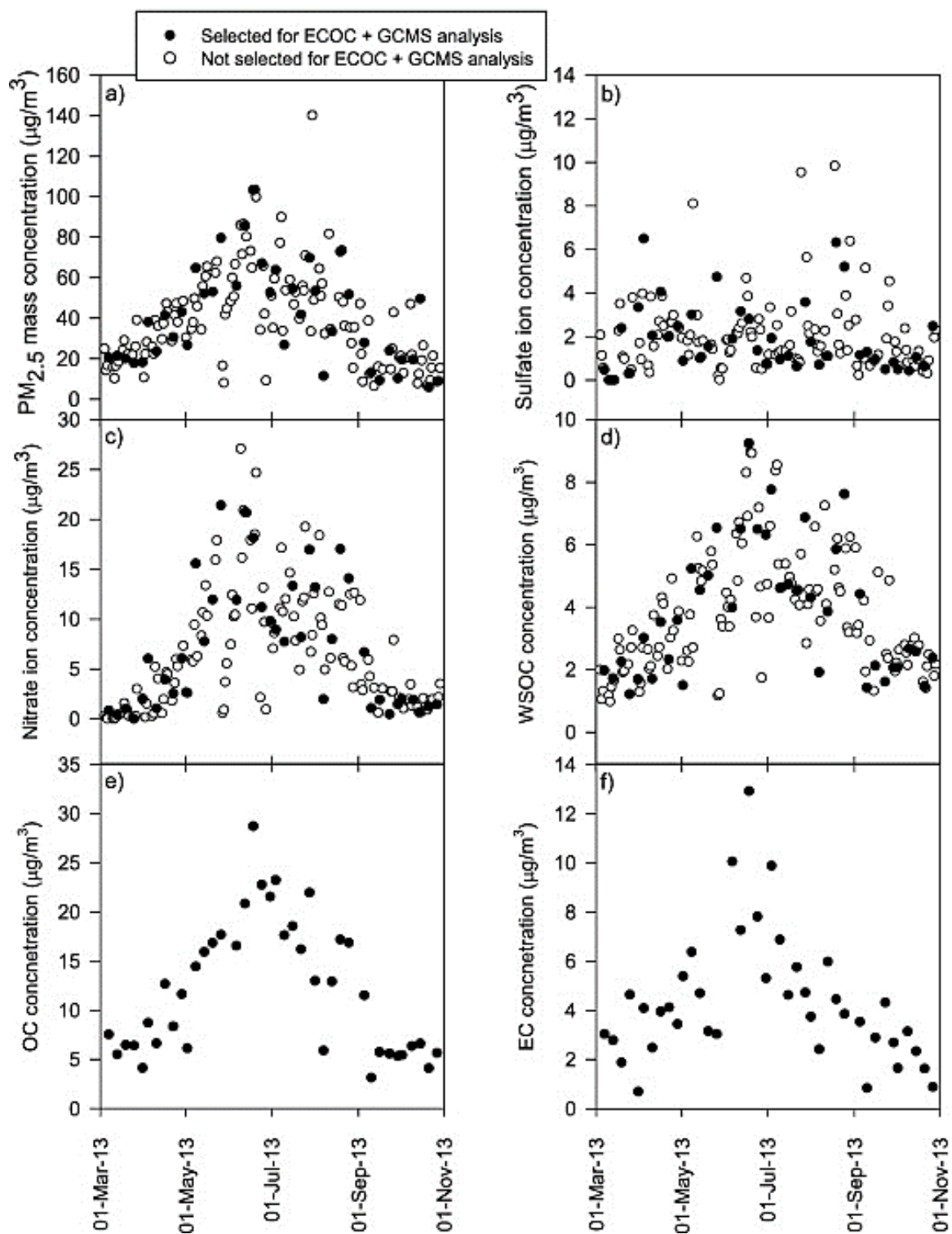


Figure 61 Concentration of a) PM_{2.5} mass, b) sulfate, c) nitrate, d) WSOC, e) OC, and f) EC in Santiago from March to October.

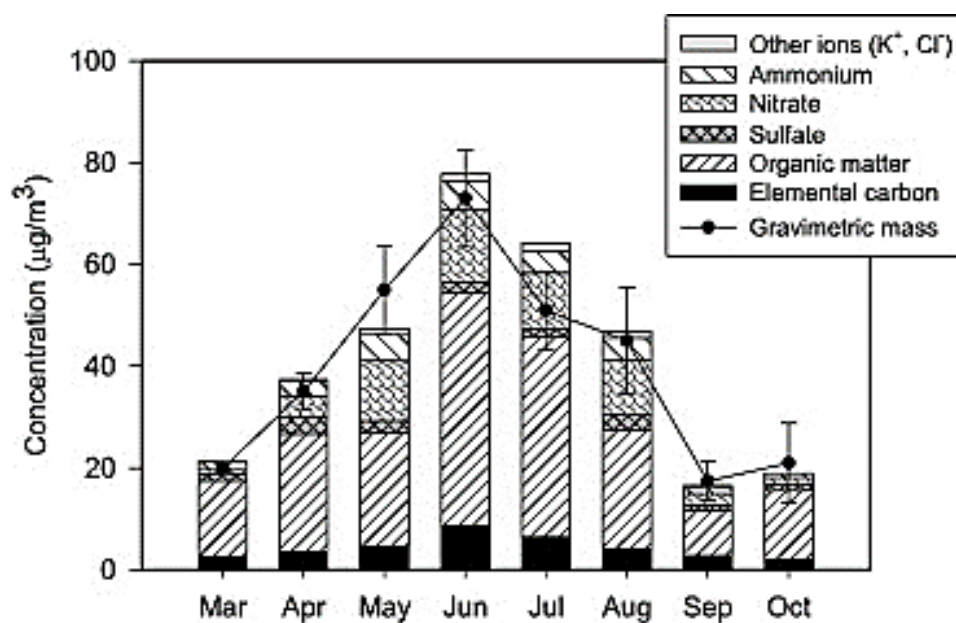


Figure 62 Monthly gravimetric $PM_{2.5}$ mass (\pm standard error) and bulk composition in Santiago from March to October.

Table 27 Monthly average gravimetric $PM_{2.5}$ mass and bulk composition (\pm standard deviation) for fine particulate matter in Santiago, Chile.

| Month | $PM_{2.5}$ mass $\mu\text{g}/\text{m}^3$ | Organic carbon $\mu\text{g}/\text{m}^3$ | Elemental carbon $\mu\text{g}/\text{m}^3$ | Sulfate $\mu\text{g}/\text{m}^3$ | Nitrate $\mu\text{g}/\text{m}^3$ | Ammonium $\mu\text{g}/\text{m}^3$ | Other ions ^a $\mu\text{g}/\text{m}^3$ |
|-------|---|--|--|-------------------------------------|-------------------------------------|--------------------------------------|---|
| Mar | 20 (± 2) | 6.0 (± 1.3) | 2.6 (± 1.5) | 1.3 (± 1.5) | 0.8 (± 0.8) | 1.4 (± 1.1) | 0.2 (± 0.2) |
| Apr | 35 (± 8) | 9.6 (± 2.5) | 3.6 (± 0.7) | 3.4 (± 1.9) | 3.9 (± 2.2) | 3.0 (± 1.2) | 0.3 (± 0.2) |
| May | 55 (± 19) | 14.2 (± 4.7) | 4.5 (± 1.4) | 2.2 (± 1.6) | 11.9 (± 7.2) | 5.4 (± 3.1) | 0.9 (± 0.6) |
| Jun | 73 (± 21) | 22.1 (± 4.4) | 8.7 (± 2.9) | 2.0 (± 1.0) | 14.4 (± 4.8) | 5.6 (± 1.9) | 1.3 (± 0.6) |
| Jul | 51 (± 17) | 19.5 (± 3.0) | 6.4 (± 2.2) | 1.6 (± 1.2) | 11.0 (± 4.0) | 4.2 (± 1.7) | 1.6 (± 0.4) |
| Aug | 45 (± 23) | 13.2 (± 4.5) | 4.1 (± 1.3) | 3.0 (± 2.6) | 10.8 (± 6.0) | 4.3 (± 2.6) | 1.3 (± 0.3) |
| Sep | 17 (± 8) | 6.3 (± 3.1) | 2.9 (± 1.3) | 0.9 (± 0.3) | 2.3 (± 2.5) | 1.5 (± 1.0) | 0.1 (± 0.2) |
| Oct | 21 (± 17) | 5.6 (± 1.0) | 1.9 (± 0.9) | 1.1 (± 0.8) | 1.3 (± 0.5) | 1.0 (± 0.4) | 0.0 (± 0.0) |

^a Includes potassium and chloride.

Mass was reconstructed through the sum of elemental carbon, organic matter (OM), sulfate, nitrate, ammonium, and other ions (chloride and potassium). Trace metals were not included in the reconstructed mass because they were not important contributors to $PM_{2.5}$. Figure 63 shows that dust concentrations calculated (Cheung et al. 2011; von Schneidmesser et al. 2010) from May to September accounted for less than 5% of $PM_{2.5}$ mass, in agreement with previous estimates for the 1999 and 2004 data (Héctor Jorquera and Barraza 2012). Organic matter concentrations were estimated using source specific OM/OC factors (Bae, Schauer, and Turner 2006), which were applied to the source apportionment results that will be shown later. As seen in Figure 62, OM was the major component of ambient $PM_{2.5}$, varying from $8.8 \mu\text{g}/\text{m}^3$ in September to $46 \mu\text{g}/\text{m}^3$ in June. In the coldest months (June–July), organic matter had the highest absolute and relative contributions, $43 \pm 5 \mu\text{g}/\text{m}^3$ and $69 \pm 7\%$ respectively.

Measured and reconstructed mass agreed well, averaging $103 \pm 12\%$.

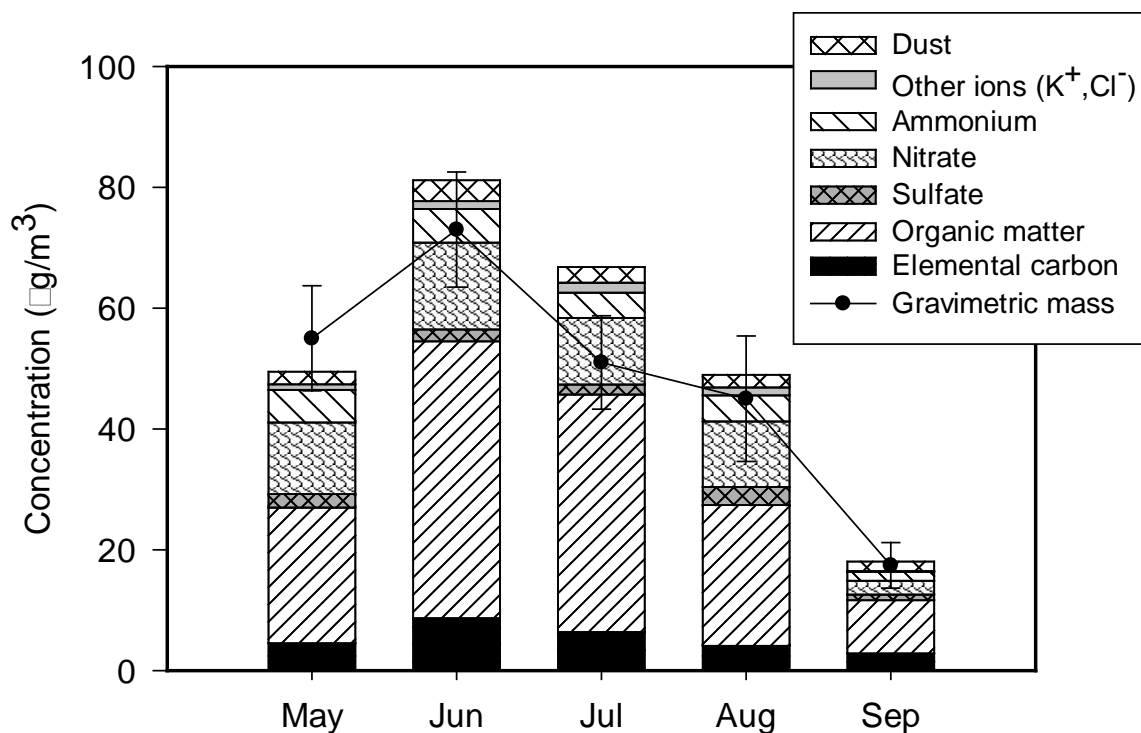


Figure 63 Monthly gravimetric $PM_{2.5}$ mass (\pm standard error) and bulk composition from May to September, including dust.

5.5.1.1. Water soluble inorganic ions

Total inorganic ions accounted for $31 \pm 19\%$ of $PM_{2.5}$ mass. Major ions were nitrate ($17.8 \pm 13.8\%$), ammonium ($8.3 \pm 4.6\%$), and sulfate ($4.9 \pm 2.3\%$), which accounted for $7.1 \pm 5.5 \mu\text{g}/\text{m}^3$, $3.3 \pm 1.8 \mu\text{g}/\text{m}^3$, and $2.0 \pm 0.90 \mu\text{g}/\text{m}^3$ respectively. As shown in Figure 62, all ions registered higher concentrations in colder months, except sulfate which lacked any pattern. In Santiago, concentrations of sulfate were low because of air quality regulations which allow a maximum of 15 ppm of sulfur content in diesel and gasoline (Ministerio del Medio Ambiente (MMA) 2014); however, nitrate and ammonium concentrations were higher. This is due to higher emissions of NO_x and ammonia, which are the precursors of these ions, and meteorological conditions that favored formation of ammonium nitrate (Toro et al. 2014). Other ions, which are the sum of chloride and potassium, only accounted for $1.5 \pm 1.1\%$ of $PM_{2.5}$ mass. Calcium and sodium concentrations were lower than $1 \mu\text{g}/\text{m}^3$.

5.5.1.2. Carbonaceous compounds

Monthly concentrations of WSOC, WIOC, and EC are shown in Figure 64a. All carbonaceous species followed the same seasonality as $PM_{2.5}$ mass; values were higher in colder months. Average EC concentration was $4.3 \pm 2.2 \mu\text{g}/\text{m}^3$ from March to October with a relative contribution to fine particles of $11 \pm 6\%$. Average OC concentrations changed from a low of $5.6 \mu\text{g}/\text{m}^3$ in October to a high of $22 \mu\text{g}/\text{m}^3$ in June. OC/EC ratios were constant from March to October, averaging 2.8 ± 0.4 . WSOC rose from a low of $1.8 \mu\text{g}/\text{m}^3$ in March to a high of $6.5 \mu\text{g}/\text{m}^3$ in June, and average WIOC concentrations were $3.5 \pm 1.8 \mu\text{g}/\text{m}^3$ in October and $16 \pm 1.8 \mu\text{g}/\text{m}^3$ in June. WSOC/OC ratios were similar during the months analyzed, averaging 0.33 ± 0.04 .

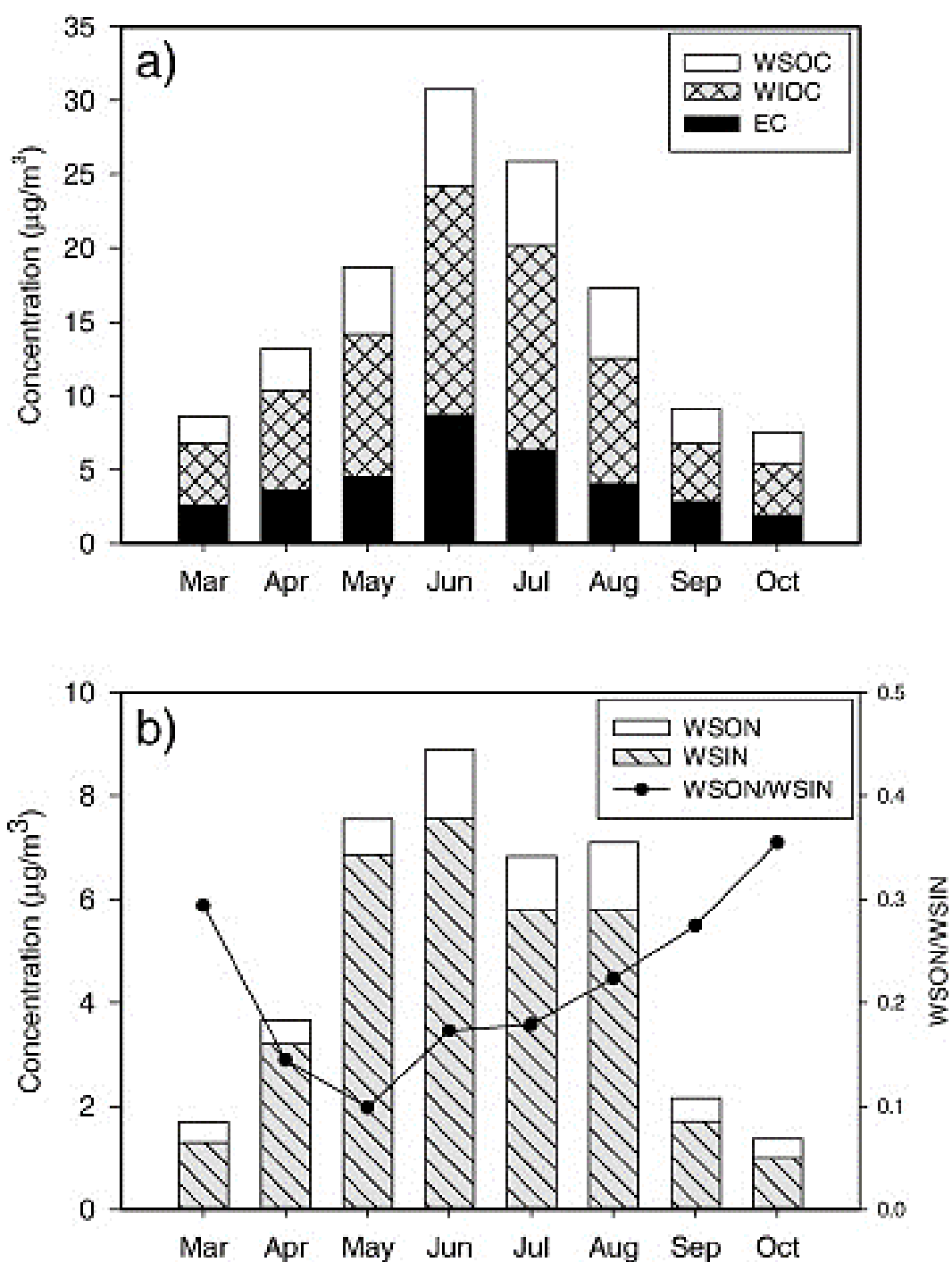


Figure 64 Monthly ambient concentrations of a) EC, WIOC, and WSOC and b) WSIN and WSON in Santiago from March to October.

5.5.1.3. Nitrogen containing species

Water soluble inorganic nitrogen (WSIN) was calculated as the sum of nitrate ion (NO_3^-) plus ammonium ion (NH_4^+), which were measured by IC. Water soluble organic nitrogen (WSON) was calculated as the difference between the water soluble total nitrogen measured in the TOC analyzer and WSIN (Lim et al. 2012; Miyazaki et al. 2011). Figure 64b shows monthly concentrations of WSIN and WSON. As expected, water soluble nitrogen concentrations were higher in colder months (May–August). Nitric acid and ammonium nitrate are semi-volatile compounds, whose partitioning to particle phase is favored at low temperatures and high relative humidity (Squizzato et al. 2013). Monthly WSON/WSIN ratios are shown in Figure 64b. The average WSON/WSIN ratio was 0.22 ± 0.09 , with peaks in warmer months (March and October). A one sample t-test showed that water soluble organic nitrogen concentrations were statistically different from zero ($p < 0.0001$). WSON could be emitted from biomass burning or formed in the atmosphere during reactions of VOCs and NO_x and partitioned to gas phase (Mace 2003). The results of this study suggest that during fall and winter WSON was associated with biomass burning and during warm months it was produced mainly by photochemical reactions of SOA with inorganic nitrogen. The peaks of WSON/WSIN in warm months were produced because a fraction of WSIN was transformed to WSON through photochemical reactions.

5.5.1.4. Organic species

Although more than one hundred organic species were detected by GC–MS, molecular markers made up a small fraction of carbonaceous aerosols. Despite their low contribution to $\text{PM}_{2.5}$, organic tracers are a useful tool to identify and quantify sources of atmospheric aerosols. Monthly concentrations of levoglucosan, polycyclic aromatic hydrocarbons (PAHs), and hopanes are shown in Figure 65.

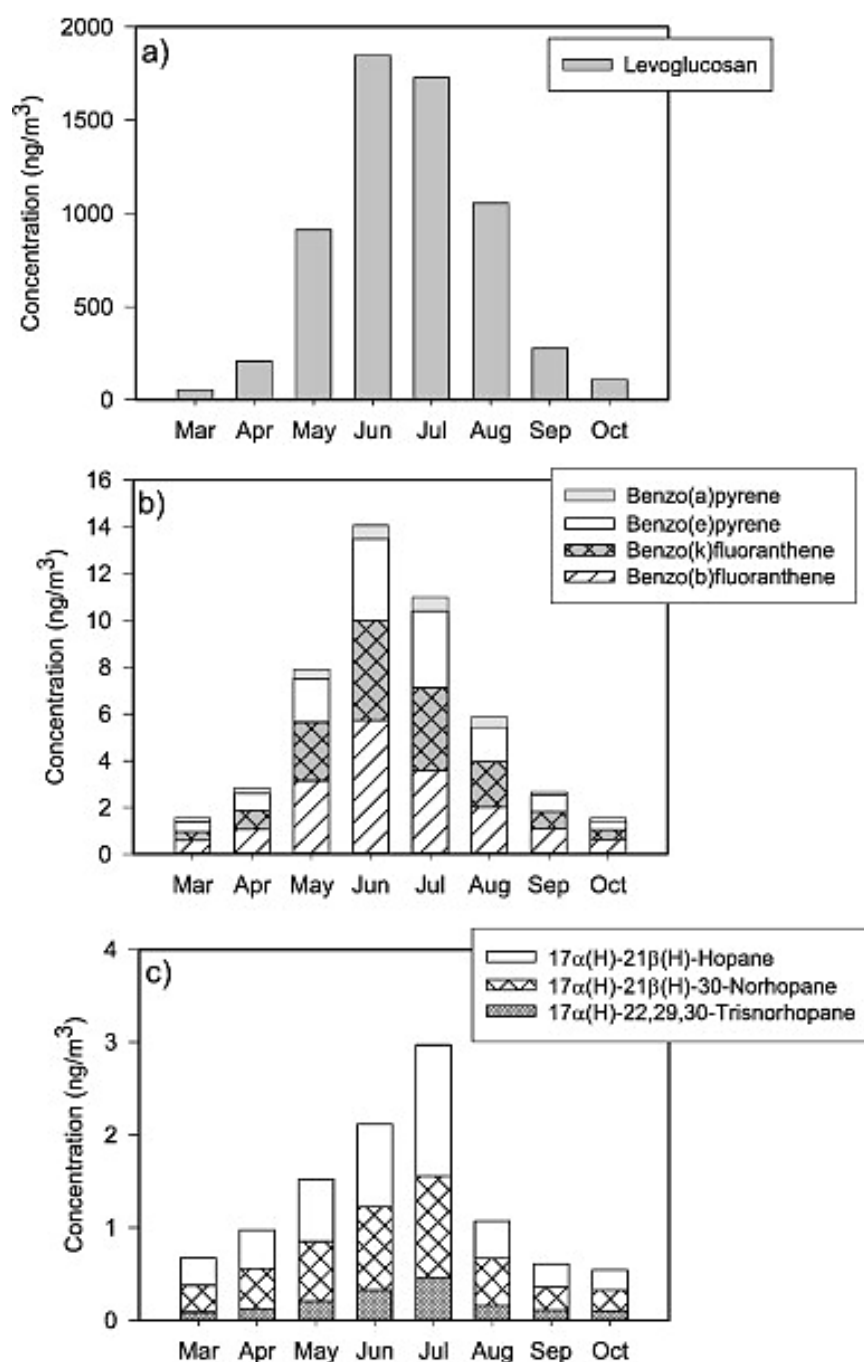


Figure 65 Monthly concentration of a) levoglucosan, b) PAHs, and c) hopanes in ambient PM_{2.5} in Santiago from March to October.

Levoglucosan, a well-established organic molecular maker for biomass burning (B.R.T. Simoneit et al. 1999), showed the highest concentrations in June and July, averaging 1789 ± 85 ng/m³ in these months. The lowest concentration was registered in March (52.9 ng/m³), and was 34 times lower than the average of June and July. Previous

studies in Santiago have reported concentrations of levoglucosan between April 25 and May 8 in the range of 206 to 1797 ng/m³, averaging 680 ng/m³ (Centro Mario Molina Chile 2009). High concentrations of levoglucosan in winter are explained by the massive consumption of residential wood for space heating in colder months.

Polycyclic aromatic hydrocarbons are made up of aromatic rings formed mainly during incomplete combustion of fossil fuels and burning vegetation at high temperatures. PAHs have been used as organic tracers for gasoline emission from mobile sources and wood combustion (Ravindra, Sokhi, and Van Grieken 2008). Several studies have reported carcinogenic properties of some PAHs, like benzo[b]fluoranthene, benzo[k]fluoranthene, and benzo[a]pyrene (Boström et al. 2002; Ravindra, Sokhi, and Van Grieken 2008; Y. Zhang et al. 2009). Concentrations of benzo[b]fluoranthene, benzo[k]fluoranthene, benzo(e)pyrene, and benzo[a]pyrene are shown in Figure 65b. Higher concentrations were registered in colder months, especially in June, when the sum of the four PAHs was 14.1 ng/m³. The lowest concentration, 1.5 ng/m³, was registered in March. The average concentration in the fall–winter period was 7.4 ± 4.5 ng/m³. Emission patterns and meteorological conditions differ from summer to winter, producing higher concentrations of PAHs in colder months (Baek et al. 1991). A previous study of these PAHs reported concentrations in August and October (1998) of 68 ng/m³ and 8.3 ng/m³ respectively (Tsapakis et al. 2002). In the present study, concentrations for these months were 5.9 ng/m³ and 1.6 ng/m³ respectively, showing a decreasing trend ascribed to the air quality regulations implemented in Santiago. Picene, which is a polycyclic aromatic hydrocarbon and a biomarker for coal combustion (Oros and Simoneit 2000), was not detected in the samples.

Hopanes are produced mainly by diesel and gasoline vehicles and fuel oil combustion (Rogge et al. 1997; James J. Schauer et al. 1996; Shrivastava et al. 2007). Figure 65c shows monthly concentrations of 17 α (H)-22,29,30-trisnorhopane, 17 α (H)-21 β (H)-30-norhopane, and 17 α (H)-21 β (H)-hopane. All measured concentrations of hopanes had a clear seasonal pattern with higher concentrations in colder months. Concentrations of the three measured hopanes ranged from a low of 0.54 ng/m³ in October

to a high of 3.0 ng/m^3 in July, averaging $1.3 \pm 0.85 \text{ ng/m}^3$. A study in Mexico City, D.F., which is another large capital city in Latin America that faces serious air pollution problems, reported 1.31 ng/m^3 as the concentration of these three hopanes during March (E. a. Stone et al. 2007). In the present study, concentration of the sum of the three hopanes was 0.61 ng/m^3 for September (similar seasons). Emission sources of hopanes do not have a seasonal pattern; consequently, the higher concentrations in colder months could be attributed only to meteorological conditions.

Concentrations of C_{27-33} n-alkanes do not have any seasonal pattern. The sum of all seven n-alkanes ranged from a low of 39.6 ng/m^3 in September to a high of 311 ng/m^3 in July, averaging $110 \pm 109 \text{ ng/m}^3$. Carbon preference index (CPI), which is the ratio of odd n-alkanes to even n-alkanes, was calculated to determine the origin of the C_{28-33} n-alkanes, which can be biogenic detritus (plant wax) and anthropogenic emissions (oil, soot) (Bernd R. T. Simoneit 1986). CPI values close to 1.0 are produced by fossil fuel emission and values higher than 2 (up to 10) indicate that the origin of n-alkanes is biogenic detritus (Rogge, Mazurek, et al. 1993; Bernd R. T. Simoneit 1986; Wils, Hulst, and den Hartog 1982). CPI values ranged from 0.70 to 1.6, averaging 0.90 (see Supplementary Fig. 7), which indicate that n-alkanes were produced by anthropogenic sources. Similar results has been previously reported (Tsapakis et al. 2002).

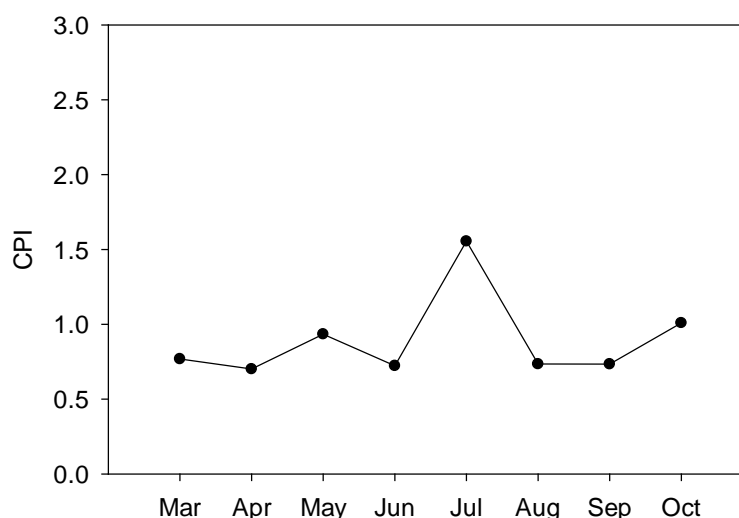


Figure 66 Monthly carbon preference indices (CPI).

5.5.2. CMB results

5.5.2.1. Source apportionment to $PM_{2.5}$ OC

The mobile source profiles included in this study were developed considering a wide range of California gasoline and diesel vehicles with model years from 1975 to 2001. The three preselected mobile sources (diesel, gasoline, and smoking vehicles) led to collinearity problems, so the CMB model was re-run including only diesel and gasoline vehicles. This sensitivity analysis showed that contribution to OC was not statistically different using the three or two mobile sources (see Figure 67). Consequently, only diesel and gasoline vehicles were included as mobile sources in the receptor model. Using source profiles from the USA could potentially add some bias to the results; however, the most comprehensive source testing programs have large uncertainties in source profiles that were shown to have limited impact on the total apportionment of mobile sources and a large impact on the split between gasoline and diesel engine emissions (Lough and Schauer 2007). Given that Santiago has cars that are similar to those in the USA and use similar petroleum based motor oil, we do not think the true mobile source profiles are outside the range of the profiles examined by Lough and Schauer (Lough and Schauer 2007).

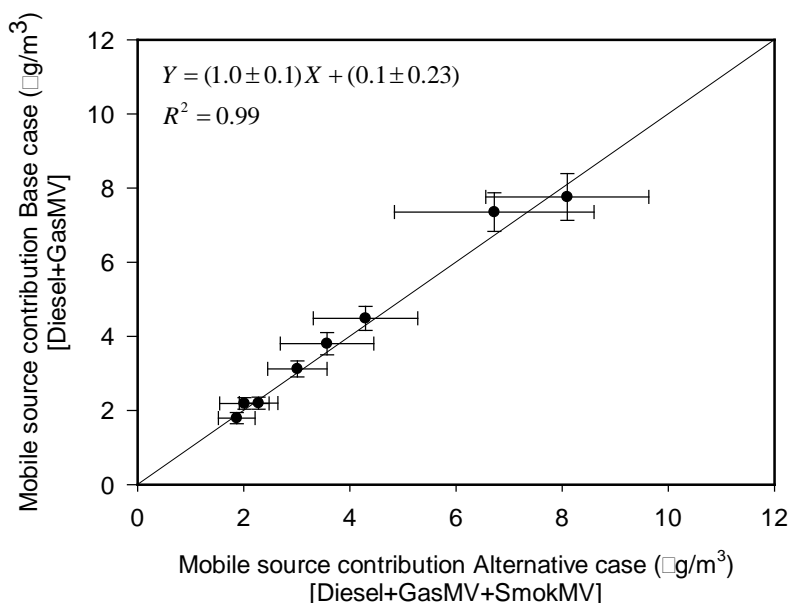


Figure 67 Linear regression between mobile source contributions of the base case and the alternative case.

The CMB model was then used to estimate source contributions to OC from wood smoke, natural gas, diesel emission, and gasoline vehicle. These sources were selected according to the organic tracer concentrations and the sensitivity analysis. “CMB Other” represents secondary organic aerosols (SOA) and unidentified primary sources, calculated as the difference of the OC and the sum of the contribution of all primary sources included in the receptor model. Source contributions and their uncertainties (standard error) are presented in Table 28 . Figure 68 shows absolute and percentage monthly contributions to OC. Only statistically significant sources were included in Figure 68.

From May to September, the largest contributor to OC was wood smoke; however, it should be noted that during the warmer months (March, April, September, and October), the sum of the mobile sources was a larger contributor to OC than wood smoke. Wood smoke in fall and winter contributed $8.16 \pm 5.94 \mu\text{g}/\text{m}^3$, and was especially important in June–July, where it contributed $14.8 \pm 2.9 \mu\text{g}/\text{m}^3$, representing an average of $71 \pm 14\%$ of OC. The second most important primary source was gasoline vehicles, contributing from $1.19 \mu\text{g}/\text{m}^3$ in October to $6.16 \mu\text{g}/\text{m}^3$ in July, with a nearly constant relative contribution to OC throughout the eight months, averaging $23.4 \pm 15.1\%$. Diesel emission contributions were lower than gasoline vehicles, contributing from a low of $0.61 \mu\text{g}/\text{m}^3$ in October to a high of $2.56 \mu\text{g}/\text{m}^3$ in June, averaging $10.5 \pm 5.0\%$ of OC. Natural gas was the lowest contributor to OC during the eight month period. It accounted for an average of $0.11 \pm 0.11 \mu\text{g}/\text{m}^3$ from March to October, which represented only $0.9 \pm 0.9\%$ of OC. In the colder months, all primary sources increased their contribution to OC. From May to September the contribution of “CMB Other” was not statistically significant. In contrast, “CMB Other” had the predominant contribution to OC during the warm months of March, April, and October, averaging $3.79 \pm 1.00 \mu\text{g}/\text{m}^3$, which represented $53.6 \pm 14.2\%$ of OC. This suggested that “CMB Other” was composed mainly of SOA, whose formation was enhanced by photochemical reactions in the warmer months; this is supported by the well-known seasonality of ozone in Santiago (Héctor Jorquera, Palma, and Tapia 2002; Elshorbany et al. 2010).

Table 28 Source contributions to ambient $PM_{2.5}$ organic carbon (OC) estimated by CMB. Statistically significant source contributions are shown in bold.

| Month | Wood smoke | | Natural gas | | Diesel emission | | Gasoline vehicles | | Other | | R^2 | χ^2 |
|-------|--------------------------|------------------|--------------------------|------------------|--------------------------|------------------|--------------------------|------------------|--------------------------|------------------|-------|----------|
| | $\mu\text{g}/\text{m}^3$ | unc ^a | $\mu\text{g}/\text{m}^3$ | unc ^a | $\mu\text{g}/\text{m}^3$ | unc ^a | $\mu\text{g}/\text{m}^3$ | unc ^a | $\mu\text{g}/\text{m}^3$ | unc ^a | | |
| Mar | 0.37 | 0.08 | 0.01 | 0.01 | 0.86 | 0.09 | 1.34 | 0.14 | 3.42 | 0.60 | 0.98 | 1.03 |
| Apr | 1.51 | 0.33 | 0.04 | 0.01 | 1.16 | 0.12 | 1.96 | 0.18 | 4.93 | 1.18 | 0.98 | 1.26 |
| May | 7.13 | 1.50 | 0.19 | 0.04 | 1.29 | 0.14 | 3.19 | 0.29 | 2.40 | 2.59 | 0.98 | 1.25 |
| Jun | 16.85 | 3.41 | 0.33 | 0.06 | 2.56 | 0.28 | 4.79 | 0.44 | - 2.45 | 3.97 | 0.96 | 2.41 |
| Jul | 12.70 | 2.69 | 0.17 | 0.05 | 1.60 | 0.20 | 6.16 | 0.60 | - 1.11 | 3.07 | 0.99 | 0.94 |
| Aug | 8.53 | 1.75 | 0.09 | 0.03 | 1.16 | 0.13 | 2.64 | 0.27 | 0.75 | 2.70 | 0.98 | 1.08 |
| Sep | 2.26 | 0.48 | 0.05 | 0.01 | 0.93 | 0.10 | 1.26 | 0.12 | 1.76 | 1.48 | 0.95 | 2.77 |
| Oct | 0.79 | 0.17 | 0.02 | 0.01 | 0.61 | 0.06 | 1.19 | 0.14 | 3.03 | 0.50 | 0.97 | 2.08 |

R^2 and χ^2 are fitting parameters of the chemical mass balance model.

^aunc = uncertainty.

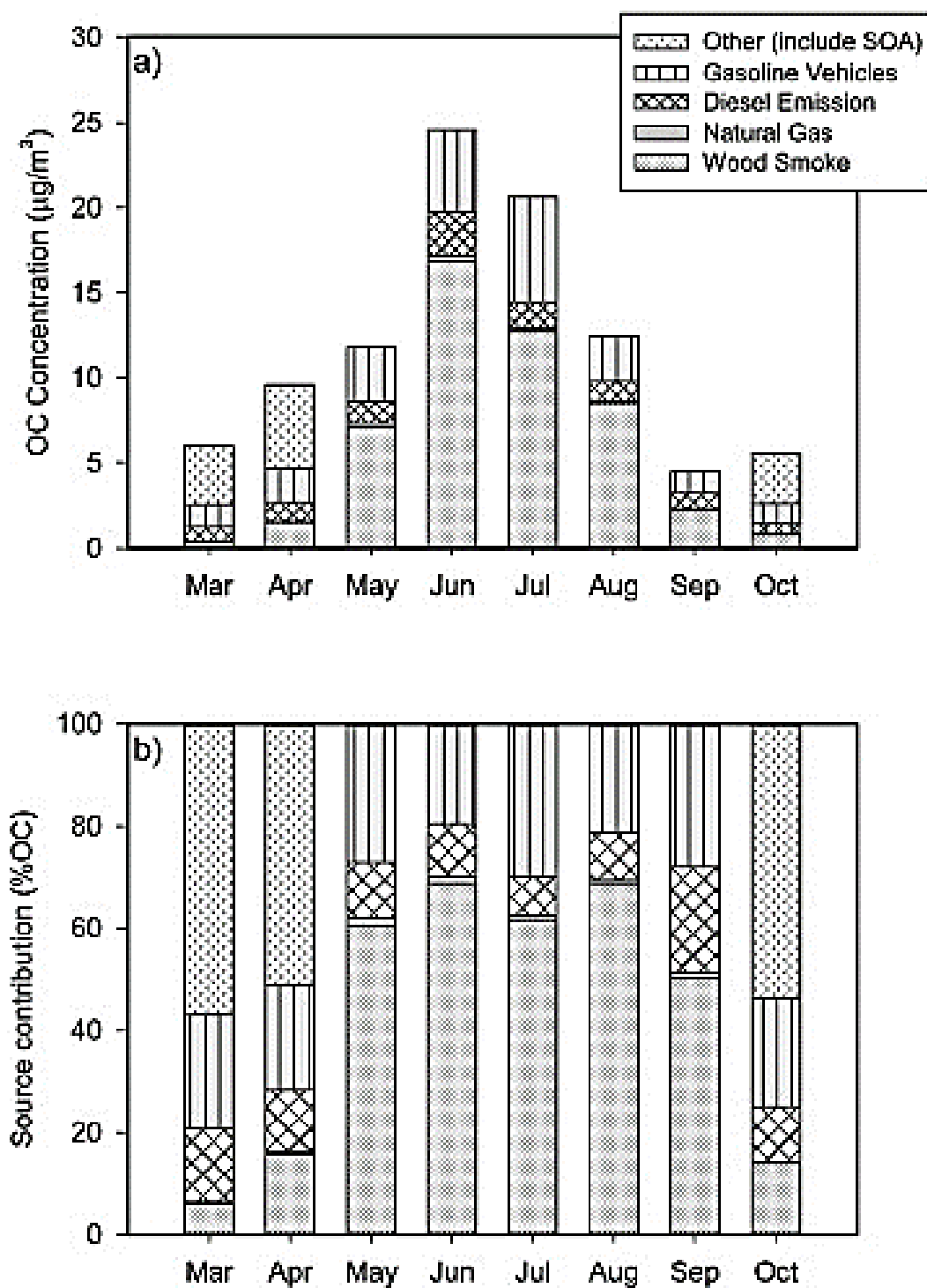


Figure 68 Monthly source contribution to $PM_{2.5}$ OC estimated using CMB model on a) absolute and b) percent scales in Santiago from March to October.

The seasonal patterns of source tracers that are shown in Figure 64 and Figure 65 provide the same conclusions about the relative impact of sources on fine particulate organic carbon that is provided by the formal source apportionment analysis shown in Figure 68. The consistency of the conclusions from the presentation of the raw data and source apportionment results is an important consistency check and provides additional confidence in the source apportionment. Furthermore, levoglucosan levels are negatively correlated with ambient temperatures as expected for the residential wood burning sources; in the cold months those emissions increase when dispersion conditions in the basin worsen, hence seasonality of levoglucosan is more marked than in the case of motor vehicles.

5.5.2.2. Source apportionment to $PM_{2.5}$ mass

Monthly source contributions to OC obtained from the CMB model were converted to source contributions to $PM_{2.5}$ using specific OC/ $PM_{2.5}$ factors for each of the four sources (Fine, Cass, and Simoneit 2004; Lough et al. 2007; Rogge, Hildemann, et al. 1993). “CMB Other” was converted to SOA using a relatively high OC/ $PM_{2.5}$ factor of 2; similar ratios have previously been used for spring and summer months (Hasheminassab et al. 2013). In addition, sulfate, nitrate, and ammonium concentrations were included as sources. The difference between the sum of all sources previously mentioned and the gravimetric $PM_{2.5}$ mass is represented as undetermined mass. Figure 69 and Table 29 show source contributions to $PM_{2.5}$ mass.

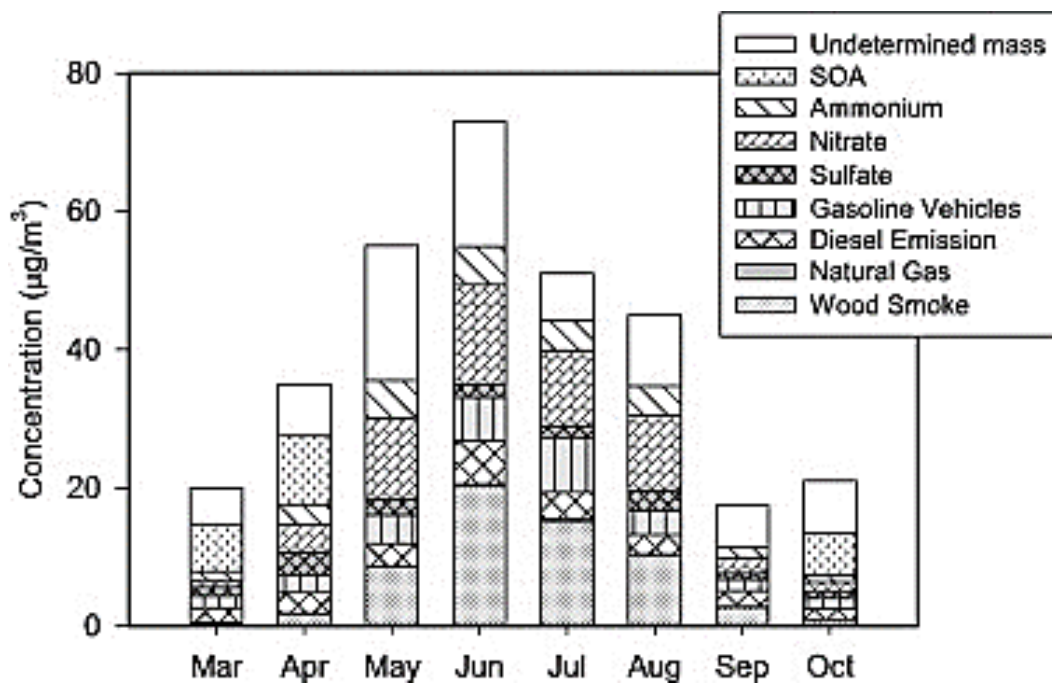


Figure 69 Monthly source contribution to ambient $PM_{2.5}$ mass in Santiago from March to October.

Table 29 *Monthly source contribution to PM_{2.5} from March to October.*

| Month | PM _{2.5} mass µg/m ³ | Wood smoke µg/m ³ | Natural gas µg/m ³ | Diesel emission µg/m ³ | Gasoline vehicles µg/m ³ | Sulfate µg/m ³ | Nitrate µg/m ³ | Ammonium µg/m ³ | SOA µg/m ³ | Undetermined mass µg/m ³ |
|-------|--|------------------------------------|----------------------------------|---|--|------------------------------|------------------------------|-------------------------------|--------------------------|--|
| Mar | 20 | 0.44 | 0.02 | 2.11 | 1.72 | 1.30 | 0.85 | 1.44 | 6.84 | 5.27 |
| Apr | 35 | 1.81 | 0.05 | 2.86 | 2.52 | 3.42 | 3.92 | 3.00 | 9.86 | 7.57 |
| May | 55 | 8.53 | 0.22 | 3.17 | 4.11 | 2.23 | 11.86 | 5.39 | 0.00 | 19.48 |
| Jun | 73 | 20.17 | 0.39 | 6.29 | 6.17 | 1.99 | 14.35 | 5.56 | 0.00 | 18.07 |
| Jul | 51 | 15.20 | 0.19 | 3.92 | 7.94 | 1.64 | 11.03 | 4.19 | 0.00 | 6.88 |
| Aug | 45 | 10.21 | 0.11 | 2.86 | 3.40 | 3.02 | 10.85 | 4.30 | 0.00 | 10.26 |
| Sep | 17 | 2.70 | 0.06 | 2.28 | 1.62 | 0.94 | 2.31 | 1.47 | 0.00 | 6.02 |
| Oct | 21 | 0.94 | 0.02 | 1.49 | 1.53 | 1.10 | 1.31 | 0.96 | 6.06 | 7.59 |

The major primary source of PM_{2.5} mass in fall and winter was wood smoke, which contributed $9.77 \pm 7.11 \mu\text{g}/\text{m}^3$ ($21.2 \pm 15.4\%$) in these seasons, with the highest relative and percentage contribution in June–July, averaging $17.69 \pm 3.51 \mu\text{g}/\text{m}^3$ ($28.53 \pm 5.66\%$). Gasoline vehicles' contribution ranged from a low of $1.53 \mu\text{g}/\text{m}^3$ in October to a high of $7.94 \mu\text{g}/\text{m}^3$ in July. In June–July it contributed to $11.4 \pm 2.0\%$ of PM_{2.5} mass. Diesel contribution was slightly lower than gasoline vehicles, and when combined these two sources contributed $19.6 \pm 0.7\%$ of fine particles in June–July. Natural gas was the smallest contributor to PM_{2.5} mass, averaging $0.13 \pm 0.13 \mu\text{g}/\text{m}^3$ which represented less than 1%. The most important secondary source of PM_{2.5} mass was nitrate, which contributed an average of $7.06 \pm 5.48 \mu\text{g}/\text{m}^3$ ($17.8 \pm 13.8\%$). As with wood smoke, this source increased its contribution in fall and winter, especially in June–July when it reached $12.7 \pm 2.4 \mu\text{g}/\text{m}^3$, representing $20.5 \pm 3.8\%$. Secondary inorganic ions (sulfate, nitrate, and ammonium) together accounted for $31.0 \pm 19.4\%$ of PM_{2.5} mass from March to October. Secondary organic aerosols contributed only in March, April, and October, averaging $29.9 \pm 7.9\%$ of PM_{2.5} mass in these three months. Undetermined mass, which represented about 30% of PM_{2.5} total mass, was generally higher in fall, mainly in May and June; however, its percentage contribution did not show any pattern. This unresolved fraction may be ascribed to a variety of industrial and commercial sources in Santiago, as well as marine aerosol contributions.

5.6. Summary and conclusions

Ambient PM_{2.5} samples collected from March to October 2013 in Santiago registered high levels of PM_{2.5} in comparison with 24-h WHO and Chilean regulations. During fall and winter, 50% of samples exceeded the 24-h Chilean national standard. Average ambient PM_{2.5} concentration from March to October was $40 \pm 20 \mu\text{g}/\text{m}^3$; the highest concentrations were registered in colder months (June–July), averaging $62 \pm 15 \mu\text{g}/\text{m}^3$. PM_{2.5} concentrations were higher in fall and winter, due to low-level thermal inversion layers which inhibit the dispersion of contaminants, and the higher emission of some sources like wood smoke. The gravimetric mass and reconstructed mass agreed well (averaging $103 \pm 12\%$).

This is the first study to apportion OC and PM_{2.5} in Santiago using molecular markers as tracers; hence novel results were obtained: i) separately resolve gasoline and diesel vehicles (previous studies have apportioned a single motor vehicle source, see Table 26), ii) clearly identifying the wood smoke source (no previous study has used levoglucosan as tracer) and iii) quantifying secondary organic aerosols and showing their strong seasonality in Santiago (no previous study has resolved this source). Molecular markers included in the CMB model were EC, hopanes, PAHs, and levoglucosan. The concentration of all of them followed the same pattern as PM_{2.5} mass; highest concentrations were registered in June and July. The CMB model determined the following contributions to OC: wood smoke, natural gas, diesel emission, and gasoline vehicles. From May to September, the main contributor to OC was wood smoke, and its contribution was especially high in June–July. In warm months, the sum of the two mobile sources contributed more than wood burning. Gasoline vehicles was the second most important single source to OC. Diesel contributions were a little lower than gasoline, and natural gas was the lowest contributor to OC. “CMB Other” only contributed in warm months, accounting in these months for more than 50% of OC. The seasonal pattern of “CMB Other” suggested that they were made up of SOA which were formed by photochemical reactions.

Wood smoke was the major primary source of $\text{PM}_{2.5}$. Its highest contribution was in June–July, reaching $17.7 \pm 3.5 \mu\text{g}/\text{m}^3$, which represented $28.5 \pm 5.6\%$. Therefore, this source needs to be further constrained to improve air quality in Santiago, given that there are alternatives for residential heating. Nitrate was the most important secondary source of $\text{PM}_{2.5}$, contributing from March to October $7.06 \pm 5.48 \mu\text{g}/\text{m}^3$ ($17.8 \pm 13.8\%$). Its highest contribution also was in June–July, averaging $12.7 \pm 2.4 \mu\text{g}/\text{m}^3$, which represented about 21% of $\text{PM}_{2.5}$ mass. Gasoline vehicle contribution was a little higher than diesel, and natural gas contributed to less than 1% of fine particles. Considering that gasoline vehicles in Santiago travel farther and consume more fuel than diesel vehicles, it seems sensible to consider a tax policy that captures the marginal damage each vehicle brings in to the city.

The three secondary inorganic ions: sulfate, nitrate, and ammonium, contributed an average of 4.9%, 17.8%, and 8.3% of $\text{PM}_{2.5}$ respectively. Sulfate comes mainly from the industrial sector because of the low sulfur content in diesel and gasoline. The apportionment of ammonium nitrate into diesel- and gasoline-powered vehicles may be estimated using a chemical transport model, provided we have reliable emission inventories for Santiago, but such task is beyond the scope of this work.

SOA contributed only in three months: March, April, and October, which are warm months; its average contribution to $\text{PM}_{2.5}$ during these months was $29.9 \pm 7.9\%$. SOA do not appear in the cold season. This is the first time SOA have been quantitatively estimated in Santiago, including their seasonal behavior.

Undetermined mass accounted for about 30% of $\text{PM}_{2.5}$ total mass, and it can be ascribed to industrial and commercial sources, as well as marine aerosol — hence local and regional sources may contribute to that unresolved mass.

5.7. Acknowledgments

Ana Villalobos was supported by Eduardo Neale Silva Memorial Scholarship at University of Wisconsin-Madison and Becas Chile CONICYT, Gobierno de Chile. We acknowledge Brandon Shelton at the Wisconsin State Laboratory of Hygiene, and Samera Hamad, Christopher Worley, and Jongbae Heo at the University of Wisconsin-Madison for their assistance with chemical and data analysis. Francisco Barraza was supported by a CONICYT doctoral fellowship grant. Héctor Jorquera was supported by FONDECYT Grant 1121054 and by Centro de Desarrollo Urbano Sustentable (CEDEUS, www.cedeus.cl), Grant CONICYT/FONDAP/15110020. The funding sources were not involved in the preparation or review of this research.

6. SUMMARY AND CONCLUSION

This chapter provides an overview of the results and conclusions mentioned in previous chapters, as well as a comparison between them. Finally, future prospects generated during this doctoral work are stated.

6.1. General Conclusions

The use of receptor models (PMF and CMB) applied to Santiago's city allowed us to identify the principal sources that contribute to ambient $PM_{2.5}$ and to identify the main sources that contribute to indoor $PM_{2.5}$. It also allowed us to identify and quantify the main sources that contribute to the levels of OC (main component of $PM_{2.5}$).

The main sources that contribute to outdoor $PM_{2.5}$ were determined separately for the years 1999 and 2004, from which the same six main sources were identified: motorized vehicles ($28\pm2.5\%$ / $31.2\pm3.4\%$), wood burning ($24.8\pm2.3\%$ / $28.9\pm3.3\%$), sulfates ($18.8\pm1.7\%$ / $16.2\pm2.5\%$), marine aerosol ($13\pm2.1\%$ / $9.9\pm1.5\%$), copper smelters ($11.5\pm1.4\%$ / $9.7\pm3.3\%$) and soil dust ($3.9\pm1.5\%$ / $4.0\pm2.4\%$), respectively. These results show that outdoor $PM_{2.5}$ is dominated by anthropogenic sources — Figure 70 —, with a high contribution of non-industrial sources which could be reduced by changing people's habits such as preferring public transport and/or shifting to cleaner space heating fuels.

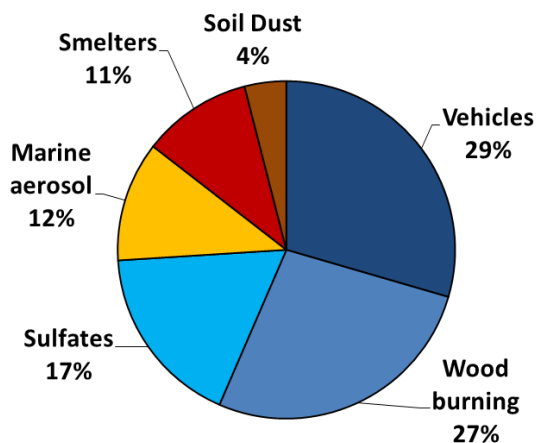


Figure 70 Santiago 2004/1999 campaigns. Summary of outdoor sources apportionment.

This work also clarifies the important regional or suburban contributions to Santiago's $PM_{2.5}$, which originate outside Santiago, identifying contributions from copper smelters from which primary emissions and secondary sulfates were resolved by the receptor model. These regional sources (including marine aerosol) were verified using wind trajectory models generated with the HYSPLIT software developed by NOAA (US National Oceanic and Atmospheric Administration).

A quantitative campaign of indoor/outdoor levels of Santiago's $PM_{2.5}$ was performed during the spring of 2012, which monitored 47 households, 44 of which were finally included in the research study. For the first time in Santiago, the PMF receptor model was applied to indoor $PM_{2.5}$. Six main contribution sources were identified; three of them had an outdoor origin: motor vehicles ($25.1 \pm 3.2\%$), street dust ($13.2 \pm 2.3\%$), and secondary sulfates ($15.5 \pm 2.3\%$), and three had an indoor origin: indoor dust ($7.3 \pm 1.4\%$), cleaning and cooking ($10.5 \pm 1.4\%$), and cooking plus environmental tobacco smoke — ETS — ($27.9 \pm 3.2\%$). Both sources explain roughly half of indoor $PM_{2.5}$ as shown in Figure 71.

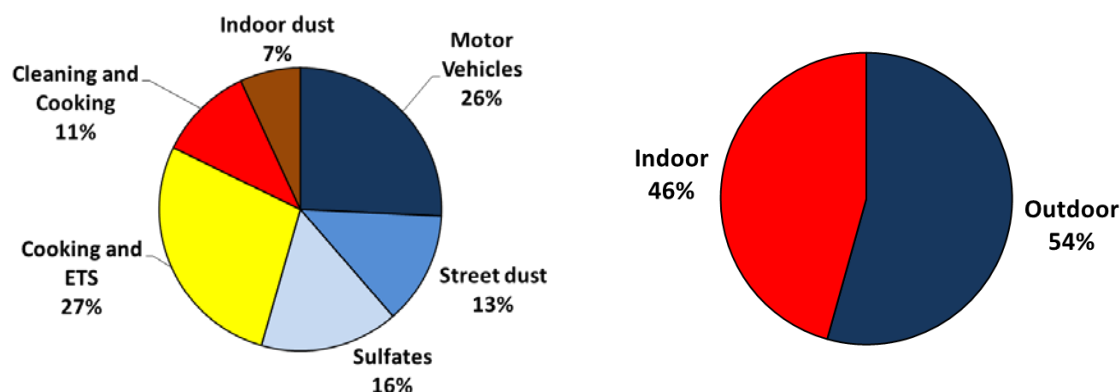


Figure 71 Santiago 2012 campaign. Indoor Source Apportionment

An outdoor campaign was performed between March and October of 2013 using the receptor model CMB, which allowed us the identification of four organic sources of combustion that contribute to $PM_{2.5}$ levels: wood smoke ($18.9 \pm 15.8\%$), diesel engine emission ($7.9 \pm 3.7\%$), gasoline vehicles ($9.2 \pm 5.9\%$), and natural gas ($0.3 \pm 0.3\%$). Wood smoke was the major contributing source during cold months, representing $28.5 \pm 5.6\%$ of

PM_{2.5} in June-July. Diesel engine emissions was the source of highest contribution during warmer months; diesel engine emissions contribute more than gasoline vehicle sources. The contribution of natural gas emissions was low during all the monitored period representing less than 1% of the total of PM_{2.5}. During the warmer months (March, April and October) those four identified sources don't represent the total OC in PM_{2.5}; the difference could be explained by the presence of secondary organic aerosol (SOA), which is formed by photochemical reactions — during the colder months the OC was represented by the four sources detected in the model.

Since OC characterization does not completely explain ambient levels of PM_{2.5} the characterization and quantification of the other non-organic chemical species was additionally performed during the 2013 campaign. We found that nitrate ($17.8 \pm 13.8\%$) was the dominant secondary contribution to PM_{2.5} followed by ammonium ($8.3 \pm 4.6\%$) and sulfate ($4.9 \pm 2.3\%$). These species, as well as organic sources, increase considerably their mass contribution during the colder months. The contribution of the four sources identified by CMB plus the contributions of the main non-organic species is illustrated in Figure 72.

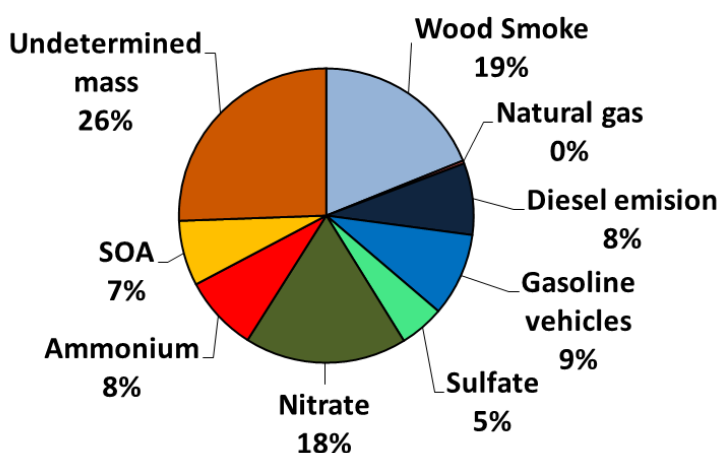


Figure 72 Santiago 2013 campaign. Outdoor Source Apportionment

While comparing the campaigns of 2013, 2004 and 1999 important similitudes of the identified sources can be seen, regardless of the difference between the methods, monitoring systems, laboratory analysis and receptor models used for the source

apportionment. For instance, during the 2004 and 1999 campaign, motor vehicles represented ~30% of the total of $PM_{2.5}$ levels; the 2013 campaign results indicate a direct (primary) contribution of ~8% and ~9% to $PM_{2.5}$ from diesel and gasoline vehicles, respectively. Then we would have to add up a large fraction of nitrate (18%), a secondary particle generated from motor vehicle emissions as well. Wood smoke represented ~27% of $PM_{2.5}$ during 2004/1999 while in 2013 it represented 19%. This difference can be explained as follows: i) in the 2004/1999 campaigns potassium was used as tracer of wood burning but it appears in other sources as well; this could have led to overestimation of that source strength, ii) an underestimation in the 2013 campaign because levoglucosan is slightly reactive, iii) a plausible decrease of wood burning emissions between 2004 and 2013 owing to contingency measures banning the use of wood in episodic days and technological improvement in woodstoves, and iv) more citizen's awareness and shifts to cleaner fuels. Nonetheless, wood smoke keeps being one of the main sources of contribution to $PM_{2.5}$ especially during cold months.

6.2. Future prospects

During the studied campaigns it was found that in Santiago there were periods where $PM_{2.5}$ were high and over the Chilean standard ($50 \mu g/m^3$ –24 hours average) and the WHO recommendation ($25 \mu g/m^3$ –24 hours average). The most critical time of year was during autumn-winter where 50% of the monitored days exceeded the Chilean standard, bringing critical urgency to initiatives that would allow to improve air quality in Santiago.

On the other hand, if we want to decrease the impact of the $PM_{2.5}$ on people's health measuring and controlling environmental levels is not enough, because people spend more 65% of their time indoors. In this regard, a contribution of this thesis was to measure indoor levels of $PM_{2.5}$ finding the following points: i) indoor $PM_{2.5}$ is higher than outdoor $PM_{2.5}$, and ii) it demonstrated that the chemical compositions of indoor $PM_{2.5}$ differs from outdoor $PM_{2.5}$ because of the contribution of indoor sources added to the

infiltrated $PM_{2.5}$ from the exterior. We think it is also necessary to determine levels of $PM_{2.5}$ in other environments such as commuting, offices or working areas, etc.

Another relevant aspect found in this thesis is that nearly 35% of the contributions to the levels of outdoor $PM_{2.5}$ come from sources from outside the city. If we aim to decrease the total concentration of $PM_{2.5}$ levels, it necessary to further reduce those regional sources (copper smelters).

Finally, it is important to highlight that the bad quality of air in Santiago especially regarding the levels of $PM_{2.5}$ is mainly caused by human activity and in order to decrease said levels it is important to make changes in the social education, habits and behavior of people. For example indoor tobacco consumption, or the excessive use of vehicles, both of which need urgently a change of mindset in Santiago's inhabitants.

7. BIBLOGRAFÍA

- Abdullahi, Karimatu L., Delgado-Saborit, Juana Maria Harrison, Roy M. 2013. "Emissions and Indoor Concentrations of Particulate Matter and Its Specific Chemical Components from Cooking: A Review." *Atmospheric Environment* 71 (0): 260–94. doi:10.1016/j.atmosenv.2013.01.061.
- Abt, E, H H Suh, P Catalano, and P Koutrakis. 2000. "Relative Contribution of Outdoor and Indoor Particle Sources to Indoor Concentrations." *Environmental Science & Technology* 34 (17): 3579–87.
- Adonis, M, and L Gil. 2001. "Indoor Air Pollution in a Zone of Extreme Poverty of Metropolitan Santiago, Chile." *Indoor and Built Environment* 10 (3-4): 138–46.
- Analitis, Antonis, Klea Katsouyanni, Konstantina Dimakopoulou, Evangelia Samoli, Aristidis K Nikoloulopoulos, Yannis Petasakis, Giota Touloumi, et al. 2006. "Short-Term Effects of Ambient Particles on Cardiovascular and Respiratory Mortality." *Epidemiology (Cambridge, Mass.)* 17 (2): 230–33. doi:10.1097/01.ede.0000199439.57655.6b.
- Anglo American. 2012. "Data from Emissions and Ambient Monitoring Surrounding Chagres Copper Smelter."
- Arden Pope, C., Richard T. Burnett, Michelle C. Turner, Aaron Cohen, Daniel Krewski, Michael Jerrett, Susan M. Gapstur, and Michael J. Thun. 2011. "Lung Cancer and Cardiovascular Disease Mortality Associated with Ambient Air Pollution and Cigarette Smoke: Shape of the Exposure-Response Relationships." *Environmental Health Perspectives* 119 (11): 1616–21. doi:10.1289/ehp.1103639.
- Artaxo, P. 1996. "Aerosol Source Apportionment at Santiago Chile Winter 1996: Technical Report for the National Commission of the Environment."
- A 1998. "Aerosol Characterization Study in Santiago de Chile Wintertime 1998: Technical Report for the National Commission of the Environment." Santiago.
- Artaxo, Paulo, Pedro Oyola, and Roberto Martinez. 1999. "Aerosol Composition and Source Apportionment in Santiago de Chile." *Nuclear Instruments and Methods in Physics Research Section B: Beam Interactions with Materials and Atoms* 150 (1-4): 409–16. doi:10.1016/S0168-583X(98)01078-7.
- Ashmore, M R, and C Dimitroulopoulou. 2009. "Personal Exposure of Children to Air Pollution." *Atmospheric Environment* 43 (1): 128–41.
- Bae, Min-Suk, James J. Schauer, and Jay R. Turner. 2006. "Estimation of the Monthly Average Ratios of Organic Mass to Organic Carbon for Fine Particulate Matter at an

- Urban Site.” *Aerosol Science and Technology* 40 (12): 1123–39. doi:10.1080/02786820601004085.
- Baek, S. O., R. A. Field, M. E. Goldstone, P. W. Kirk, J. N. Lester, and R. Perry. 1991. “A Review of Atmospheric Polycyclic Aromatic Hydrocarbons: Sources, Fate and Behavior.” *Water, Air, and Soil Pollution* 60 (3-4): 279–300. doi:10.1007/BF00282628.
- Barraza, Francisco, Héctor Jorquera, Gonzalo Valdivia, and Lupita D. Montoya. 2014. “Indoor PM_{2.5} in Santiago, Chile, Spring 2012: Source Apportionment and Outdoor Contributions.” *Atmospheric Environment* 94 (September): 692–700. doi:10.1016/j.atmosenv.2014.06.014.
- Begum, Bilkis A, Samir K Paul, M Dildar Hossain, Swapan K Biswas, and Philip K Hopke. 2009. “Indoor Air Pollution from Particulate Matter Emissions in Different Households in Rural Areas of Bangladesh.” *Building and Environment* 44 (5): 898–903.
- Belis, C.A. A, F. Karagulian, B.R. R Larsen, and P.K. K Hopke. 2013. “Critical Review and Meta-Analysis of Ambient Particulate Matter Source Apportionment Using Receptor Models in Europe.” *Atmospheric Environment* 69 (0): 94–108. doi:10.1016/j.atmosenv.2012.11.009.
- Bell, Michelle L, Devra L Davis, Nelson Gouveia, Víctor H Borja-aburto, and Luis A Cifuentes. 2006. “The Avoidable Health Effects of Air Pollution in Three Latin American Cities: Santiago, São Paulo, and Mexico City.” *Environmental Research* 100 (3): 431–40. doi:10.1016/j.envres.2005.08.002.
- Bernstein, Jonathan A, Neil Alexis, Hyacinth Bacchus, I Leonard Bernstein, Pat Fritz, Elliot Horner, Ning Li, et al. 2008. “The Health Effects of Nonindustrial Indoor Air Pollution.” *Journal of Allergy and Clinical Immunology* 121 (3): 585–91.
- Boström, Carl-Elis, Per Gerde, Annika Hanberg, Bengt Jernström, Christer Johansson, Titus Kyrklund, Agneta Rannug, Margareta Törnqvist, Katarina Victorin, and Roger Westerholm. 2002. “Cancer Risk Assessment, Indicators, and Guidelines for Polycyclic Aromatic Hydrocarbons in the Ambient Air.” *Environmental Health Perspectives* 110 Suppl : 451–88. doi:10.1289/ehp.02110s3451.
- Burgos, Soledad, Pablo Ruiz, and Rosalina Koifman. 2013. “Changes to Indoor Air Quality as a Result of Relocating Families from Slums to Public Housing.” *Atmospheric Environment (Oxford, England: 1994)* 70 (0): 179–85. doi:10.1016/j.atmosenv.2012.12.044.
- Caceres, D, M Adonis, C Retamal, P Ancic, M Valencia, X Ramos, N Olivares, and L Gil. 2001. “Indoor Air Pollution in a Zone of Extreme Poverty of Metropolitan Santiago.” *Revista Medica de Chile* 129 (1): 33–42.

- Cao, Jun-Ji, Zhen-Xing Shen, Judith C. Chow, John G. Watson, Shun-Cheng Lee, Xue-Xi Tie, Kin-Fai Ho, Ge-Hui Wang, and Yong-Ming Han. 2012. "Chemical Compositions in Fourteen Chinese Cities." *Journal of the Air & Waste Management Association* 62 (10): 1214–26. doi:10.1080/10962247.2012.701193.
- Centro Mario Molina Chile. 2009. "Análisis de Las Concentraciones de MP10 Y MP2.5 Asociadas a Las Emisiones de Quema de Leña Residencial En La Región Metropolitana de Santiago." available at: http://www.ced.cl/ced/wp-content/uploads/2012/03/resumen-ejecutivo-lena_cgp.pdf (2009) (in Spanish).
- Cesaroni, Giulia, Chiara Badaloni, Claudio Gariazzo, Massimo Stafoggia, Roberto Sozzi, and Marina Davoli. 2013. "Long-Term Exposure to Urban Air Pollution and Mortality in a Cohort of More than a Million Adults in Rome." *Environmental Health Perspectives* 121 (3): 324–31.
- Chao, C. Y.H. H, T. C. W. Tung, and J. Burnett. 1998. "Influence of Different Indoor Activities on the Indoor Particulate Levels in Residential Buildings." *Indoor and Built Environment* 7 (2): 110–21. doi:10.1177/1420326X9800700205.
- Chen, Chun, and Bin Zhao. 2011. "Review of Relationship between Indoor and Outdoor Particles: I/O Ratio, Infiltration Factor and Penetration Factor." *Atmospheric Environment* 45 (2): 275–88. doi:10.1016/j.atmosenv.2010.09.048.
- Cheung, Kalam, Nancy Daher, Martin M Shafer, Zhi Ning, James J Schauer, and Constantinos Sioutas. 2011. "Diurnal Trends in Coarse Particulate Matter Composition in the Los Angeles Basin." *Journal of Environmental Monitoring: JEM* 13 (11). The Royal Society of Chemistry: 3277–87. doi:10.1039/c1em10296f.
- Chow, Judith C., John G. Watson, Hampden Kuhns, Vicken Etyemezian, Douglas H. Lowenthal, Dale Crow, Steven D. Kohl, Johann P. Engelbrecht, and Mark C. Green. 2004. "Source Profiles for Industrial, Mobile, and Area Sources in the Big Bend Regional Aerosol Visibility and Observational Study." *Chemosphere* 54 (2): 185–208. doi:10.1016/j.chemosphere.2003.07.004.
- COCHILCO. 2012. "Statistics on Chilean and Worldwide Copper Production."
- Daher, Nancy, Ario Ruprecht, Giovanni Invernizzi, Cinzia De Marco, Justin Miller-Schulze, Jong Bae Heo, Martin M. Shafer, James J. Schauer, and Constantinos Sioutas. 2011. "Chemical Characterization and Source Apportionment of Fine and Coarse Particulate Matter inside the Refectory of Santa Maria Delle Grazie Church, Home of Leonardo Da Vincis 'Last Supper.'" *Environmental Science and Technology* 45 (24): 10344–53. doi:10.1021/es202736a.
- Daher, Nancy, Ario Ruprecht, Giovanni Invernizzi, Cinzia De Marco, Justin Miller-Schulze, Jong Bae Heo, Martin M. Shafer, Brandon R. Shelton, James J. Schauer, and Constantinos Sioutas. 2012. "Characterization, Sources and Redox Activity of Fine

- and Coarse Particulate Matter in Milan, Italy.” *Atmospheric Environment* 49. Elsevier Ltd: 130–41. doi:10.1016/j.atmosenv.2011.12.011.
- Deshmukh, Dhananjay K.; Manas K. Deb; Ying I. Tsai;, and Stelyus L. Mkoma. 2011. “Water Soluble Ions in PM2.5 and PM1 Aerosols in Durg City, Chhattisgarh, India.” *Aerosol and Air Quality Research*, no. 11: 696–708. doi:doi:10.4209/aaqr.2010.04.0025.
- Didyk, Borys M, Bernd R.T Simoneit, L Alvaro Pezoa, M Luis Riveros, and a Anselmo Flores. 2000. “Urban Aerosol Particles of Santiago, Chile.” *Atmospheric Environment* 34 (8): 1167–79. doi:10.1016/S1352-2310(99)00403-3.
- Dockery, D W, C A Pope, X Xu, J D Spengler, J H Ware, M E Fay, B G Ferris, and F E Speizer. 1993. “An Association between Air Pollution and Mortality in Six U.S. Cities.” *The New England Journal of Medicine* 329 (24). MASS MEDICAL SOC, 10 SHATTUCK, BOSTON, MA 02115: 1753–59. doi:10.1056/NEJM199312093292401.
- Dockery, Douglas W, and Peter H Stone. 2007. “Cardiovascular Risks from Fine Particulate Air Pollution.” *The New England Journal of Medicine* 356 (5): 511–13. doi:10.1056/NEJMe068274.
- Du, Liuliu, Stuart Batterman, Christopher Godwin, Jo-Yu Chin, Edith Parker, Michael Breen, Wilma Brakefield, Thomas Robins, and Toby Lewis. 2012. “Air Change Rates and Interzonal Flows in Residences, and the Need for Multi-Zone Models for Exposure and Health Analyses.” *International Journal of Environmental Research and Public Health* 9 (12): 4639–61.
- ECLAC: Economic Commission for Latin America. 2012. “Statistical Data for Latin America.”
- ECLAC. 2014. “Statistical Data for Latin America. Data for GINI.”
- Elshorbany, Y. F., J. Kleffmann, R. Kurtenbach, E. Lissi, M. Rubio, G. Villena, E. Gramsch, a. R. Rickard, M. J. Pilling, and P. Wiesen. 2010. “Seasonal Dependence of the Oxidation Capacity of the City of Santiago de Chile.” *Atmospheric Environment* 44 (40). Elsevier Ltd: 5383–94. doi:10.1016/j.atmosenv.2009.08.036.
- Fabian, P., G. Adamkiewicz, and J. I. Levy. 2012. “Simulating Indoor Concentrations of NO2 and PM2.5 in Multifamily Housing for Use in Health-Based Intervention Modeling.” *Indoor Air* 22 (1): 12–23. doi:10.1111/j.1600-0668.2011.00742.x.
- Fernández-Caliani, J. C., C. Barba-Brioso, I. González, and E. Galán. 2009. “Heavy Metal Pollution in Soils around the Abandoned Mine Sites of the Iberian Pyrite Belt (Southwest Spain).” *Water, Air, and Soil Pollution* 200 (1-4): 211–26. doi:10.1007/s11270-008-9905-7.

- Fiebig-Wittmaack, M., E. Schultz, a. M. Córdova, and C. Pizarro. 2006. "A Microscopic and Chemical Study of Airborne Coarse Particles with Particular Reference to Sea Salt in Chile at 30° S." *Atmospheric Environment* 40 (19): 3467–78. doi:10.1016/j.atmosenv.2006.02.008.
- Fine, Philip M., Glen R. Cass, and Bernd R. T. Simoneit. 2004. "Chemical Characterization of Fine Particle Emissions from the Fireplace Combustion of Wood Types Grown in the Midwestern and Western United States." *Environmental Engineering Science* 21 (3). MARY ANN LIEBERT INC PUBL, 2 MADISON AVENUE, LARCHMONT, NY 10538 USA: 387–409. doi:10.1089/109287504323067021.
- Flores, C., M.T. Solís, A Fortt, and G. Valdivia. 2010. "Síntomatología Respiratoria Y Enfermedad Pulmonar Obstructiva Crónica Y Su Asociación a Contaminación Intradomiciliaria En El Área Metropolitana de Santiago: Estudio Platino." *Revista Chilena de Enfermedades Respiratorias* 26 (2): 72–80.
- Fujiwara, Fabián, Raúl Jiménez Rebagliati, Laura Dawidowski, Darío Gómez, Griselda Polla, Victoria Pereyra, and Patricia Smichowski. 2011. "Spatial and Chemical Patterns of Size Fractionated Road Dust Collected in a Megacity." *Atmospheric Environment* 45 (8): 1497–1505.
- Gallardo, L., G. Olivares, J. Langner, and B. Arrhus. 2002. "Coastal Lows and Sulphur Air Pollution in Central Chile." *Atmospheric Environment* 36: 3829–41.
- Garcia-Menendez, Fernando, Aika Yano, Yongtao Hu, and M. Talat Odman. 2010. "An Adaptive Grid Version of CMAQ for Improving the Resolution of Plumes." *Atmospheric Pollution Research* 1: 239–49. doi:10.5094/APR.2010.031.
- Garreaud, RenéD., JoséA. Rutllant, and Humberto Fuenzalida. 2002. "Coastal Lows along the Subtropical West Coast of South America: Mean Structure and Evolution." *Monthly Weather Review* 130 (1): 75–88. doi:10.1175/1520-0493(2002)130<0075:CLATSW>2.0.CO;2.
- Gidhagen, L., H. Kahelin, P. Schmidt-Thomé, and C. Johansson. 2002. "Anthropogenic and Natural Levels of Arsenic in PM10 in Central and Northern Chile." *Atmospheric Environment* 36 (23): 3803–17. doi:10.1016/S1352-2310(02)00284-4.
- González R., Nelly, Francisco Torres-Avilés, Elena Carrasco P., Francisca Salas P., and Francisco Pérez B. 2013. "Estudio Temporal de Diabetes Mellitus Tipo 1 En Chile: Asociación Con Factores Ambientales Durante El Período 2000-2007." *Revista Medica de Chile* 141 (5): 595–601. doi:10.4067/S0034-98872013000500007.
- Gramsch, E; Cereceda-Balic, F;, and D; Oyola, P; Vonbaer. 2006. "Examination of Pollution Trends in Santiago de Chile with Cluster Analysis of PM10 and Ozone

- Data.” *Atmospheric Environment* 40 (28): 5464–75. doi:10.1016/j.atmosenv.2006.03.062.
- Hasheminassab, Sina, Nancy Daher, James J. Schauer, and Constantinos Sioutas. 2013. “Source Apportionment and Organic Compound Characterization of Ambient Ultrafine Particulate Matter (PM) in the Los Angeles Basin.” *Atmospheric Environment* 79. Elsevier Ltd: 529–39. doi:10.1016/j.atmosenv.2013.07.040.
- Hedberg, Emma, Lars Gidhagen, and Christer Johansson. 2005. “Source Contributions to PM₁₀ and Arsenic Concentrations in Central Chile Using Positive Matrix Factorization.” *Atmospheric Environment* 39 (3): 549–61. doi:10.1016/j.atmosenv.2004.11.001.
- Heo, Jongbae, Muaz Dulger, Michael R. Olson, Jerome E. McGinnis, Brandon R. Shelton, Aiko Matsunaga, Constantinos Sioutas, and James J. Schauer. 2013. “Source Apportionments of PM_{2.5} Organic Carbon Using Molecular Marker Positive Matrix Factorization and Comparison of Results from Different Receptor Models.” *Atmospheric Environment* 73. Elsevier Ltd: 51–61. doi:10.1016/j.atmosenv.2013.03.004.
- Hopke, P K, K Ito, T Mar, W F Christensen, D J Eatough, R C Henry, E Kim, et al. 2006. “PM Source Apportionment and Health Effects: 1. Intercomparison of Source Apportionment Results.” *Journal of Exposure Science and Environmental Epidemiology* 16 (3): 275–86.
- Hopke, Philip K., Ying Xie, Taisto Raunemaa, Steven Biegalski, Sheldon Landsberger, Willy Maenhaut, Paulo Artaxo, and David Cohen. 1997. “Characterization of the Gent Stacked Filter Unit PM₁₀ Sampler.” *Aerosol Science and Technology* 27 (6): 726–35. doi:10.1080/02786829708965507.
- Hopke, PK. 2005. “PM Source Apportionment and Health Effects: I. Intercomparison of Source Apportionment Results.” *J Expo Anal Environ Epidemiol* 1 (1-12).
- INE: Instituto Nacional de Estadísticas. 2012. “Population Data for Census 2002.”
- Jorquera, Hector. 2009. “Source Apportionment of PM₁₀ and PM_{2.5} at Tocopilla, Chile (22A Degrees 05' S, 70A Degrees 12' W).” *Environmental Monitoring and Assessment* 153 (1-4): 235–51.
- Jorquera, Héctor, and Francisco Barraza. 2012. “Source Apportionment of Ambient PM_{2.5} in Santiago, Chile: 1999 and 2004 Results.” *Science of the Total Environment* 435-436 (October). Elsevier B.V.: 418–29. doi:10.1016/j.scitotenv.2012.07.049.
- Jorquera. 2013. “Source Apportionment of PM₁₀ and PM_{2.5} in a Desert Region in Northern Chile.” *Science of the Total Environment* 444. Elsevier B.V.: 327–35. doi:10.1016/j.scitotenv.2012.12.007.

- Jorquera, Hector, and Julio Castro. 2010. "Analysis of Urban Pollution Episodes by Inverse Modeling." *Atmospheric Environment* 44 (1): 42–54. doi:10.1016/j.atmosenv.2009.09.040.
- Jorquera, Hector, German Orrego, Julio Castro, and Velisa Vesovic. 2004. "Trends in Air Quality and Population Exposure in Santiago, Chile, 1989-2001." *International Journal of Environment and Pollution* 22 (4): 507–30. doi:10.1504/IJEP.2004.005684.
- Jorquera, Héctor, Wilfredo Palma, and José Tapia. 2000. "An Intervention Analysis of Air Quality Data at Santiago, Chile." *Atmospheric Environment* 34 (24): 4073–84. doi:10.1016/S1352-2310(00)00161-8.
- Jorquera. 2002. "A Ground-Level Ozone Forecasting Model for Santiago, Chile." *Journal of Forecasting* 21 (July): 451–72. doi:10.1002/for.836.
- Junninen, Heikki, Jacob Monster, Maria Rey, Jose Cancelinha, Kevin Douglas, Matthew Duane, Vittorio Forcina, et al. 2009. "Quantifying the Impact of Residential Heating on the Urban Air Quality in a Typical European Coal Combustion Region." *Environmental Science & Technology* 43 (20): 7964–70.
- Kavouras, I G, P Koutrakis, F Cereceda-Balic, and P Oyola. 2001. "Source Apportionment of PM10 and PM2.5 in Five Chilean Cities Using Factor Analysis." *Journal of the Air & Waste Management Association (1995)* 51 (3): 451–64.
- Klepeis, Neil E., and William W. Nazaroff. 2006. "Modeling Residential Exposure to Secondhand Tobacco Smoke." *Atmospheric Environment* 40 (23): 4393–4407. doi:10.1016/j.atmosenv.2006.03.018.
- Koutrakis, Petros, Sonja N Sax, Jeremy a Sarnat, Brent Coull, Phil Demokritou, Pedro Oyola, Javier Garcia, and Ernesto Gramsch. 2005. "Analysis of PM10, PM2.5, and PM2.5-10 Concentrations in Santiago, Chile, from 1989 to 2001." *Journal of the Air & Waste Management Association (1995)* 55 (3): 342–51. doi:10.1080/10473289.2005.10464627.
- Lai, S C, K F Ho, Y Y Zhang, S C Lee, Yu Huang, and S C Zou. 2010. "Characteristics of Residential Indoor Carbonaceous Aerosols: A Case Study in Guangzhou, Pearl River Delta Region." *Aerosol and Air Quality Research* 10 (5): 472–78.
- Leiva, Manuel A, Daniela A Santibanez, Sergio Ibarra E, Patricia Matus C, and Rodrigo Seguel. 2013. "A Five-Year Study of Particulate Matter (PM2.5) and Cerebrovascular Diseases." *Environmental Pollution* 181 (October): 1–6.
- Lepeule, Johanna, Francine Laden, Douglas Dockery, and Joel Schwartz. 2012. "Chronic Exposure to Fine Particles and Mortality: An Extended Follow-up of the Harvard Six

- Cities Study from 1974 to 2009.” *Environmental Health Perspectives* 120 (7): 965–70. doi:10.1289/ehp.1104660.
- Lim, Stephen S., Theo Vos, Abraham D. Flaxman, Goodarz Danaei, Kenji Shibuya, Heather Adair-Rohani, Markus Amann, et al. 2012. “A Comparative Risk Assessment of Burden of Disease and Injury Attributable to 67 Risk Factors and Risk Factor Clusters in 21 Regions, 1990-2010: A Systematic Analysis for the Global Burden of Disease Study 2010.” *The Lancet* 380 (9859): 2224–60. doi:10.1016/S0140-6736(12)61766-8.
- Lough, Glynis C, Charles G Christensen, James J Schauer, James Tortorelli, Erin Mani, Douglas R Lawson, Nigel N Clark, and Peter a Gabele. 2007. “Development of Molecular Marker Source Profiles for Emissions from on-Road Gasoline and Diesel Vehicle Fleets.” *Journal of the Air & Waste Management Association (1995)* 57 (10): 1190–99. doi:10.3155/1047-3289.57.10.1190.
- Lough, Glynis C, and James J Schauer. 2007. “Sensitivity of Source Apportionment of Urban Particulate Matter to Uncertainty in Motor Vehicle Emissions Profiles.” *Journal of the Air & Waste Management Association (1995)* 57 (10): 1200–1213. doi:10.3155/1047-3289.57.10.1200.
- Mace, Kimberly a. 2003. “Water-Soluble Organic Nitrogen in Amazon Basin Aerosols during the Dry (biomass Burning) and Wet Seasons.” *Journal of Geophysical Research* 108 (D16). doi:10.1029/2003JD003557.
- MacNeill, M., L. Wallace, J. Kearney, R.W. W Allen, K. Van Ryswyk, S. Judek, X. Xu, et al. 2012. “Factors Influencing Variability in the Infiltration of PM_{2.5} Mass and Its Components.” *Atmospheric Environment* 61 (0): 518–32. doi:10.1016/j.atmosenv.2012.07.005.
- Malm, William C., James F. Sisler, Dale Huffman, Robert A. Eldred, Thomas A. Cahill, and A Malm, C Sisler, James F Cahill. 1994. “Spatial and Seasonal Trends in Particle Concentration and Optical Extinction in the United States.” *Journal of Geophysical Research* 99 (D1): 1347–70. doi:10.1029/93JD02916.
- Mansbach, David K., and Joel R. Norris. 2007. “Low-Level Cloud Variability over the Equatorial Cold Tongue in Observations and Models.” *Journal of Climate* 20 (8): 1555–70. doi:10.1175/JCLI4073.1.
- Marple, Virgil a., Kenneth L. Rubow, William Turner, and John D. Spengler. 1987. “Low Flow Rate Sharp Cut Impactors for Indoor Air Sampling: Design and Calibration.” *Japca* 37 (11): 1303–7. doi:10.1080/08940630.1987.10466325.
- McGrath, J.A. A, M.A. A Byrne, M.R. R Ashmore, A.C. C Terry, and C. Dimitroulopoulou. 2014. “A Simulation Study of the Changes in PM_{2.5} Concentrations due to Interzonal Airflow Variations Caused by Internal Door

- Opening Patterns.” *Atmospheric Environment* 48 (1): 183–88.
doi:10.1016/j.atmosenv.2014.01.050.
- Mena-Carrasco, Marcelo, Pablo Saide, Rodrigo Delgado, Pablo Hernandez, Scott Spak, Luisa Molina, Gregory Carmichael, and Xiaoyan Jiang. 2014. “Regional Climate Feedbacks in Central Chile and Their Effect on Air Quality Episodes and Meteorology.” *Urban Climate* 10 (December): 771–81.
doi:10.1016/j.uclim.2014.06.006.
- Meng, Q Y, B J Turpin, L Korn, C P Weisel, M Morandi, S Colome, J F J Zhang, et al. 2005. “Influence of Ambient (outdoor) Sources on Residential Indoor and Personal PM_{2.5} Concentrations: Analyses of RIOPA Data.” *Journal of Exposure Analysis and Environmental Epidemiology* 15 (1): 17–28.
- Meng, Qing Yu, Dalia Spector, Steven Colome, and Barbara Turpin. 2009. “Determinants of Indoor and Personal Exposure to PM_{2.5} of Indoor and Outdoor Origin during the RIOPA Study.” *Atmospheric Environment* 43 (36): 5750–58.
- Meng, Qing Yu, Barbara J Turpin, Jong Hoon Lee, Andrea Polidori, Clifford P Weisel, Maria Morandi, Steven Colome, Junfeng Zhang, Thomas Stock, and Arthur Winer. 2007. “How Does Infiltration Behavior Modify the Composition of Ambient PM_{2.5} in Indoor Spaces? An Analysis of RIOPA Data.” *Environmental Science & Technology* 41 (21): 7315–21.
- Meng, Qing Yu, Barbara J. Turpin, Andrea Polidori, Jong Hoon Lee, Clifford Weisel, Maria Morandi, Steven Colome, Thomas Stock, Arthur Winer, and Jenfeng F Zhang. 2005. “PM_{2.5} of Ambient Origin: Estimates and Exposure Errors Relevant to PM Epidemiology.” *Environmental Science & Technology* 39 (14): 5105–12.
doi:10.1021/es048226f.
- Ministerio de Transporte. 2014. “Statistics of Fuel Consumption and Km Travelled per Vehicle Class in Chilean Cities.”
- Ministerio del Medio Ambiente (MMA). 2014. “Progress Report on Santiago’s Pollution Prevention Plan.”
- Miyazaki, Y., K. Kawamura, J. Jung, H. Furutani, and M. Uematsu. 2011. “Latitudinal Distributions of Organic Nitrogen and Organic Carbon in Marine Aerosols over the Western North Pacific.” *Atmospheric Chemistry and Physics* 11 (7): 3037–49.
doi:10.5194/acp-11-3037-2011.
- MMA: Ambiente Ministerio del Medio. 2012. “A Cost Benefit Analysis for a Proposed Revision of the Emission Standard for Copper Smelters in Chile.”
- MMA: Ministerio del Medio Ambiente. 2012. “Operational PM₁₀ Forecast for Santiago.”

- Moreno, Francisco, Ernesto Gramsch, Pedro Oyola, and Maria Angélica Rubio. 2010. "Modification in the Soil and Traffic-Related Sources of Particle Matter between 1998 and 2007 in Santiago de Chile." *Journal of the Air & Waste Management Association* 60 (12): 1410–21. doi:10.3155/1047-3289.60.12.1410.
- Muñoz, Ricardo C., and Ricardo I. Alcañiz. 2012. "Variability of Urban Aerosols over Santiago, Chile: Comparison of Surface PM₁₀ Concentrations and Remote Sensing with Ceilometer and Lidar." *Aerosol and Air Quality Research* 12 (1): 8–14. doi:10.4209/aaqr.2011.08.0133.
- Muñoz, Ricardo C., Angella a. Undurraga, Ricardo C Muñoz, Angella a. Undurraga, Ricardo C. Muñoz, and Angella a. Undurraga. 2010. "Daytime Mixed Layer over the Santiago Basin: Description of Two Years of Observations with a Lidar Ceilometer." *Journal of Applied Meteorology and Climatology* 49 (8): 1728–41. doi:10.1175/2010JAMC2347.1.
- Nolte, Christopher G., James J. Schauer, Glen R. Cass, and Bernd R T Simoneit. 2002. "Trimethylsilyl Derivatives of Organic Compounds in Source Samples and in Atmospheric Fine Particulate Matter." *Environmental Science and Technology* 36 (20): 4273–81. doi:10.1021/es020518y.
- Ohura, Takeshi, Takashi Amagai, Xueyou Shen, Shuang Li, Ping Zhang, and Lizhong Zhu. 2009. "Comparative Study on Indoor Air Quality in Japan and China: Characteristics of Residential Indoor and Outdoor VOCs." *Atmospheric Environment* 43 (40): 6352–59.
- Okin, Gregory S., Joanna E. Bullard, Richard L. Reynolds, John Andrew C Ballantine, Kerstin Schepanski, Martin C. Todd, Jayne Belnap, Matthew C. Baddock, Thomas E. Gill, and Mark E. Miller. 2011. "Dust: Small-Scale Processes with Global Consequences." *Eos* 92 (29): 241–42. doi:10.1029/2011EO290001.
- Olivares, G., L. Gallardo, J. Langner, and B. Aarhus. 2002. "Regional Dispersion of Oxidized Sulfur in Central Chile." *Atmospheric Environment* 36 (23): 3819–28. doi:10.1016/S1352-2310(02)00286-8.
- Oros, D. R., and B. R T Simoneit. 2000. "Identification and Emission Rates of Molecular Tracers in Coal Smoke Particulate Matter." *Fuel* 79 (5): 515–36. doi:10.1016/S0016-2361(99)00153-2.
- Ott, Wayne, Lance Wallace, and David Mage. 2000. "Predicting Particulate (PM₁₀) Personal Exposure Distributions Using a Random Component Superposition Statistical Model." *Journal of the Air & Waste Management Association* 50 (8): 1390–1406. doi:10.1080/10473289.2000.10464169.

- Paatero, Pentti. 1997. "Least Squares Formulation of Robust Non-Negative Factor Analysis." *Chemometrics and Intelligent Laboratory Systems* 37 (1): 23–35. doi:10.1016/S0169-7439(96)00044-5.
- Paatero. 1999. "The Multilinear Engine—A Table-Driven, Least Squares Program for Solving Multilinear Problems, Including the N -Way Parallel Factor Analysis Model." *Journal of Computational and Graphical Statistics* 8 (4). Taylor & Francis Group: 854–88. doi:10.1080/10618600.1999.10474853.
- Paatero, P Hopke, P, S Begun, B Biswas, Pentti Paatero, Philip K Hopke, Bilkis A Begum, and Swapan K Biswas. 2005. "A Graphical Diagnostic Method for Assessing the Rotation in Factor Analytical Models of Atmospheric Pollution." *Atmospheric Environment* 39 (1): 193–201. doi:10.1016/j.atmosenv.2004.08.018.
- Pant, Pallavi, and Roy M. Harrison. 2012. "Critical Review of Receptor Modelling for Particulate Matter: A Case Study of India." *Atmospheric Environment* 49 (March): 1–12. doi:10.1016/j.atmosenv.2011.11.060.
- Pant. 2013. "Estimation of the Contribution of Road Traffic Emissions to Particulate Matter Concentrations from Field Measurements: A Review." *Atmospheric Environment* 77 (0): 78–97. doi:10.1016/j.atmosenv.2013.04.028.
- Pino, P, T Walter, M Oyarzun, R Villegas, and I Romieu. 2004. "Fine Particulate Matter and Wheezing Illnesses in the First Year of Life." *Epidemiology* 15 (6): 702–8.
- Polissar, Alexandr V., Philip K. Hopke, William C. Malm, and James F. Sisler. 1998. "Atmospheric Aerosol over Alaska: 1. Spatial and Seasonal Variability." *Journal of Geophysical Research* 103 (D15): 19035. doi:10.1029/98JD01365.
- Polissar, Alexandr V., Philip K. Hopke, Pentti Paatero, William C. Malm, and James F. Sisler. 1998. "Atmospheric Aerosol over Alaska: 2. Elemental Composition and Sources." *Journal of Geophysical Research* 103 (D15): 19045. doi:10.1029/98JD01212.
- Pope, C Arden. 2007. "Mortality Effects of Longer Term Exposures to Fine Particulate Air Pollution: Review of Recent Epidemiological Evidence." *Inhalation Toxicology* 19 Suppl 1 (October 2006): 33–38. doi:10.1080/08958370701492961.
- Pope, C. Arden, Richard T. Burnett, George D. Thurston, Michael J. Thun, Eugenia E. Calle, Daniel Krewski, and John J. Godleski. 2004. "Cardiovascular Mortality and Long-Term Exposure to Particulate Air Pollution: Epidemiological Evidence of General Pathophysiological Pathways of Disease." *Circulation* 109 (1): 71–77. doi:10.1161/01.CIR.0000108927.80044.7F.

- Pope, C. Arden, and Douglas W. Dockery. 2006. "Health Effects of Fine Particulate Air Pollution: Lines That Connect." *Journal of the Air & Waste Management Association* 56 (6): 709–42. doi:10.1080/10473289.2006.10464485.
- Rappenglück, Bernhard, Pedro Oyola, Ignacio Olaeta, and Peter Fabian. 2000. "The Evolution of Photochemical Smog in the Metropolitan Area of Santiago de Chile." *Journal of Applied Meteorology* 39 (3): 275–90. doi:10.1175/1520-0450(2000)039<0275:TEOPSI>2.0.CO;2.
- Ravindra, Khaiwal, Ranjeet Sokhi, and René Van Grieken. 2008. "Atmospheric Polycyclic Aromatic Hydrocarbons: Source Attribution, Emission Factors and Regulation." *Atmospheric Environment* 42 (13): 2895–2921. doi:10.1016/j.atmosenv.2007.12.010.
- Reff, Adam, Shelly I Eberly, and Prakash V Bhawe. 2007. "Receptor Modeling of Ambient Particulate Matter Data Using Positive Matrix Factorization: Review of Existing Methods." *Journal of the Air & Waste Management Association* 57 (2): 146–54. doi:10.1080/10473289.2007.10465319.
- Riley, W J, T E McKone, A C K Lai, and W W Nazaroff. 2002. "Indoor Particulate Matter of Outdoor Origin: Importance of Size-Dependent Removal Mechanisms." *Environmental Science & Technology* 36 (2): 200–207.
- Rogge, Wolfgang F., Lynn M. Hildemann, Monica a. Mazurek, Glen R. Cass, and B. R T Simoneit. 1997. "Sources of Fine Organic Aerosol. 8. Boilers Burning No. 2 Distillate Fuel Oil." *Environmental Science and Technology* 31 (10): 2731–37. doi:10.1021/es9609563.
- Rogge, Wolfgang F., Lynn M. Hildemann, Monica a. Mazurek, Glen R. Cass, and Bernd R. T. Simoneit. 1993. "Sources of Fine Organic Aerosol. 5. Natural Gas Home Appliances." *Environmental Science & Technology* 27 (13): 2736–44. doi:10.1021/es00049a012.
- Rogge, Wolfgang F., Monica A. Mazurek, Lynn M. Hildemann, Glen R. Cass, and Bernd R.T. Simoneit. 1993. "Quantification of Urban Organic Aerosols at a Molecular Level: Identification, Abundance and Seasonal Variation." *Atmospheric Environment. Part A. General Topics* 27 (8): 1309–30. doi:10.1016/0960-1686(93)90257-Y.
- Rojas, Carlos M., Paulo Artaxo, René Van Grieken, and René Van Grieken. 1990. "Aerosols in Santiago de Chile: A Study Using Receptor Modeling with X-Ray Fluorescence and Single Particle Analysis." *Atmospheric Environment. Part B. Urban Atmosphere* 24 (2): 227–41. doi:10.1016/0957-1272(90)90028-S.
- Rojas-Bracho, Leonora, Helen H Suh, Pedro Oyola, and Petros Koutrakis. 2002. "Measurements of Children's Exposures to Particles and Nitrogen Dioxide in Santiago, Chile." *Science of The Total Environment* 287 (3): 249–64. doi:10.1016/S0048-9697(01)00987-1.

- Rolph, G.D. 2012. "Real-Time Environmental Applications and Display sYstem (READY)." Silver Spring, MD.
- Ruiz, Pablo a, Claudia Toro, Jorge Cáceres, Gianni López, Pedro Oyola, Petros Koutrakis, Jorge Caceres, Gianni Lopez, Pedro Oyola, and Petros Koutrakis. 2010. "Effect of Gas and Kerosene Space Heaters on Indoor Air Quality: A Study in Homes of Santiago, Chile." *Journal of the Air & Waste Management Association* 60 (1): 98–108. doi:10.3155/1047-3289.60.1.98.
- Rutllant, JoséA., and RenéD. Garreaud. 2004. "Episodes of Strong Flow down the Western Slope of the Subtropical Andes." *Monthly Weather Review* 132 (2): 611–22. doi:10.1175/1520-0493(2004)132<0611:EOSFDT>2.0.CO;2.
- Saide, Pablo E., Gregory R. Carmichael, Scott N. Spak, Laura Gallardo, Axel E. Osses, Marcelo A. Mena-Carrasco, and Mariusz Pagowski. 2011. "Forecasting Urban PM10 and PM2.5 Pollution Episodes in Very Stable Nocturnal Conditions and Complex Terrain Using WRF–Chem CO Tracer Model." *Atmospheric Environment* 45 (16): 2769–80. doi:10.1016/j.atmosenv.2011.02.001.
- Saraga, Dikaia E, Thomas Maggos, Constantinos G Helmis, John Michopoulos, John G Bartzis, and Christos Vasilakos. 2010. "PM10 and PM2.5 Ionic Composition and VOCs Measurements in Two Typical Apartments in Athens, Greece: Investigation of Smoking Contribution to Indoor Air Concentrations." *Environmental Monitoring and Assessment* 167 (1-4): 321–31.
- Sarnat, Jeremy a., Christopher M. Long, Petros Koutrakis, Brent a. Coull, Joel Schwartz, and Helen H. Suh. 2002. "Using Sulfur as a Tracer of Outdoor Fine Particulate Matter." *Environmental Science & Technology* 36 (24): 5305–14. doi:10.1021/es025796b.
- Sax, Sonja N, Petros Koutrakis, Pablo A Ruiz Rudolph, Francisco Cereceda-Balic, Ernesto Grarnsch, and Pedro Oyola. 2007. "Trends in the Elemental Composition of Fine Particulate Matter in Santiago, Chile, from 1998 to 2003." *Journal of the Air & Waste Management Association* 57 (7): 845–55.
- Schauer, J. J., B. T. Mader, J. T. Deminter, G. Heidemann, M. S. Bae, J. H. Seinfeld, R. C. Flagan, et al. 2003. "ACE-Asia Intercomparison of a Thermal-Optical Method for the Determination of Particle-Phase Organic and Elemental Carbon." *Environmental Science and Technology* 37 (5): 993–1001. doi:10.1021/es020622f.
- Schauer, James J., Wolfgang F. Rogge, Lynn M. Hildemann, Monica A. Mazurek, Glen R. Cass, and Bernd R.T. Simoneit. 1996. "Source Apportionment of Airborne Particulate Matter Using Organic Compounds as Tracers." *Atmospheric Environment* 30 (22): 3837–55. doi:10.1016/1352-2310(96)00085-4.

- Schmitz, Rainer. 2005. "Modelling of Air Pollution Dispersion in Santiago de Chile." *Atmospheric Environment* 39 (11): 2035–47. doi:10.1016/j.atmosenv.2004.12.033.
- Shrivastava, Manish K., R. Subramanian, Wolfgang F. Rogge, and Allen L. Robinson. 2007. "Sources of Organic Aerosol: Positive Matrix Factorization of Molecular Marker Data and Comparison of Results from Different Source Apportionment Models." *Atmospheric Environment* 41 (40): 9353–69. doi:10.1016/j.atmosenv.2007.09.016.
- Simoneit, B.R.T., J.J. Schauer, C.G. Nolte, D.R. Oros, V.O. Elias, M.P. Fraser, W.F. Rogge, and G.R. Cass. 1999. "Levoglucosan, a Tracer for Cellulose in Biomass Burning and Atmospheric Particles." *Atmospheric Environment* 33 (2): 173–82. doi:10.1016/S1352-2310(98)00145-9.
- Simoneit, Bernd R. T. 1986. "Characterization of Organic Constituents in Aerosols in Relation to Their Origin and Transport: A Review." *International Journal of Environmental Analytical Chemistry* 23 (3). Taylor & Francis Group: 207–37. doi:10.1080/03067318608076446.
- SINCA. 2012. "National System of Air Quality Monitoring Information SINCA." 2015. <http://sinca.mma.gob.cl/>.
- Singer, B. C., W. W. Delp, P. N. Price, and M. G. Apte. 2012. "Performance of Installed Cooking Exhaust Devices." *Indoor Air* 22 (3): 224–34. doi:10.1111/j.1600-0668.2011.00756.x.
- Sohn, Michael D., Michael G. Apte, Richard G. Sextro, and Alvin C.K. Lai. 2007. "Predicting Size-Resolved Particle Behavior in Multizone Buildings." *Atmospheric Environment* 41 (7): 1473–82. doi:10.1016/j.atmosenv.2006.10.010.
- Squizzato, S., M. Masiol, a. Brunelli, S. Pistollato, E. Tarabotti, G. Rampazzo, and B. Pavoni. 2013. "Factors Determining the Formation of Secondary Inorganic Aerosol: A Case Study in the Po Valley (Italy)." *Atmospheric Chemistry and Physics* 13 (4): 1927–39. doi:10.5194/acp-13-1927-2013.
- Stone, E. a., D. C. Snyder, R. J. Sheesley, a. P. Sullivan, R. J. Weber, and J. J. Schauer. 2007. "Source Apportionment of Fine Organic Aerosol in Mexico City during the MILAGRO Experiment 2006." *Atmospheric Chemistry and Physics Discussions* 7 (4): 9635–61. doi:10.5194/acpd-7-9635-2007.
- Stone, Elizabeth, James Schauer, Tauseef a. Quraishi, and Abid Mahmood. 2010. "Chemical Characterization and Source Apportionment of Fine and Coarse Particulate Matter in Lahore, Pakistan." *Atmospheric Environment* 44 (8). Elsevier Ltd: 1062–70. doi:10.1016/j.atmosenv.2009.12.015.

- Street, James O., Raymond J. Carroll, and David Ruppert. 1988. "A Note on Computing Robust Regression Estimates Via Iteratively Reweighted Least Squares." *The American Statistician* 42 (2): 152–54. doi:10.1080/00031305.1988.10475548.
- Sun, R, S Moorthi, H Xiao, and C R Mechoso. 2010. "Simulation of Low Clouds in the Southeast Pacific by the NCEP GFS: Sensitivity to Vertical Mixing." *Atmospheric Chemistry and Physics* 10 (24): 12261–72.
- Toro, Richard a., Mauricio Canales, Robert G. Flocchini, Raúl G E Morales, and Manuel a. Leiva G. 2014. "Urban Atmospheric Ammonia in Santiago City, Chile." *Aerosol and Air Quality Research* 14 (1): 33–44. doi:10.4209/aaqr.2012.07.0189.
- Troncoso, Rodrigo, Louis De Grange, and Luis A Cifuentes. 2012. "Effects of Environmental Alerts and Pre-Emergencies on Pollutant Concentrations in Santiago, Chile." *Atmospheric Environment* 61: 550–57.
- Tsapakis, Manolis, Evaggelia Lagoudaki, Euripides G. Stephanou, Ilias G. Kavouras, Petros Koutrakis, Pedro Oyola, and Dietrich Von Baer. 2002. "The Composition and Sources of PM_{2.5} Organic Aerosol in Two Urban Areas of Chile." *Atmospheric Environment* 36 (23): 3851–63. doi:10.1016/S1352-2310(02)00269-8.
- U.S. Environmental Protection Agency. 1999. "Compendium Method 10-3.3. Determination of Metals in Ambient Particulate Matter Using X-Ray Fluorescence (XRF) Spectroscopy." Cincinnati, Ohio.
- U.S. Environmental Protection Agency. 2004. "PMF3.0 Software." U.S. Environmental Protection Agency. 2012a. "PMF3.0 Software."
- U.S. Environmental Protection Agency. 2012b. "PMF3.0 Software and User Guide."
- U.S. Environmental Protection Agency. 2015. "Chemical Mass Balance (CMB) Model."
- U.S. Environmental Protection Agency. 1997. "Guidance for Network Design and Optimum Site Exposure for PM_{2.5} and PM₁₀, EPA-454/R-99-022, December, 1997."
- U.S. Environmental Protection Agency. 1999. "Compendium of Methods for the Determination of Inorganic Compounds in Ambient Air Compendium. Method IO-3.3 Determination of Metals in Ambient Particulate Matter Using X-Ray Fluorescence (XRF) Spectroscopy."
- U.S. Environmental Protection Agency. 2004. "Air Quality Criteria for Particulate Matter: Final Report." Washington DC.
- Valdes, Ana, Antonella Zanobetti, Jaana I Halonen, Luis Abdón Cifuentes, Diego Morata, Joel Schwartz, Ana Valdés, et al. 2012. "Elemental Concentrations of Ambient

- Particles and Cause Specific Mortality in Santiago, Chile: A Time Series Study.” *Environmental Health* 11 (1): 82. doi:10.1186/1476-069X-11-82.
- Viale, Maximiliano, and René Garreaud. 2014. “Summer Precipitation Events over the Western Slope of the Subtropical Andes.” *Monthly Weather Review* 142 (3): 1074–92. doi:10.1175/MWR-D-13-00259.1.
- Von Schneidemesser, Erika, Elizabeth a. Stone, Tauseef a. Quraishi, Martin M. Shafer, and James J. Schauer. 2010. “Toxic Metals in the Atmosphere in Lahore, Pakistan.” *Science of the Total Environment* 408 (7). Elsevier B.V.: 1640–48. doi:10.1016/j.scitotenv.2009.12.022.
- Wang, Ying, Guoshun Zhuang, Aohan Tang, Hui Yuan, Yele Sun, Shuang Chen, and Aihua Zheng. 2005. “The Ion Chemistry and the Source of PM_{2.5} Aerosol in Beijing.” *Atmospheric Environment* 39 (21): 3771–84. doi:10.1016/j.atmosenv.2005.03.013.
- Watson, John G, L W Anthony Chen, Judith C Chow, Prakash Doraiswamy, and Douglas H Lowenthal. 2008. “Source Apportionment: Findings from the US Supersites Program.” *Journal of the Air & Waste Management Association* 58 (2): 265–88.
- Watson, John G., John A. Cooper, and James J. Huntzicker. 1984. “The Effective Variance Weighting for Least Squares Calculations Applied to the Mass Balance Receptor Model.” *Atmospheric Environment (1967)* 18 (7): 1347–55. doi:10.1016/0004-6981(84)90043-X.
- Weschler, Charles J., and Helen C. Shields. 1997. “Potential Reactions among Indoor Pollutants.” *Atmospheric Environment* 31 (21): 3487–95. doi:10.1016/S1352-2310(97)00219-7.
- WHO. 2002. “The World Health Report 2002 - Reducing Risks, Promoting Healthy Life.”
- WHO. 2015. “Indoor Air Pollution: Global Burden of Disease due to Indoor Air Pollution.”
- WHO: World Health Organization. 2005. “WHO Air Quality Guidelines for Particulate Matter, Ozone, Nitrogen Dioxide and Sulfur Dioxide, Global Update 2005, Summary of Risk Assessment.”
- Willis, R.D. 2000. “Workshop on UNMIX and PMF as Applied to PM_{2.5}. U.S. EPA, Report No. EPA/600/A-00/048.”
- Wils, E.R.J., A.G. Hulst, and J.C. den Hartog. 1982. “The Occurrence of Plant Wax Constituents in Airborne Particulate Matter in an Urbanized Area.” *Chemosphere* 11 (11): 1087–96. doi:10.1016/0045-6535(82)90113-8.

- Xu, Haiming M, Shang Ping Xie, and Yuqing Q Wang. 2005. "Subseasonal Variability of the Southeast Pacific Stratus Cloud Deck." *Journal of Climate* 18 (1): 131–42. doi:10.1175/JCLI3250.1.
- Yamamoto, N., D. G. Shendell, a. M. Winer, and J. Zhang. 2010. "Residential Air Exchange Rates in Three Major US Metropolitan Areas: Results from the Relationship among Indoor, Outdoor, and Personal Air Study 1999-2001." *Indoor Air* 20 (1): 85–90. doi:10.1111/j.1600-0668.2009.00622.x.
- Yang, Hong, Qianfeng Li, and Jian Zhen Yu. 2003. "Comparison of Two Methods for the Determination of Water-Soluble Organic Carbon in Atmospheric Particles." *Atmospheric Environment* 37 (6): 865–70. doi:10.1016/S1352-2310(02)00953-6.
- Zhang, Qunfang, Roja H Gangupomu, David Ramirez, and Yifang Zhu. 2010. "Measurement of Ultrafine Particles and Other Air Pollutants Emitted by Cooking Activities." *International Journal of Environmental Research and Public Health* 7 (4). Molecular Diversity Preservation International: 1744–59. doi:10.3390/ijerph7041744.
- Zhang, Yanxu, Shu Tao, Huizhong Shen, and Jianmin Ma. 2009. "Inhalation Exposure to Ambient Polycyclic Aromatic Hydrocarbons and Lung Cancer Risk of Chinese Population." *Proceedings of the National Academy of Sciences of the United States of America* 106 (50): 21063–67. doi:10.1073/pnas.0905756106.
- Zhao, Weixiang, Philip K. Hopke, Erwin W. Gelfand, and Nathan Rabinovitch. 2007. "Use of an Expanded Receptor Model for Personal Exposure Analysis in Schoolchildren with Asthma." *Atmospheric Environment* 41 (19): 4084–96. doi:10.1016/j.atmosenv.2007.01.037.
- Zhao, Weixiang X, Philip K. Hopke, Gary Norris, Ron Williams, and Pentti Paatero. 2006. "Source Apportionment and Analysis on Ambient and Personal Exposure Samples with a Combined Receptor Model and an Adaptive Blank Estimation Strategy." *Atmospheric Environment* 40 (20): 3788–3801. doi:10.1016/j.atmosenv.2006.02.027.

ANNEXES

ANNEX A: ETHICAL ISSUES

All protocols and documents used in this study were subjected to evaluation by the ethics committee of the Engineering and Medicine School at the Catholic University of Chile. Also an informed consent was requested from the participants, in which the characteristics and scope of measurements was informed, in addition to their rights as volunteers in this study.